2010

Establishment of a suitable dynamic formula for the construction control of driven piles and its calibration for Load and Resistance Factor Design

Matthew John Roling
Iowa State University

Establishment of a suitable dynamic formula for the construction control of driven piles and its calibration for Load and Resistance Factor Design

by

Matthew John Roling

A thesis submitted to the graduate faculty

in partial fulfillment of the requirements for the degree of

MASTER OF SCIENCE

Major: Civil Engineering (Structural Engineering)

Program of Study Committee:
Sri Sritharan, Major Professor
Fouad Fanous
Peter Sherman
Muhannad Suleiman

Iowa State University

Ames, Iowa

2010

TABLE OF CONTENTS

LIST OF FIGURES

LIST OF TABLES

ABSTRACT

Dynamic pile driving formulas have been available for the field prediction of the static bearing capacity of pile foundations for well over 180 years. On account of the immense number of different formulas that have been amassed during this time frame, a review of published literature was performed to identify the most common dynamic pile driving formulas utilized in the United States and their documented reliability. The results of this review indicated that no one dynamic pile driving formula is consistently better than all the rest; however, the Hiley, Janbu, Pacific Coast Uniform Building Code (PCUBC), and Gates formulas were shown to provide, on average, the best predictions of ultimate pile capacity. In contrast, the Engineering News Record (ENR) formula, which has been probably the most widely used dynamic formula within the United States, was shown to be among the worst predictors of pile capacity.

For well over 100 years, the Working Stress Design (WSD) approach has been the traditional basis for geotechnical design with regard to settlements or failure conditions. However, considerable effort has been put forth over the past couple of decades in relation to the adoption of the Load and Resistance Factor Design (LRFD) approach into geotechnical design. With the goal of producing engineered designs with consistent levels of reliability, the Federal Highway Administration (FHWA) issued a policy memorandum on June 28, 2000, requiring all new bridges initiated after October 1, 2007, to be designed according to the LRFD approach. Likewise, regionally calibrated LRFD resistance factors have been permitted by the American Association of State Highway Officials (AASHTO) to improve the economy of bridge foundation elements. Thus, the bulk of this study focused on the development of regionally calibrated LRFD resistance factors for the construction control of driven pile foundations via a suitable dynamic pile driving formula.

Using data from pile load tests performed in the State of Iowa, which was analyzed for reliability and placed in a newly designed relational database management system termed PILOT-IA, the efficiency of seven dynamic pile driving formulas (i.e., the Gates, FHWA Gates, ENR, Iowa Department of Transportation (DOT) Modified ENR, Janbu, PCUBC, and Washington DOT (WSDOT) formulas) was investigated. In addition to verifying the poor performance of the ENR formula, it was demonstrated that the efficiency of the Iowa DOT

Modified ENR formula, which is presently specified in the Iowa DOT's *Standard Specifications for Highway and Bridge Construction* manual, is sufficient to allow for its recommended use with steel H-shaped and timber pile foundations driven in any soil type; these two driven pile foundation types were found to be the most commonly used in Iowa via the results of both a state- and county-level survey. More specifically, LRFD resistance factors were calibrated and verified on a pile and soil type basis for the Iowa DOT Modified ENR formula using the first-order, second-moment (FOSM) reliability approach and the findings obtained from nine full-scale field load tests performed throughout the State of Iowa on steel H-shaped piles. For a target probability of failure of 1%, LRFD resistance factors of 0.49, 0.62, and 0.50 have been recommended for use with steel H-shaped piles driven in sand, clay, and mixed soil profiles, respectively, with a factor of 0.35 having been cautiously recommended for use with timber piles driven in any soil type.

Finally, a displacement-based signal matching technique was recommended for use with PDA measured data to arrive at prediction correlations for soil quake values, Smith damping factors, and the degree-of-degradation of such parameters with respect to pile penetration depth. Although an insufficient amount of data was analyzed to even begin to develop such correlations, the accuracy, uniqueness, and theoretical basis of the displacement-based signal matching approach over the more commonly employed Case Pile Wave Analysis Program (CAPWAP) approach was demonstrated. Provided the future establishment of such prediction correlations from the increased use of this proposed technique, it was suggested that a one-dimensional pile-soil model could be used in conjunction with a dynamic pile driving formula to design driven pile foundations.

CHAPTER 1: INTRODUCTION

1.1 PILE FOUNDATION PRELUDE

Piles are structural members, typically constructed from timber, concrete, and/or steel, that are used to transmit surface loads to lower levels of a soil mass. This transfer may be by vertical distribution of the load along the pile shaft or a direct application of the load to a lower stratum through the pile toe (Bowles 1996). In such instances, a vertical distribution of the load is made using a friction (or floating) pile, while a direct application of the load is made using a point (or end-bearing) pile. This distinction is purely one of convenience since all piles carry load as a combination of side resistance and point bearing, expect for the case in which a pile penetrates an extremely soft soil mass before making contact with a solid base (Bowles 1996).

As acknowledged by Bowles (1996), piles are commonly used for the following purposes:

- to carry vertical and/or lateral superstructure loads into or through a soil stratum;
- to resist uplift forces, such as those arising from the placement of a basement mat below the groundwater table, and/or overturning forces, such as those induced at the supports for tower legs as a result of the imposition of lateral wind loads upon the structure;
- to compact loose, cohesionless deposits through a combination of pile volume displacement and driving vibrations;
- to control settlements when, for example, a spread footing or mat foundation is located on a marginal soil or underlain by a highly compressible stratum;
- to stiffen the soil beneath machine foundations to control both vibration amplitudes as well as the natural frequency of the system;
- to provide an additional safety factor beneath bridge abutments and/or piers, particularly if the potential for scour is a concern; and
- to transmit loads, originating above the water surface, through the water and into the underlying soil, as witnessed in offshore construction where, for example, partially

embedded piling is subjected to vertical as well as lateral loads and the potential for buckling failure is a significant concern.

1.2 PILE BEARING CAPACITY ESTIMATION METHODS

On account of the poor subsurface conditions typically encountered at the locations of bridge-type structures, realization of a sound support system frequently implores the use of pile foundations. The failure of these foundation elements beneath a bridge-type superstructure presents the possibility for infliction of catastrophic consequences; however, the elevated cost of the piling elements themselves makes the practice of overdesigning extremely inefficient. Therefore, in order to be able to design economical bridge foundations, an engineer must be able to accurately predict the bearing capacity of nearly every pile.

In the American Society of Civil Engineers' (1946) *Manual of Engineering Practice* No. 27, the term bearing capacity is defined as follows:

> "Bearing capacity may be defined as that load which can be sustained by a pile foundation without producing objectionable settlement or material movement—initial or progressive—resulting in damage to the structure or interfering with its use."

With this definition in mind, Jumikis (1971) suggested that the bearing capacity of a pile is dependent upon the following items:

- type and properties of the soil;
- surface and/or groundwater regimen;
- geometry of the pile (i.e., solid, hollow, rectangular, straight, or tapered);
- pile material (i.e., timber, concrete, or steel);
- size of pile (i.e., cross-sectional area and length);
- property of mantle surface of pile (i.e., rough or smooth);
- driving depth of pile;
- method of embedding the pile into the soil (i.e., driving, jacking, jetting, vibrating, or casting in place);
- vertical pile alignment; and

- spacing of piles in a pile group.

Given the severity and complexity of this problem (i.e., the prediction of pile bearing capacity), pile designers have discovered the imperative benefits associated with alternative pile capacity estimation methods. Thus, the three most commonly available sources of pile bearing capacity estimates are:

- those derived from analyses of soil-boring information, standard penetration testing (SPT), or cone penetration testing (CPT) (i.e., static analysis methods);
- those based on nearby static load tests (SLTs) of similar piling; and
- those based on the driving record and pile driving equipment characteristics for a particular pile (i.e., dynamic analysis methods, which includes both the detailed methods derived from wave propagation theory as well as the much simpler dynamic pile driving formulas obtained from work-energy theory).

1.3 FOUNDATION DESIGN AND CONSTRUCTION PROCESS

To fully understand the timely application of the aforementioned pile capacity estimation methods, the typical design and construction process for pile foundations, provided in Figure 1.1, must be expounded. Simply put, design procedures begin with a detailed site investigation and soil parameter evaluation, which vary in quality and quantity according to the importance of the project and the complexity of the subsurface. Subsequently, potential foundation schemes are identified based upon the results of the site investigation, superstructure loading requirements, and local practice. All potential foundation schemes are then evaluated via static analysis methods (e.g., α-Tomlinson, Nordlund and Thurman, Meyerhof SPT, Schmertmann CPT, etc.). In addition, a drivability analysis is conducted for hammer evaluation as well as the determination of installation feasibility and structural adequacy of the pile. In summary, the pile foundation design procedures combine structural and geotechnical analyses to determine the best substructure design in advance of the bidding procedures. In other words, this process establishes quantity estimates to be used in construction bidding documents.

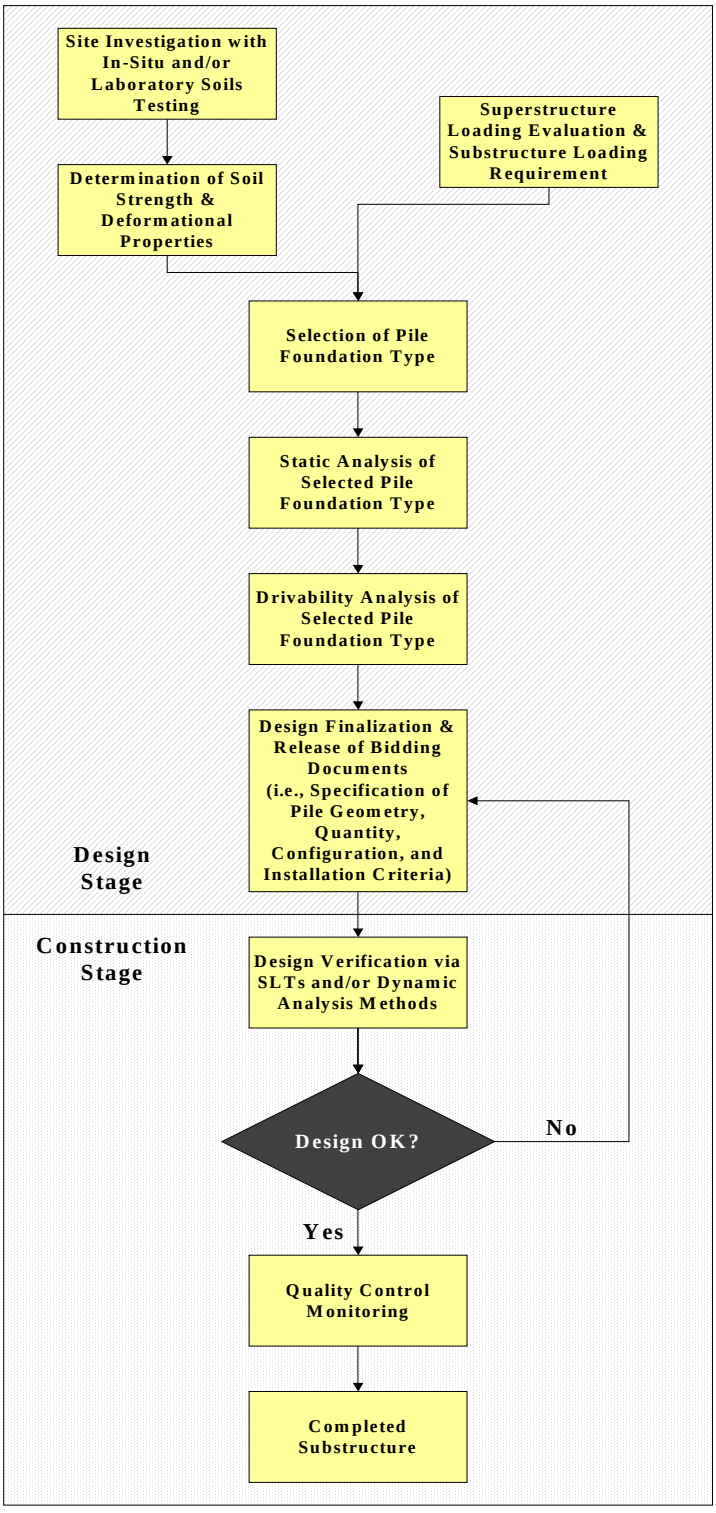

Figure 1.1: Typical Design and Construction Process for Driven Pile Foundations

Upon construction initiation, SLTs and/or dynamic analyses based on driving resistance (e.g., Wave Equation Analysis Approach (WEAP) (Pile Dynamics Inc. 2005), Pile Driving Analyzer (PDA) (Pile Dynamics Inc. 1992), CAse Pile Wave Analysis Program (CAPWAP) (Pile Dynamics Inc. 2000), and/or dynamic pile driving formula) are carried out on selected elements of the original design for pile capacity verification purposes. If the original design compares favorably with what is measured in the field for the select foundation elements, then construction sequences, which include quality control monitoring, are allowed to progress normally toward substructure completion. However, should the original design differ substantially from that measured in the field, then design modifications, which may include changes to the pile type, size, length or quantity, based on the construction phase testing results must be made before construction sequences are allowed to progress normally. In the end, two requirements are evident from this process: (1) pile evaluation is carried out in both the design and construction stages, and (2) these evaluations should result in foundation elements of the same reliability, but a potentially different number and length of elements depending on the information available in each stage (Paikowsky et al. 2004).

Based upon the results of a survey conducted by AbdelSalam et al. (2010) regarding the current pile foundation design and construction practices encountered nationwide, it was determined that a majority of the State Departments of Transportation (DOTs) adhere to a slightly different process than that depicted in Figure 1.1. Essentially, the main difference between the typical pile foundation design and construction process and that currently employed by various State DOTs is realized in the construction stage. Whereas the typical process of Figure 1.1 relies on SLTs and various dynamic analysis methods for the design verification and construction control of driven pile foundations, the Iowa DOT, for example, relies either on the results of WEAP analyses or the driving of piling to refusal or end-bearing on bedrock, which is an uneconomical practice (AbdelSalam et al. 2010). Moreover, in regards to the design stage, most of the geotechnical engineers in the State of Iowa rely solely on the results of SPTs and/or CPTs for the determination of site specific soil parameters; in other words, sophisticated laboratory soil tests are not typically conducted for the determination of soil strength and deformation properties. It is important to point out that

the practices of the Iowa DOT have been singled out here because of the fact that the data acquired for the analyses presented in this thesis was obtained from bridge foundation projects performed within this state.

Seeing as the aforementioned discussion pertained to pile foundation design and construction practices encountered at the state level, it seems appropriate to address any differences in practice that may be encountered at the county level. Again, focusing on the practices carried out within the boundaries of the State of Iowa, the key difference is manifested in the construction stage. Whereas the results of WEAP analyses are entrusted for the design verification and construction control of driven pile foundations at the state level, the predictions of dynamic pile driving formulas are used at the county level. Even though it is well recognized that dynamic pile driving formulas, such as the Engineering News Record (ENR) formula, are too simplistic in nature to model accurately all complexities associated with the relationship between pile bearing, hammer performance, and pile penetration resistance (Allen 2007), their ability to provide a simple and quick assessment of pile bearing capacity is an extremely desirable characteristic for many county engineering offices located within the State of Iowa. Thus, it is the intent of this thesis to focus solely on the construction control of driven pile foundations in the State of Iowa via a suitable dynamic pile driving formula, where the term suitable refers to a dynamic pile driving formula in which inaccuracies have been notably reduced without forfeiture of the formula's inherent ease of use.

1.4 Background to Design Methodologies

Regardless of the pile capacity estimation method selected for use in the design or construction stage of driven pile foundations, multiple design methodologies exist for the evaluation of such predicted pile capacities. More specifically, the Working Stress Design (WSD) and Load and Resistance Factor Design (LRFD) approaches delineate the most commonly employed design methodologies. Information concerning the use of both approaches for geotechnical design has been provided in the following subsections.

1.4.1 WSD

For over 100 years, the WSD approach, also referred to as the Allowable Stress Design (ASD) approach, has been the traditional basis for geotechnical design relating to settlements or failure conditions (Fenton and Griffiths 2008). Under this approach, the design loads, which consist of the actual forces estimated to be applied to the substructure (or a particular element of the substructure), are compared to the capacity of the substructure, or the resistance, by means of a factor of safety (FS). As recommended in the 1997 version of the *Standard Specifications for Highway Bridges* (AASHTO 1997), the selection of such an appropriate FS is made based upon the desired level of control to be had in the design and/or construction stages of driven pile foundations. However, seeing as such code requirements are merely intended to guide the designer, selection of an appropriate FS is ultimately made based upon the experience and subjective judgment of the design engineer(s) (Paikowsky et al. 2004). Nonetheless, such factors of safety fail to consider the different degrees of uncertainty associated with the applied loads and predicted pile foundation capacities. Hence, standard bridge design specifications based on the WSD approach cannot be expected to ensure the consistent and reliable performance of structures.

1.4.2 LRFD

The LRFD approach has now been in use for the design of superstructures for about fifty years (Goble 2005) and has been progressively developed with the objective of ensuring the uniform reliability of structures since about the mid-1980s. Even though the LRFD approach, as it applies to the design of structural elements, has been well established and implemented in design codes around the world, its adoption into geotechnical design has been relatively slow (DiMaggio et al. 1999). Unlike the WSD approach, which manages all uncertainties associated with the applied load and predicted pile foundation capacity via a lone, arbitrarily defined FS, the LRFD approach separates the uncertainties in these design components and rationally quantifies them using probability-based methods aimed at achieving engineered designs with consistent levels of reliability. Consequently, in the LRFD approach, the characteristic load effect values are increased through multiplication with a load factor, while the nominal pile penetration resistance values are decreased through multiplication with a resistance factor. The advantages associated with the use of the LRFD

approach over the more tradition WSD approach in the evaluation of predicted pile capacities can be summarized as follows:

- The uncertainties associated with the design parameters, i.e., load effect and pile penetration resistance, are handled in a rational framework of probability theory.
- The reliability, or risk, is quantified through a consistent measure, resulting in the assurance of a uniform level of safety.
- The levels of safety in both the superstructure and substructure are provided with more consistency given the fact that both are designed using the same loads for predicted or target probabilities of failure.

In response to these documented advantages, the Federal Highway Administration (FHWA) issued a policy memorandum on June 28, 2000, requiring all new bridges initiated after October 1, 2007, to be designed according to the LRFD approach. As alluded to previously, this approach for designing foundation elements has substantially more challenges associated with it than, for example, the design of superstructure elements following the same design approach. These challenges develop mainly from the inherently high variability of soil properties across, as well as within, regions and the ability to predict the realistic pile capacity and driving stresses. Since the foundation is a critical element of the bridge system, conservative LRFD resistance factors have been recommended for their design (AASHTO 2007) to ensure safe foundation design practices. In this process, soil variability expected at the national level was given consideration, contributing to the conservativeness of the recommended LRFD resistance factors. However, for economical reasons, an unnecessarily conservative design method should not be adopted since foundation systems typically account for as much as thirty percent of the total bridge cost. Consequently, regionally calibrated LRFD resistance factors have been permitted by the American Association of State Highway and Transportation Officials (AASHTO) in order to improve the economy of the bridge foundation elements.

1.5 SCOPE OF RESEARCH

As indicated in Section 1.4, the FHWA has mandated the use of the LRFD approach on the design and construction of all new bridges initiated after October 1, 2007. Seeing as current LRFD pile design and construction control specifications have not been written for direct application in the State of Iowa and those recommended in the most recent edition of the *AASHTO LRFD Bridge Design Specifications* (AASHTO 2007) are conservative in nature, the main goal of this research project is to develop regionally calibrated LRFD resistance factors, as permitted by AASHTO, for the design and construction control of Iowa driven pile foundations. Although it is the intent of this thesis to focus solely on the LRFD calibration procedures related to the construction control of driven pile foundations in the State of Iowa via a suitable dynamic pile driving formula, additional information concerning the regional calibration of LRFD resistance factors for the design of driven pile foundations via various static analysis methods as well as their construction control via alternative dynamic analysis methods (e.g., WEAP, PDA, and CAPWAP) can be found in the PhD dissertations of AbdelSalam (2010) and Ng (2011), respectively. More specifically, this thesis will focus on addressing the following objectives to achieve the proposed goal:

- Identify the most common dynamic pile driving formulas utilized in the United States and in different counties throughout the State of Iowa for the construction control of driven pile foundations and their documented reliability via a comprehensive literature review.
- Assist in the conduction of a national survey of State DOTs as well as a local survey of Iowa county engineers to acquire information related to current pile design and construction practices.
- Develop an electronic pile load test database, consisting of both static and dynamic data collected from pile load tests performed in the State of Iowa, for use in the establishment of regionally calibrated LRFD resistance factors for the design and construction control of driven pile foundations.
- Participate in the collection of information from nine full-scale field load tests performed on steel H-piles installed in different soil profiles throughout the State of Iowa for verification of the regionally calibrated LRFD resistance factors. In addition

to being statically load tested to failure, the proposed test piles will be instrumented with strain gauges and dynamically monitored during driving and restrikes. Additionally, the subsurface conditions at the locations of the test piles will be characterized by the application of laboratory (e.g., moisture content, grain-size distribution, Atterberg limits, consolidation, and Triaxial Consolidated-Undrained (TX-CU) compression tests) and in-situ (e.g., standard penetration test (SPT), cone penetration test (CPT), and borehole shear test (BST)) tests, with ground instrumentation used to continuously capture horizontal and porewater pressure data.

- Establish regionally calibrated LRFD resistance factors for the construction control of driven pile foundations via a selected number of dynamic pile driving formulas.
- Establish enhanced LRFD resistance factors, which account for field capacity verification by means of dynamic pile driving formulas, for the design of driven pile foundations via static analysis methods.
- Recommend, based upon the results of efficiency comparisons, a single dynamic pile driving formula together with an appropriate LRFD resistance factor for use in the construction control of Iowa driven pile foundations.
- Investigate the potential of a one-dimensional pile-soil model to estimate the permanent pile displacement experienced by an embedded pile subjected to a single hammer blow; ultimately enabling for the use of dynamic pile driving formulas in design.

1.6 THESIS OUTLINE

This thesis consists of seven chapters detailing the establishment of regionally calibrated LRFD resistance factors for the construction control of Iowa driven pile foundations via seven distinct dynamic pile driving formulas. In addition, a theoretical design model is proposed for the estimation of axial pile capacity by the application of dynamic pile driving formulas. A summary of the content of each chapter is presented below.

- ***Chapter 1 – Introduction***: This chapter provides a brief introduction into the available methods for pile bearing capacity estimation, including dynamic pile

driving formulas, and their situation in the overall pile foundation design and construction process. Additionally, background information related to the WSD and LRFD approaches for the evaluation of predicted pile capacities is presented.

- ***Chapter 2 – Literature Review***: This chapter provides a comprehensive review concerning the history, development, assumptions, and improvements for several dynamic pile driving formulas used for the construction control of driven pile foundations. A review of published studies documenting the evaluated reliability of such dynamic pile driving formulas is also presented. This chapter concludes with a review of published studies focused on the calibration of LRFD resistance factors for the construction control of driven pile foundations.
- ***Chapter 3 – State of the Practice and PILOT-IA Development***: This chapter presents the major findings associated with the use of dynamic pile driving formulas for the construction control of driven piles from a national survey of state DOTs as well as a local survey of Iowa county engineers, both of which were conducted for delineation of the current state of practice. Additionally, this chapter provides a detailed description of the database for PIle LOad Tests in Iowa (PILOT-IA), which was specifically developed for use in the establishment of regionally calibrated LRFD resistance factors for the design and construction control of driven pile foundations.
- ***Chapter 4 – Summary of Field Testing of Steel H-Piles***: This chapter provides a brief description of the steel H-pile testing program implemented at nine distinct locations within the State of Iowa. In addition, a summary of the results obtained from static and dynamic pile load tests as well as in-situ and laboratory soil tests is presented for each test site.
- ***Chapter 5 – Calibration of LRFD Resistance Factors***: This chapter presents the methodology and framework utilized for the calibration of LRFD resistance factors for the construction control of driven pile foundations via seven dynamic pile driving formulas. In addition to presenting the pertinent calibration results, this chapter provides enhanced LRFD resistance factors, which account for field capacity verification by means of dynamic pile driving formulas, for the design of driven pile foundations via static analysis methods.

- ***Chapter 6 – A Theoretical Dynamic Model for Pile Capacity Estimation***: This chapter presents the details of a one-dimensional finite element model created in SAP2000 for the estimation of the permanent pile displacement experienced at different stages of driving. With the success of the model dependent on the accurate quantification of the dynamic properties of soil, a displacement-based signal matching technique used for the estimation of these dynamic soil properties as well as their variation with changes in soil type and depth is proposed and verified.
- ***Chapter 7 – Summary, Conclusions, and Recommendations***: This chapter presents a summary of the regionally calibrated LRFD resistance factors developed for the construction control of driven pile foundations via dynamic pile driving formulas and conclusions drawn from the study reported in this thesis. In addition to recommending a suitable dynamic pile driving formula for the construction control of driven pile foundations in the State of Iowa, this chapter summarizes the proposed theoretical design model for pile capacity estimation by means of dynamic pile driving formulas. Furthermore, this chapter provides suggestions concerning the potential for future research.

CHAPTER 2: LITERATURE REVIEW

2.1 INTRODUCTION

Dynamic pile driving formulas have been available for the prediction of the static bearing capacity of pile foundations for well over 180 years (Fragaszy, Higgins, and Lawton 1985). As a consequence of the immense effort and ingenuity put forth by engineers in their development, a multitude of different formulas have been amassed. In fact, Smith (1962) reported that in the early 1960s the editors of *Engineering News Record* had 450 such formulas on file. Accordingly, this chapter presents a comprehensive review detailing the development, assumptions, and improvements for several of the most common dynamic pile driving formulas used for the construction control of driven pile foundations. Additionally, a review of published studies documenting the evaluated reliability of such dynamic pile driving formulas is presented. Given the focus of this thesis, this chapter also provides a review of published studies focused on the calibration of LRFD resistance factors for the construction control of driven pile foundations.

2.2 DEVELOPMENT OF A GENERAL DYNAMIC PILE DRIVING FORMULA

Even though a multitude of different dynamic pile driving formulas are in existence, all such formulas are based on the assumption that the ultimate capacity of the pile under static loading can be directly related to the driving resistance of the pile during its last stages of embedment (Fragaszy, Higgins, and Lawton 1985). With this in mind, it can also be shown that while a small percentage of the available dynamic pile driving formulas are empirical in nature, the majority are based on Newton's law of impact and conservation of energy principles. In the crudest of fashions, the hammer energy is equated to the work done on the soil by the following equation:

$$W_R \cdot h = R \cdot s \tag{2.1}$$

where: W_R = weight of the pile driving ram,

h = drop height (stroke) of the ram,

R = resistance to pile penetration, and

s = pile penetration distance under one hammer blow, i.e., pile set.

As was acknowledged by Cummings (1940), these definitions of *R* and *s* contain certain implied assumptions as to the nature of their quantities. To begin with, the definition of *s* does not explicitly state whether the permanent pile penetration or the maximum pile penetration is to be used. The maximum pile penetration, which includes the temporary elastic compression of the pile and the soil, can only be measured with the aid of special instrumentation. Thus, the permanent pile penetration, which is significantly easier to obtain, is almost always the chosen form of pile penetration measured and recorded on a pile driving project. Furthermore, the definition of *R* suggests that *R* is assumed to be constant throughout the full depth of penetration, representing an average value of a variable resistance to penetration.

To further elaborate on the issues of pile penetration and resistance to pile penetration, Cummings (1940) suggested the three diagrams reproduced in Figure 2.1. For starters, Figure 2.1a was intended to be a graphic representation of Eq. (2.1), where the pile penetration is assumed to be an exact quantity defined by the distance from the origin, *O*, to a point, *s*, on the penetration axis and the resistance is assumed to be uniform over the full depth of the pile penetration. In other words, the work done in moving the pile a distance *s* against a resistance *R*, represented by the shaded area of Figure 2.1a, is equivalent to the available work in the hammer at the bottom of its stroke assuming there were no losses in energy ($W_R \cdot h$).

Conversely, in actual pile driving, the resistance versus penetration diagram would not resemble that of Figure 2.1a on account of the presence of some temporary elastic compression of the pile and surrounding soil. Although very little information is available on the concept of resistance to pile penetration, Cummings (1940) suggests that the probability in favor of a variable resistance is much greater than that in favor of a constant resistance. In addition to showing the temporary elastic compression of the pile and the surrounding soil, Figure 2.1b and Figure 2.1c offer two possibilities of variable resistance to pile penetration. In an effort to show how actual pile driving differs from the assumptions on which Eq. (2.1) and Figure 2.1a are based, the shaded area of Figure 2.1a has been superimposed on both Figure 2.1b and Figure 2.1c.

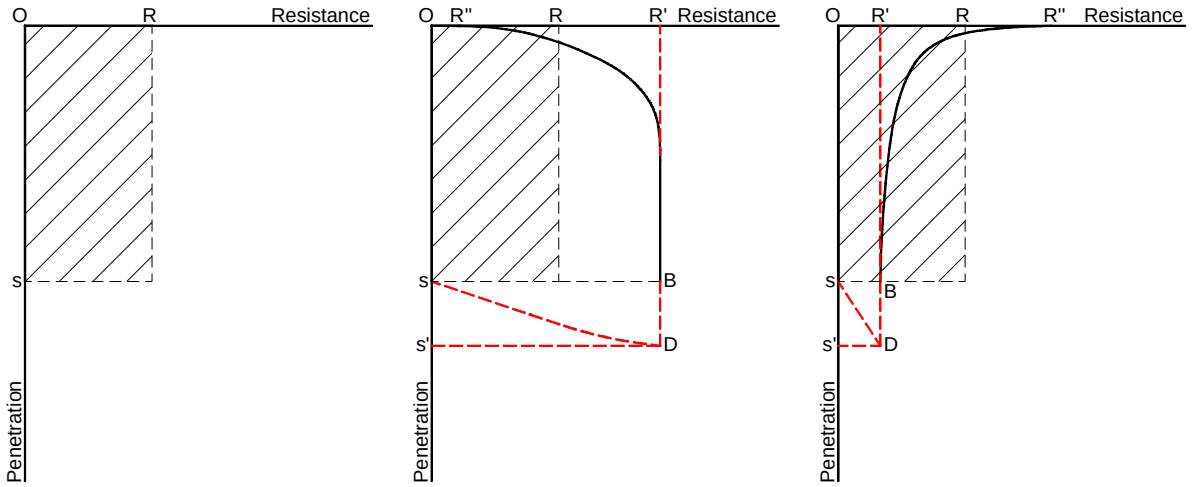

(a) Constant Resistance **(b) Variable Resistance (Sand)** **(c) Variable Resistance (Clay)**

Figure 2.1: Relationship between Resistance and Penetration under a Single Hammer Blow (After: Cummings 1940)

Commencing with the problem of resistance to pile penetration, Figure 2.1b assumes that the initial resistance, R'', is very small and that with an increasing depth of pile penetration this resistance increases to an asymptotic value of R'; a phenomenon characteristic of a pile driven into a sand soil where the resistance to pile penetration increases as the moving pile compacts the sand. On the other hand, Figure 2.1c assumes a high initial resistance, R'', which decreases with an increasing depth of pile penetration to an asymptotic value of R'; a phenomenon characteristic of a pile driven into a clay soil where the high initial resistance to pile penetration would be explained by the circumstance of soil "set-up" experienced by such soils during a temporary interruption in driving. In either case, the resistance at the end of pile penetration, R', is not the same as the uniform resistance to pile penetration, R, assumed in Figure 2.1a. However, Cummings (1940) proposed that the aforementioned quantities are related by the following equation:

$$R' = C \cdot R \tag{2.2}$$

where: C = proportionality coefficient that assumes values greater or less than one depending on whether the resistance versus penetration diagram more closely resembles that of Figure 2.1c or Figure 2.1b respectively.

Advancing on to the question of pile penetration, Figure 2.1b and Figure 2.1c depict the permanent pile penetration, *s*, and the maximum pile penetration, *s′*. The distance defined by *s*-*s′* on the penetration axis represents the temporary elastic compression of the pile that occurs during impact. As is to be expected, this temporary elastic pile compression produces an energy loss that can be quantified by the triangular area *s*-*B*-*D* evidenced in both diagrams.

Taking into account the aforementioned items, Eq. (2.1) can be modified to more closely represent the actual dynamics of pile driving. The revised equation, as suggested by Cummings (1940) is as follows:

$$W_R \cdot h = C \cdot R \cdot s + Q \tag{2.3}$$

where: Q = all energy losses that occur during impact.

In spite of the fact that work diagrams such as those provided in Figure 2.1 and the field measurements required to produce such diagrams represent the most rational approach to the dynamics of pile driving as stated by Cummings (1940), relatively few engineers have used such methods to develop dynamic pile driving formulas. Other than the ENR formula, which was derived by A. M. Wellington in 1888 on the basis of his experience and a work diagram similar to that found in Figure 2.1c, practically all of the other dynamic pile driving formulas that are to be found in literature have been derived by means of mathematics and theoretical mechanics. In such cases, Eq. (2.1) is used as a starting point and the ensuing dynamic pile driving formula is derived based upon assumptions concerning the energy losses that occur during impact. Consequently, the great number of dynamic pile driving formulas that can be found in literature is an indication of the wide variety of assumptions that have been made concerning such energy losses.

2.3 EXAMINATION OF COMMON DYNAMIC PILE DRIVING FORMULAS

As was indicated in the previous section, the vast majority of dynamic pile driving formulas found in literature were derived from Eq. (2.1) by means of varying assumptions concerning the energy losses that occur during the impact from a single hammer blow upon

the head of an embedded pile. The three most common types of energy loss deductions, as suggested by Cummings (1940), are as follows:

a) the energy losses associated with only the temporary elastic compressions of the cap, pile, and/or soil;
b) the energy loss associated with only the Newtonian theory of impact, as described by the coefficient of restitution; and
c) the energy losses associated with both the temporary elastic compressions of the cap, pile, and/or soil as well as the Newtonian theory of impact.

In the following subsections, numerous dynamic pile driving formulas will be summarized according to which one of the three main assumptions concerning energy loss deductions was made in their respective derivations. Afterward, several empirically based formulas will be presented for completeness. However, an examination of dynamic pile driving formulas possessing the exact form of Eq. (2.1) must first be taken.

2.3.1 Dynamic Formulas Excluding Energy Losses

As discussed previously, Eq. (2.1) was derived based upon the fact that no energy losses associated with the temporary elastic compressions of the cap, pile, and/or soil as well as the Newtonian theory of impact occurred during the impact from a single hammer blow, with an assumed mechanical efficiency of 100 percent, upon the head of an embedded pile. With this in mind, Major John Sanders and Merriman each published dynamic pile driving formulas taking the exact form of Eq. (2.1), but with the application of dissimilar factors of safety. More precisely, the Sanders formula, proposed in 1851, was obtained by applying a purported factor of safety of 8 to Eq. (2.1), while Merriman only applied a purported factor of safety 6 (Chellis 1961). However, Beardsley (1907) noted that Sanders' purported factor of safety of 8 was established from experiments conducted in the river mud of the Delaware River and that a factor of safety of about ten would appear to be more appropriate. Nonetheless, Eqs. (2.4) and (2.5) present the exact forms of the Sanders and Merriman dynamic pile driving formulas respectively.

$$R_a = \frac{W_R \cdot h}{8 \cdot s} \qquad \textit{Sanders Formula} \qquad (2.4)$$

$$R_a = \frac{W_R \cdot h}{6 \cdot s} \qquad \textit{Merriman Formula} \qquad (2.5)$$

where: R_a = allowable resistance to pile penetration.

Additionally, the Goodrich dynamic pile driving formula, which is a simplification of a more comprehensive formula containing 25 terms covering conditions of the pile, hammer, cap, and ground, adheres to the same direct relation presented in Eq. (2.1). Seeing as the more comprehensive formula was too complicated and unwieldy for practical use, Ernest P. Goodman evaluated a number of terms with the aid of experiments conducted under proper conditions for pile driving in good practice. By substituting the values thus obtained, and inserting suitable numerical values for the dimensions and weights of the pile and hammer, the expression presented in Eq. (2.6) was derived circa 1902 (Jacoby and Davis 1914). As a consequence of these simplifying procedures, Goodrich's formula was only intended for use with timber piles and gravity hammers exhibiting a set of approximately one inch and a stroke of about fifteen feet, respectively (Jacoby and Davis 1914). Although, under these conditions Goodrich believed that his formula was capable of predicting the ultimate pile bearing capacity to within a ten percent error of that predicted by the more comprehensive formula (Jacoby and Davis 1914).

$$R_u = \frac{10 \cdot W_R \cdot h}{3 \cdot s} \qquad \textit{Goodrich Formula} \qquad (2.6)$$

where: R_u = ultimate resistance to pile penetration.

Having now introduced the three most basic dynamic pile driving formulas available, a more complete dissection of the remaining multitude of formulas can be given in light of the assumptions made in their respective derivations concerning energy loss deductions. To begin with, the following subsection will examine those dynamic pile driving formulas derived from Eq. (2.1) by assuming that the only energy losses that occur during the impact of a single hammer blow upon the head of an embedded pile are those associated with the temporary elastic compressions of the cap, pile, and/or soil.

2.3.2 Dynamic Formulas Incorporating Only Energy Losses from Temporary Elastic Compressions

As has been stated, some dynamic pile driving formulas are based upon the assumption that the elastic compressions of the cap, pile, and/or soil are the only energy losses that must be considered. Inserting the formula for the strain energy of a compressed strut, as obtained from static theory, into Eq. (2.1) yields the following equation:

$$W_R \cdot h = R \cdot s + \frac{R^2 \cdot L}{2 \cdot A \cdot E} \tag{2.7}$$

where: L = length of the pile,

A = cross-sectional area of the pile, and

E = Young's modulus for the pile material.

In other words, Eq. (2.7) states that some of the hammer energy is used up by the temporary elastic compression of the pile, ignoring the temporary elastic compressions of the cap and soil, and that the remainder of the energy is available to drive the pile a distance, *s*, against a resistance, *R*. It is from this equation that the Weisbach dynamic pile driving formula was developed circa 1850 (Jumikis 1971).

The Weisbach formula presented in Eq. (2.8) was obtained by directly solving Eq. (2.7) for *R*.

$$R_u = -\frac{s \cdot A \cdot E}{L} + \sqrt{\frac{2 \cdot W_R \cdot h \cdot A \cdot E}{L} + \left(\frac{s \cdot A \cdot E}{L}\right)^2} \qquad \textit{Weisbach Formula} \tag{2.8}$$

However, as expressed by Cummings (1940), the last term of Eq. (2.7) is open to serious criticism on at least two counts. First, the expression is taken from static theory and it is well known that the elastic compression under impact is something entirely different from the elastic compression due to a static force. Second, the expression is derived on the assumption that all of the resistance, *R*, is applied at the point of the pile. Thus, when part of the resistance is applied along the sides of the pile, the expression shown in Eq. (2.8) becomes invalid.

In order to take into account the fact that part of the resistance might be developed along the sides of the pile, Rankine proposed the use of half the actual pile length for the effective length, *L*, in Eq. (2.7) (Cummings 1940). In other words, assuming that the distance from the pile toe to the center of resistance can be expressed as *L*/2 for a fully embedded friction pile, the Rankine formula, which is presented in Eq. (2.9), was derived from Eq. (2.7) by substituting in *L*/2 for *L* and solving the resulting expression for *R*.

$$R_u = \frac{2 \cdot A \cdot E \cdot s}{L} \cdot \left(\sqrt{1 + \frac{W_R \cdot h \cdot L}{s^2 \cdot E \cdot A}} - 1 \right) \qquad \textit{Rankine Formula} \qquad (2.9)$$

In contrast to the aforementioned Weisbach and Rankine formulas, the ENR formula, which was first published in 1888 by A. M. Wellington, accounts not only for energy losses resulting from the temporary elastic compression of the pile, but also energy losses resulting from the temporary elastic compressions of the pile cap and soil by means of a constant term of value 1.0 inches per blow. Wellington derived this dynamic pile driving formula by equating the applied energy (i.e., the driving energy) to the energy obtained by graphically integrating the area under typical load-settlement curves for timber piles driven by gravity hammers (Chellis 1961). The original form of the ENR formula has been provided in Eq. (2.10), with the recommended application of a factor of safety of six as suggested by Wellington.

$$R_u = \frac{W_R \cdot h}{s + 1.0} \qquad \textit{ENR Formula: Gravity Hammers} \qquad (2.10)$$

where: s = pile penetration distance under one hammer blow, i.e., pile set, expressed in inches per blow.

Noting that the original ENR formula of Eq. (2.10) was developed at a time when all piles were made of timber and were driven with gravity hammers, modifications were proposed by Wellington when the single-acting steam hammer was introduced and again when the double-acting steam hammer was introduced. These modifications were also empirical in nature and were meant to compensate for the lubricant action of the soil that occurred as a result of the more rapid strokes of the new hammers (Argo 1987). These two

modified forms of the ENR formula, which were again developed for use with timber piles driven by either single-acting or double-acting steam hammers, are provided in Eqs. (2.11) and (2.12), respectively, with the retained recommendation for the application of a factor of safety of six in both instances.

$$R_u = \frac{W_R \cdot h}{s + 0.1} \qquad \textit{ENR Formula: Single-Acting Steam Hammers} \qquad (2.11)$$

$$R_u = \frac{E_h}{s + 0.1} \qquad \textit{ENR Formula: Double-Acting Steam Hammers} \qquad (2.12)$$

where: E_h = rated hammer energy per blow, and

s = pile penetration distance under one hammer blow, i.e., pile set, expressed in inches per blow.

When Eqs. (2.11) and (2.12) are expressed in terms of the blow count (n), i.e., the number of hammer blows inflicted upon the head of a pile per foot of pile penetration, as opposed to the pile set (s), Eqs. (2.13) and (2.14) are obtained. As acknowledged by Chellis (1961), these equations are more commonly referred to as the Vulcan Iron Works pile driving formulas and they call for the same recommended application of a factor of safety of six.

$$R_u = \frac{120 \cdot N}{120 + N} \cdot (W_R \cdot h) \qquad \textit{Vulcan Iron Works Formula: Single-Acting Steam Hammers} \qquad (2.13)$$

$$R_u = \frac{120 \cdot N}{120 + N} \cdot E_h \qquad \textit{Vulcan Iron Works Formula: Double-Acting Steam Hammers} \qquad (2.14)$$

where: N = number of hammer blows per foot of pile penetration, i.e., blow count.

Although Wellington's ENR formula has been probably the most widely used dynamic pile driving formula in use for the construction control of driven pile foundations in the United States (Fragaszy, Higgins, and Lawton 1985), a couple of modifications have been suggested over the years in an attempt to improve upon the original formula's pile bearing capacity prediction capabilities, while still maintaining its desirable qualities of simplicity and ease of use. As reported by Chellis (1961), the United States Steel Company modified

the ENR formula by varying the constant in the numerator as observed in Eqs. (2.15), (2.16), and (2.17).

$$R_a = \frac{F \cdot W_R \cdot h}{s + 1.0} \qquad \textit{United States Steel Formula: Gravity Hammers} \qquad (2.15)$$

$$R_a = \frac{F \cdot W_R \cdot h}{s + 0.1} \qquad \textit{United States Steel Formula: Single-Acting Steam Hammers} \qquad (2.16)$$

$$R_a = \frac{F \cdot h \cdot \left(W_R + A_p \cdot p\right)}{s + 0.1} \qquad \textit{United States Steel Formula: Double-Acting Steam Hammers} \qquad (2.17)$$

where: F = 2 for piles driven to refusal or practical refusal in all materials,

F = 6 for piles driven easily in sands and/or gravels,

F = 4 for piles driven easily in hard or sandy clays,

F = 3 for piles driven easily in mixed mediums consisting of clays and sands or sands and silts,

F = 2 for piles driven easily in alluvial deposits, soft clays, and silts,

A_p = effective area of piston,

p = mean effective pressure of steam or air, and

s = pile penetration distance under one hammer blow, i.e., pile set, expressed in inches per blow.

Furthermore, the Bureau of Yards and Docks modified the ENR formula by changing the constant term in the denominator, which accounts for all energy losses experienced as a result of temporary elastic compressions in the cap, pile, and soil, from 1.0 inches per blow to 0.3 inches per blow as shown in Eq. (2.18) (Chellis 1961). Still, the application of a factor of safety of six is recommended for this formula.

$$R_u = \frac{W_R \cdot h}{s + 0.3} \qquad \textit{Bureau of Yards and Docks Formula} \qquad (2.18)$$

Finally, by returning to the assumption made in the derivation of the Weisbach and Rankine formulas, namely that the energy loss associated with only the temporary elastic compression of the pile is of significance, the foundation for Sörensen and Hansen's Danish

dynamic pile driving formula, which is sometimes referred to as the S_O formula, is established. Based upon a study done using dimensional and statistical analyses, this formula was ultimately obtained by simplifying some of the more complicated dynamic pile driving formulas presented later in Section 2.3.4 of this report (Fragaszy, Higgins, and Lawton 1985). For as Sörensen and Hansen (1957) so eloquently stated in their report:

> "Due to the fact that all the practical formulae are fundamentally wrong on several points, it cannot be assumed or even expected that the best formula is the one that considers the greatest numbers of energy losses or appears to be the most comprehensive. The only criterion by which any sound judgment can be made is the statistical analysis of the agreement between formula and load tests, and if simplicity can be combined with accuracy, so much the better."

Proposed in the year 1957, the Danish formula, which is presented in Eq. (2.19), contains a term (S_O) for the elastic compression of the pile, should all of the available hammer energy be used solely for this pile compression, i.e., all other potential types of energy loss deductions are disregarded (Agerschou 1962). Accordingly, it is recommended that a factor of safety within the range of three to six be applied to the value for the ultimate resistance to pile penetration produced by the Danish formula (Fragaszy, Higgins, and Lawton 1985).

$$R_u = \frac{W_R \cdot h}{s + \frac{1}{2} \cdot S_O} \qquad \textit{Danish/}S_O\textit{ Formula} \qquad (2.19)$$

where: $S_O = \sqrt{\frac{2 \cdot W_R \cdot h \cdot L}{A \cdot E}}$. (2.20)

In summary, the numerous dynamic pile driving formulas presented in this subsection were all derived under the assumption that the energy losses associated with only the temporary elastic compressions of the driving cap, pile, and soil are of significance. However, as indicated by Cummings (1940), it should not be expected that such temporary elastic compressions can be calculated with any reasonable degree of accuracy by means of expressions taken from static theory without modification for use in a problem of dynamic nature. In fact, it is only through accurate field measurements of the behavior of the pile during driving that quantities for such temporary elastic compressions can be confidently

attained. Thus, in the eyes of Cummings (1940), all of the dynamic pile driving formulas presented in this subsection are not appropriate.

2.3.3 Dynamic Formulas Incorporating Only Energy Losses from Newtonian Impact Theory

As evidenced from the preceding subsection, numerous dynamic pile driving formulas have been proposed under the assumption that the elastic compressions of the cap, pile, and/or soil are the only energy losses that must be considered. Nonetheless, just as many dynamic pile driving formulas have been proposed under the assumption that the energy losses associated with only the Newtonian theory of impact are of significance. The Newtonian theory of impact involves a coefficient of restitution that is used to indicate how much of the original kinetic energy remains after the impact of two objects. For the type of collision known as direct central impact, which assumes the line of impact passes through the centers of gravity of the colliding bodies and coincides with the direction of the motion, the Newtonian theory gives the following equation for the amount of lost energy (Fuller and Johnston 1915):

$$E_1 - E_2 = \left(\frac{1}{2}\right) \cdot (1 - e^2) \left(\frac{M_1 \cdot M_2}{M_1 + M_2}\right) \cdot (v_2 - v_1)^2 \tag{2.21}$$

where: E_1 = total kinetic energy of the two bodies in the system before impact,

E_2 = total kinetic energy of the two bodies in the system after impact,

M_1 = mass of the first colliding body in the system,

M_2 = mass of the second colliding body in the system,

v_1 = velocity of the first colliding body prior to impact,

v_2 = velocity of the second colliding body prior to impact, and

e = Newton's coefficient of restitution; Table 2.1 presents representative values of this variable.

Table 2.1: Representative Values of the Coefficient of Restitution for use in Dynamic Pile Driving Formulas (ASCE 1941)

Material	***e***
Broomed Wood	0
Wood Piles (Nondeteriorated End)	0.25
Compact Wood Cushion on Steel Pile	0.32
Compact Wood Cushion over Steel Pile	0.40
Steel-on-Steel Anvil on Either Steel or Concrete Pile	0.50
Cast-Iron Hammer on Concrete Pile without Cap	0.40

If the variables M_1 and v_1 of Eq. (2.21) refer to the pile driving hammer, then:

$$M_1 = \frac{W_R}{g} \tag{2.22}$$

$$v_1 = \sqrt{2 \cdot g \cdot h} \tag{2.23}$$

where: $g =$ the acceleration of gravity.

Likewise, if the variables M_2 and v_2 of Eq. (2.21) refer to the pile element, then:

$$M_2 = \frac{W_p}{g} \tag{2.24}$$

$$v_2 = 0 \tag{2.25}$$

where: $W_p =$ weight of the pile, driving cap, follower, and mandrel as driven.

Thus, when the values for M_1, M_2, v_1, and v_2, as expressed in Eqs. (2.22), (2.23), (2.24), and (2.25), are substituted into Eq. (2.21), an equation for the amount of lost energy, as obtained from only the Newtonian theory of impact, that occurs during the impact from a single hammer blow upon the head of an embedded pile is attained, i.e., Eq. (2.26).

$$E_1 - E_2 = (W_R \cdot h) \cdot \frac{W_p \cdot (1 - e^2)}{W_R + W_p} \tag{2.26}$$

When the energy loss defined by Eq. (2.26) is added to the right-hand side of Eq. (2.1) and simplified, the expression provided in Eq. (2.27) is obtained.

$$R \cdot s = (W_R \cdot h) \cdot \frac{W_R + e^2 \cdot W_p}{W_R + W_p} \tag{2.27}$$

In fact, Eq. (2.27) has been used as the basis for several well-known dynamic pile driving formulas. To begin with, Eytelwein's dynamic pile driving formula, which has been provided in its original form in Eq. (2.28) (Chellis 1961), is obtained by solving Eq. (2.27) for R and assuming a perfectly inelastic impact between the pile driving hammer and embedded pile, i.e., $e = 0$. This formula, which was proposed in 1820, was developed during a time in which steel and concrete piles were being used more frequently in place of timber piles, resulting in heavier piles and contemporaneously higher driving energies (Fragaszy, Higgins, and Lawton 1985); thus, providing evidence for the notion that energy losses associated with the Newtonian theory of impact were of great significance. Since Eytelwein's original dynamic pile driving formula, i.e., Eq. (2.28), was only intended for use with gravity hammers, modifications were proposed by Eytelwein to allow for its use with the increasingly popular single-acting and double-acting steam hammers. These modified forms of the Eytelwein formula have been presented in Eqs. (2.29) and (2.30) (Chellis 1961). Furthermore, it is important to note that statistical studies suggest that all three forms of the Eytelwein dynamic pile driving formula should be used with a factor of safety of six (Chellis 1961).

$$R_u = \frac{W_R \cdot h}{s \cdot \left(1 + \frac{W_p}{W_R}\right)} \qquad \textit{Eytelwein Formula: Gravity Hammers} \tag{2.28}$$

$$R_u = \frac{W_R \cdot h}{s + 0.1 \cdot \left(\frac{W_p}{W_R}\right)} \qquad \textit{Eytelwein Formula: Single-Acting Steam Hammers} \tag{2.29}$$

$$R_u = \frac{h \cdot \left(W_R + A_p \cdot p\right)}{s + 0.1 \cdot \left(\frac{W_p}{W_R}\right)} \qquad \textit{Eytelwein Formula: Double-Acting Steam Hammers} \tag{2.30}$$

where: s = pile penetration distance under one hammer blow, i.e., pile set, expressed in inches per blow for Eqs. (2.29) and (2.30).

If the ratio between the weight of the pile and the weight of the pile driving hammer in the denominator of Eq. (2.28) is modified by a factor of $0.3 \cdot s$ instead of $1.0 \cdot s$, then the Navy-McKay formula of Eq. (2.31) is obtained (Chellis 1961). Although this dynamic pile driving formula is no longer used by the Navy, it is still recommended that a factor of safety of six be applied when used.

$$R_u = \frac{W_R \cdot h}{s \cdot \left(1 + 0.3 \cdot \frac{W_p}{W_R}\right)} \qquad \textit{Navy-McKay Formula} \quad (2.31)$$

On the other hand, if Eq. (2.28) is rewritten in such a way as to set the ultimate resistance to pile penetration equal to the product of two fractional terms, then the Dutch formula of Eq. (2.32) is obtained. With this formula, which is best known in the United Kingdom of Great Britain and Northern Ireland, it is customary to use a factor of safety of ten when driving with a gravity hammer and of six when driving with a steam hammer (Chellis 1961).

$$R_u = \frac{W_R \cdot h}{s} \cdot \left(\frac{W_R}{W_R + W_p}\right) \qquad \textit{Dutch Formula} \quad (2.32)$$

Furthermore, the Ritter formula of Eq. (2.33) is the same as the Dutch formula of Eq. (2.32), with the inclusion of additional terms to account for the weights of the pile driving hammer and pile (Chellis 1961). However, little more is known regarding the history and development of this dynamic pile driving formula.

$$R_u = \frac{W_R \cdot h}{s} \cdot \left(\frac{W_R}{W_R + W_p}\right) + W_R + W_p \qquad \textit{Ritter Formula} \quad (2.33)$$

Like the Ritter formula, few details exist in literature concerning the history and development of the Brix dynamic pile driving formula. However, what is known regarding this formula is that it was established by modifying the Dutch formula of Eq. (2.32) to account for the energy given to the pile during the impact from a single hammer blow (Faber et al. 1947). With the recommended application of a factor of safety of three or greater, the

Brix formula presented in Eq. (2.34) is intended for use with piles driven only by gravity hammers in sandy soils (Jumikis 1971).

$$R_u = \frac{W_R^2 \cdot W_p \cdot h}{\left(W_R + W_p\right)^2 \cdot s} \qquad \textit{Brix Formula} \quad (2.34)$$

In brief, the numerous dynamic pile driving formulas presented in this subsection were all derived under the assumption that pile driving is strictly a problem in Newtonian impact theory. However, as Cummings (1940) so expertly indicated, Newton himself excluded from his impact theory the case of "…bodies…which suffer some such extension as occurs under the strokes of a hammer." Moreover, Newton deduced his impact theory as a part of the proof of his third law of motion, which explained the behavior of two colliding bodies displaying unhindered motions apart from the actual collision. With this in mind, Cummings (1940) concluded that a dynamic pile driving formula cannot be based on simple Newtonian impact theory since the restraining effect of the earth surrounding the pile is sufficient enough to put the pile driving problem beyond its scope. Thus, according to Cummings (1940), the validity of the dynamic pile driving formulas presented in this subsection is questionable, to say the least.

2.3.4 Dynamic Formulas Incorporating Energy Losses from Both Temporary Elastic Compressions and Newtonian Impact Theory

Combining the assumptions made in the preceding two subsections concerning the energy losses that occur during the impact from a single hammer blow upon the head of an embedded pile yields this next class of dynamic pile driving formulas. In other words, the dynamic pile driving formulas presented in this subsection were derived under the assumption that the energy losses associated with both the temporary elastic compressions of the cap, pile, and/or soil as well as the Newtonian theory of impact are of significance. To begin this discussion, J. F. Redtenbacher, in the year 1859, put forward the expression revealed in Eq. (2.35), which has often been referred to as the "complete" dynamic pile driving formula on account of the fact that it incorporates deductions for all of the aforementioned sources of energy losses (Jumikis 1971).

$$W_R \cdot h = R \cdot s + \left[W_R \cdot h \cdot \left(\frac{W_p \cdot (1 - e^2)}{W_R + W_p}\right)\right] + \left\{\frac{R \cdot C_1}{2} + \frac{R \cdot C_2}{2} + \frac{R \cdot C_3}{2}\right\} \quad (2.35)$$

where: $C_1 = \frac{R \cdot L'}{A' \cdot E'}$ = temporary elastic compression of the driving cap, (2.36)

$C_2 = \frac{R \cdot L}{A \cdot E}$ = temporary elastic compression of the pile, (2.37)

C_3 = temporary elastic compression of the soil surrounding the pile,

L' = length of the driving cap,

A' = cross-sectional area of the driving cap, and

E' = Young's modulus for the driving cap material.

In fact, it is from this expression shown in Eq. (2.35) that Alfred Hiley derived his renowned dynamic pile driving formula. Used extensively in the United Kingdom of Great Britain and Northern Ireland as well as in Europe, the Hiley formula of Eq. (2.38) was developed in an attempt to eliminate some of the errors associated with the theoretical evaluation of energy absorption by a pile-soil system during driving (Olson and Flaate 1967).

$$R_u = \frac{e_h \cdot W_R \cdot h}{s + \frac{1}{2} \cdot (C_1 + C_2 + C_3)} \cdot \left(\frac{W_R + e^2 \cdot W_p}{W_R + W_p}\right) \quad \textit{Hiley Formula} \quad (2.38)$$

where: e_h = efficiency of striking hammer; Table 2.2 presents representative values of this variable for hammers in reasonably good operating condition.

Table 2.2: Representative Values of Hammer Efficiency for use in Dynamic Pile Driving Formulas (Bowles 1996)

Type	Hammer Efficiency, e_h
Drop Hammers	0.75-1.00
Single-Acting Steam Hammers	0.75-0.85
Double-Acting Steam Hammers	0.85
Diesel Hammers	0.85-1.00

Recognizing the complexity associated with determining the temporary elastic compressions of the cap and soil (i.e., C_1 and C_3), Hiley established recommended values for these variables as shown in Table 2.3 and Table 2.4, respectively. As a final point, the application

of a factor of safety of three is recommended for use with the Hiley dynamic pile driving formula (Fragaszy, Higgins, and Lawton 1985).

Table 2.3: Recommended Values for C_1 (inches/blow) - Temporary Elastic Compression of the Pile Head and Driving Cap (Chellis 1961)

Material to which Hammer Blow is Applied	Driving Stresses on Pile Head or Driving Cap (ksi)			
	0.50	1.00	1.50	2.00
Head of steel H-shaped or pipe piling	0	0	0	0
Head of timber pile	0.05	0.10	0.15	0.20
Precast concrete pile with 3.0 – 4.0 inches of packing inside driving cap	0.12	0.25	0.37	0.50
Precast concrete pile with only 0.5 – 1.0 inch mat pad on head	0.025	0.05	0.075	0.10
Steel-covered cap containing wood packing for steel H-shaped or pipe piling	0.04	0.05	0.12	0.16
3/16 inch fiber disk between two 3/8 inch steel plates for use with Monotube piles subjected to severe driving conditions	0.02	0.04	0.06	0.08

Note: For driving stresses larger than 2.00 ksi, use the value of C_1 provided in the last column.

Table 2.4: Recommended Values for C_3 (inches/blow) - Temporary Elastic Compression of the Soil Surrounding the Pile (Chellis 1961)

Type of Pile	Driving Stresses on Horizontal Projection of Pile Toe (ksi)			
	0.50	1.00	1.50	2.00
Piles of Constant Cross Section	0 – 0.10	0.10	0.10	0.10

In an effort to further alleviate the difficulty associated with the determination of Hiley's rebound coefficients, i.e., C_1, C_2, and C_3, the federal government of Canada adopted a dynamic pile driving formula for the construction control of driven pile foundations in their first edition of the Canadian National Building Code (CNBC) that modified empirically these coefficients. Although the CNBC formula presented in Eq. (2.39) is no longer specified in the National Building Code of Canada, it was recommended that a factor of safety of three be applied when used (Chellis 1961).

$$R_u = \frac{n \cdot W_R \cdot h}{s + \frac{C}{2}} \qquad \textit{CNBC Formula} \quad (2.39)$$

where: $n = \frac{W_R + e^2 \cdot W_p}{W_R + W_p}$ for friction piles, (2.40)

$$n = \frac{W_R + 0.5 \cdot e^2 \cdot W_p}{W_R + W_p} \text{ for refusal, and} \tag{2.41}$$

$$C = \frac{3 \cdot R_u}{A} \cdot \left(\frac{L}{E} + 0.0001 \text{ in}^3/\text{kip} \right). \tag{2.42}$$

Given that the CNBC formula of Eq. (2.39) was intended for use with piles driven by trigger activated gravity hammers, when single-acting steam hammers and winch drag gravity hammers are used, the resulting value for the ultimate resistance to pile penetration, as obtained from Eq. (2.39), should be multiplied by 0.90 and 0.80, respectively (Chellis 1961).

With a similar motivation, the Pacific Coast Building Officials, later referred to as the International Conference of Building Officials (ICBO), adopted a modified version of the Hiley dynamic pile driving formula for the construction control of driven pile foundations in their first edition of the Uniform Building Code (UBC), which was published in 1927. This formula, which is most commonly referred to as the Pacific Coast Uniform Building Code (PCUBC) formula, attempts to account for the energy losses associated with the temporary elastic compressions of the driving cap and soil by using twice the average energy loss associated with the temporary elastic compression of the pile (Chellis 1961). Although the PCUBC dynamic pile driving formula was removed from the UBC in 1976, its use is still permitted provided that a factor of safety of four is applied to obtain an allowable resistance to pile penetration (Bowles 1996).

$$R_u = \frac{W_R \cdot h \cdot \dfrac{W_R + k \cdot W_p}{W_R + W_p}}{s + \dfrac{R_u \cdot L}{A \cdot E}} \qquad \textit{PCUBC Formula} \tag{2.43}$$

where: k = 0.25 for steel piles and 0.10 for all other piles.

If it is assumed that energy losses resulting from the temporary elastic compressions of the driving cap and soil can be neglected, then Eq. (2.35) can be rewritten as:

$$W_R \cdot h = R \cdot s + \left[W_R \cdot h \cdot \left(\frac{W_p \cdot (1 - e^2)}{W_R + W_p} \right) \right] + \left\{ \frac{R^2 \cdot L}{2 \cdot A \cdot E} \right\} \tag{2.44}$$

When Eq. (2.44) is solved directly for *R*, the resulting dynamic pile driving formula, which has been provided in Eq. (2.45), is referred to as the Universal or Stern formula (Chellis 1961). However, it is important to note that, other than being established in the year 1908, little is known concerning the history associated with this dynamic pile driving formula.

$$R_u = \frac{A \cdot E}{L} \cdot \left[-s + \sqrt{s^2 + W_R \cdot h \cdot \left(\frac{W_R + e^2 \cdot W_p}{W_R + W_p} \right) \cdot \left(\frac{2 \cdot L}{A \cdot E} \right)} \right] \quad \textit{Universal/Stern Formula} \quad (2.45)$$

As a special case of the Universal/Stern formula of Eq. (2.45), J. F. Redtenbacher proposed a dynamic pile driving formula by assuming the occurrence of a perfectly inelastic impact between the pile driving hammer and embedded pile, i.e., $e = 0$ (Chellis 1961). Although Redtenbacher, as stated previously, is often times credited with the development of the "complete" dynamic pile driving formula, this engineer is more frequently associated with the simplified formula provided in Eq. (2.46).

$$R_u = \frac{A \cdot E}{L} \cdot \left[-s + \sqrt{s^2 + \left(\frac{W_R^2 \cdot h}{W_R + W_p} \right) \cdot \left(\frac{2 \cdot L}{A \cdot E} \right)} \right] \quad \textit{Redtenbacher Formula} \quad (2.46)$$

Like the Universal/Stern and Redtenbacher formulas, the Janbu formula, proposed by N. Janbu in 1953 (Gulhati and Datta 2005), is based upon the assumption that energy losses resulting from the temporary elastic compressions of the driving cap and soil can be neglected. Although this formula does not directly involve the Newtonian theory of impact, Janbu attempted to account for it by factoring out a series of variables, which proved to be difficult to evaluate, from the general conservation of energy equation, i.e., Eq. (2.3), and then combining them to form what is termed the driving coefficient, C_d. More specifically, this driving coefficient includes terms representing the difference between static and dynamic capacity, the ratio associated with the transfer of load into the soil as a function of depth, and hammer efficiency (Fragaszy, Higgins, and Lawton 1985). Furthermore, the driving coefficient is correlated with the ratio of the weight of the pile to the weight of the pile driving hammer in an effort to account for the variability in the energy available at the close of the period of restitution. As a result, the Janbu formula, in its simplest form, may be

expressed as shown in Eq. (2.47), with the recommended application of a factor of safety of three, as reported by Gulhati and Datta (2005).

$$R_u = \left(\frac{e_h \cdot W_R \cdot h}{s}\right)\left(\frac{1}{K_u}\right) \qquad \textit{Janbu Formula} \quad (2.47)$$

$$\text{where: } K_u = C_d \cdot \left[1 + \left(1 + \frac{\lambda_e}{C_d}\right)^{1/2}\right], \qquad (2.48)$$

$$C_d = 0.75 + 0.15 \cdot \left(\frac{W_p}{W_R}\right), \text{ and} \qquad (2.49)$$

$$\lambda_e = \frac{e_h \cdot W_R \cdot h \cdot L}{A \cdot E \cdot s^2}. \qquad (2.50)$$

If it is again assumed that energy losses resulting from the temporary elastic compression of the soil, together with the temporary elastic compression of the pile, are significant, then for a perfectly inelastic impact between the pile driving hammer and embedded pile, i.e., e = 0, Schenk proposed the dynamic pile driving formula presented in Eq. (2.51) (Chellis 1961). Notice that in this formula, the temporary elastic compressions of the pile and soil are measured from a load-settlement curve, which is obtained via a static pile load test, near to or beyond the failure load, as defined by an appropriate method (e.g., De Beer (1967), Chin (1970) and (1971), Davisson (1972), etc.).

$$R_u = \frac{s}{\tan\varphi_e} \cdot \left[-1 + \sqrt{1 + \left(\frac{W_R^2 \cdot h}{W_R \cdot W_p}\right) \cdot \left(\frac{2 \cdot \tan\varphi_e}{s^2}\right)}\right] \qquad \textit{Schenk Formula} \quad (2.51)$$

where: $\tan\varphi_e$ = tangent of the angle formed between a horizontal line and the elastic pile rebound line, as encountered on a load-settlement curve constructed from static pile load test data.

As indicated in Section 2.3.2, several modifications to Wellington's ENR formula have been made over the years in an attempt to improve upon the original formula's pile bearing capacity prediction capabilities while still maintaining its desirable qualities of simplicity and ease of use. Since the various modifications presented in Section 2.3.2 follow the original formula's assumption that the energy losses associated with only the temporary

elastic compressions of the cap, pile, and soil need to be considered, it seems appropriate to now address those modified forms of the ENR formula that additionally account for the energy losses associated with the Newtonian theory of impact. Proposed in 1965 by the Michigan State Highway Commission (MSHC) as the product of an extensive study focused on comparing the efficacy of several dynamic pile driving formulas to predict the ultimate bearing capacity of driven piles, the MSHC Modified ENR formula, which is presented in Eq. (2.52), modifies the original ENR formula through the multiplication of an additional factor to account for the available kinetic energy after the impact from a single hammer blow upon the head of an embedded pile (Fragaszy, Higgins, and Lawton 1985). As with Wellington's original ENR formula, it is recommended that a factor of safety of six be applied to the value for the ultimate resistance to pile penetration produced by the MSHC Modified ENR formula.

$$R_u = \left[\frac{W_R \cdot h}{s + 0.1}\right] \cdot \left[\frac{W_R + e^2 \cdot W_p}{W_R + W_p}\right] \qquad \textit{MSHC Modified ENR Formula} \quad (2.52)$$

where: s = pile penetration distance under one hammer blow, i.e., pile set, expressed in inches per blow.

If it is assumed that a perfectly inelastic impact occurs between the pile driving hammer and embedded pile, i.e., e = 0, and if the constant term in the denominator of the MSHC Modified ENR formula, which accounts for all energy losses experienced as a result of temporary elastic compressions in the cap, pile, and soil, is altered to account for various hammer-pile combinations, then the Iowa DOT Modified ENR formula, which is presented in Eq. (2.53), is attained. Incorporated into the Iowa DOT's *Standard Specifications for Highway and Bridge Construction* manual, the Iowa DOT Modified ENR formula is to be used only in situations where there is no excessive bounce exhibited by the pile driving hammer subsequent to the impartation of the driving blow (Iowa DOT 2008). Furthermore, it is recommended that a factor of safety of four be applied to the value for the ultimate resistance to pile penetration produced by Eq. (2.53) when a gravity hammer or diesel hammer is used to drive timber, steel H-shaped, or steel shell type piles and when a steam hammer is used to drive any pile type. However, statistical studies suggest that factors of

safety of $2\frac{2}{3}$ and $1\frac{5}{7}$ should be used when either a gravity hammer or diesel hammer is utilized to drive a concrete pile, respectively.

$$R_u = \left[\frac{W_R \cdot h}{s+z}\right] \cdot \left[\frac{W_R}{W_R + W_p}\right] \qquad \textit{Iowa DOT Modified ENR Formula} \quad (2.53)$$

where: z = 0.35 inches per blow for timber, steel H-shaped, or steel shell piles driven by a gravity hammer; 0.20 inches per blow for concrete piles driven by a gravity hammer; and 0.10 inches per blow for all piles driven by either a diesel hammer or a steam hammer.

Finally, the Gow formula, which modified, based on experience and intuition, the denominator of the ENR formula to account for the energy-absorbing characteristics of precast concrete piles, is presented in Eqs. (2.54), (2.55), and (2.56) (Fragaszy, Higgins, and Lawton 1985). As with the original ENR formula, the application of a factor of safety of six is recommended for the Gow formula.

$$R_u = \frac{W_R \cdot h}{s + 1.0 \cdot \left(\frac{W_p}{W_R}\right)} \qquad \textit{Gow Formula: Gravity Hammers} \quad (2.54)$$

$$R_u = \frac{W_R \cdot h}{s + 0.1 \cdot \left(\frac{W_p}{W_R}\right)} \qquad \textit{Gow Formula: Single-Acting Steam Hammers} \quad (2.55)$$

$$R_u = \frac{E_h}{s + 0.1 \cdot \left(\frac{W_p}{W_R}\right)} \qquad \textit{Gow Formula: Double-Acting Steam Hammers} \quad (2.56)$$

where: s = pile penetration distance under one hammer blow, i.e., pile set, expressed in inches per blow.

In brief, the numerous dynamic pile driving formulas presented in this subsection account for the energy losses associated with both the temporary elastic compressions of the cap, pile, and soil as well as the Newtonian theory of impact. However, as stated in Section 2.3.3, Newton's theory of impact is based on what is now called the coefficient of restitution and, by definition, the coefficient of restitution includes all of the energy losses that occur in a given case of Newtonian impact, including those in the form of elastic distortions

(Cummings 1940). Thus, as recognized by Cummings (1940), the energy losses associated with the temporary elastic compressions of the driving cap, pile, and soil and those associated with the Newtonian theory of impact are in fact mutually exclusive and only one or the other of them should be accounted for in any given dynamic pile driving formula. Hence, when both are considered, some of the energy losses are actually deducted twice. Furthermore, the dynamic pile driving formulas of this subsection are based on the same questionable assumptions as those presented in Sections 2.3.2 and 2.3.3, namely that it is possible to calculate the temporary elastic compressions of the driving cap, pile, and soil from the expressions contained within the braces of Eq. (2.35) and that inertial energy losses can be calculated by the elementary Newtonian impact theory (Cummings 1940). Therefore, although it is true that some of the hammer energy provided to a driven pile foundation is dissipated in producing temporary elastic compressions of the driving cap, pile, and soil, and that the inertia of the pile is a factor in the pile driving problem, these approaches are only remotely related to the phenomena of actual pile driving. A phenomena that, Cummings (1940) concludes, cannot be solved by mathematics and theoretical mechanics alone.

2.3.5 Empirically Derived Dynamic Formulas

Although some of the dynamic pile driving formulas presented in the preceding subsections were obtained through empirical modifications to established relationships derived based on assumptions concerning the energy losses that occur during the impact from a single hammer blow upon the head of an embedded pile, a dynamic formula that is strictly empirical in nature has yet to be introduced. The Gates formula, proposed by Marvin Gates in 1957, is a strictly empirical relationship between hammer energy, final pile set, and measured static pile load test results (Jumikis 1971). The general structure of the formula was developed based on two relationships established by Gates, namely that the resistance to pile penetration is directly proportional to the square root of the net hammer energy as well as the logarithm of the final pile set. Through the application of statistical methods and a curve-fitting approach, the final form of the Gates formula was established as revealed in Eq. (2.57) (Gates 1957). Although it is known that the statistical adjustments employed in the development of this formula were based on the results from approximately one hundred static pile load tests, Gates (1957) failed to report on the amount of scatter exhibited by this data in

addition to whether or not the used dataset encompassed all soil types. Nonetheless, Gates (1957) recommends that a factor of safety of four be applied to the value for the ultimate resistance to pile penetration obtained from his formula.

$$R_u = \left(\frac{6}{7}\right) \cdot \sqrt{e_h \cdot E_h} \cdot \log\left(\frac{10}{s}\right) \qquad \textit{Gates Formula} \quad (2.57)$$

where: R_u = ultimate resistance to pile penetration expressed in tons,
E_h = rated hammer energy per blow expressed in foot-pounds per blow, and
s = pile penetration distance under one hammer blow, i.e., pile set, expressed in inches per blow.

The Gates formula of Eq. (2.57) was further enhanced by Richard Cheney of the FHWA (Paikowsky et al. 2004), based on statistical correlations with data from additional static pile load tests, as a means to help offset the original formulas tendency to overpredict pile penetration resistance at low driving resistances and underpredict pile penetration resistance at high driving resistances. Generally referred to as the FHWA Modified Gates formula, it is recommended in the current edition of the *AASHTO LRFD Bridge Design Specifications* (AASHTO 2007) that this dynamic pile driving formula be used before all other dynamic pile driving formulas in the construction control of driven pile foundations. Provided in Eq. (2.58) is the exact form of the FHWA Modified Gates formula as it appears in the current edition of the *AASHTO LRFD Bridge Design Specifications* (AASHTO 2007).

$$R_u = 1.75 \cdot \sqrt{W_R \cdot h} \cdot \log(10 \cdot N_b) - 100 \qquad \textit{FHWA Modified Gates Formula} \quad (2.58)$$

where: R_u = ultimate resistance to pile penetration expressed in kips,
W_R = weight of the pile driving ram expressed in pounds,
h = drop height (stroke) of the ram expressed in feet, and
N_b = number of hammer blows for one inch of pile permanent set.

In a similar manner, the Washington State Department of Transportation (WSDOT) used an expanded database established by Paikowsky et al. (2004), which was comprised of data from numerous static pile load tests conducted throughout the United States, to statistically enhance the original Gates dynamic pile driving formula. As with the FHWA

Modified Gates formula, the WSDOT dynamic pile driving formula was developed to maintain the low prediction variability of the original Gates formula, but at the same time minimize its tendency to under- or over-predict the ultimate pile penetration resistance (Allen 2005). As presented by Allen (2007), the WSDOT formula takes the following form:

$$R_u = 6.6 \cdot F_{eff} \cdot W_R \cdot h \cdot \ln(10 \cdot N_b) \qquad \textit{WSDOT Formula} \quad (2.59)$$

where: R_u = ultimate resistance to pile penetration expressed in kips,

F_{eff} = 0.55 for air/steam hammers with all pile types, 0.37 for open-ended diesel hammers with concrete or timber piles, 0.47 for open-ended diesel hammers with steel piles, 0.35 for closed-ended diesel hammers with all pile types, 0.58 for hydraulic hammers with all pile types, and 0.28 for gravity hammers with all pile types,

W_R = weight of the pile driving ram expressed in kips,

h = drop height (stroke) of the ram expressed in feet, and

N_b = number of hammer blows for one inch of pile permanent set, averaged over the last four inches of driving.

Finally, described as a combination static and dynamic formula, the Rabe formula is a comprehensive formula that takes into account most of the factors that influence pile capacity (Spangler and Mumma 1958). Developed empirically from the results of over 100 pile driving and pile testing projects, this formula can be rather cumbersome to use on account of the fact that it requires extensive computations and several trial estimates of load (Spangler and Mumma 1958). Thus, it is often times necessary to perform many of the computations required by the formula prior to driving; otherwise it becomes exceedingly difficult to use in the field. With an inherent theoretical factor of safety of two, the Rabe formula is the only dynamic pile driving formula that attempts to account for the soil types and soil conditions into which the pile is being driven. Without further introduction, the Rabe formula, as presented by Spangler and Mumma (1958), is as follows:

$$R_a = \left(\frac{M \cdot F'}{s + C'}\right) \cdot \left(\frac{W_R}{W_R + \frac{W_p}{2}}\right) \cdot B \qquad \textit{Rabe Formula} \quad (2.60)$$

where: R_a = allowable resistance to pile penetration expressed in pounds,

M = 4.0 for winch drag gravity hammers, 4.75 for trigger activated gravity hammers, 5.0 for single-acting steam hammers of the Vulcan type, 5.25 for differential-acting steam hammers of the Vulcan type, and 6.0 for double-acting steam hammers of the McKiernan-Terry type,

F' = $W_R \cdot h$ for gravity and single-acting steam hammers or E_h for differential and double-acting steam hammers expressed in foot-pounds per blow,

s = pile penetration distance under one hammer blow, i.e., pile set, expressed in inches per blow,

W_R = weight of the pile driving ram expressed in pounds,

h = drop height (stroke) of the ram expressed in feet,

C' = temporary elastic compression of the driving cap, pile and soil expressed in inches per blow ($C' = C_1' + C_2' + C_3'$),

W_p = weight of the pile, driving cap, follower, and mandrel as driven expressed in pounds, and

B = static supplement factor ($B = B_s \cdot B_l \cdot B_c$).

In order to compute C_1', C_2', and C_3' as well as B_s, B_l, and B_c, additional formulas, tables, and figures are required. For C_1':

$$C_1' = \frac{R_a \cdot \left(\frac{W_R + \frac{W_p}{2}}{W_R}\right)}{6{,}000{,}000 \cdot B} \cdot \frac{h}{3} \qquad (2.61)$$

However, for single-acting and for double-acting or differential-acting hammers, the $h/3$ term is considered to be equal to the value of one. For C_2':

$$C_2' = \frac{12 \cdot V \cdot R_a \cdot L}{A \cdot E \cdot B} \qquad (2.62)$$

where: L = length of the pile expressed in feet,

V = a factor that takes into account the amount of taper of the pile and the vertical arrangement of the soil and is obtained from Table 2.5,

E = Young's modulus for the pile material expressed in pounds per square inch, and

A = average cross-sectional area of the pile apparatus as driven including equivalent transformed section properties in the case of piles composed of several materials expressed in square inches.

Furthermore, C_3' is equal to a constant value of 0.04 inches per blow. Focusing now on B_c, B_l, and B_s, the variable B_c represents a pile cross-section factor that is determined through the use of Figure 2.2. To use this figure, the average, horizontal cross-sectional area of soil displaced by the pile over the entire penetrated length in units of square inches is required; for steel H-piles, this quantity is assumed to be equal to two times the cross-sectional area of the pile since B_c is intended to account for friction surface as well as displacement. Subsequently, the variable B_l represents a pile length factor that is determined through the use of Figure 2.3. To use this figure, the value for length of pile penetration in units of feet is required. Finally, the variable B_s represents a soil factor that is determined through the use of Table 2.6. More specifically, the soil profile encountered at the location of the driven pile foundation under examination, in conjunction with Table 2.6, is used in the following manner to determine B_s:

1) Divide the total penetrated depth into its various types of soil and choose a soil factor for each from Table 2.6.
2) Select equal depth intervals of four to twenty feet and assign a B_s value to each. Multiply by progression numbers, beginning at the head and increasing to the toe of the pile, which give more weight to soil near the toe than at the ground level. The progression numbers are 1, 4, 8, 12, 17, 22, 28, 34, 40, 46, 53, 60, 67, 74, 81, 88, 95, 102, 109, and 116.

3) After multiplying the B_s selected for each depth interval by its progression number, take the sum of these and divide it by the sum of the progression numbers used. This value is B_s for the penetrated depth of the pile.
4) If the soil immediately below the toe has a lower B_s than that determined for the entire embedded length, an average of the two values should be used.
5) The value of B_s should not be increased due to contact with rock.

Table 2.5: Values for the *V* Factor in Rabe's Formula (Spangler and Mumma 1958)

Vertical Arrangement of Soil†	Pile Characteristics							
	Steel H-Shaped w/ Filler Near End	No Taper	Length in Feet Corresponding to a Taper of 1 inch					
			Over 20	20	16	12	8	4
Point bearing; rock or other hard material at point; poor soil above	1.00	1.00	1.00	1.00	1.00	1.00	1.00	1.00
Point bearing; rock or other hard material at point; fairly good soil above	0.95	0.95	0.95	0.93	0.92	0.91	0.89	0.87
Point bearing; rock or other hard material at point; very good soil above	0.90	0.88	0.85	0.82	0.79	0.76	0.72	0.68
Abrupt increase in firmness of soil near point, but not reaching rock or other hard material	0.88	0.80	0.75	0.70	0.66	0.62	0.55	0.49
Uniform firmness; full penetration (soft, medium, or hard)	0.85	0.75	0.70	0.63	0.57	0.52	0.44	0.36

† With reference to center of resistance to driving.

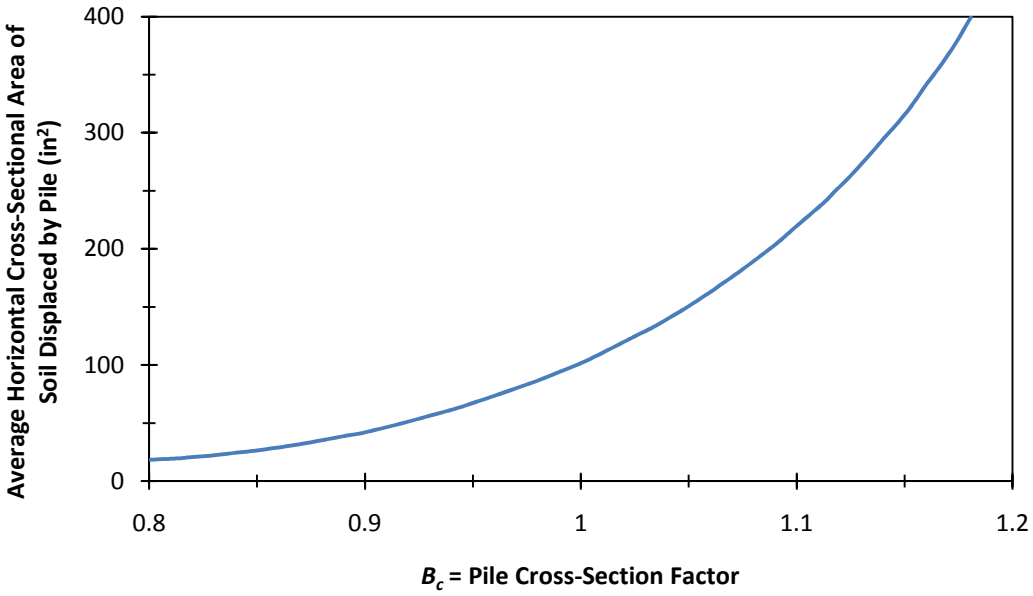

Figure 2.2: Pile Cross-Section Factor (B_c) in Rabe's Formula (Spangler and Mumma 1958)

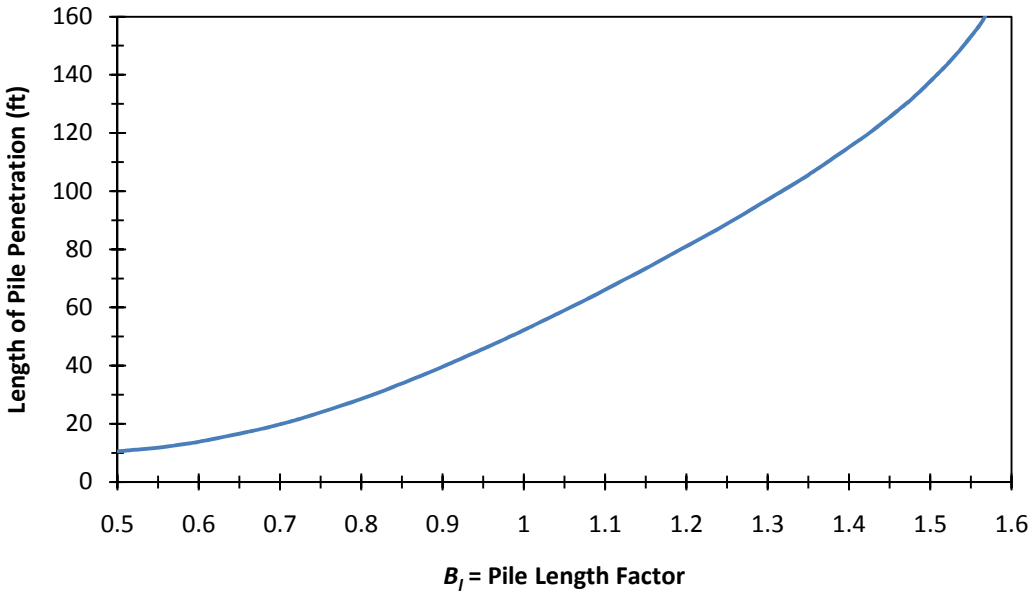

Figure 2.3: Pile Length Factor (B_l) in Rabe's Formula (Spangler and Mumma 1958)

Table 2.6: Values for the Soil Factor (B_s) in Rabe's Formula (Spangler and Mumma 1958)

Soil Type	B_s
Muck	0.20 – 0.35
Loam	0.20 – 0.50
Very wet plastic clay or silt	0.30
Soft clay or silt	0.50
Medium clay or silt	0.70
Hard clay or silt	0.85
Dense sandy silt	1.00
Loose sand, or sand and gravel	0.85
Moderately compact sand, or sand and gravel	1.00
Very compact sand, or sand and gravel	1.25
Shale	1.00 – 1.50
Hardpan	1.00 – 1.50

2.4 COMPARATIVE STUDIES OF DYNAMIC PILE DRIVING FORMULAS

Although a multitude of dynamic pile driving formulas exist for the construction control of driven pile foundations, the act of determining which one is best suited for a given situation or which one is most accurate overall is a particularly difficult task. Nonetheless, it can be assumed that the ideal dynamic pile driving formula, if one were to exist, would be accurate enough to provide a safe yet economical design, in addition to being suitable for varying soil conditions and pile types. With this in mind, numerous studies have been conducted over the past sixty years in an effort to determine the correlation between the bearing capacity of a statically load tested pile and the estimated pile bearing capacity as obtained via dynamic pile driving formulas. In the following subsections, a comprehensive review of these studies will be presented in chronological fashion. It is important to note that, although many of the studies presented in the following subsections were identified by Fragaszy, Higgins, and Lawton (1985) in their report to the Washington State Transportation Center, they have been included here so that a clear historical progression regarding the perceived accuracy of specific dynamic pile driving formulas can be realized.

2.4.1 Chellis, 1949

One of the oldest references to have cited comparisons between the predicted pile bearing capacity obtained via dynamic pile driving formulas and the corresponding measured bearing capacity attained from static pile load test results is Chellis (1949). Using the results

from 45 static pile load tests conducted in predominately cohesionless soils and encompassing several different pile types (i.e., mandrel-driven corrugated shell, fluted steel shell, precast concrete, timber, and steel H-shaped piles) and pile driving hammers (i.e., double-acting, differential-acting, and gravity hammers), Chellis compared the measured ultimate pile capacity, defined as the load on the net settlement versus load curve where the rate of movement begins to increase sharply in proportion to the increase in load, against that predicted by the ENR, Hiley, MSHC Modified ENR, Eytelwein, Modified Eytelwein (where the ratio between the weight of the pile and the weight of the pile driving hammer in the denominator of Eq. (2.29) was modified by a factor of 0.3 instead of 0.1), Navy-McKay, CNBC, and PCUBC dynamic pile driving formulas. Based on the results of this comparison, which have been reproduced in Table 2.7, Chellis (1949) concluded that the Hiley, PCUBC, and CNBC dynamic pile driving formulas performed sufficiently well, given the fact that they demonstrated the provision of a safe yet economical design through application of the recommended factors of safety. Furthermore, it was also concluded that the ENR and Eytelwein formulas were inefficient methods for the prediction of ultimate pile capacity considering their respective mean and variance statistics reported in Table 2.7; a reality that has been seemingly ignored given the widespread use of the ENR formula yet today.

Table 2.7: Summary of Results from Chellis (1949) (From: Fragaszy, Higgins, and Lawton 1985)

Dynamic Pile Driving Formula	Ratio of Predicted Load to Measured Ultimate Load (%)	
	Average	Range
Hiley	92	55-125
PCUBC	112	55-220
CNBC	80	55-140
ENR	289	100-700
MSHC Modified ENR	182	98-430
Eytelwein	292	90-1800
Modified Eytelwein	202	98-508
Navy-McKay	-	99-∞

2.4.2 Sörensen and Hansen, 1957

Sörensen and Hansen (1957) used data from 78 static pile load tests conducted on concrete, steel, and timber piles bearing on sand, or in a few instances hard moraine clay, to

evaluate the performance of their numerically integrated wave equation, which describes the mechanics of force transmission along an elastic rod subjected to an impact force, and the following four dynamic pile driving formulas: Janbu, Hiley, Eytelwein, and Danish. The results of this study have been reproduced in Figure 2.4, where the ratio of the measured to predicted pile bearing capacity (μ) is plotted against the percentage of load tests producing a value less than μ. Since the plot displayed in Figure 2.4 is a normal probability plot, a straight line on this plot corresponds to a normal or Gaussian distribution of results. With this in mind, it can be observed from Figure 2.4 that the predictive capacities of all dynamic pile driving formulas considered in this study follow approximately a normal distribution, save for the Eytelwein formula. Sörensen and Hansen (1957) concluded their study by noting that the Danish, Hiley, and Janbu formulas all performed at a similar level of accuracy to that exhibited by the numerically integrated wave equation, but that the Eytelwein formula was an exceedingly inaccurate method.

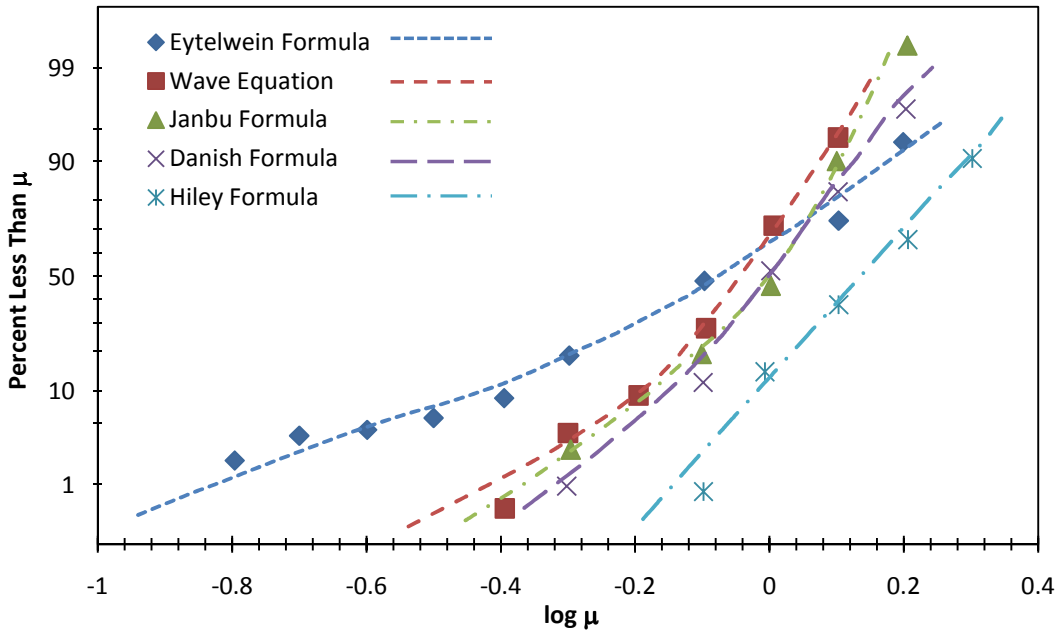

Figure 2.4: Statistical Distribution of the Results from Sörensen and Hansen (1957) (From: Ng, Simons, and Bruce 2004)

2.4.3 Spangler and Mumma, 1958

Spangler and Mumma (1958) compared the allowable bearing capacities predicted by the ENR, PCUBC, Eytelwein, and Rabe dynamic pile driving formulas with the

corresponding measured bearing capacities attained from the results of 58 static pile load tests conducted in locales spanning the entire United States. In other words, this comparative study covered a wide variety of soil conditions and pile types (i.e., steel H-shaped, concrete, timber, Raymond step-tapered, and pipe piles). For each of the aforementioned static pile load tests, the measured ultimate pile capacity was defined by Spangler and Mumma (1958) to be the average value resulting from the application of the following four procedures upon the obtained load versus displacement results:

a) the load at which net settlement equals 0.25 inches is defined as the failure load,
b) the load at which the incremental gross settlement divided by the incremental load exceeds 0.03 inches per ton is defined as the failure load,
c) the load at which the gross settlement curve breaks and passes into a deep straight tangent is defined as the failure load, and
d) the load at which the tangents to the early flat portion and the steep portion of the load-settlement curve intersect is defined as the failure load.

With this information at hand, an actual factor of safety was determined by dividing the measured ultimate pile capacity by the allowable bearing capacity predicted by the four dynamic pile driving formulas considered in this study. The results of this comparison have been reproduced in Table 2.8.

Table 2.8: Summary of Results from Spangler and Mumma (1958) (From: Fragaszy, Higgins, and Lawton 1985)

Factor of Safety	Number of Cases			
	ENR	Eytelwein	PCUBC	Rabe
<1.0	4	6	0	0
1.0-1.5	10	7	1	1
1.5-2.0	10	7	2	13
2.0-3.0	21	21	12	30
3.0-4.0	7	7	5	13
4.0-5.0	5	7	11	1
5.0-8.0	1	3	20	0
>8.0	0	0	7	0
Range	***0.83-5.38***	***0.72-5.49***	***1.22-9.27***	***1.30-4.00***

Defining an unsafe or uneconomical prediction in pile bearing capacity by the event in which the actual factor of safety assumed a value that was less than 1.5 or greater than 4.0, respectively, Spangler and Mumma (1958) arrived at the following general conclusions:

1) The ENR dynamic pile driving formula is often “unsafe” for piles with small sets, i.e., pile sets of 0.10 inches per blow or less.
2) The actual factor of safety for the ENR formula is usually between 1.5 and 3.0, as opposed to the recommended value of 6.0, when used in conjunction with combination end-bearing and friction pile foundations.
3) For friction piles, the ENR formula generally provided an actual factor of safety that was greater than 3.0.
4) The Eytelwein dynamic pile driving formula produced larger scatter for the actual factor of safety values than the ENR formula and was considered to be unreliable for use with heavy piles driven by light hammers.
5) Although the PCUBC dynamic pile driving formula produced the largest scatter for the actual factor of safety values, it generated safe results and was more conservative than both the ENR and Eytelwein formulas.
6) The PCUBC formula was considered to be most reliable for use with long piles driven by heavy hammers.
7) Although very difficult to use, the Rabe dynamic pile driving formula produced the best results of the four formulas examined.

2.4.4 Agerschou, 1962

Agerschou (1962) used the results of up to 171 static pile load tests, in which the pile tips penetrated into either sand or gravel, to evaluate the performance of Sörensen and Hansen’s (1957) numerically integrated wave equation and the following six dynamic pile driving formulas: Hiley, ENR, Eytelwein, Janbu, Danish, and Weisbach. Using the seven methods to predict the ultimate pile bearing capacity, Agerschou (1962) was able to determine the ratio of the measured ultimate pile capacity, defined as either the load at which the total settlement equals ten percent of the pile diameter or the maximum load that can be reached by way of hydraulic jacking procedures, to the predicted ultimate pile capacity for

each pile. Using the common logarithms of these ratios as a basis for the statistical evaluation of each method, the analysis returned a nominal factor of safety required to assure that for 98 percent of the time the allowable resistance to pile penetration will be less than or equal to the measured ultimate resistance. Additionally, for each dynamic formula, Agerschou (1962) calculated the upper limit for the actual factor of safety, which was defined to be the maximum value obtained from comparisons between the measured ultimate pile capacity and the predicted allowable pile capacity, i.e., the predicted ultimate pile capacity divided by the previously established nominal factor of safety for 98 percent safety. The pertinent results of this study have been summarized in Table 2.9.

Table 2.9: Summary of Statistical Analysis by Agerschou (1962) (From: Fragaszy, Higgins, and Lawton 1985)

Dynamic Pile Driving Formula	Number of Load Tests	Nominal Factor of Safety	Standard Deviation on log $\frac{Q_{Measured}}{Q_{Predicted}}$	Upper Limit for 98% Safety if Lower Limit is 1.0
ENR	171	0.86	0.78	26.0
Eytelwein	78	7.10	0.57	17.0
Hiley	50	1.40	0.27	3.8
Janbu	78	2.30	0.25	3.6
Danish	78	2.00	0.26	3.8
Weisbach	123	2.60	0.36	6.0
Sörensen and Hansen's (1957) Wave Equation	78	2.60	0.23	3.9

From the results provided in Table 2.9, Agerschou (1962) concluded that the ENR formula was an unreliable method for the prediction of the ultimate bearing capacity of piles. This conclusion was based on the fact that the ENR formula generated the largest standard deviation of the seven methods studied as well as the fact that it would require a nominal factor of safety of 0.86 for 98 percent assurance of safety; not to mention the fact that factors of safety reaching as high as 26 would have to be accepted if such a nominal factor of safety was to be adopted. Finally, Agerschou (1962) deemed the Hiley, Janbu, and Danish pile driving formulas as well as Sörensen and Hansen's (1957) numerically integrated wave equation as acceptable methods for the prediction of ultimate pile capacity given their documented accuracy, i.e., small standard deviation.

2.4.5 Flaate, 1964

Flaate (1964) investigated the accuracy of the Janbu, Hiley, and ENR formulas by comparing them with data from 116 static pile load tests carried out on timber, concrete, and steel piles embedded in sandy soils. In all cases, the measured ultimate pile capacity was defined using the method proposed by Davisson (1972). Reinforcing the conclusions reached by Agerschou (1962) regarding the unreliability of the ENR formula in the prediction of the ultimate bearing capacity of piles penetrating into either sand or gravel soil mediums, the results of this study also showed that there is relatively little difference between the Janbu and Hiley formulas, although the former is perhaps the more reliable overall and provides good results when used with timber and concrete piles; however, Hiley's formula also provided reasonable results when used with timber piles.

2.4.6 Michigan State Highway Commission, 1965

In 1965, the Michigan State Highway Commission (Kerkhoff, Oehler, and Housel 1965) undertook a comprehensive pile testing program in which 88 piles were driven and statically load tested to failure as shown in Table 2.10. With this information at hand, the correlation between the bearing capacity of the load tested piles and the estimated pile bearing capacity as obtained from selected dynamic pile driving formulas was investigated and the results have been summarized in Table 2.11. The formulas selected for examination in this study included the ENR, Hiley, PCUBC, Redtenbacher, Eytelwein, Navy-McKay, Rankine, CNBC, MSHC Modified ENR, Gates, and Rabe formulas. In addition to identifying the inability of dynamic pile driving formulas to provide a reliable means for the estimation of the long-term bearing capacity of piles, the investigative efforts of the Michigan State Highway Commission (Kerkhoff, Oehler, and Housel 1965) revealed the following important and pertinent results:

1) In several instances, the allowable pile capacities predicted by the ENR, Navy-McKay, and Rankine formulas experienced actual factors of safety of less than unity when compared with the measured ultimate pile capacities determined from the results of static load tests.

2) In several instances, the allowable pile capacities predicted by the Hiley, PCUBC, Redtenbacher, and CNBC formulas experienced actual factors of safety greater than nine when compared with the measured ultimate pile capacities determined from the static load test results.
3) In general, the allowable pile capacities predicted by the MSHC Modified ENR and Gates formulas experienced actual factors of safety in the range of 1.5 to 6.

The general conclusion from the Michigan State Highway Commission's research study states that while dynamic pile driving formulas leave much to be desired as a basis for estimating pile bearing capacity, it is strongly recommended that they be retained for rapid determination and control of pile capacity in the field. Defending this conclusion, the MSHC Modified ENR formula was implemented into their state-specific project specifications.

Table 2.10: Summary of Piles Driven in the Michigan State Highway Commission Test Program (From: Bowles 1996)

Pile Type	Dimensions (in)	Weight (lb/ft)	Manufacturer	Approximate Range in Length (ft)	Number of Piles Driven
HP 12×53	12 (depth)	53.0	U.S. Steel	44-88	48
12 in outside diameter pipe piles (mandrel-driven)	0.25 (wall thickness)	31.4	Armco	44-178	16
	0.23 (wall thickness)	29.7			6
	0.18 (wall thickness)	22.6			11
Monotube piles, fluted tapered, F 12-7 (30 ft taper section) and an N 12-7 extension	12 (nominal diameter)	F 19.6 N 24.5	Union Metal Manufacturing Company	55-80	5
Step-tapered shells with 8 ft sections	9.5 outside toe diameter	Varied	Raymond International	58-67	2

Table 2.11: Summary of Results from the Michigan State Highway Commission's Research Study (From: Bowles 1996)

Dynamic Formula	Upper and Lower Limits of SF = P_u/P_d* for Ranges of P_u (kips) Values		
	0 to 900	900 to 1800	1800 to 3100
ENR	1.1-2.4	0.9-2.1	1.2-2.7
Hiley	1.1-4.2	3.0-6.5	4.0-9.6
PCUBC	2.7-5.3	4.3-9.7	8.8-16.5
Redtenbacher	1.7-3.6	2.8-6.5	6.0-10.9
Eytelwein	1.0-2.4	1.0-3.8	2.2-4.1
Navy-McKay	0.8-3.0	0.2-2.5	0.2-3.0
Rankine	0.9-1.7	1.3-2.7	2.3-5.1
CNBC	3.2-6.0	5.1-11.1	10.1-19.9
MSHC Modified ENR	1.7-4.4	1.6-5.2	2.7-5.3
Gates	1.8-3.0	2.5-4.6	3.8-7.3
Rabe	1.0-4.8	2.4-7.0	3.2-8.0

*P_u = ultimate test load
P_d = design capacity, using the factor of safety recommended for the equation (values range from 2 to 6, depending the dynamic formula)

2.4.7 Housel, 1966

Aside from presenting the data gathered by the Michigan State Highway Commission (Kerkhoff, Oehler, and Housel 1965) for their comprehensive pile testing program, Housel (1966) compared the predicted pile capacities obtained from the ENR and MSHC Modified ENR formulas with the measured ultimate pile capacities garnered from the results of nineteen additional static pile load tests. Of these nineteen test piles, fourteen were twelve-inch (outside-diameter) steel piles filled with concrete and driven closed-ended, two were H-shaped steel piles, and three were open-ended pipe piles, with one of these three being driven in granular soil and the remaining two being driven in clayey soils. Although the results of this study showed that the MSHC Modified ENR formula gave somewhat better predictions of pile bearing capacity than the original ENR formula, Housel (1966) concluded the study with the following statement:

> "From the standpoint of a reliable estimate of capacity, the range of variation improved only slightly and there seems to be no practicable way of increasing the formula's (MSHC Modified ENR) accuracy in predicting pile capacity for the great variety of field conditions under which piles must be driven."

2.4.8 Olson and Flaate, 1967

Olson and Flaate (1967) used the results from 93 static pile load tests conducted on piles driven into sandy soils to evaluate the performance of the ENR, Gow, Hiley, PCUBC, Janbu, Danish, and Gates dynamic pile driving formulas. Although several different criteria were used to determine the measured ultimate pile capacities of the 93 tested piles, Olson and Flaate (1967) state that this produces a scatter in the results of about fifteen percent instead of providing specific information regarding the static pile load test results themselves. Nevertheless, the measured versus predicted ultimate pile capacities were plotted on an *x*-*y* graph and a linear least squares fit was used to find the slope (*A*) and y-intercept (*B*) of the best fit line through the data points as well as the associated correlation coefficient (*r*). A summary of this statistical data, as compiled by Olson and Flaate (1967), has been provided in Table 2.12. It is important to note that in an ideal situation the slope (*A*) would be equal to one, the *y*-intercept (*B*) would be equal to zero, and the correlation coefficient (*r*) would be equal to one.

For all cases presented in Table 2.12, Olson and Flaate (1967) found that the ENR and Gow formulas were clearly inferior to the other five formulas based solely on their remarkably low correlation coefficients. Although no formula was deemed best for use with concrete piles due to the small number of such piles analyzed, the Janbu formula was found to be the most accurate when used with timber and steel piles. Furthermore, the Janbu, Danish, and Gates formulas produced the highest average correlation coefficients under the consideration of all pile types, although those associated with the PCUBC and Hiley formulas were only slightly lower.

Before concluding their study, Olson and Flaate (1967) adjusted the three best formulas to produce values of one and zero for the slope and *y*-intercept, respectively, of the best fit line through the data points. Finally, an adjusted form of the Gates formula was recommended for use with precast concrete, timber, and steel piles simply on account of its ease-of-use qualities. These three adjusted forms of the Gates formula have been provided in Eqs. (2.63), (2.64), and (2.65).

$$R_u = 7.2 \cdot \sqrt{e_h \cdot E_h} \cdot \log\left(\frac{10}{s}\right) - 17 \qquad \textit{Timber Piles} \qquad (2.63)$$

$$R_u = 9.0 \cdot \sqrt{e_h \cdot E_h} \cdot \log\left(\frac{10}{s}\right) - 27 \qquad \textit{Precast Concrete Piles} \quad (2.64)$$

$$R_u = 123.0 \cdot \sqrt{e_h \cdot E_h} \cdot \log\left(\frac{10}{s}\right) - 83 \qquad \textit{Steel Piles} \quad (2.65)$$

where: R_u = ultimate resistance to pile penetration expressed in tons,

E_h = rated hammer energy per blow expressed in inch-tons per blow, and

s = pile penetration distance under one hammer blow, i.e., pile set, expressed in inches per blow.

Table 2.12: Summary of Statistical Parameters from Olson and Flaate (1967) (From: Fragaszy, Higgins, and Lawton 1985)

Pile Type	Dynamic Pile Driving Formula	*N*	*A*	*B* (tons)	*r*
Timber	ENR	37	0.45	16	0.28
	Gow	37	0.37	18	0.43
	Hiley	37	0.64	19	0.77
	PCUBC	37	0.80	14	0.74
	Janbu (C_d = 1)	37	0.98	9	0.86
	Danish	37	0.71	9	0.86
	Gates	37	1.30	-17	0.86
Concrete	ENR	15	0.20	72	0.11
	Gow	15	0.32	69	0.12
	Hiley	15	1.08	24	0.43
	PCUBC	15	1.57	-19	0.75
	Janbu (C_d = 1)	15	0.66	23	0.64
	Danish	15	0.60	11	0.69
	Gates	15	1.62	-27	0.65
Steel	ENR	41	0.28	43	0.37
	Gow	41	0.28	42	0.38
	Hiley	41	1.14	-10	0.76
	PCUBC	41	1.07	0	0.79
	Janbu (C_d = 1)	41	0.91	7	0.83
	Danish	41	0.89	-16	0.82
	Gates	41	2.34	-83	0.84
All	ENR	93	0.33	37	0.29
	Gow	93	0.32	37	0.36
	Hiley	93	0.92	7	0.72
	PCUBC	93	1.04	2	0.76
	Janbu (C_d = 1)	93	0.87	10	0.81
	Danish	93	0.77	-2	0.81

2.4.9 Mansur and Hunter, 1970

Mansur and Hunter (1970) compared the measured ultimate pile capacities attained from the results of 12 static pile load tests, which were conducted on four steel pipe, two concrete, two steel H-shaped, and one timber pile driven in cohesionless soils, with the ultimate pile capacities predicted by the PCUBC, Janbu, and ENR formulas. As did Spangler and Mumma (1958), Mansur and Hunter (1970) defined the measured ultimate pile capacity for each of the aforementioned pile load tests as the average value resulting from the application of the following four procedures upon the obtained load versus displacement results:

a) the load on the load-gross settlement curve where the slope equals 0.01 inches per ton is defined as the failure load,
b) the load on the net movement curve where the settlement equals 0.25 inches is defined as the failure load,
c) the load where the tangents to the initial and final portions of the load-gross settlement curve intersect is defined as the failure load, and
d) the load where the slope of the gross movement curve becomes disproportionate to the load applied is defined as the failure load.

Based upon comparisons of the ratios of measured to predicted ultimate pile capacity, Mansur and Hunter (1970) determined that the PCUBC and Janbu formulas generated the best correlations between measured and predicted ultimate pile capacity. In fact, the average value of this ratio was found to be 1.07 for both the PCUBC and Janbu formulas, as opposed to 0.64 for the ENR formula. Likewise, the range in values employed by this ratio of measured to predicted ultimate pile capacity was found to be 0.85-1.34, 0.88-1.43, and 0.48-0.93 for the PCUBC, Janbu, and ENR formulas, respectively. Furthermore, Mansur and Hunter (1970) observed that, on average, the PCUBC and Janbu formulas tend to underpredict the measured ultimate pile capacity, with the ENR formula overpredicting this capacity in all instances by factors ranging from approximately 1.1 to 2.1.

2.4.10 Poplin, 1971

In 1971, Poplin (1971) examined and evaluated test pile data collected by the Louisiana Department of Highways between 1950 and 1970. Among the many tasks undertaken during the project was a comparison of measured ultimate pile capacities attained from the results of 24 static pile load tests, which were conducted on square precast concrete piles (14 inch and 16 inch), with the allowable pile capacities predicted by the ENR formula. The average ratio of measured ultimate pile capacity, defined as the load at the onset of large displacement or the load at which one inch of settlement occurs, to predicted allowable pile capacity was determined by Poplin (1971) to be about 0.506, which indicated that the actual factor of safety provided by the ENR formula was about two. On the other hand, the range in values employed by this ratio (0.107 to 1.0) was found to be quite large. Thus, as has been the case with most of the comparative studies discussed so far, Poplin (1971) concluded that the ENR dynamic pile driving formula yields extremely variable results. In addition, Poplin (1971) also examined the performance of a static analysis method for the prediction of pile capacity using the same 24 precast concrete test piles mentioned previously. Even though this static analysis method only exhibited, on average, slightly better accuracy than the ENR formula, the range of actual factors of safety was considerably reduced.

2.4.11 Ramey and Hudgins, 1975

Ramey and Hudgins (1975) used the results from 153 static pile load tests conducted in Alabama and adjacent southeastern states to evaluate the performance of the ENR, Gates, Danish, Hiley, and MSHC Modified ENR dynamic pile driving formulas in addition to the wave equation, as proposed by Smith (1962). For this study, the measured ultimate pile capacity was defined as the load at which the slope of the load-settlement curve reached 0.01 inches per kip. Moreover, of the 153 analyzed test piles, 48 were steel H-shaped piles, 38 were steel pipe piles, 32 were precast concrete piles, and 35 were timber piles, with 48 of these piles begin driven in predominantly cohesive soils and the remaining 105 being driven in predominantly cohesionless soils. In contrast to the conclusions reached by all of the comparative studies presented thus far, Ramey and Hudgins (1975) found that, of the five dynamic formulas studied, the ENR formula was the most consistent, with the Gates formula performing at a close second. Surprisingly enough, the Hiley formula was found to be the

worst overall. With these results at hand, Ramey and Hudgins (1975) modified the original ENR formula using the same techniques presented by Olson and Flaate (1967) and ultimately made a recommendation for the use of this adjusted ENR formula.

Finally, in regards to Smith's (1962) wave equation, the authors discovered that this method for the prediction of pile bearing capacity produced even better results than that of the ENR formula. As a result, Ramey and Hudgins (1975) concluded their study by recommending the development of an efficient wave equation computer program to be used for the construction control of driven pile foundation in lieu of the adjusted ENR formulas presented earlier in their study.

2.4.12 Kazmierowski and Devata, 1978

Kazmierowski and Devata (1978) compared the pile capacities estimated by the Hiley, Gates, Janbu, and MSHC Modified ENR formulas with the measured ultimate pile capacities obtained from the results of five static pile load tests. These five test piles consisted of a steel H-shaped pile, a closed-ended steel pipe pile filled with concrete, two precast concrete piles, and one timber pile. Furthermore, all of these piles were driven by a diesel hammer into a soil profile characterized by irregular layers of cohesive clayey silt with traces of sand and gravel, combined with occasional layers of silt to silty sands. Through comparisons of the variations in the predicted pile capacities and the measured ultimate pile capacities, which were defined to be the average value resulting from the application of Davisson's Method (1972) and two additional, yet unfamiliar, methods, for each test pile, the following observations were made:

1) The Hiley, Janbu, and Gates formulas provided acceptable results for the five piles studied, while the MSHC Modified ENR formula furnished very inconsistent results.
2) The Gates formula provided the best prediction of ultimate pile capacity for the closed-ended steel pipe and timber piles.
3) The Janbu formula provided the best prediction of ultimate pile capacity for the two precast concrete piles.
4) The Hiley formula provided the best prediction of ultimate pile capacity for the steel H-shaped pile.

2.4.13 Morris and Barksdale, 1982

Employing the same least squares linear regression analysis used by Olson and Flaate (1967), Morris and Barksdale (1982) compared the ultimate pile capacities estimated by the ENR and Gates formulas with the measured ultimate pile capacities obtained from the results of 306 pile static load tests carried out on timber, steel, and precast concrete piles. This plethora of pile load test data represents the compilation of information obtained from the following sources: Olson and Flaate (1967), Ramey and Hudgins (1975) and (1977), and Gutierrez (1978). Based upon the results of this analysis, which have been reproduced in Table 2.13, Morris and Barksdale (1982) found that the Gates formula was superior to the ENR formula for all pile types analyzed, as indicated by the higher correlation coefficient values observed. Using this information, Morris and Barksdale (1982) ultimately adjusted the Gates dynamic pile driving formula on a pile type basis in such a way as to produce values of one and zero for the slope and y-intercept, respectively, of the best fit line through the data points. These three modified forms of the Gates formula, which are recommended by Morris and Barksdale (1982) for estimating ultimate pile capacity during driving conditions where pile load tests are not practical, have been provided in Eqs. (2.66), (2.67), and (2.68).

$$R_u = 6.33 \cdot \sqrt{e_h \cdot E_h} \cdot \log\left(\frac{10}{s}\right) - 2.18 \qquad \textit{Timber Piles} \qquad (2.66)$$

$$R_u = 12.99 \cdot \sqrt{e_h \cdot E_h} \cdot \log\left(\frac{10}{s}\right) - 78.1 \qquad \textit{Precast Concrete Piles} \qquad (2.67)$$

$$R_u = 11.76 \cdot \sqrt{e_h \cdot E_h} \cdot \log\left(\frac{10}{s}\right) - 48.1 \qquad \textit{Steel Piles} \qquad (2.68)$$

where: R_u = ultimate resistance to pile penetration expressed in tons,

E_h = rated hammer energy per blow expressed in inch-tons per blow, and

s = pile penetration distance under one hammer blow, i.e., pile set, expressed in inches per blow.

Table 2.13: Summary of Statistical Parameters from (Morris and Barksdale 1982)

Dynamic Pile Driving Formula	Pile Type	N	A	B (tons)	r	Standard Deviation (tons)
Gates	Timber	78	1.13	-2.18	0.819	31.7
ENR			0.22	41.8	0.563	31.6
Gates	Steel	173	2.10	-48.1	0.723	86.9
ENR			0.24	66.3	0.632	87.4
Gates	Precast Concrete	55	2.32	-78.1	0.869	169.3
ENR			0.19	73.1	0.855	169.3
Gates	All	306	2.12	-54.4	0.820	105.4
ENR			0.21	64.2	0.778	105.5

2.4.14 Folse, McManis, and Elias, 1989

Folse, McManis, and Elias (1989) used the results from various static pile load tests performed in the State of Louisiana to evaluate the performance of Smith's (1962) wave equation and the following five dynamic pile driving formulas: ENR, Hiley, Gates, Janbu, and PCUBC. In all cases, the measured ultimate pile capacity was defined using the method proposed by C. Van der Veen (1953). Unlike all of the comparative studies presented thus far, Folse, McManis, and Elias (1989) recognized that the failure load at the EOD condition is not the same as the failure load at the time of static load testing as a result of setup or relaxation. Therefore, in an attempt to improve the uniformity of the comparisons made in this study, such time effects were estimated by applying a setup factor to the EOD side friction capacity; i.e., the estimated failure load at the time of static load testing was divided by the input setup factor (*SUF*) defined in Eq. (2.69) to obtain the estimated failure load at the EOD condition.

$$SUF = S(P_s) + 1.0 \cdot (P_t) \tag{2.69}$$

where: P_s = fraction of total pile resistance coming from side friction at the EOD condition; 0.95 if the final blow count is less than 3.5 times the average blow count, 0.75 if the final blow count is between 3.5 and 4.0 times the average blow count, or 0.50 if the final blow count is more than 4.0 times the average blow count,

P_t = fraction of total pile resistance coming from end-bearing at the EOD condition, and

S = 1.0 if predominant side soil has high permeability (sand or gravel), 2.0 if predominant side soil is medium to stiff clay, 3.0 if predominant side soil is soft to medium clay, and 4.0 if predominant side soil is very soft to soft clay.

Based upon comparisons of the ratio of the estimated failure load at the time of static load testing to the predicted ultimate pile capacity, it was shown that the Hiley and Gates dynamic pile driving formulas provided the most reliable, or accurate and consistent, predictions of ultimate pile capacity. Furthermore, comparisons of the ratio of the estimated failure load at the EOD condition to the predicted ultimate pile capacity yielded more efficient predictions of ultimate pile capacity from the PCUBC and Janbu dynamic pile driving formulas, with a reduction in the reliability previously associated with the Hiley and Gates dynamic pile driving formulas. Consequently, Folse, McManis, and Elias (1989) concluded that, in spite of everything, the quantification of time effects on ultimate pile capacity remains a difficult component in the use of dynamic methods.

2.4.15 Fragaszy, Argo, and Higgins, 1989

In an effort to determine whether the WSDOT should replace the ENR formula with another dynamic pile driving formula for the estimation of ultimate pile capacity, Fragaszy, Argo, and Higgins (1989) studied the relative performance of the following ten formulas: ENR, MSHC Modified ENR, Hiley, Gates, Janbu, Danish, PCUBC, Eytelwein, Weisbach, and Navy-McKay. Using the data collected from 63 static pile load tests conducted in western Washington and northwest Oregon on open and closed ended steel pipe, steel H-shaped, timber, concrete, hollow concrete, and Raymond step-tapered piles, the ratio of the predicted to measured ultimate pile capacity was determined for each test pile using each of the aforementioned dynamic pile driving formulas. In all cases, the measured ultimate pile capacity was defined to be the interception of the line generated by offsetting the pile elastic compression line by a distance equal to the pile diameter divided by 30 with the overall load-settlement curve.

Based upon analyses of the coefficient of variation of the aforementioned ratio for each of the ten investigated dynamic pile driving formulas, Fragaszy, Argo, and Higgins

(1989) found the Gates formula to be the most accurate, and the ENR formula to be among the worst. In fact, the coefficient of variation, which is a normalized measure of dispersion defined as the ratio of the standard deviation to the mean, of the predicted to measured ultimate pile capacity for the ENR formula was approximately two to three times higher than that for the Gates formula. As an alternative comparison, a measure of safety was determined for each formula to be the percentage of piles for which the measured ultimate pile capacity was expected to be lower than the predicted ultimate pile capacity. From this information, the Gates formula was again found to be the best, with the ENR formula once again ranking near the bottom. Finally, Fragaszy, Argo, and Higgins (1989) conducted economic analyses which showed that for the same level of safety, the Gates formula resulted, on average, in higher allowable capacities and consequentially lower foundation costs.

2.4.16 Summary of Comparative Studies

The various comparative studies presented in the preceding subsections clearly indicate that no one dynamic pile driving formula is consistently better than all of the others. Even when specific combinations of pile, hammer, and/or soil type are considered, it is nearly impossible to predict which formula is best suited for a given situation. Nonetheless, it does appear as though the Hiley, Janbu, PCUBC, and Gates dynamic pile driving formulas are better on average than the remaining multitude of formulas in existence. Likewise, the ENR formula seems to be among the worst performing dynamic pile driving formulas in all comparative studies presented, which date back to 1949, save for the investigation carried out by Ramey and Hudgins (1975).

The lack of consistency witnessed between these various comparative studies can be explained by a lack of data quality assurance. In other words, unless static load test datasets are first checked for completeness, validity, consistency, and accuracy, it cannot be expected that the results obtained from applications involving these datasets will provide an actual portrayal of reality. In many of the studies presented in this section, dataset completeness was not maintained when considering soil profile delineation. Besides the obvious fact that some datasets simply did not provide any information on the subsurface profiles in which the various test piles were driven, the generalization of such profiles by the remaining datasets

came without a clear definition of the classification rules applied; thus, yielding inconsistencies in the interpretations obtained from one individual to the next and making reliable soil specific recommendations for the use of dynamic pile driving formulas almost impossible. Furthermore, dataset accuracy and consistency was disregarded on multiple accounts when considering the way in which the measured ultimate pile capacity was obtained from the results of static load tests. More specifically, many datasets presented in this section utilized subjective interpretations of the static load versus pile displacement behavior to define the measured ultimate capacity, which prohibited data reproducibility and introduced an unsystematic statistical bias. Hence, in light of these data quality assurance issues, the inconsistencies observed in the conclusions drawn from one study to the next should come as no surprise.

2.5 LRFD Resistance Factor Calibration Investigations

As mentioned in the introductory chapter of this thesis, one key aspect of the LRFD approach, as it relates to the design of pile foundations, is that uncertainties associated with the applied loads and predicted pile foundation capacities are handled separately through the application of load and resistance factors. Reliability theory can be used to calibrate these load and resistance factors so that a consistent level of reliability is achieved. In the following subsections, reviews of three published investigations will be presented in which statistical parameters, generated by comparative studies similar to those presented in the previous section, were used in differing ways (i.e., first-order, second-moment (FOSM) approach, first-order reliability method (FORM), and Monte Carlo simulations) to calibrate LRFD resistance factors for the construction control of driven pile foundations via dynamic pile driving formulas, given that this is the main focus of this thesis. Although the details associated with the FOSM approach are thoroughly presented in Section 5.2.2, the reader is asked to refer to Ayyub and Assakkaf (1999) and Allen et al. (2005) for detailed descriptions of the FORM and Monte Carlo simulation method, respectively.

2.5.1 McVay et al., 2000

Using the rigorous probability-based framework of the LRFD approach, McVay et al. (2000) evaluated the performance of eight dynamic methods in predicting the ultimate

capacity of driven pile foundations. Of particular interest to this thesis is the fact that four of these eight methods were dynamic pile driving formulas, i.e., ENR, MSHC Modified ENR, Gates, and FDOT. Given that the FDOT formula was not introduced in Section 2.3, it is important to note that it was derived in much the same way as the Gow formula and is reproduced in Eq. (2.70).

$$R_u = \frac{2 \cdot E_h}{s + 0.1 + 0.01 \cdot W_p} \qquad \textit{FDOT Formula} \qquad (2.70)$$

where: E_h = rated hammer energy per blow expressed in foot-tons per blow, and

s = pile penetration distance under one hammer blow, i.e., pile set, expressed in inches per blow.

Based upon measured data obtained from pile static and dynamic load tests carried out on 247 piles of various types (e.g., square concrete, round concrete, pipe, and steel H-shaped), the ratio of the measured ultimate pile capacity, which was defined according to Davisson's (1972) criteria, to the predicted pile capacity (obtained from the four dynamic pile driving formulas) was determined for each of the test piles at the end-of-driving (EOD) and beginning-of-restrike (BOR) conditions. Using the statistical parameters acquired from the distributions of measured to predicted pile capacity ratios for each of the four dynamic pile driving formulas, the first-order, second-moment (FOSM) reliability approach (Thoft-Christensen and Baker 1982) was employed for computation of the respective LRFD resistance factors. As presented by Barker et al. (1991) and Withiam et al. (1997), the FOSM relation for the calculation of LRFD resistance factors, assuming a lognormal distribution for the pile vertical load resistance and only dead and live load effects, can be expressed as follows:

$$\phi = \frac{\bar{\lambda}_R \left(\frac{\gamma_D Q_D}{Q_L} + \gamma_L\right) \sqrt{\frac{\left(1 + COV_{Q_D}^2 + COV_{Q_L}^2\right)}{\left(1 + COV_{\lambda_R}^2\right)}}}{\left(\frac{\bar{\lambda}_{Q_D} Q_D}{Q_L} + \bar{\lambda}_{Q_L}\right) \exp\left\{\beta_T \sqrt{\ln\left[\left(1 + COV_{\lambda_R}^2\right)\left(1 + COV_{Q_D}^2 + COV_{Q_L}^2\right)\right]}\right\}} \qquad (2.71)$$

where: ϕ = resistance factor,

$\bar{\lambda}_R$ = resistance bias factor (the mean ratio of the measured static load test pile capacity, which was based on Davisson's (1972) approach, to the estimated dynamic pile driving formula pile capacity),

COV_{Q_D}, COV_{Q_L} = coefficient of variation (the ratio of the standard deviation, σ, to the mean) of the dead and live loads, repectively,

COV_{λ_R} = coefficient of variation of the resistance bias factor,

β_T = target reliability index,

γ_D, γ_L = dead and live load factors, respectively,

Q_D/Q_L = dead to live load ratio, and

$\bar{\lambda}_D, \bar{\lambda}_L$ = dead and live load bias factors, respectively.

Assuming the same probabilistic characteristics for the dead (D) and live (L) random variables as those used in the *AASHTO LRFD Highway Bridges Design Specifications* (1994) and recapitulated in Table 2.14, a dead to live load ratio of 1.58, which was based on an average bridge span length of approximately 90 feet, and target reliability indices of 1.96 (corresponding to 2.50% probability of failure) and 2.50 (corresponding to 0.62% probability of failure) as recommended by AASHTO (1994) for redundant and non-redundant piles, respectively, McKay et al. (2000) computed LRFD resistance factors for each of the four dynamic pile driving formulas at the EOD and BOR conditions. The associated results have been summarized in Table 2.15 and Table 2.16.

Table 2.14: Load Statistics used by McKay et al. (2000) for the Computation of LRFD Resistance Factors (AASHTO 1994)

Load (Q)	Load Factor (γ)	Load Bias ($\bar{\bar{\lambda}}_Q$)	Coefficient of Variation (COV_Q)	Distribution Type
Dead (D)	1.25	1.08	0.13	Lognormal
Live (L)	1.75	1.15	0.18	Lognormal

Table 2.15: Statistical Details of Dynamic Pile Driving Formula Predictions Performed at EOD Conditions for Driven Piles and Calculated LRFD Resistance and Efficiency Factors (McVay et al. 2000)

Dynamic Pile Driving Formula	N	$\bar{\lambda}_R$	σ_{λ_R}	COV_{λ_R}	β_T = 1.96		β_T = 2.50	
					φ	φ/$\bar{\lambda}_R$†	φ	φ/$\bar{\lambda}_R$
FDOT	72	2.381	1.341	0.563	0.91	0.382	0.67	0.281
ENR	77	0.299	0.159	0.532	0.12	0.405	0.09	0.301
MSHC Modified ENR	61	0.446	0.267	0.599	0.16	0.357	0.12	0.258
Gates	74	1.742	0.787	0.452	0.82	0.472	0.63	0.363

†Efficiency Factor → Indicates the percentage of the measured ultimate pile capacity that can be utilized for design to reach a predefined reliability index.

Table 2.16: Statistical Details of Dynamic Pile Driving Formula Predictions Performed at BOR Conditions for Driven Piles and Calculated LRFD Resistance and Efficiency Factors (McVay et al. 2000)

Dynamic Pile Driving Formula	N	$\bar{\lambda}_R$	σ_{λ_R}	COV_{λ_R}	β_T = 1.96		β_T = 2.50	
					φ	φ/$\bar{\lambda}_R$	φ	φ/$\bar{\lambda}_R$
FDOT	63	2.574	1.293	0.502	1.10	0.429	0.83	0.323
ENR	71	0.235	0.160	0.681	0.07	0.306	0.05	0.215
MSHC Modified ENR	63	0.363	0.246	0.676	0.11	0.308	0.08	0.217
Gates	71	1.886	0.715	0.379	1.02	0.541	0.81	0.429

Based upon these results, McVay et al. (2000) concluded that the accuracy of any dynamic pile driving formula or, to be more general, any pile bearing capacity estimation method is indicated by the coefficient of variation of the pile vertical load resistance and not the absolute value of the LRFD resistance factor. This is due in large part to the fact that each method is defined by its own bias factor, i.e., the mean ratio of measured to predicted ultimate pile capacity. In other words, an under predictive method ($\bar{\lambda}_R$ < 1) infers that the method contains a "built-in" safety margin and hence a higher resistance factor is required to achieve the same target reliability as would be obtained from a method that predicts, on average, more accurately the ultimate pile capacity ($\bar{\lambda}_R \approx 1$). With this in mind, McVay et al. (2000) found that the Gates formula was the most accurate of the four dynamic pile driving formulas analyzed, with the ENR and MSHC Modified ENR formulas displaying the worst accuracy. In accordance with these findings, the Gates formula was also found to be the most efficient or economical of the four dynamic pile driving formulas analyzed based on comparisons of the efficiency factors (φ/$\bar{\lambda}_R$) presented in Table 2.15 and Table 2.16, with the

ENR and MSHC Modified ENR formulas again displaying poor performance. Finally, although testing at the BOR condition provides important information on the issue of soil/pile set-up, it was shown that such testing provides no increase in the accuracy or efficiency of a particular dynamic pile capacity estimation method; in fact, testing at the BOR condition only alters the bias and recommended resistance factors for a given method. As a result, it was recommended that dynamic pile driving formulas be used with the EOD condition considering the fact that testing at the BOR condition may introduce addition costs as well as production delays.

2.5.2 Paikowsky et al., 2004

With the intent of rewriting AASHTO's Deep Foundation Specifications, National Cooperative Highway Research Program (NCHRP) Project 24-17, which was led by Samuel G. Paikowsky of the University of Massachusetts, evaluated the performance of various static and dynamic analysis methods in predicting the ultimate capacity of driven pile foundations. Of particular interest to this thesis is the fact that three of the dynamic analysis methods analyzed were dynamic pile driving formulas, i.e., ENR, Gates, and FHWA Modified Gates. Moreover, LRFD resistance factors were developed for the various methods using statistical analyses compatible with common practice in the field of structural engineering.

Using measured data obtained from pile static and dynamic load tests carried out on 210 driven piles of various types (e.g., 37 steel H-shaped, 10 open-ended steel pipe, 61 closed-ended steel pipe, 35 voided concrete, 60 square concrete, three octagonal concrete, two timber, and two Monotube piles), the ratio of the measured ultimate pile capacity, which was defined according to Davisson's (1972) criteria, to the predicted ultimate pile capacity obtained from the three dynamic pile driving formulas was determined for each of the test piles at the EOD and BOR conditions, when applicable. Via the statistical parameters acquired from the distributions of measured to predicted pile capacity ratios for each of the three dynamic pile driving formulas, the first-order reliability method (FORM) approach, as developed by Hasofer and Lind (1974), was used for computation of the respective LRFD resistance factors. As stated previously, this invariant approach was deemed necessary on account of the consistency provided with the current structural code. Although the FORM approach requires only first and second moment information on resistances and loads (i.e.,

means and variances) and an assumption of distribution shape (e.g., normal, lognormal, etc.), the actual calibration process is quite complex and involves an iterative approach.

Assuming the same probabilistic characteristics for the dead and live random variables as those used in the *AASHTO LRFD Bridge Design Specifications* (2000) and recapitulated in Table 2.17, a dead to live load ratio of 2.00, and target reliability indices of 2.33 (corresponding to 1.00% probability of failure) and 3.00 (corresponding to 0.10% probability of failure) for redundant and non-redundant pile cap configurations, respectively, Paikowsky et al. (2004) computed LRFD resistance factors for each of the three aformentioned dynamic pile driving formulas at a general time-of-driving condition (i.e., the EOD and BOR data was not handled separately for such LRFD resistance factor computations). The associated results have been summarized in Table 2.18, which were ultimately used by AASHTO to recommend resistance factors of 0.40 and 0.10 for the FHWA Modified Gates and ENR formulas, respectively, in the 2007 version of the *AASHTO LRFD Bridge Design Specifications*.

Table 2.17: Load Statistics used by Paikowsky et al. (2004) for the Computation of LRFD Resistance Factors (AASHTO 2000)

Load (Q)	Load Factor (γ)	Load Bias ($\bar{\bar{\lambda}}_Q$)	Coefficient of Variation (COV_Q)	Distribution Type
Dead (D)	1.25	1.05	0.10	Lognormal
Live (L)	1.75	1.15	0.20	Lognormal

Table 2.18: Statistical Details of Dynamic Pile Driving Formula Predictions Performed at EOD and BOR Conditions for Driven Piles and Calculated LRFD Resistance and Efficiency Factors (Paikowsky et al. 2004)

Dynamic Pile Driving Formula	N	$\bar{\lambda}_R$	σ_{λ_R}	COV_{λ_R}	β_T = 2.33		β_T = 3.00	
					φ	$\varphi/\bar{\lambda}_R$	φ	$\varphi/\bar{\lambda}_R$
ENR	384	1.602	1.458	0.910	0.26	0.162	0.15	0.094
Gates	384	1.787	0.849	0.475	0.73	0.409	0.53	0.297
FHWA Modified Gates	384	0.940	0.472	0.502	0.36	0.383	0.26	0.277

Based upon these results, Paikowsky et al. (2004) concluded that most dynamic pile capacity estimation methods used for the construction control of driven pile foundations tend to underpredict the measured ultimate pile capacity obtained from static load testing.

Conversely, most static pile capacity estimation methods used for the design of driven pile foundations were found to over-predict the measured ultimate pile capacity obtained from static load testing. By way of these findings, Paikowsky et al. (2004) demonstrated the shortcomings of safety evaluation based solely on resistance factors and the need for an efficiency measurement index to objectively assess the performance of various analysis methods. In accordance with the recommendations provided by McVay et al. (2000), Paikowsky et al. (2004) recommends the use of an efficiency factor ($\varphi/\bar{\lambda}_R$) to account for the bias of the analysis method as well as to provide an objective evaluation regarding the effectiveness of the pile capacity estimation method. With this in mind, Paikowsky et al. (2004) found that the Gates formula was the most efficient of the three dynamic pile driving formulas analyzed, with the ENR formula displaying the worst efficiency. Furthermore, although testing at the BOR condition can provide important information regarding the issue of soil/pile set-up, Paikowsky et al. (2004) did not handle this condition separately in the establishment of LRFD resistance factors for dynamic pile driving formulas. In other words, the LRFD resistance factors recommended in the NCHRP 507 report for dynamic pile driving formulas were developed using both EOD and BOR data; an approach that has the potential to yield misleading resistance bias and efficiency factors for the pile capacity estimation methods investigated on account of the many-to-one nature of the employed dataset, where the predicted and measured pile capacities represent members of the domain and range, respectively.

2.5.3 Allen, 2005

Using the results of a 1996 in-house study focused on updating the pile driving formula used for pile driving acceptance in the WSDOT Standard Specifications, Allen used Monte Carlo simulations to perform the reliability analyses required for the development of LRFD resistance factors for the WSDOT dynamic pile driving formula. Additionally, the FHWA Modified Gates and ENR dynamic pile driving formulas were analyzed and LRFD resistance factors were developed and recommended for these methods as well.

Based upon measured data obtained from pile static load tests carried out on 131 piles of various types (e.g., closed-ended steel pipe, open-ended steel pipe, concrete, and steel H-shaped), in both end-bearing and friction pile situations, and containing penetration

resistance values (i.e., blow count values) at the EOD and BOR conditions, the ratio of the measured ultimate pile capacity, which was defined according to Davisson's (1972) criteria, to the predicted pile capacity obtained from the three aforementioned dynamic pile driving formulas was determined for each of the test piles at the EOD condition. Using the statistical parameters acquired from theoretical distributions that were best-fit to the tail regions of the measured to predicted pile capacity ratio sample distributions for each of the three dynamic pile driving formulas, Monte Carlo simulations, as described by Allen et al. (2005), were used to estimate the reliability index, β, and the LRFD resistance factor, φ, needed to achieve the target value of β (i.e., either 2.33 or 3.00 for redundant and non-redundant pile cap configurations, respectively).

Assuming the same probabilistic characteristics for the dead and live random variables as those used in the *AASHTO LRFD Bridge Design Specifications* (2006) and recapitulated in Table 2.19 and dead to live load ratios ranging from 2.00 to 5.00, Allen (2005) computed LRFD resistance factors for each of the three aformentioned dynamic pile driving formulas using the estimated developed energy of the pile driving hammer, as opposed to the rated hammer energy, at the EOD condition. The associated results have been summarized in Table 2.20.

Table 2.19: Load Statistics used by Allen (2005) for the Computation of LRFD Resistance Factors (AASHTO 2006)

Load (Q)	Load Factor (γ)	Load Bias ($\bar{\bar{\lambda}}_Q$)	Coefficient of Variation (COV_Q)	Distribution Type
Dead (D)	1.25	1.05	0.10	Normal
Live (L)	1.75	1.15	0.18	Normal

Table 2.20: Statistical Details of Dynamic Pile Driving Formula Predictions Performed at EOD Conditions for Driven Piles and Calculated LRFD Resistance Factors (Allen 2005)

Dynamic Pile Driving Formula	N	$\bar{\lambda}_R$	σ_{λ_R}	COV_{λ_R}	φ at β_T = 2.33 for Q_D/Q_L =			φ at β_T = 3.00 for Q_D/Q_L =
					2	3	5	3
WSDOT	131	0.850	0.190	0.224	0.61	0.60	0.59	0.50
FHWA Modified Gates	131	0.970	0.345	0.356	-	0.51	-	0.40
ENR	131	0.280	0.130	0.464	-	0.11	-	0.08

Based upon these results, Allen (2005) concluded that the dead to live load ratio has only a minor effect on the magnitude of the resistance factor required to achieve a predetermined target reliability index. Allen (2005) also noted that this is most likely due to the fact that the uncertainty in the dead and live load random variables is much less than the uncertainty in the pile vertical resistance random variable. Consequently, it was considered feasible by Allen (2005) to recommend one resistance factor that was independent of the dead to live load ratio for each dynamic pile driving formula analyzed. Allen's (2005) final recommendations on LRFD resistance and efficiency factors for two of the three pile driving formulas investigated have been reproduced in Table 2.21. Although a resistance factor was initially determined for the ENR formula, as seen in Table 2.20, Allen (2005) does not recommend that the ENR formula be used for the construction control of driven pile foundations on account of the large degree of uncertainty associated with the method; therefore, a LRFD resistance factor was not given for this dynamic pile driving formula in Table 2.21. Lastly, when comparing the WSDOT and FHWA Modified Gates formulas, Allen (2005) notes that the WSDOT formula provides the least amount of relative conservatism and is thus the most efficient method of the two.

Table 2.21: Recommended LRFD Resistance and Efficiency Factors for the Construction Control of Driven Pile Foundations using the Estimated Developed Hammer Energy at the EOD Condition (Allen 2005)

Dynamic Pile Driving Formula	β_T = 2.33		β_T = 3.00	
	φ	$\varphi/\bar{\lambda}_R$	φ	$\varphi/\bar{\lambda}_R$
WSDOT	0.55	0.647	0.45	0.529
FHWA Modified Gates	0.45	0.464	0.40	0.412

2.5.4 Summary of LRFD Investigations

The various investigations presented in the preceding subsections indicate that there exists three main approaches for the performance of reliability analyses required for the development of LRFD resistance factors for pile bearing capacity estimation methods; i.e., FOSM, FORM, and Monte Carlo simulations. Although each of these three reliability approaches will generate LRFD resistance factors in such a way as to ensure a consistent level of reliability is achieved, the performance of any given pile bearing capacity estimation

method should not be assessed by the magnitude of these values alone. In other words, an efficiency measurement index (i.e., efficiency factor) should be used so that the bias of a particular pile capacity estimation method is accounted for; thus, leading to an objective evaluation regarding the effectiveness of a given pile capacity estimation method. Based on these efficiency factors, both McVay et al. (2000) and Paikowsky et al. (2004) found that the Gates formula was the most efficient or economical of the dynamic pile driving formulas analyzed in each study for the construction control of driven pile foundations. Allen (2005), on the other hand, did not consider the original Gates formula in his analysis, but found an enhanced version of this formula (i.e., the WSDOT formula), which specifically addressed energy transfer efficiencies for particular hammer and pile type combinations, to be the most efficient or economical. Moreover, all three investigations presented in this section found the ENR formula to be the least efficient of the dynamic pile driving formulas analyzed. A summary of the LRFD resistance and efficiency factors developed under the three investigations presented in this section for various dynamic pile driving formulas has been provided in Table 2.22 for completeness.

Table 2.22: Summary of Recommended LRFD Resistance and Efficiency Factors for Dynamic Pile Driving Formulas at the EOD Condition and Redundant Pile Cap Configurations

Dynamic Pile Driving Formula	(McVay et al. 2000)		(Paikowsky et al. 2004)		(Allen 2005)	
	φ	$\varphi/\bar{\lambda}_R$	φ	$\varphi/\bar{\lambda}_R$	φ	$\varphi/\bar{\lambda}_R$
FDOT	0.91	0.382	-	-	-	-
ENR	0.12	0.405	0.26	0.162	-	-
MSHC Modified ENR	0.16	0.357	-	-	-	-
Gates	0.82	0.472	0.73	0.409	-	-
FHWA Modified Gates	-	-	0.36	0.383	0.45	0.464
WSDOT	-	-	-	-	0.55	0.647

As with the comparative studies presented in Section 2.4, the three investigations summarized in this section failed to comment on the quality of data used in the calibration of their respective LRFD resistance factors. Although Davisson's (1972) objective criteria was consistently used in each study to define the measured ultimate pile capacity, a clear definition of the classification rules applied for the generalization of the subsurface profiles

in which the various test piles were driven was lacking. Thus, these three static load test datasets were incomplete, allowing room for inconsistencies in the interpretations obtained from one individual to the next and making reliable soil specific resistance factor recommendations almost meaningless. In other words, the assurance of data quality is an important task in any study to guarantee that the corresponding results provide as actual a portrayal of reality as is humanly possible. As a final point, none of the investigations presented in this or the preceding section attempted to actually quantify how the energy imparted by one hammer blow is dissipated by a specific pile-soil system; a reality that is fundamental to the understanding of why or how one dynamic pile driving formula is superior to all the rest.

CHAPTER 3: STATE OF THE PRACTICE AND PILOT-IA DEVELOPMENT

3.1 INTRODUCTION

Before comparative analyses and subsequent LRFD resistance factor calibration efforts can be carried out on a predetermined set of the most commonly used dynamic pile driving formulas, a comprehensive review of lessons learned from LRFD pile foundation design practices in other states as well as a historical perspective on the driven pile foundation design process adopted by the Iowa DOT is first examined. Given this current state of practice, historical and recent pile load test data obtained in the State of Iowa is then formulated to aid with the performance of the aforementioned comparative analyses and LRFD resistance factor calibration efforts. Thus, for delineation of the current state of practice, this chapter presents the major findings associated with a nationwide survey of state DOTs as well as a local survey of Iowa county engineers and consulting firms involved in the design of county bridge foundations. Additionally, this chapter provides a detailed description of the database for PIle LOad Tests in Iowa (PILOT-IA), which is an amalgamated, electronic source of information consisting of both static and dynamic data for pile load tests conducted in the State of Iowa. By ensuring consistency and quality, the PILOT-IA formulation was intended for use in the establishment of LRFD resistance factors for the design and construction control of driven pile foundations.

3.2 NATIONWIDE SURVEY OF STATE DOTS

In order to determine the current design and construction practices of deep foundations nationwide, a study was conducted by means of a web-based survey. In addition to the basic questions related to the implementation of the LRFD methods in bridge foundation design practice, information on design and construction practices of bridge deep foundations was gathered and analyzed in the following topic areas: (1) pile analysis and design, (2) pile drivability, (3) pile design verification methods, and (4) quality control of pile construction. Although the main conclusions of this survey, which was the first of its kind to be conducted following the FHWA's policy memorandum requiring all new bridges initiated after October 1, 2007, to be designed according to the LRFD approach, have been

presented herein, the reader is referred to AbdelSalam et al. (2010) for a comprehensive documentation of the major findings of this survey. Based on the responses received from the FHWA Eastern Federal Lands Highway Division, Alberta (Canada) Infrastructure and Transportation, and 31 different state DOTs, the important conclusions drawn from the study are as follows:

1) As of June 2008, 52% of the state DOTs whom responded to the survey have already adopted the LRFD approach for the design of bridge deep foundations, while 33% are in a transition phase from ASD to LRFD and the remaining 15% still follow the ASD approach with a factor of safety ranging from 2 to 2.5. Of those currently using the LRFD approach, six state DOTs are using geotechnical resistance factors obtained from fitting to ASD calibration efforts, eight state DOTs are following the recommendations provided in the *AASHTO LRFD Bridge Design Specifications* (2007), and twelve state DOTs have adopted their own regionally calibrated LRFD resistance factors using reliability theory.
2) A summary of the reported regionally calibrated geotechnical LRFD resistance factors is provided in Tables 3.1, 3.2, 3.3, and 3.4. As observed in these summary tables, the LRFD regionally calibrated resistance factors reported for piles driven in sand and clay type soils are either equal to or greater than the values recommended in the *AASHTO LRFD Bridge Design Specifications* (2007). More specifically, for piles driven in sand soils, the reported LRFD resistance factors are as much as 50% greater than those recommended in the *AASHTO LRFD Bridge Design Specifications* (2007), while for piles driven in clay soils, the reported LRFD resistance factors are as much as 100% greater than those recommended in the *AASHTO LRFD Bridge Design Specifications* (2007). As one may surmise, such large increases in geotechnical LRFD resistance factors will ultimately lead to an overall reduction in the cost of bridge deep foundations.

Table 3.1: Summary of Responses to a Nationwide Survey on the use of LRFD for Bridge Deep Foundations (AbdelSalam et al. 2010)

State	Soil/Rock Type	Pile Type	Static Analyses		Dynamic Analyses	Dynamic Formulas	Reported LRFD Resistance Factors					
			Cohesive	Cohesionless			Sand	Clay	Mixed	Glacial	Loess	Alluvial
AK	Alluvium	CIDH[1]	α-Method	SPT Method	Not Used	Not Used	0.45	N/A	N/A	N/A	N/A	N/A
CA	Glacial	Steel H-Piles	CPT Method	Nordlund	P + C + W[2]	FHWA-G[3]	0.45	0.35	N/A	N/A	N/A	N/A
CO	Alluvium	CIDH	SPT Method	SPT Method	P + C + W	ENR, G[4], FHWA-G	0.10	0.90	0.50	0.30	0.70	0.70
CT	Limestone	Prestressed	In-House	In-House	P + C + W	Not Used	0.65	0.65	0.65	N/A	N/A	N/A
FL	Alluvium	CIDH	CPT Method	Nordlund	P + C + W	In-House	0.65	0.65	0.65	0.65	0.65	0.65
HI	Mud	Steel H-Piles	β-Method	β-Method	P + C + W	Not Used	0.65	0.65	0.65	0.65	0.65	0.65
IA	Glacial	Steel H-Piles	In-House	In-House	Not Used	Not Used	0.73	0.73	0.73	0.73	0.73	0.73
ID	Alluvium	Steel H-Piles	β-Method	SPT Method	P + C + W	FHWA-G	0.45	0.45	0.45	N/A	N/A	0.45
IL	Alluvium	Open-Ended Pipe	α-Method	Nordlund	Not Used	Not Used	0.70	0.70	0.70	N/A	N/A	0.70
MA	N/A	Open-Ended Pipe	In-House	Nordlund	P + C + W	Not Used	0.65	0.65	0.65	0.65	0.65	0.65
NH	Glacial	Closed-Ended Pipe	α-Method	Nordlund	P + C + W	Not Used	0.45	0.35	N/A	N/A	N/A	N/A
NJ	Alluvium	CIDH	α-Method	Nordlund	P + C + W	Not Used	0.45	0.35	0.40	N/A	N/A	N/A
NM	Alluvium	Steel H-Piles	β-Method	Nordlund	P + C + W	ENR, G, FHWA-G	0.35	0.45	N/A	N/A	N/A	N/A
NV	N/A	Steel H-Piles	α-Method	Nordlund	Not Used	Not Used	0.35	0.25	N/A	N/A	N/A	N/A
PA	Alluvium	Steel H-Piles	β-Method	Nordlund	P + C + W	Not Used	0.50	0.50	0.50	0.50	0.50	0.50
PA	Alluvium	Steel H-Piles	λ-Method	SPT Method	P + C + W	Not Used	0.45	0.55	0.55	0.50	0.50	0.50
UT	Alluvium	Steel H-Piles	α-Method	Nordlund	Not Used	Not Used	0.50	0.70	0.70	0.50	0.50	0.50
WA	Glacial	Steel H-Piles	In-House	In-House	WEAP	FHWA-G	0.50	0.50	0.50	0.50	0.50	0.50
WY	Alluvium	Steel H-Piles	CPT Method	Nordlund	Not Used	Not Used	0.45	0.35	0.35	0.35	N/A	0.35

[1]CIDH = Cast-In-Drilled-Hole Shaft; [2]P + C + W = PDA, CAPWAP, and WEAP; [3]FHWA-G = FHWA Modified Gates Formula; and [4]G = Gates Formua

Table 3.2: Mean Values and Standard Deviations of the Reported Regional LRFD Resistance Factors According to Different Pile and Soil Types (AbdelSalam, Sritharan, and Suleiman 2010)

Pile Type	Reported Factors in Sand			Reported Factors in Clay			Reported Factors in Mixed Soil		
	N[1]	Mean	S.D.[2]	N	Mean	S.D.	N	Mean	S.D.
Steel H-Shaped	11	0.48	0.11	12	0.48	0.15	8	0.55	0.13
CIDH	4	0.40	0.23	3	0.60	0.28	3	0.50	0.13
Open-Ended Pipe	2	0.65	N/A	2	0.67	N/A	2	0.67	N/A

[1]N = Sample Size
[2]S.D. = Standard Deviation

Table 3.3: Mean Values and Standard Deviations of the Reported Regional LRFD Resistance Factors According to Different Static Analysis Methods and Soil Types (AbdelSalam, Sritharan, and Suleiman 2010)

Static Analysis Method	Reported Factors in Sand			Reported Factors in Clay			Reported Factors in Mixed Soil		
	N	Mean	S.D.	N	Mean	S.D.	N	Mean	S.D.
Nordlund	11	0.50	0.12	-	-	-	4	0.53	0.17
SPT Method	3	0.45	0.25	-	-	-	3	0.53	0.11
α-Method	-	-	-	6	0.47	0.19	-	-	-
β-Method	-	-	-	4	0.49	0.13	-	-	-
CPT Method	-	-	-	3	0.45	0.17	-	-	-
In-House	3	0.62	0.11	4	0.63	0.10	3	0.62	0.11

Table 3.4: Comparison of the Reported Regional LRFD Resistance Factors with those Recommended in the NCHRP 507 Report and the *2007 AASHTO LRFD Bridge Design Specifications* (AbdelSalam, Sritharan, and Suleiman 2010)

Soil Type	Static Analysis Method	NCHRP 507 (Paikowsky et al. 2004)	AASHTO (2007)	Mean of Reported Resistance Factors
Sand	SPT Method	0.45	0.30	0.45
	β-Method	0.30	N/A	0.65
	Nordlund	0.45	0.45	0.50
	In-House	N/A	N/A	0.62
Clay	α-Method	0.45	0.35	0.47
	β-Method	0.20	0.25	0.49
	In-House	N/A	N/A	0.63

3) In the design stages of a deep foundation project, state DOTs are using static analysis methods to determine the ultimate driven pile capacities. For cohesive soils, the most commonly used methods are the α- and β-methods. Alternatively, for cohesionless soils, the most commonly used methods are the Nordlund and SPT methods. Furthermore, most of the respondents chose the α-method and the Nordlund method to be the most accurate methods for predicting the ultimate capacity of piles driven in cohesive and cohesionless soils, respectively.
4) During the construction of deep foundations, state DOTs employ either a dynamic analysis method or a dynamic pile driving formula to verify the pile capacity estimated by a static analysis method in the design stages. Although all of the respondents noted that they use WEAP as a dynamic analysis method, 75% of respondents indicated that they use a combination of PDA and CAPWAP in addition to WEAP. Of those respondents using dynamic pile driving formulas for driven pile capacity verification, the majority either use the FHWA Modified Gates formula or a locally developed/enhanced formula.

3.3 LOCAL SURVEY OF IOWA COUNTY ENGINEERS

To determine the present pile design and construction practices at the county-level and understand how they differ from those at the state-level, a study of Iowa county engineers as well as consulting firms involved in the design of county bridge foundations was conducted by means of a web-based survey. By way of this survey, information was collected regarding the design method, dynamic pile driving formulas, and analysis procedures used for driven pile foundation design. More specifically, this survey acquired the aforementioned general information via an organizational structure defined by the following four focal areas: (1) foundation practice, (2) timber pile usage, (3) pile analysis and design, and (4) drivability, testing, and quality control. In the following subsections, the major results of this survey, which received complete responses from engineers located in 44 different counties within the State of Iowa, as seen in Figure 3.1, and eight civil engineering consulting firms, will be presented, first for the responding Iowa county engineers according to the four focal areas previously delineated, and then for the responding consulting firms.

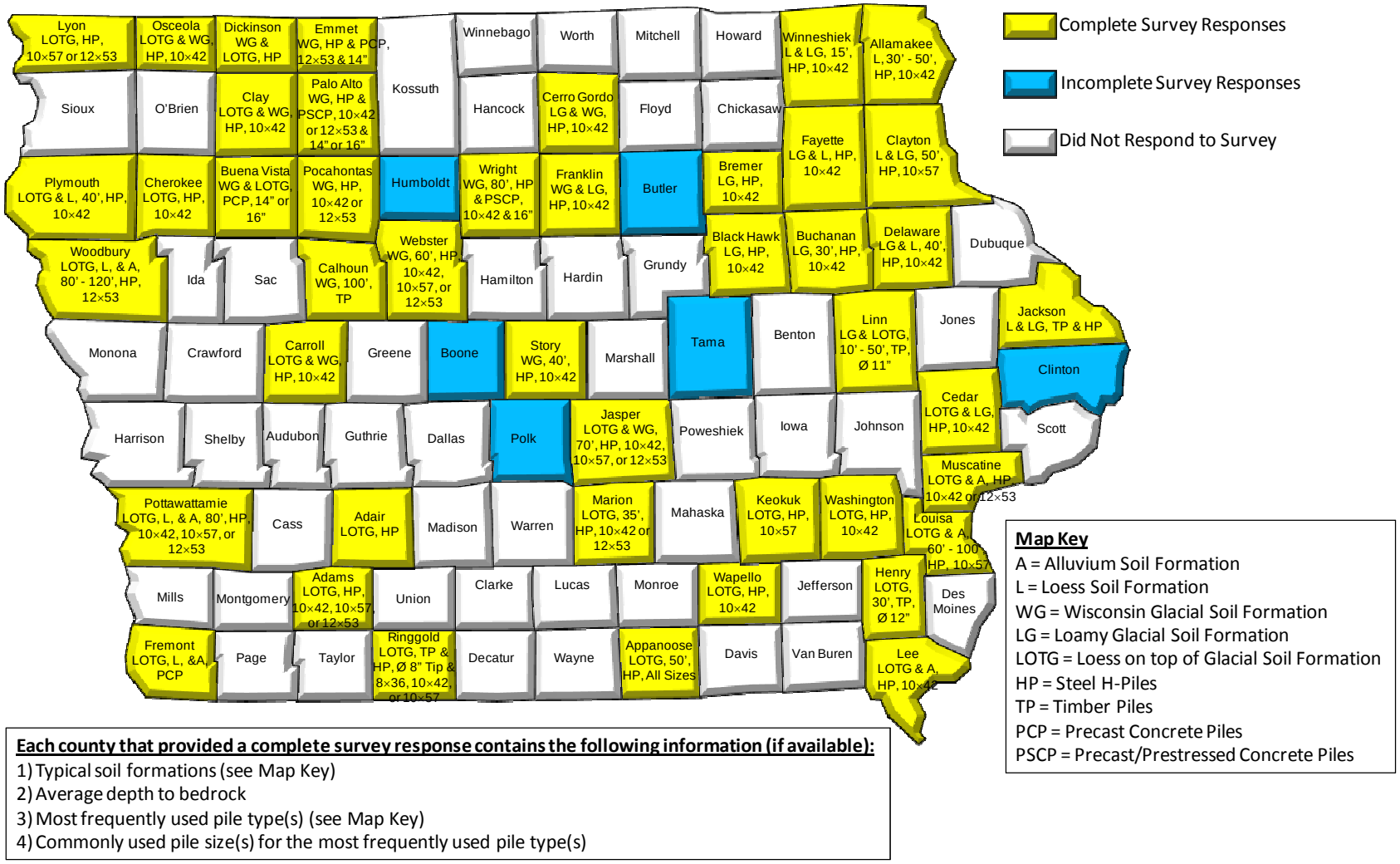

Figure 3.1: Iowa County Map Showing Survey Respondents, Typical Soil Formations, Average Depth to Bedrock, and Most Frequently Used Pile Types and Sizes

3.3.1 Foundation Practice

The questions contained within this first section of the survey focused on obtaining information regarding typical soil formations, average depths to bedrock, routine soil in-situ and laboratory tests, the main criteria used for the selection of a given type of driven pile, the most commonly used types of driven piles, as well as the selection potential of drilled shafts over driven piles on future bridge projects. Figure 3.1 presents a summary of results obtained for the common foundation practice in different Iowa counties. Included in this figure are the typical soil formations, the average depth to bedrock, and the most frequently used pile types and sizes. It is important to point out that the soil formations identified for each county in Figure 3.1 were determined based on the survey responses as well as the typical soil formations found in geological maps (NRCS 2010). Furthermore, for questions regarding the use of in-situ and/or laboratory tests to establish soil parameters for pile design, 61% of respondents indicated that no such tests are performed, while the remaining 39% unanimously cited the use of the Standard Penetration Test (SPT), despite its subjective nature.

Based upon the responses received, as summarized in Figure 3.2, it was found that 54.5% of Iowa county engineers rely on past design experience when it comes to the selection of a given type of driven pile foundation, whereas 18.2% cited economy as the main criterion, 15.9% stated that the selection criteria differs between projects, 13.6% reported using the same type of driven pile foundation for all bridge projects, 9.1% cited available construction equipment as the main criteria, and the remaining 11.4% stated that a particular selection criteria other than those defined formerly was used.

With all respondents preferring the use of driven pile foundations for present and future applications over drilled shafts, no further information was obtained regarding the percentage of usage of different types of drilled shafts. However, a distribution of the most commonly used types of driven pile foundations for bridge type structures was attained and is presented in Figure 3.3. Explicitly put, all respondents indicated the use of steel H-shaped piles, while 43.2% indicated the use of timber piles, 22.7% cited the use of precast concrete piles, 20.5% reported the use of prestressed concrete piles, 2.3% indicated the use of closed-ended steel pipe piles, and the remaining 2.3% reported the use of driven pile types other

than those defined formerly. Although the unanimous use of steel H-shaped piles by respondents of this survey is consistent with the results obtained at the state-level (AbdelSalam et al. 2010), the significant use of timber piles as a foundation practice was not found in the state-level survey; thus, providing valuable new insight into the pile foundation practice of Iowa.

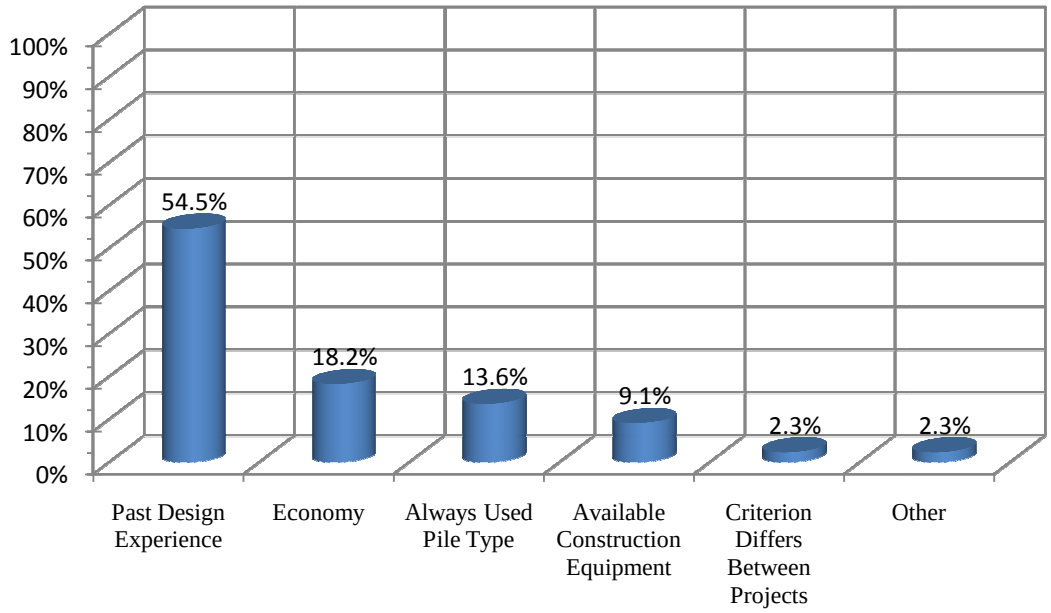

Figure 3.2: Main Criterion Used for Driven Pile Type Selection

Furthermore, the respondents were asked to identify the most common pile size(s) used for the pile types reported in Figure 3.3. This information has been included in Figure 3.1, which shows that steel H-shaped piles are commonly used in almost all Iowa counties. However, in North Central Iowa where the soil formation is mainly defined as glacial till, precast and prestressed concrete piles are also used with increased frequency. Likewise, in East Central Iowa where the soil formation is mainly composed of loess and glacial tills, timber piles are used with more frequency.

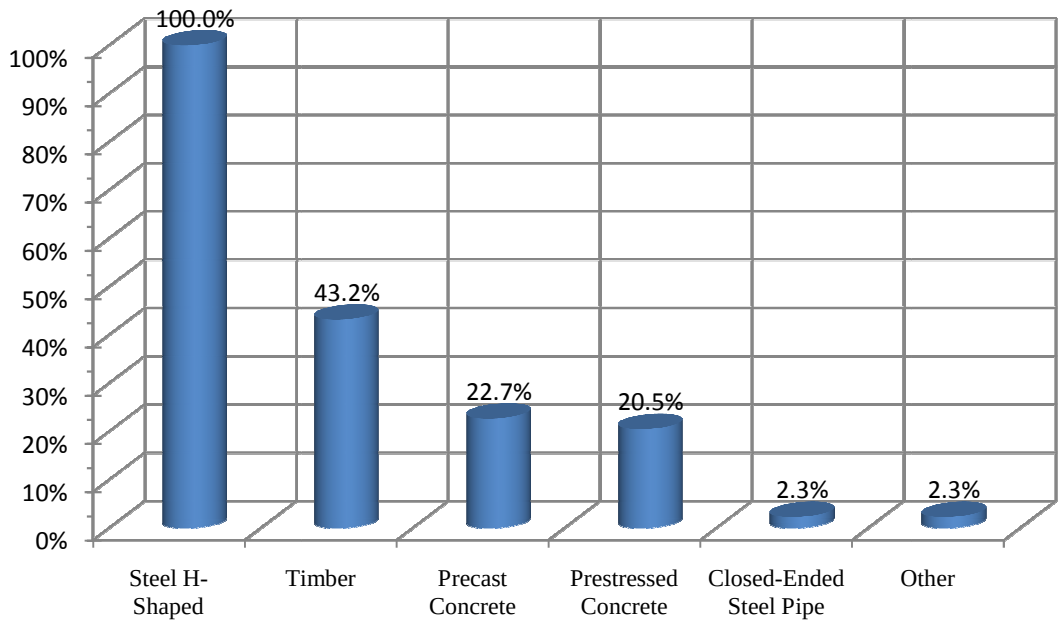

Figure 3.3: Distribution of the Most Commonly Used Types of Driven Pile Foundations for Bridge Type Structures

3.3.2 Timber Pile Usage

In this second section of the survey, questions were asked to those who had reported the use of timber type driven pile foundations to justify the need to establish regional LRFD resistance factors for this specific pile type. These questions gathered information regarding the bridge types recommended for support by a deep foundation system consisting of driven timber piles as well as the soil types recommended for use with driven timber piles. Based upon the responses received (see Figure 3.4), it was found that 72.2% of Iowa county engineers use a deep foundation system comprised of timber piles to support low-volume bridges, 55.6% use such a pile type for short span bridges, 16.7% do not recommend the use of deep foundation systems comprised of timber piles for bridge type structures, and 5.6% use such a pile type for pedestrian bridges. The findings associated with the soil types recommended for use with driven timber piles, the results were widespread, as shown in Figure 3.5, and no one soil type is recommended over another.

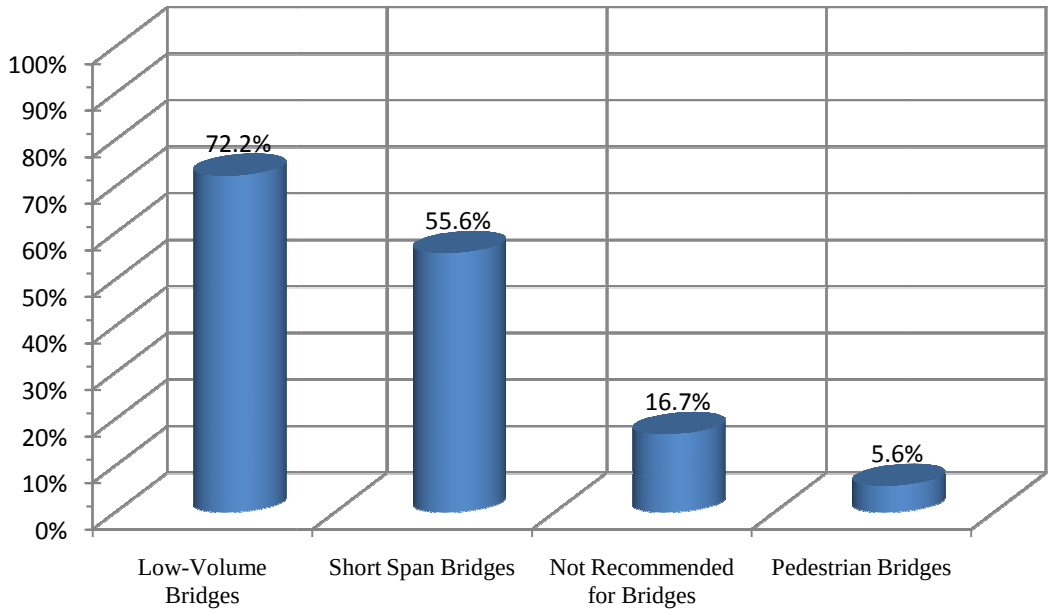

Figure 3.4: Distribution of Bridge Types Recommended for Support by Deep Foundation Systems Comprised of Driven Timber Piles

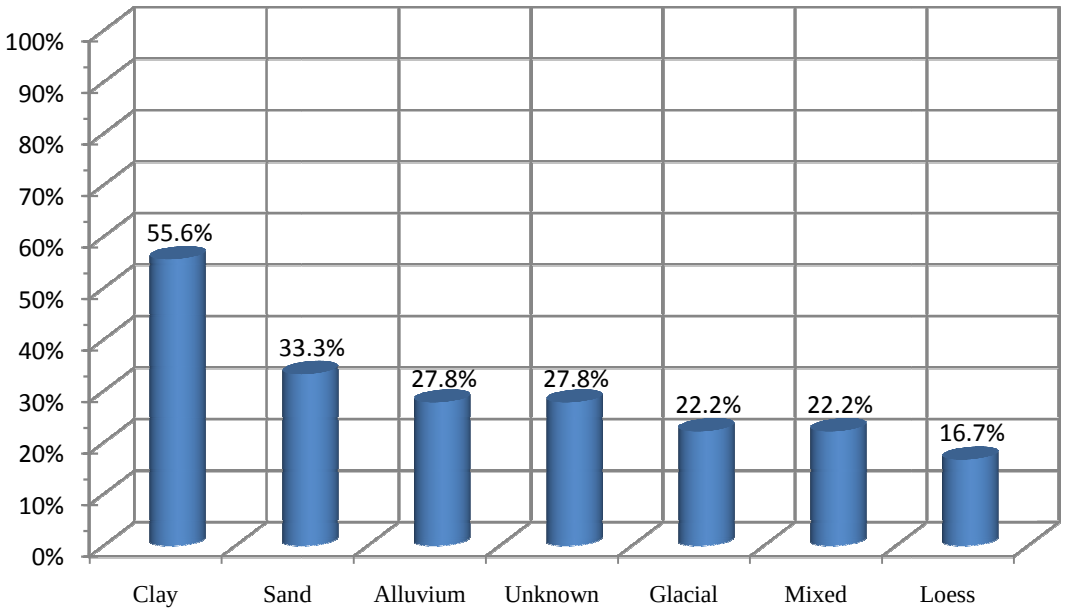

Figure 3.5: Distribution of Soil Types Recommended for Use with Driven Timber Piles

3.3.3 Pile Analysis and Design

For the pile analysis and design section of the survey, the questions were directed to obtain information regarding the individuals responsible for the design of driven pile foundations for bridge type structures, the specifications used for their design, and the method of analysis most commonly called upon for driven pile foundation design. Based upon the responses received, it was found that 59% of Iowa county engineers actually perform the design of driven pile foundations for bridge type structures themselves, whereas 39% enlist the services of private engineering consulting firms and the remaining 2% seek the aid of the Iowa DOT or an outside agency for their design.

For those Iowa county engineers whom reportedly perform the design of driven pile foundations for bridge type structures themselves, 73% cited the *Iowa County Bridge Standards* (Iowa DOT 2009) as their primary driven pile design specification, 15% acknowledged use of the *Iowa ASD/LFD Bridge Design Manual* (Iowa DOT 2010), 4% made use of the *AASHTO LRFD Bridge Design Specifications* (2007), and the remaining 8% cited pile design specifications other than those defined formerly. It is important to point out that the aforementioned list of primary driven pile design specifications utilized by Iowa county engineers does not include the *Iowa LRFD Bridge Design Manual* (Iowa DOT 2010).

On the other hand, for those Iowa counties reporting the enlistment of private engineering consulting firms for the performance of driven pile design procedures, 45% solicited the services of Calhoun-Burns & Associates, Inc. (CB&A); 14% made use of the services offered by HGM Associates, Inc.; 9% enlisted either the assistance of IIW Engineers and Surveyors, PC (IIW), Shuck-Britson, Inc., or Kirkham Michael, Inc.; 5% solicited the services of either Terracon Consultants, Inc. or Sundquist Engineering, PC; and the remaining 4% made use of the services offered by WHKS & Co., as presented in Figure 3.6. Given this information, an enhanced version of the survey issued to the Iowa county engineers was sent to the aforementioned private engineering consulting firms to better understand the county-level foundation design practice in Iowa. The results of this survey have been presented in Section 3.3.5.

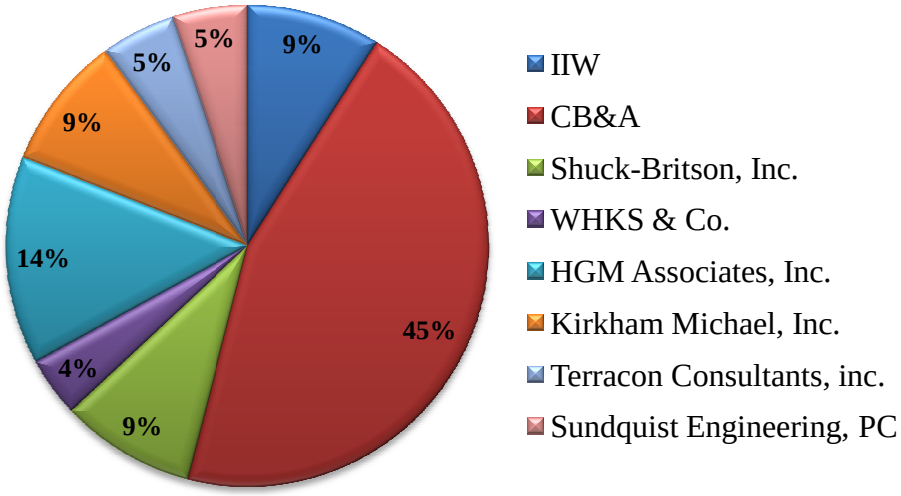

Figure 3.6: Private Engineering Consulting Firms Enlisted by Iowa Counties for the Performance of Driven Pile Foundation Design Procedures

Finally, in regards to the method of analysis most commonly used by Iowa county engineers for the design of driven pile foundations, 86% of respondents cited the use of dynamic pile driving formulas for this particular task, with the remaining 14% reporting the use of static analysis methods. In particular, the unanimous dynamic pile driving formula of choice for the design of driven pile foundations by Iowa county engineers was the ENR formula, which has been shown in Chapter 2 to be inappropriate since about 1950, with the unanimous static analysis method of choice being the α-method regardless of the foundation soil type.

3.3.4 Drivability, Testing, and Quality Control

The questions contained within this final section of the survey focused on obtaining information regarding the methods for determining pile driving termination, the use of static pile load tests for design verification, and the frequency of performance of quality control tests. Based upon the responses received, it was found that 61.4% of Iowa county engineers use a WEAP analysis and field observations to determine the termination of the pile driving process, 29.5% make use of dynamic pile driving formulas for this same purpose, and 9.1% rely on the initial results produced by static analysis methods in the design stages of the project and consequently make no adjustments to the lengths of production piles, as presented in Figure 3.7. Interestingly, 15.9% of respondents noted that they drive piles until

refusal regardless of the pile penetration length estimated in the design stages of the project, where pile refusal is defined by an observed penetration of less than one inch per ten hammer blows, while 6.8% indicated that they prefer to drive piles until bedrock has been reached. The remaining 4.5% of respondents stated that they use no well defined method for determining pile driving termination. Although not nearly as common as the methods presented in Figure 3.7, 9% of respondents did indicate the use of static pile load tests for the verification of design pile capacities.

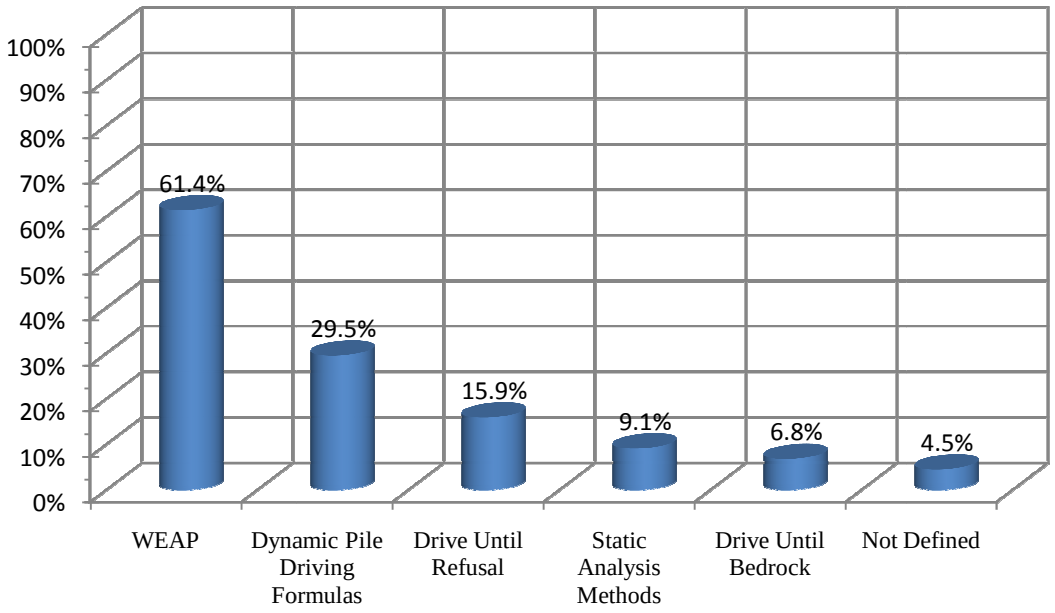

Figure 3.7: Methods for Determining Pile Driving Termination

Furthermore, Iowa county engineers were asked to report on the frequency to which quality control tests, such as pile verticality measurements and inspections of welds used for splicing, are performed on driven pile foundations. As illustrated in Figure 3.8, about 22% of respondents indicated that such quality control tests are always performed on 5% of the installed piles, with 3% of respondents stating that these tests are performed on a more frequent basis (i.e., greater than 5% of the installed piles) and another 19% suggesting that these tests are performed on a less frequent basis (i.e., less than 5% of the installed piles). The remaining 56% of respondents indicated that quality control tests for driven pile foundations are never performed.

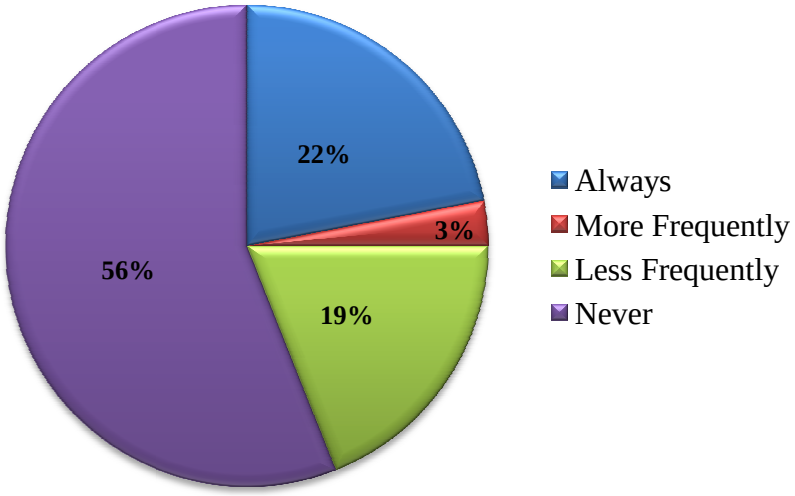

Figure 3.8: Frequency of Performance of Quality Control Tests on Driven Pile Foundations by the County Office

3.3.5 Contribution from Engineering Consulting Firms

As previously mentioned, 39% of respondents, or about 17 different Iowa county engineers, indicated the enlistment of private engineering consulting companies/firms for the conduction of bridge deep foundation design procedures, especially for large-scale projects. Consequently, the survey distributed to the Iowa county engineers was modified and dispersed again to the most commonly used consulting firms reported in Figure 3.6. After sending the survey to nine different local and nationwide private engineering consulting firms, eight complete responses were received. In this section, a summary of the received responses concerning the four main topic areas of the survey is provided, including a brief comparison showing the main differences between the practices of local county engineers and consulting firms.

For the first section of the survey concerning foundation practice, 50% of the consulting firms indicated that they perform soil in-situ and laboratory tests to establish different soil parameters; SPT was the most commonly used in-situ soil test, with soil classification and Atterberg limits comprising the typical laboratory tests. Interestingly, only one respondent indicated the performance of the one-dimensional consolidation test, with another respondent indicating the use of the triaxial test for large-scale projects. With regards to the main criterion used for the selection of a given type of driven pile foundation,

about 44% of the consulting firms indicated a reliance on past design and construction experience, 28% cited economy as the main criterion, and the remaining 28% stated that the criterion is dictated by either available construction equipment or some alternative means. All respondents indicated that steel H-shaped piles are the most commonly used pile type within their respective regions, followed closely by closed-ended steel pipe piles and precast concrete piles, in that order. Interestingly, only one respondent denoted the use of timber piles, which happened with a frequency of about 14%. Finally, all respondents expressed their desire to use driven piles over drilled shafts.

In the pile analysis and design section of the survey, 50% of the responding consulting firms cited the *Iowa LRFD Bridge Design Manual* (Iowa DOT 2010) as their primary driven pile design specification, whereas 37.5% of respondents acknowledged the use of the *Iowa County Bridge Standards* (Iowa DOT 2009) and the remaining 12.5% made use of the *AASHTO LRFD Bridge Design Specifications* (2007). Therefore, it is evident that design engineers still prefer local design manuals over the AASHTO specifications, seeing as the latter is characterized by unnecessary conservatism to account for soil variations across the country (AbdelSalam et al. 2010). Furthermore, to attain a more inclusive image concerning the design and construction practices enacted at the county-level, several questions related to different pile analysis methods were asked. Survey results showed that 60% of the consulting firms rely on dynamic analysis methods to determine design pile capacities, with WEAP analyses based on the SPT N-value soil input method (i.e., SA-method) being the most common, whereas the remaining 40% of respondents indicated the use of conventional static analysis methods based on SPT data. Finally, questions regarding the performance of serviceability limit checks during the design of deep foundations were asked. All responses received from the engineering consulting firms indicated that the vertical settlement of a single pile or group of piles is not accounted for in design, while half of the respondents indicated that lateral displacements are accounted for in design, an important design consideration, which was addressed by only 22% of the county engineers, given the common use of integral abutments in practice.

The last section of the survey acquired information regarding pile drivability and quality control aspects. As expected, more than 75% of respondents indicated that pile

design verification is accomplished through WEAP analyses, while the remainder of respondents indicated a reliance on the original design capacity produced by static analysis methods or that offered by dynamic formulas. Of particular interest were the responses received regarding the effect of soil setup on pile capacity. About 70% of the responding engineering consulting firms indicated that this effect on pile capacity is neglected in design. However, one respondent indicated that soil setup affected pile capacity in a range from 5 to 10%, with another respondent indicating that soil setup can increase pile capacities from anywhere between 11 and 20%, depending on the soil type. Finally, in terms of pile capacity verification by means of the SLT, none of the respondents reported the use of such a test, as it is a sophisticated, expensive, and time consuming test (AbdelSalam et al. 2010). Likewise, in regards to the use of other quality control measures, 80% of respondents reported that such tasks are never performed; thus, leading to a hidden increase in the cost of the deep foundation that could have been significantly reduced through the conduction of either simple or sophisticated quality control tests.

3.4 DATABASE OF PILE LOAD TESTS IN IOWA (PILOT-IA)

Having defined the current state of practice in Iowa regarding the design and construction of deep foundations at both the state- and county-level, it is now appropriate to examine the collection of data associated with pile load tests conducted within Iowa. This information, as previously noted, will be used for the performance of comparative analyses and subsequent LRFD resistance factor calibration efforts on a predetermined set of the most commonly used dynamic pile driving formulas. The collected dataset, which consists of a historically collected subset that was used for the performance of preliminary analyses and a recently collected subset that was used for verification of the results obtained from the preliminary analyses, was assessed for quality and then correspondingly placed in a relational database management system to allow for the efficient performance of filtering, sorting, and querying procedures required by the aforementioned LRFD resistance factor calibration process. In the following subsections, the importance of PILOT-IA will be detailed together with a brief discussion of the structure and key parameters used in the development of this database. A detailed description of the historical dataset upon which the database was originally fashioned will also be provided, before a comprehensive review of all fields

contained within the database is given. For a detailed hardcopy listing of all pile load test information stored within the electronic framework of PILOT-IA, the reader is asked to refer to Roling et al. (2010).

3.4.1 Significance of PILOT-IA

In response to AASHTO's permittance of regionally calibrated LRFD resistance factors for the design of driven pile foundations, which was introduced in Chapter 1, many states across the nation have made an effort to develop such factors so as to improve the economy of bridge foundation elements. More specifically, Florida (McVay et al. 2000), Illinois (Long, Hendrix, and Baratta 2009), Washington (Allen 2005), and Wisconsin (Long, Hendrix, and Jaromin 2009) have all published studies recommending LRFD resistance factors for the design of driven pile foundations by means of static analysis methods and the construction control of driven pile foundations by means of dynamic analysis methods, which includes dynamic pile driving formulas. While these studies provide valuable information including the identification of available regional pile load test data, in all cases, except for the State of Florida study, the reported LRFD resistance factor calibrations were accomplished through the use of national databases such as the FHWA's Deep Foundation Load Test Database (DFLTD), which contains 1500 deep foundation load test records from nearly 850 sites covering various parts of the world. Such procedures were adopted due to the absence of quality assurance provisions and required geotechnical and load test data for the regionally reported static pile load tests.

According to McVay et al. (2000), the University of Florida has been collecting pile load test data for the Florida DOT since 1989. The resultant database, termed PILEUF, contains data for 247 piles of various types (e.g., square concrete, round concrete, pipe, and steel H-shaped), with 180 of those piles being located in the State of Florida. Although it is unknown as to whether PILEUF exists in an electronic form, its general characteristics resemble those of PILOT-IA. With the goal of becoming a model database for an effective regional LRFD calibration process that can be refined as more data becomes available, PILOT-IA is based on a well-defined hierarchical classification scheme, in addition to an appealing user-friendly interface, that has not yet been seen with other databases such as DFLTD and PILEUF. Furthermore, imposition of a strict acceptance criterion for each of the

three hierarchical pile load test dependability classifications, expounded in the subsequent section, ensures that the resulting data available in PILOT-IA for LRFD regional calibration is of superior quality and consistency. These aforementioned qualities delineate the importance of establishing databases such as PILOT-IA at the state and national levels.

3.4.2 Key Terminology Used for Data Quality Assurance

As mentioned in Chapter 1, an estimate of a pile's capacity can be achieved through the use of static and/or dynamic methods. Employing a static method requires a detailed site investigation for the evaluation of soil parameters, while for a dynamic method driving record information and reported pile driving equipment characteristics are typically required. Consequently, it was determined during the formulation of PILOT-IA that a well-defined hierarchical classification scheme would be required to clearly identify those pile load tests containing sufficient information for the estimation of pile capacity by means of both static and dynamic methods. Furthermore, based upon the reality that not every pile load test yielded dependable results, an additional level in the hierarchical classification scheme was deemed necessary for initial separation of the reliable pile load tests from the entirety of the PILOT-IA database.

The unique classification system developed for PILOT-IA catalogs pile load tests as "reliable," "usable-static," and "usable-dynamic." The first tier of the hierarchical system, which was originally termed by Dirks and Kam (1989), assigns the reliable classification to a pile static load test that has achieved the displacement based criteria for pile capacity, as defined by Davisson (1972), prior to the pull-out of any anchor piles. The second tier assigns the usable-static classification, which identifies those pile load tests possessing sufficient information for the prediction of pile capacity by means of static methods, to a reliable pile static load test that has soil boring information and SPT data within one hundred feet of the test pile. Furthermore, the third tier assigns the usable-dynamic classification, which identifies those pile load tests containing sufficient information for the prediction of pile capacity by means of dynamic methods, to a usable-static pile load test that has complete driving records and information concerning characteristics of the pile driving equipment for the test pile under consideration.

As a final means of ensuring data quality and consistency within PILOT-IA, distinct classification rules, which were missing from the numerous databases presented in Sections 2.4 and 2.5, were established for generalization of the soil profile located along the test pile embedded length. In other words, a test pile is classified as being embedded in a sand soil profile when at least 70% of the soil located along the shaft of the pile is classified as a sand or non-cohesive material according to the Unified Soil Classification System (USCS). Likewise, a test pile is classified as being embedded in a clay soil profile when at least 70% of the soil located along the shaft of the pile is classified as a clay or cohesive material according to the USCS. However, when neither of the aforementioned classifications is achieved, the test pile is classified as being embedded in a mixed soil profile. In light of the key terminology defined in this subsection, a descriptive summary of the historical data subset upon which PILOT-IA was originally fashioned is presented below.

3.4.3 Descriptive Summary of PILOT-IA Historical Data Subset

Over a twenty-four year period defined by the years from 1966 to 1989, information concerning 264 pile static load tests (SLTs) conducted in the State of Iowa on steel H-shaped, timber, pipe, Monotube, and concrete piles (Figure 3.9) was collected by the Iowa Department of Transportation (Iowa DOT). During this time period, the entirety of the aforementioned collected information, although not always wholly available, included details concerning the site location, subsurface conditions, pile type, hammer characteristics, EOD blow count, and static load test results. All of this information was stored by the Iowa DOT in hardcopy format, making its usage for the LRFD resistance factor calibration process cumbersome and almost impractical. As a part of the research outlined in this thesis, the electronic database for PIle LOad Tests in Iowa (PILOT-IA) was developed using Microsoft Office Access™ and in conjunction with the Iowa DOT to allow for the efficient performance of reference and/or analysis procedures on the amassed dataset, as stated previously. In the following subsections, a descriptive summary of the historical data subset is presented as a function of pile type.

3.4.1.1 Steel H-Pile SLTs

Of the 264 pile SLTs conducted by the Iowa DOT, 164 were performed on H-shaped steel piles. A distribution of the number of static pile load tests conducted on the various sizes of steel H-shaped piles has been provided in Figure 3.10. Likewise, a distribution indicating the various embedded lengths for the 164 steel H-shaped test piles is depicted in Figure 3.11, for which the mean and standard deviation are 53.20 and 18.56 feet, respectively.

Of considerable interest and value to the objectives of this thesis is the fact that a total of 141 steel H-pile load tests were classified in PILOT-IA as reliable, with 82 of those being classified as usable-static and 34 of those 82 being grouped as usable-dynamic. For the 82 usable-static steel H-pile load tests, distributions amongst Iowa's five predominant soil regions, Iowa's 99 counties, and the predominant soil medium encountered along the shaft of the pile have been provided in Figure 3.12, Figure 3.13, and Figure 3.14, respectively. Likewise, for the 34 usable-dynamic steel H-pile load tests, distributions amongst Iowa's five predominant soil regions, Iowa's 99 counties, and the predominant soil medium encountered along the shaft of the pile have been provided in Figure 3.15, Figure 3.16, and Figure 3.17, respectively.

Lastly, to assist with future investigations concerning the effect of soil setup on pile capacity, the time interval between the EOD condition and the actual SLT was established for each of the 82 usable-static steel H-pile load tests. With this information, distributions for both the usable-static and usable-dynamic data subsets were generated and have been provided in Figure 3.18 and Figure 3.19, respectively. More specifically, the usable-static distribution of Figure 3.18 possesses a mean of 5.3 days and a standard deviation of 3.8 days, whereas the usable-dynamic distribution of Figure 3.19 possesses a mean of 5.8 days and a standard deviation of 5.2 days. When considering only those steel H-piles embedded in a clay soil profile, for which the influence of soil setup is greatest on account of a characteristically slow time rate of consolidation, the mean and standard deviation for the distribution of the time interval between the EOD condition and the actual SLT become 4.6 days and 1.9 days, respectively, for the usable-static records and 3.9 days and 0.8 days, respectively, for the usable-dynamic records.

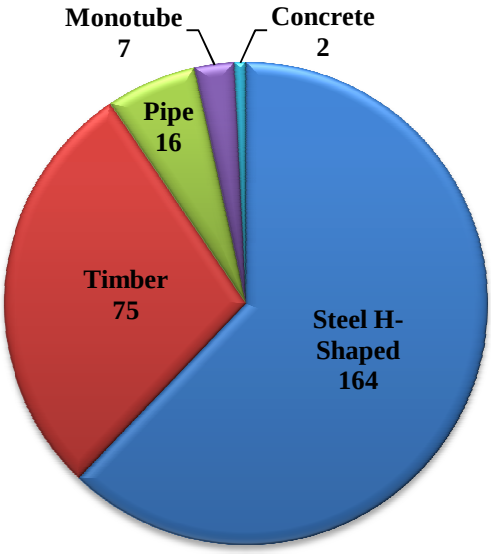

Figure 3.9: Distribution of Historical Iowa Pile SLTs by Pile Type

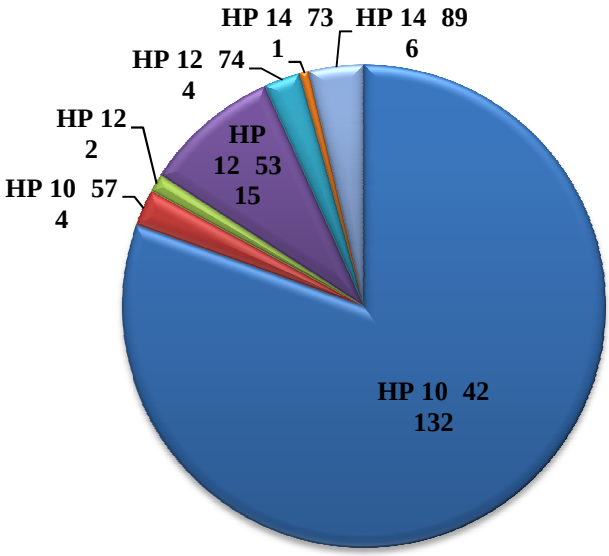

Figure 3.10: Distribution of Historical Steel H-Pile SLTs by Pile Size

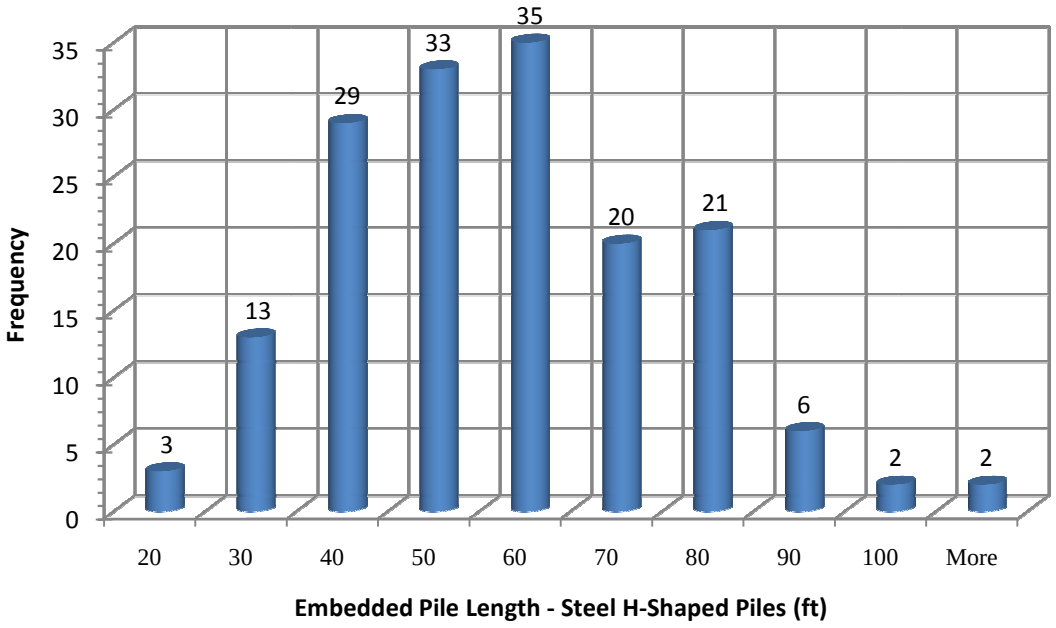

Figure 3.11: Distribution of Embedded Pile Lengths for Historical Steel H-Pile Dataset

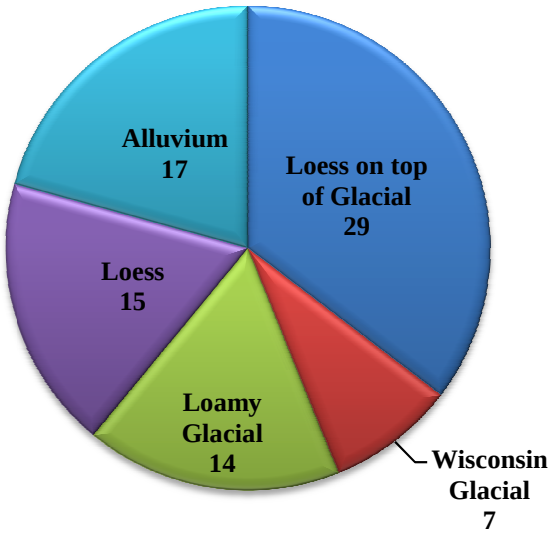

Figure 3.12: Distribution of Historical Usable-Static Steel H-Pile SLTs amongst Iowa's Predominant Soil Regions

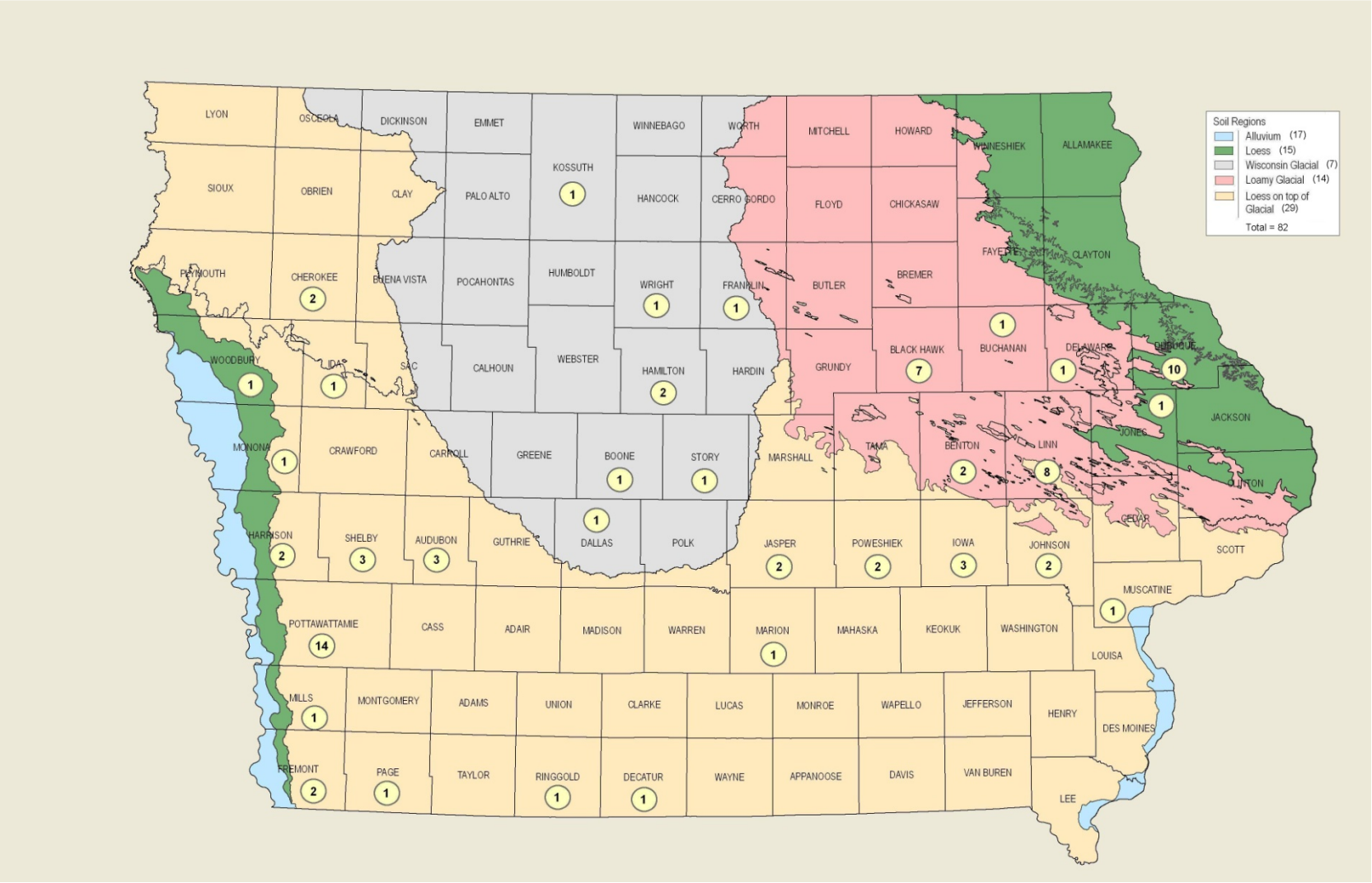

Figure 3.13: Distribution of Historical Usable-Static Steel H-Pile SLTs amongst Iowa's Predominant Soil Regions and 99 Counties

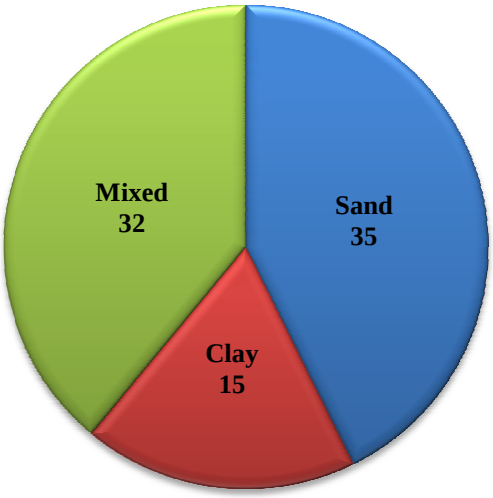

Figure 3.14: Distribution of Historical Usable-Static Steel H-Pile SLTs by Test Site Soil Classification

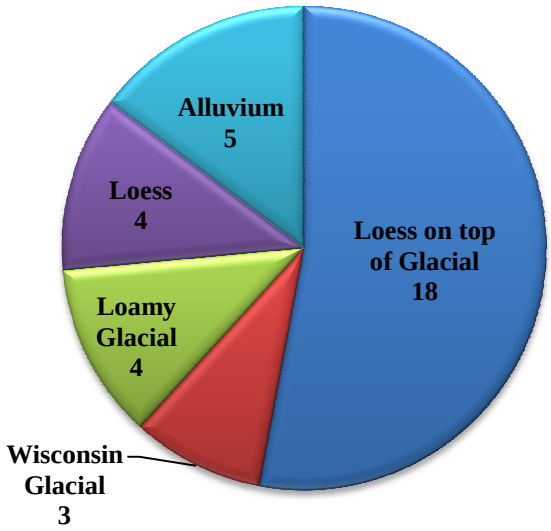

Figure 3.15: Distribution of Historical Usable-Dynamic Steel H-Pile SLTs amongst Iowa's Predominant Soil Regions

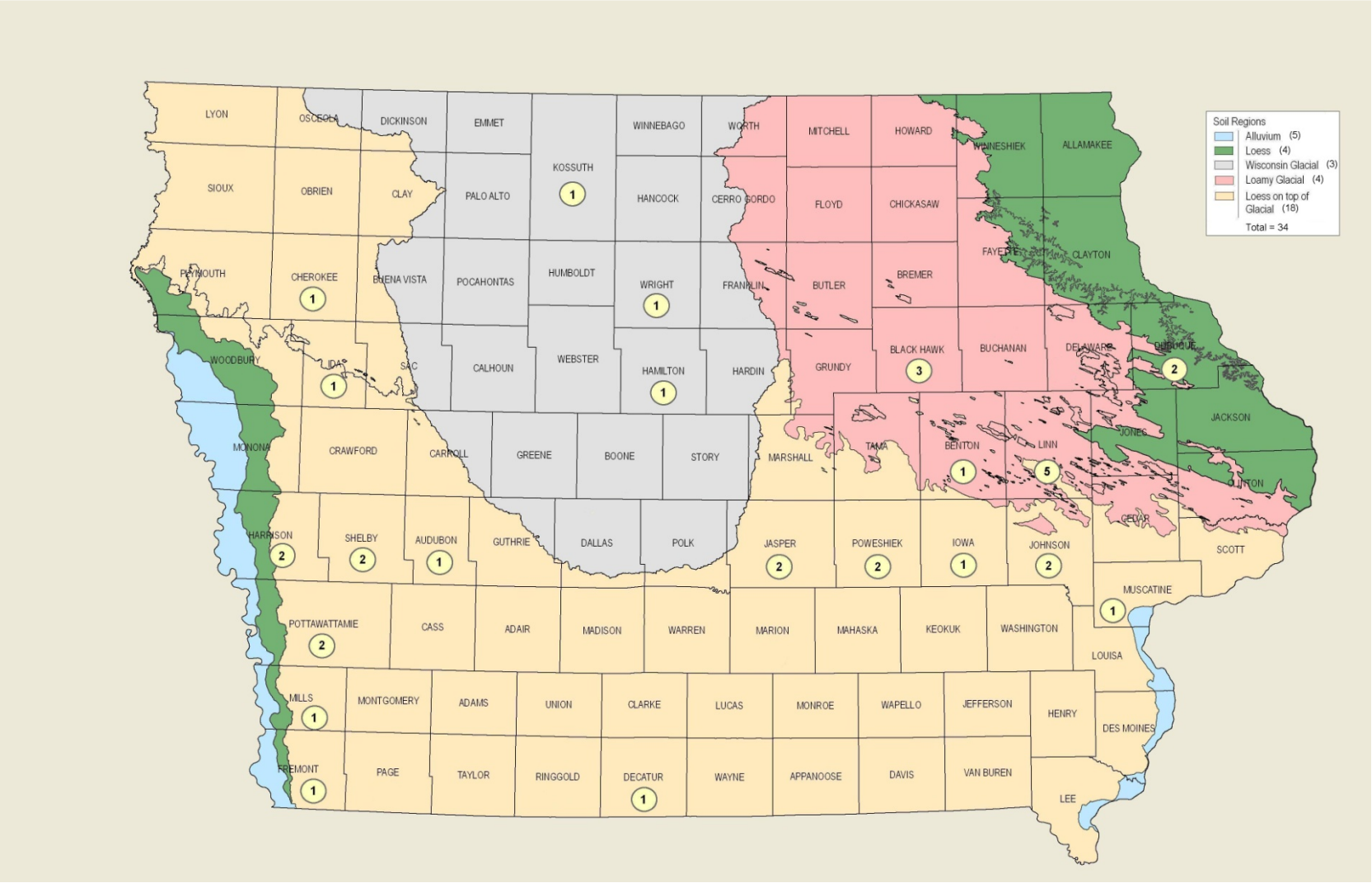

Figure 3.16: Distribution of Historical Usable-Dynamic Steel H-Pile SLTs amongst Iowa's Predominant Soil Regions and 99 Counties

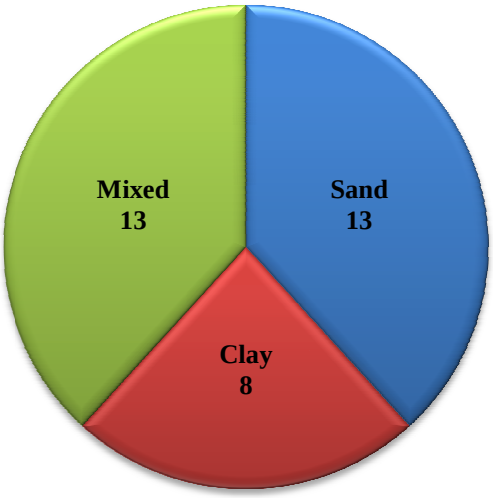

Figure 3.17: Distribution of Historical Usable-Dynamic Steel H-Pile SLTs by Test Site Soil Classification

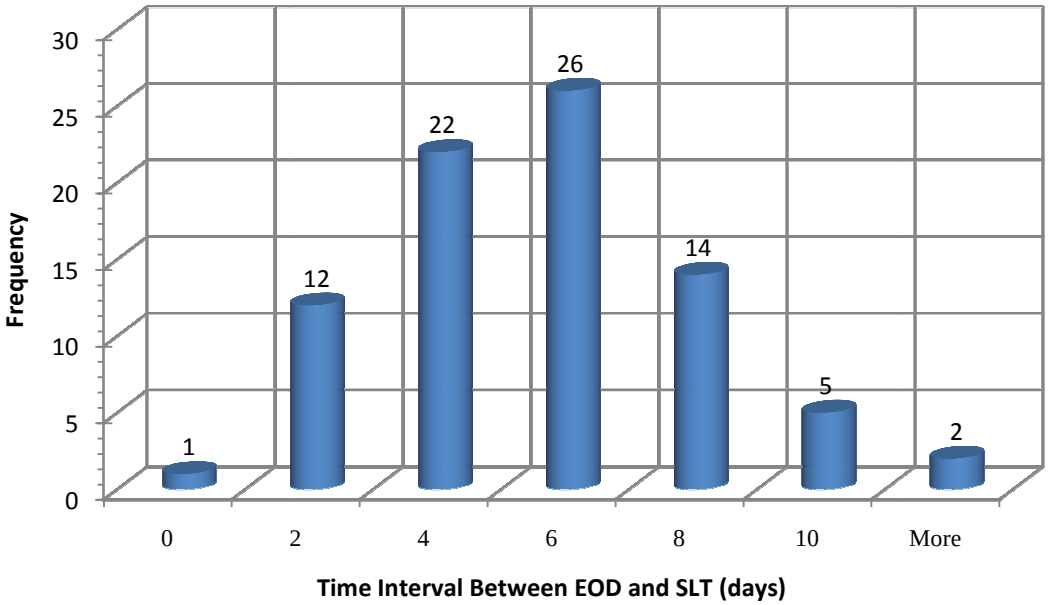

Figure 3.18: Distribution of Time Interval between EOD and SLT for Historical Usable-Static Steel H-Pile SLTs

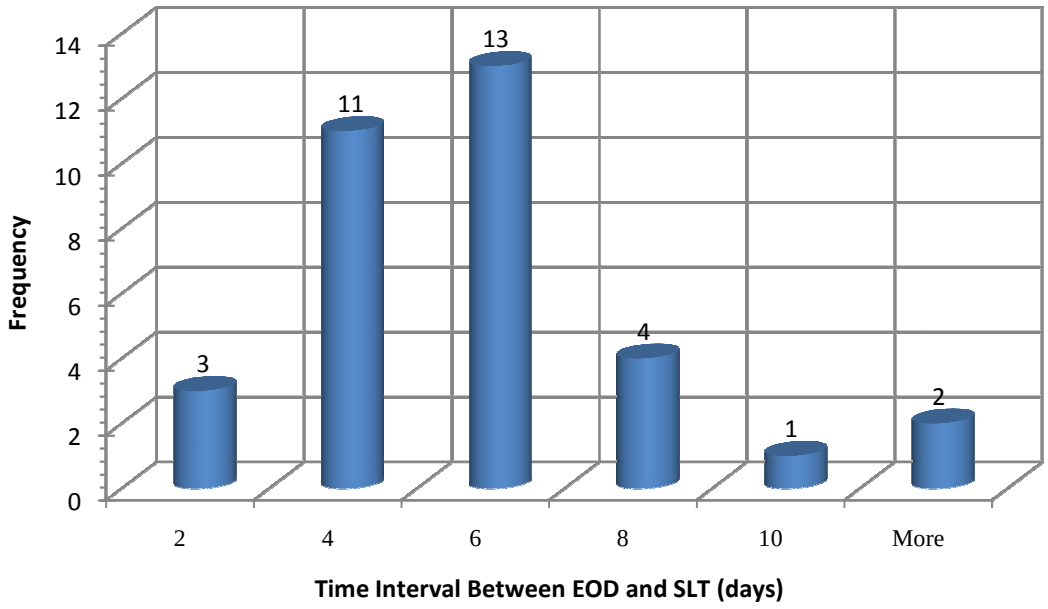

Figure 3.19: Distribution of Time Interval between EOD and SLT for Historical Usable-Dynamic Steel H-Pile SLTs

3.4.1.2 Timber Pile SLTs

Of the 264 pile SLTs conducted by the Iowa DOT, 75 were performed on timber piles. For the entirety of this timber pile load test data subset, it was presumed that all test piles were 10 inches in diameter as a consequence of inadequate size classification information. This assumption follows that made by Dirks and Kam (1989) in their derivation of the skin friction and end bearing design charts found in *Foundation Soils Information Chart: Pile Foundation*. The various embedded lengths for these 75 timber piles have been provided in the distribution presented in Figure 3.20, for which the mean and standard deviation are 29.00 and 10.68 feet.

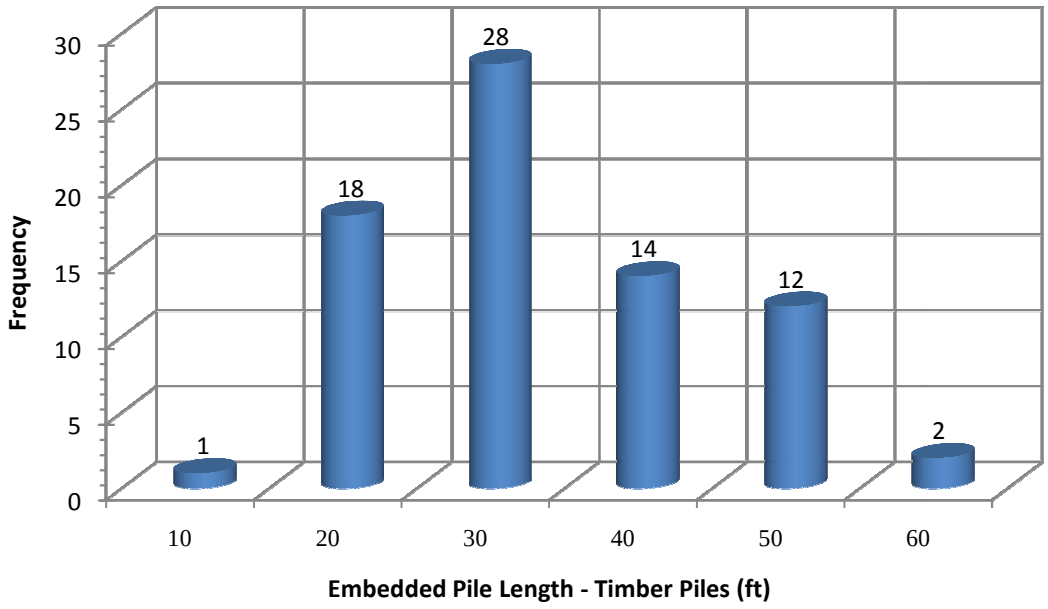

Figure 3.20: Distribution of Embedded Pile Lengths for Historical Timber Pile Dataset

Out of the 75 total timber pile SLTs conducted by the Iowa DOT, 47 were classified in PILOT-IA as reliable, with 24 of those being classified as usable-static and 9 of those 24 being grouped as usable-dynamic. For the 24 usable-static timber pile load tests, distributions amongst Iowa's five predominant soil regions, the predominant soil medium encountered along the shaft of the pile, and Iowa's 99 counties have been provided in Figure 3.21, Figure 3.22, and Figure 3.23, respectively. Similarly, for the 9 usable-dynamic timber pile load tests, distributions amongst Iowa's five predominant soil regions, the predominant soil medium encountered along the shaft of the pile, and Iowa's 99 counties have been provided in Figure 3.24, Figure 3.25, and Figure 3.26, respectively.

To finish, distributions of the time interval between the EOD condition and the actual SLT for both the usable-static and usable-dynamic timber pile data subsets have been provided in Figure 3.27 and Figure 3.28, respectively. More specifically, the usable-static distribution of Figure 3.27 possesses a mean of 5.8 days and a standard deviation of 2.7 days, whereas the usable-dynamic distribution of Figure 3.28 possesses a mean of 5.0 days and a standard deviation of 3.2 days.

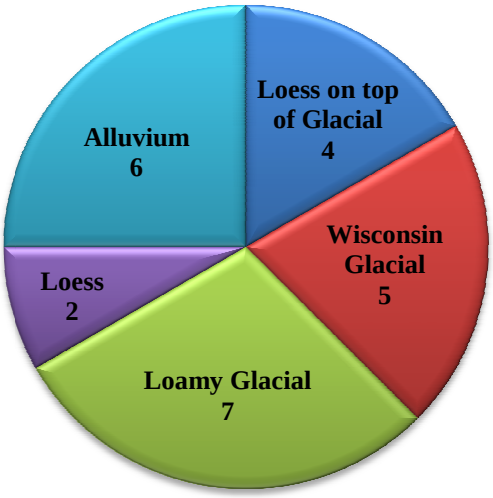

Figure 3.21: Distribution of Historical Usable-Static Timber Pile SLTs amongst Iowa's Predominant Soil Regions

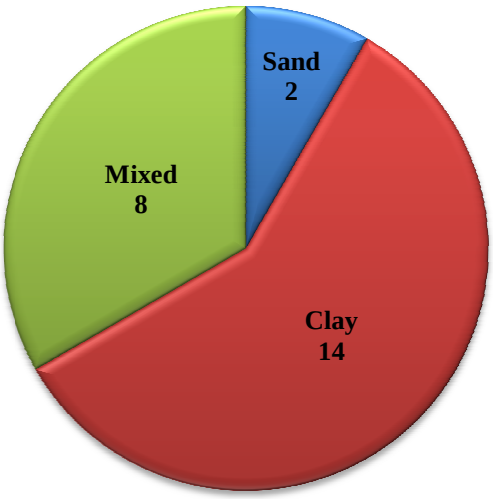

Figure 3.22: Distribution of Historical Usable-Static Timber Pile SLTs by Test Site Soil Classification

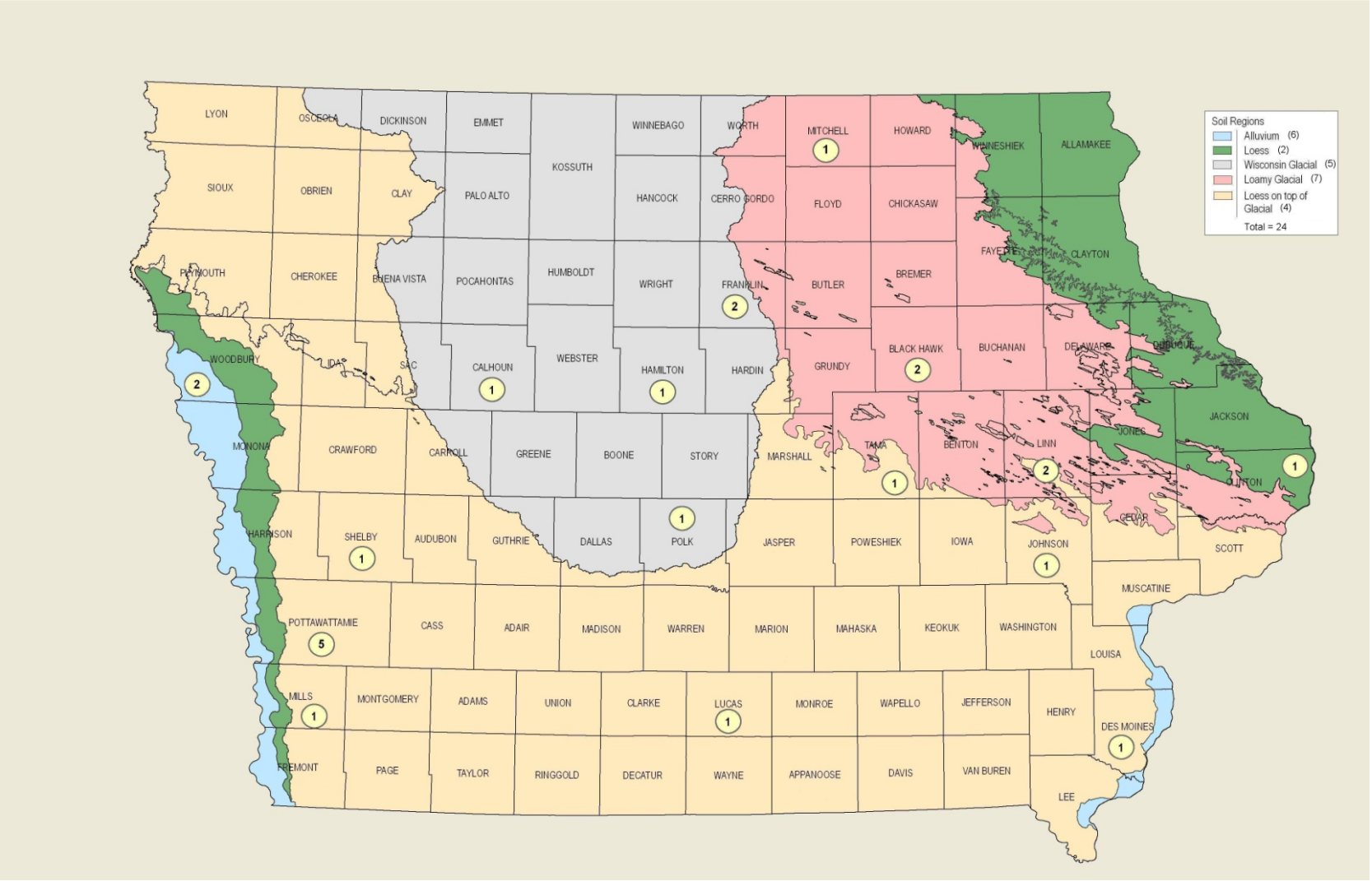

Figure 3.23: Distribution of Historical Usable-Static Timber Pile SLTs amongst Iowa's Predominant Soil Regions and 99 Counties

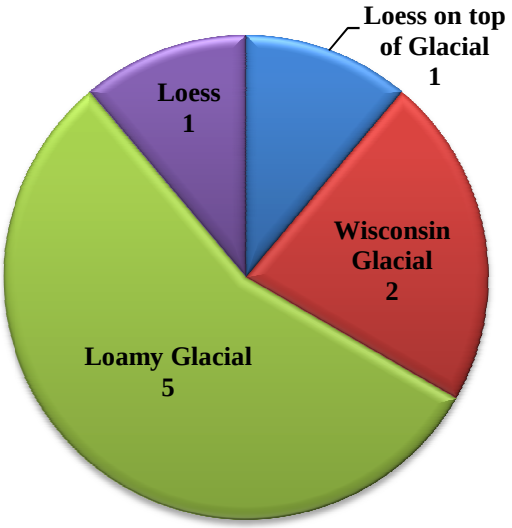

Figure 3.24: Distribution of Historical Usable-Dynamic Timber Pile SLTs amongst Iowa's Predominant Soil Regions

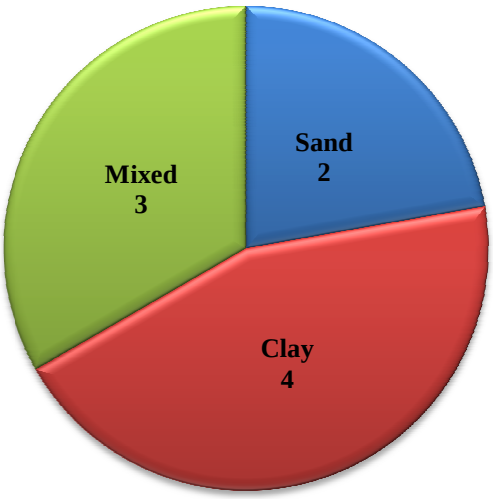

Figure 3.25: Distribution of Historical Usable-Dynamic Timber Pile SLTs by Test Site Soil Classification

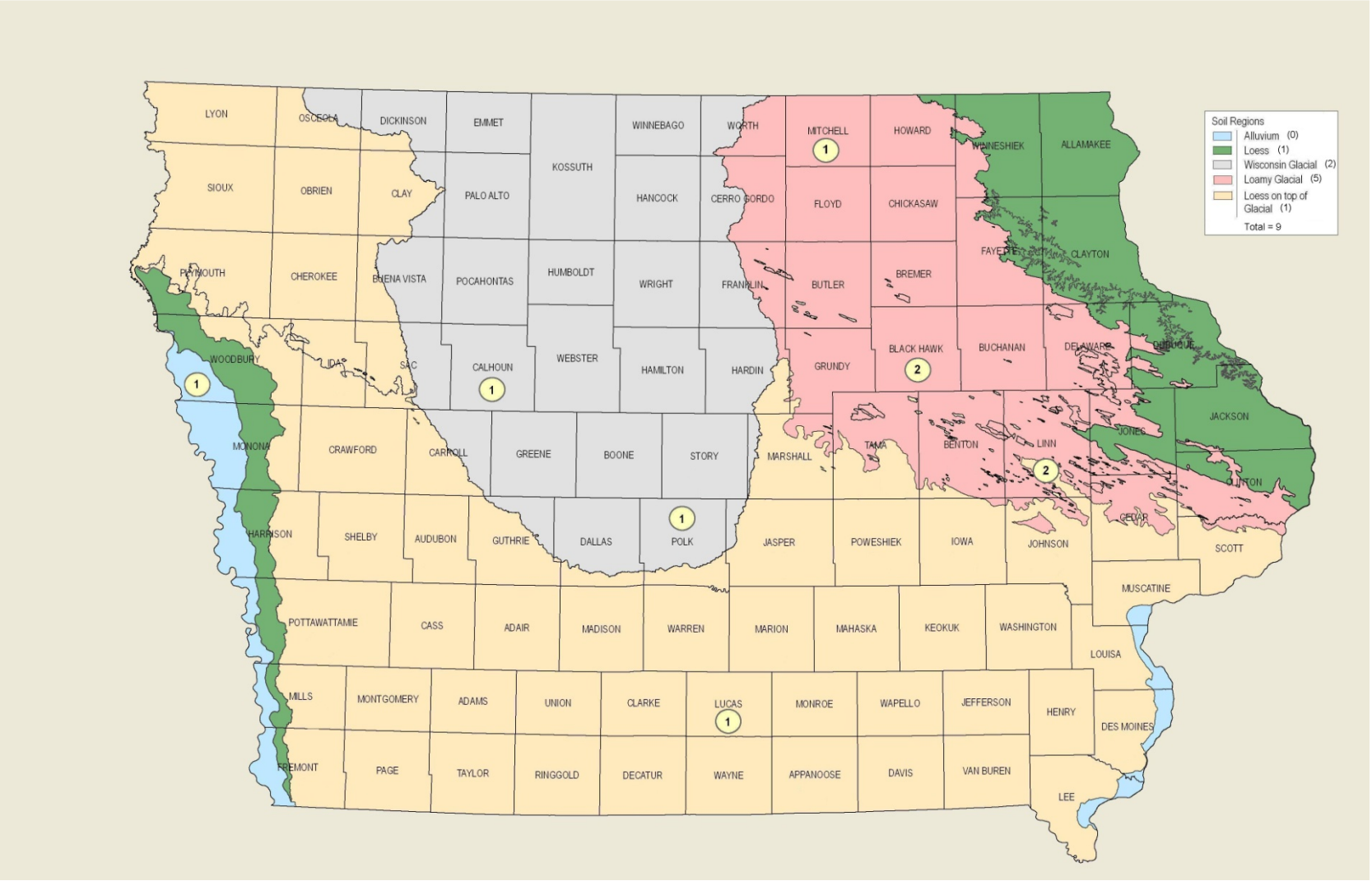

Figure 3.26: Distribution of Historical Usable-Dynamic Timber Pile SLTs amongst Iowa's Predominant Soil Regions and 99 Counties

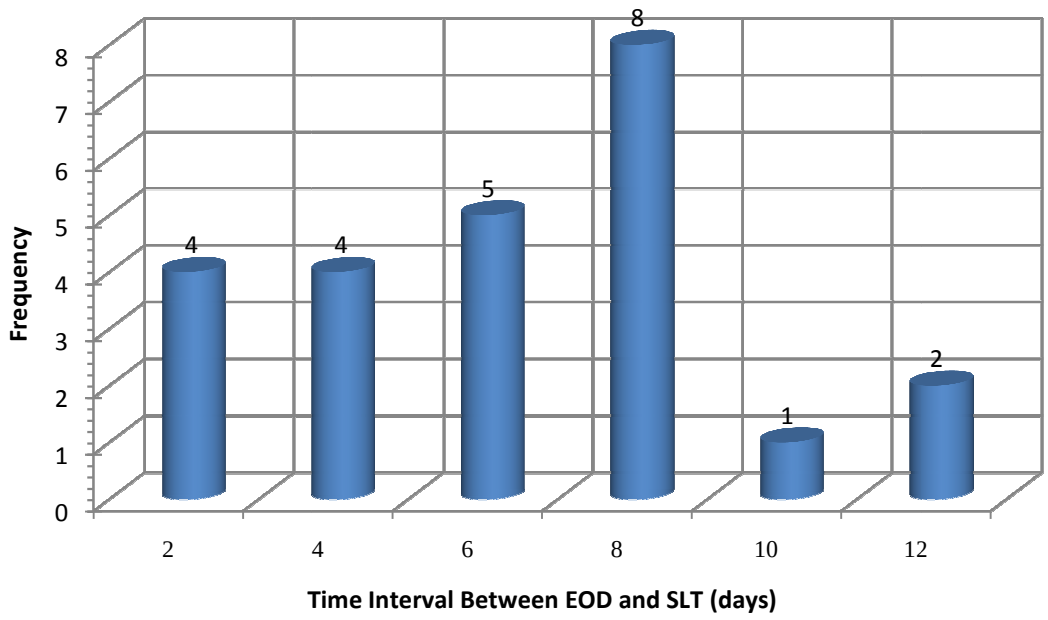

Figure 3.27: Distribution of Time Interval between EOD and SLT for Historical Usable-Static Timber Pile SLTs

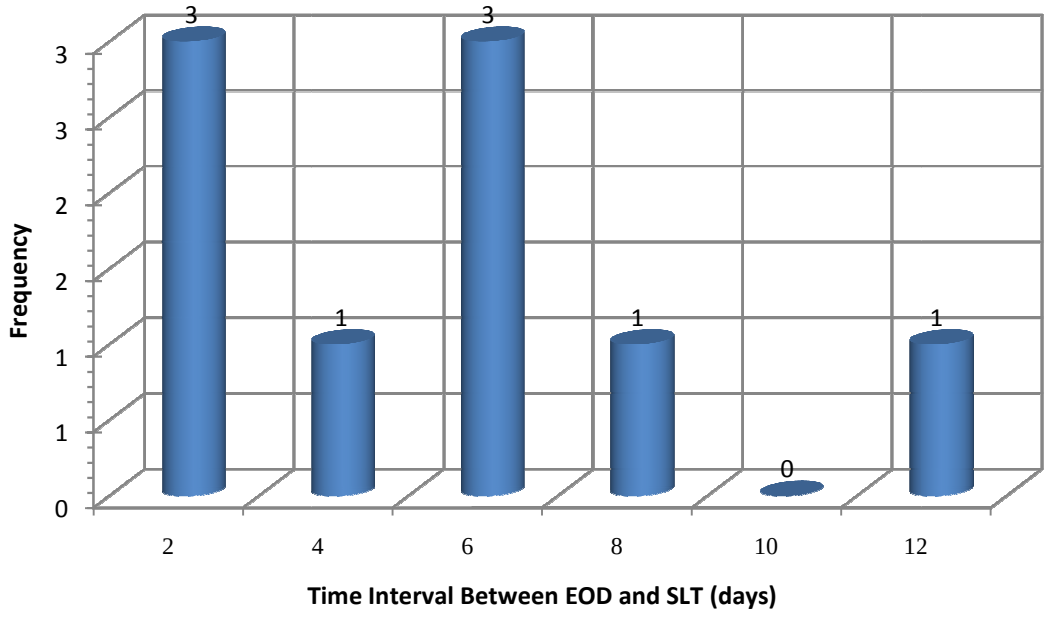

Figure 3.28: Distribution of Time Interval between EOD and SLT for Historical Usable-Dynamic Timber Pile SLTs

3.4.1.3 Pipe, Monotube, and Concrete Pile SLTs

Finally, the 25 remaining pile SLTs conducted by the Iowa DOT were performed on steel pipe, Monotube, and prestressed concrete piles. More specifically, sixteen pile SLTs were performed on steel pipe piles, seven were performed on Monotube piles, which are essentially steel pipe piles with fluted walls and a tapered cross-section, and two were performed on prestressed concrete piles. A distribution showing the number of pile SLTs conducted on the various types and sizes of steel pipe, Monotube, and prestressed concrete piles has been provided in Figure 3.29. In addition, the various embedded lengths for these 25 steel pipe, Monotube, and prestressed concrete piles have been provided in the distribution presented in Figure 3.30, for which the mean and standard deviation are 41.47 feet and 16.21 feet, respectively.

Of the 25 total pile SLTs conducted on steel pipe, Monotube, and prestressed concrete piles, 21 were classified in PILOT-IA as reliable (i.e., 15 steel pipe, 5 Monotube, and 1 prestressed concrete pile SLT), with 17 of those being classified as usable-static (i.e., 14 steel pipe and 3 Monotube pile SLTs) and 2 of those 17 being grouped as usable-dynamic (i.e., 2 steel pipe SLTs). For the 17 usable-static steel pipe and Monotube pile load tests, distributions amongst Iowa's five predominant soil regions, the predominant soil medium encountered along the shaft of the pile, and Iowa's 99 counties have been provided in Figure 3.31, Figure 3.32, and Figure 3.33, respectively. As for the two usable-dynamic steel pipe pile load tests, one was performed in Iowa's loess on top of glacial soil region, while the other was performed in the loess soil region. Additionally, one of the two usable-dynamic steel pipe pile load tests was performed in Shelby County, while the other was performed in Woodbury County. Finally, a mixed soil medium was encountered along the shaft of both usable-dynamic steel pipe piles.

To conclude, a distribution of the time interval between the EOD condition and the actual SLT for the usable-static steel pipe and Monotube pile data subset has been provided in Figure 3.34, where the mean and standard deviation are 10.4 and 11.2 days, respectively. As for the two usable-dynamic steel pipe pile load tests, the one driven in Shelby County was statically load tested to failure seven days after the EOD, while the one driven in Woodbury County was statically loaded to failure fourteen days after the EOD.

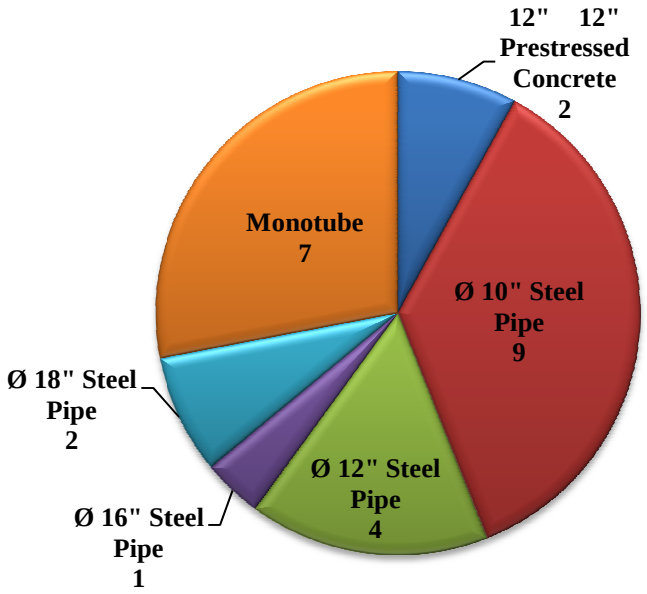

Figure 3.29: Distribution of Historical Steel Pipe, Monotube, and Prestressed Concrete Pile SLTs by Type and Size

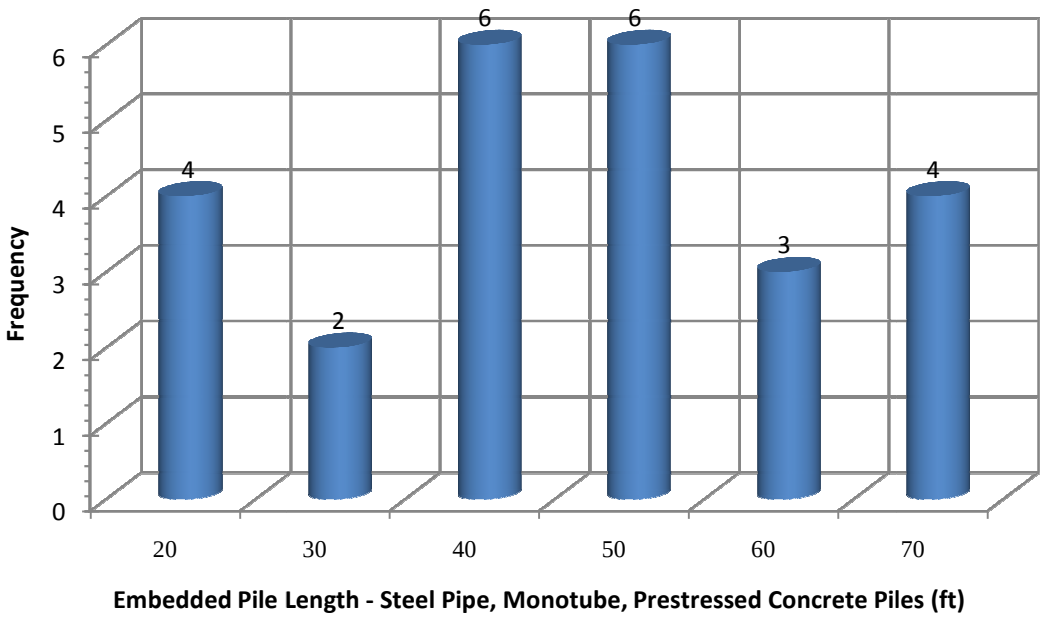

Figure 3.30: Distribution of Embedded Pile Lengths for Historical Steel Pipe, Monotube, and Prestressed Concrete Piles

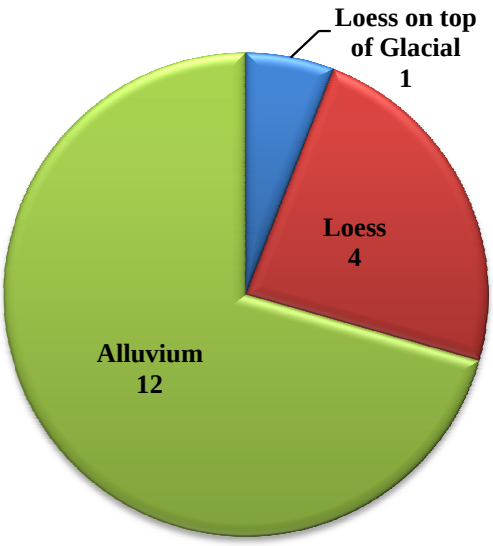

Figure 3.31: Distribution of Historical Usable-Static Steel Pipe, Monotube, and Prestressed Concrete Pile SLTs amongst Iowa's Predominant Soil Regions

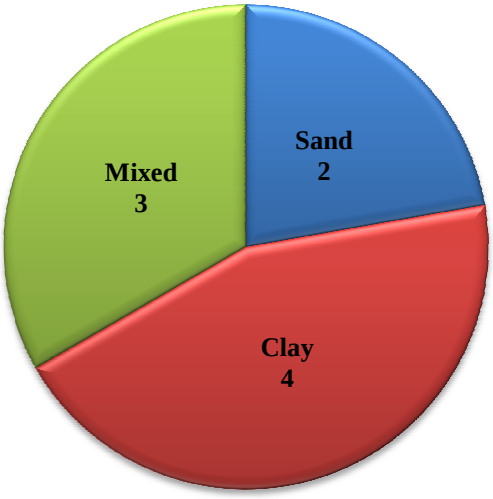

Figure 3.32: Distribution of Historical Usable-Static Steel Pipe and Monotube Pile SLTs by Test Site Soil Classification

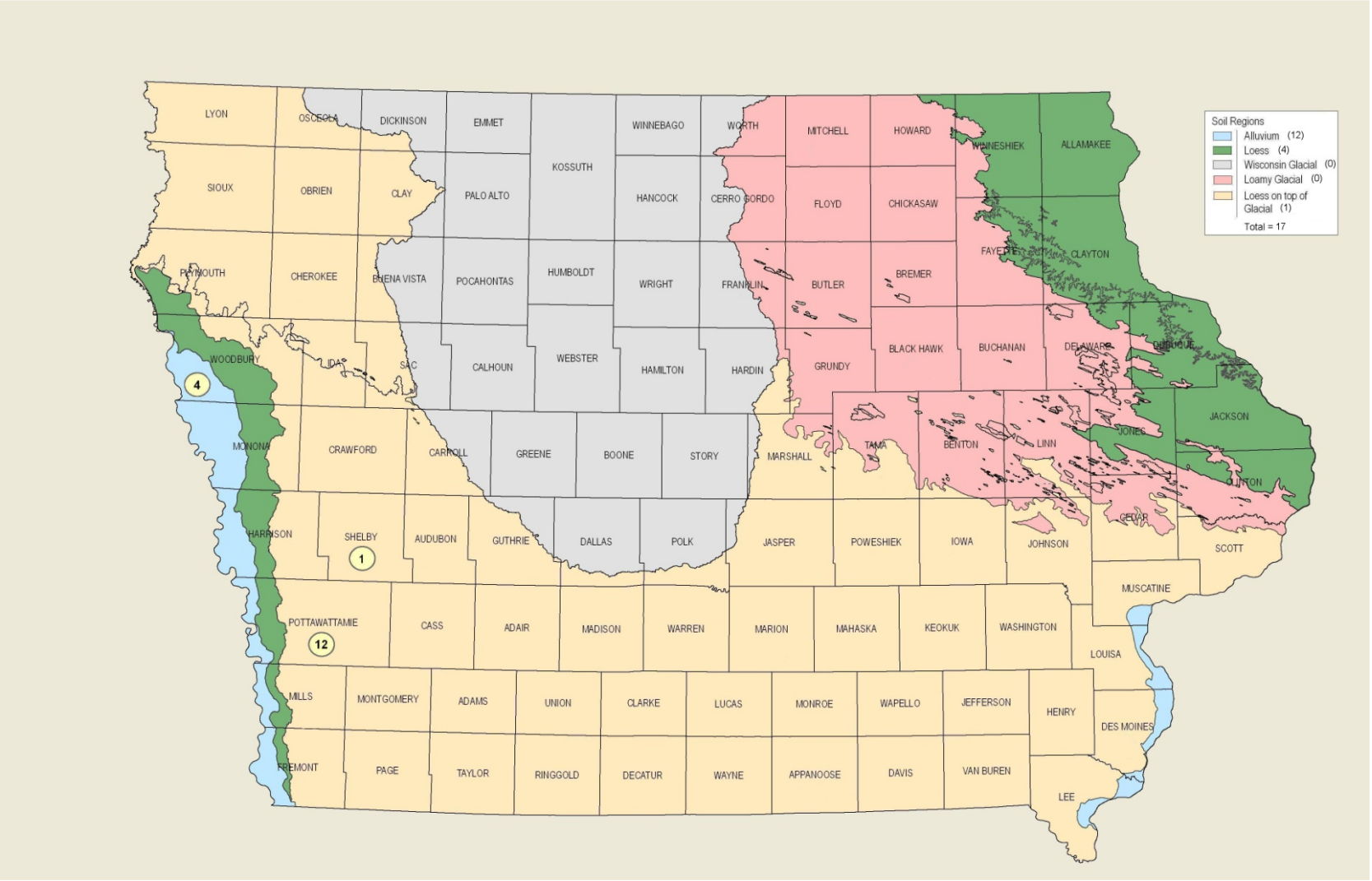

Figure 3.33: Distribution of Historical Usable-Static Steel Pipe and Monotube Pile SLTs amongst Iowa's Predominant Soil Regions and 99 Counties

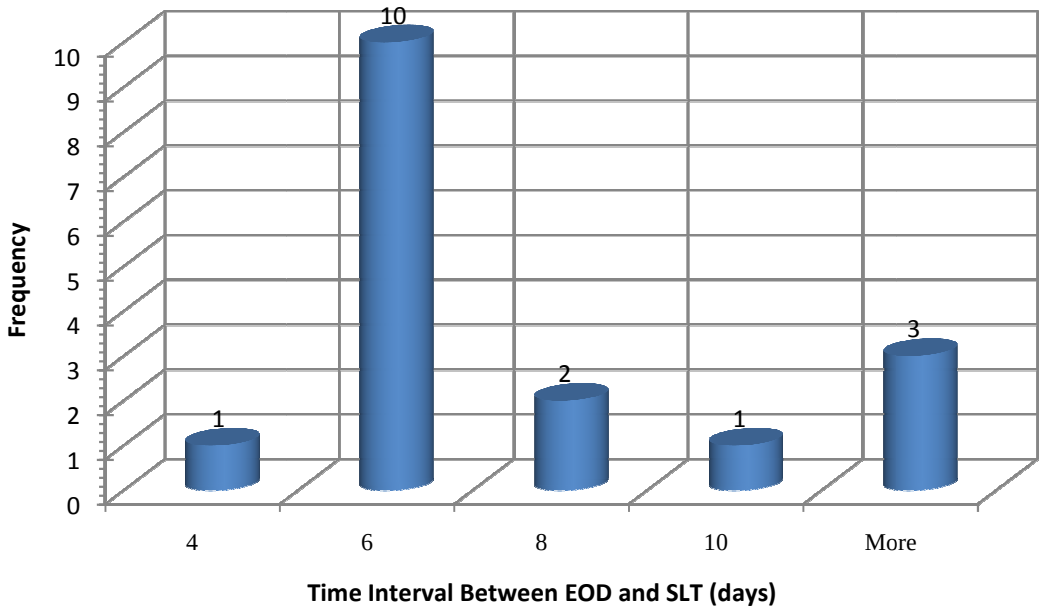

Figure 3.34: Distribution of Time Interval between EOD and SLT for Historical Usable-Static Steel Pipe and Monotube Pile SLTs

3.4.4 PILOT-IA User Manual

As alluded to previously, PILOT-IA was developed to provide a means for all past, present, and future Iowa DOT bridge pile load test data to be stored in electronic form for subsequent reference and/or analysis. The purpose of the following user manual is to provide a comprehensive explanation of the many features incorporated into PILOT-IA, the details of how the quality of data was ensured, as well as information on how to add new SLT data and the minimum required extent of details for these new tests.

3.4.2.1 Accessing PILOT-IA

To download and save a copy of the most recent version of PILOT-IA, follow the steps listed below:

1) Open the *My Computer* system folder on a computer to which PILOT-IA will be installed.
2) Insert the PILOT-IA CD-ROM into the computer's CD-ROM drive. Once the PILOT-IA CD-ROM has been placed in the computer's CD-ROM drive, the CD drive found in the *My Computer* system folder will display the name PILOT-IA.

3) Open the PILOT-IA CD-ROM by double-clicking with the mouse on the CD drive icon found in the *My Computer* system folder.
4) Drag the PILOT-IA folder found on the PILOT-IA CD-ROM to the Local Disk (C:) drive. The computer will now begin copying the PILOT-IA folder to the Local Disk (C:) drive; note that this process may take a few minutes. (Should one wish to save the PILOT-IA folder to a location other than the Local Disk (C:) drive, simply drag the PILOT-IA folder found on the PILOT-IA CD-ROM to the desired location.)
5) Once the PILOT-IA folder has been successfully copied to the desired location, PILOT-IA can be opened by first double-clicking with the mouse on the recently copied PILOT-IA folder.
6) Upon opening the PILOT-IA folder, locate and open the Database folder by double-clicking with the mouse.
7) Once the Database folder has been successfully opened, locate and open the Microsoft Office Access™ 2007 file named "PILOT-IA.accdb" by double-clicking with the mouse. (Note that PILOT-IA is best viewed at a screen resolution of 1600 by 1200 pixels.)

3.4.2.2 Description of PILOT-IA Database Fields

The first screen one will see upon properly opening the Microsoft Access 2007 file named "PILOT-IA.accdb" is shown in Figure 3.35. As illustrated in this figure, the values located under the "ID" column contain a hyperlink to the complete Pile Load Test Record Form (PLTRF) for the specified pile SLT. A screenshot of the PLTRF is provided in Figure 3.36 and the database fields identified in this figure are described in detail in the following subsections.

Click here to open a blank Pile Load Test Record Form

Click here to open a form that provides information on PILOT-IA

Use this drop down menu to quickly apply filters to PILOT-IA

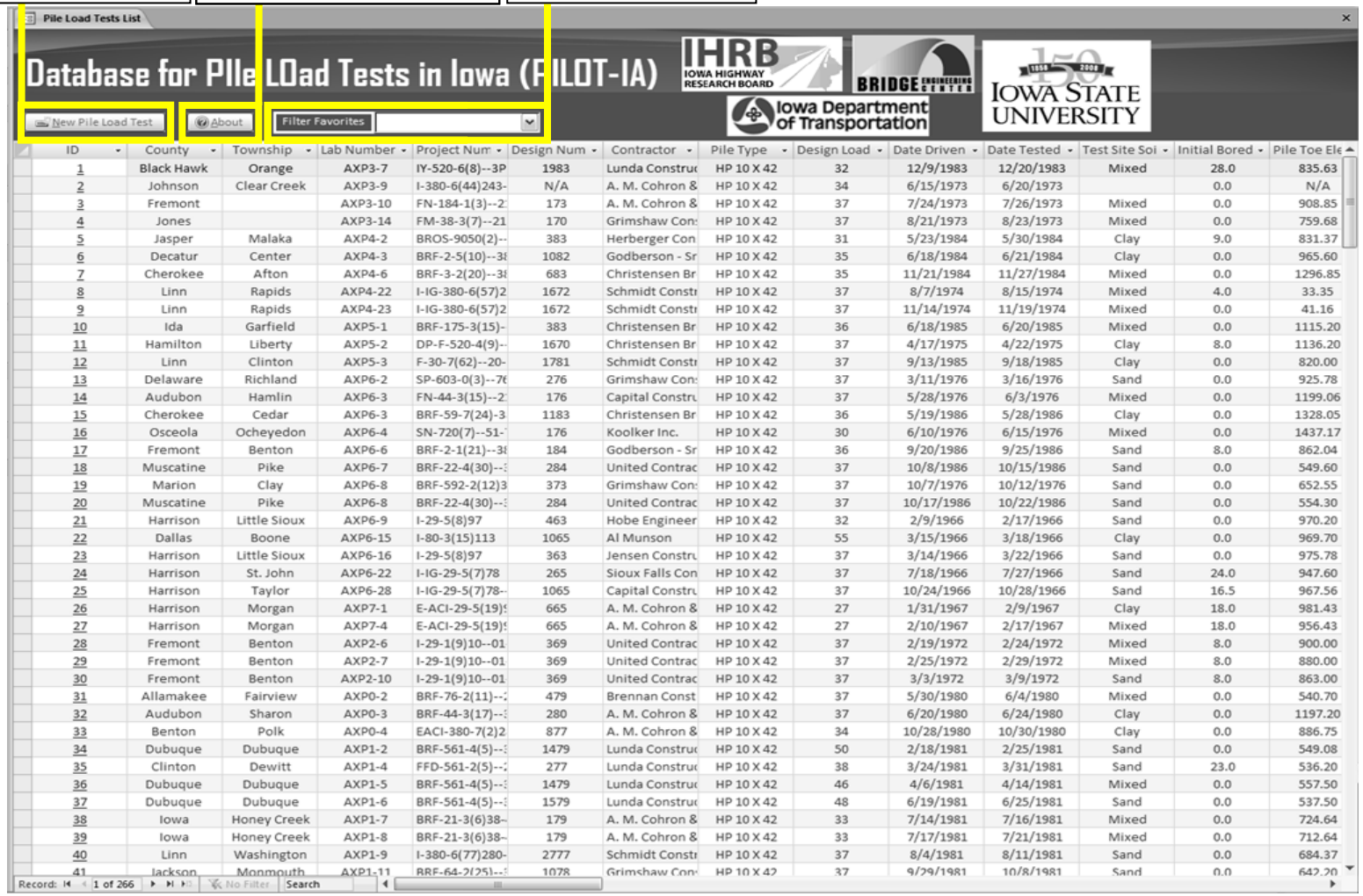

ID	County	Township	Lab Number	Project Num	Design Num	Contractor	Pile Type	Design Load	Date Driven	Date Tested	Test Site Soi	Initial Bored	Pile Toe Ele
1	Black Hawk	Orange	AXP3-7	IY-520-6(8)--3P	1983	Lunda Construc	HP 10 X 42	32	12/9/1983	12/20/1983	Mixed	28.0	835.63
2	Johnson	Clear Creek	AXP3-9	I-380-6(44)243-	N/A	A. M. Cohron &	HP 10 X 42	34	6/15/1973	6/20/1973		0.0	N/A
3	Fremont		AXP3-10	FN-184-1(3)--2	173	A. M. Cohron &	HP 10 X 42	37	7/24/1973	7/26/1973	Mixed	0.0	908.85
4	Jones		AXP3-14	FM-38-3(7)--21	170	Grimshaw Con:	HP 10 X 42	37	8/21/1973	8/23/1973	Mixed	0.0	759.68
5	Jasper	Malaka	AXP4-2	BROS-9050(2)--	383	Herberger Con	HP 10 X 42	31	5/23/1984	5/30/1984	Clay	9.0	831.37
6	Decatur	Center	AXP4-3	BRF-2-5(10)--3	1082	Godberson - Sr	HP 10 X 42	35	6/18/1984	6/21/1984	Clay	0.0	965.60
7	Cherokee	Afton	AXP4-6	BRF-3-2(20)--3	683	Christensen Br	HP 10 X 42	35	11/21/1984	11/27/1984	Mixed	0.0	1296.85
8	Linn	Rapids	AXP4-22	I-IG-380-6(57)2	1672	Schmidt Constr	HP 10 X 42	37	8/7/1974	8/15/1974	Mixed	4.0	33.35
9	Linn	Rapids	AXP4-23	I-IG-380-6(57)2	1672	Schmidt Constr	HP 10 X 42	37	11/14/1974	11/19/1974	Mixed	0.0	41.16
10	Ida	Garfield	AXP5-1	BRF-175-3(15)-	383	Christensen Br	HP 10 X 42	36	6/18/1985	6/20/1985	Mixed	0.0	1115.20
11	Hamilton	Liberty	AXP5-2	DP-F-520-4(9)--	1670	Christensen Br	HP 10 X 42	37	4/17/1975	4/22/1975	Clay	8.0	1136.20
12	Linn	Clinton	AXP5-3	F-30-7(62)--20-	1781	Schmidt Constr	HP 10 X 42	37	9/13/1985	9/18/1985	Clay	0.0	820.00
13	Delaware	Richland	AXP6-2	SP-603-0(3)--76	276	Grimshaw Con:	HP 10 X 42	37	3/11/1976	3/16/1976	Sand	0.0	925.78
14	Audubon	Hamlin	AXP6-3	FN-44-3(15)--2	176	Capital Constru	HP 10 X 42	37	5/28/1976	6/3/1976	Mixed	0.0	1199.06
15	Cherokee	Cedar	AXP6-3	BRF-59-7(24)-3	1183	Christensen Br	HP 10 X 42	36	5/19/1986	5/28/1986	Clay	0.0	1328.05
16	Osceola	Ocheyedon	AXP6-4	SN-720(7)--51-	176	Koolker Inc.	HP 10 X 42	30	6/10/1976	6/15/1976	Mixed	0.0	1437.17
17	Fremont	Benton	AXP6-6	BRF-2-1(21)--3	184	Godberson - Sr	HP 10 X 42	36	9/20/1986	9/25/1986	Sand	8.0	862.04
18	Muscatine	Pike	AXP6-7	BRF-22-4(30)--:	284	United Contrac	HP 10 X 42	37	10/8/1986	10/15/1986	Sand	0.0	549.60
19	Marion	Clay	AXP6-8	BRF-592-2(12)3	373	Grimshaw Con:	HP 10 X 42	37	10/7/1976	10/12/1976	Sand	0.0	652.55
20	Muscatine	Pike	AXP6-8	BRF-22-4(30)--:	284	United Contrac	HP 10 X 42	37	10/17/1986	10/22/1986	Sand	0.0	554.30
21	Harrison	Little Sioux	AXP6-9	I-29-5(8)97	463	Hobe Engineer	HP 10 X 42	32	2/9/1966	2/17/1966	Sand	0.0	970.20
22	Dallas	Boone	AXP6-15	I-80-3(15)113	1065	Al Munson	HP 10 X 42	55	3/15/1966	3/18/1966	Clay	0.0	969.70
23	Harrison	Little Sioux	AXP6-16	I-29-5(8)97	363	Jensen Constru	HP 10 X 42	37	3/14/1966	3/22/1966	Sand	0.0	975.78
24	Harrison	St. John	AXP6-22	I-IG-29-5(7)78	265	Sioux Falls Con	HP 10 X 42	37	7/18/1966	7/27/1966	Sand	24.0	947.60
25	Harrison	Taylor	AXP6-28	I-IG-29-5(7)78--	1065	Capital Constru	HP 10 X 42	37	10/24/1966	10/28/1966	Sand	16.5	967.56
26	Harrison	Morgan	AXP7-1	E-ACI-29-5(19)9	665	A. M. Cohron &	HP 10 X 42	27	1/31/1967	2/9/1967	Clay	18.0	981.43
27	Harrison	Morgan	AXP7-4	E-ACI-29-5(19)9	665	A. M. Cohron &	HP 10 X 42	27	2/10/1967	2/17/1967	Mixed	18.0	956.43
28	Fremont	Benton	AXP2-6	I-29-1(9)10--01	369	United Contrac	HP 10 X 42	37	2/19/1972	2/24/1972	Mixed	8.0	900.00
29	Fremont	Benton	AXP2-7	I-29-1(9)10--01	369	United Contrac	HP 10 X 42	37	2/25/1972	2/29/1972	Mixed	8.0	880.00
30	Fremont	Benton	AXP2-10	I-29-1(9)10--01	369	United Contrac	HP 10 X 42	37	3/3/1972	3/9/1972	Sand	8.0	863.00
31	Allamakee	Fairview	AXP0-2	BRF-76-2(11)--2	479	Brennan Const	HP 10 X 42	37	5/30/1980	6/4/1980	Mixed	0.0	540.70
32	Audubon	Sharon	AXP0-3	BRF-44-3(17)--:	280	A. M. Cohron &	HP 10 X 42	37	6/20/1980	6/24/1980	Clay	0.0	1197.20
33	Benton	Polk	AXP0-4	EACI-380-7(2)2	877	A. M. Cohron &	HP 10 X 42	34	10/28/1980	10/30/1980	Clay	0.0	886.75
34	Dubuque	Dubuque	AXP1-2	BRF-561-4(5)--:	1479	Lunda Construc	HP 10 X 42	50	2/18/1981	2/25/1981	Sand	0.0	549.08
35	Clinton	Dewitt	AXP1-4	FFD-561-2(5)--2	277	Lunda Construc	HP 10 X 42	38	3/24/1981	3/31/1981	Sand	23.0	536.20
36	Dubuque	Dubuque	AXP1-5	BRF-561-4(5)--:	1479	Lunda Construc	HP 10 X 42	46	4/6/1981	4/14/1981	Mixed	0.0	557.50
37	Dubuque	Dubuque	AXP1-6	BRF-561-4(5)--:	1579	Lunda Construc	HP 10 X 42	48	6/19/1981	6/25/1981	Sand	0.0	537.50
38	Iowa	Honey Creek	AXP1-7	BRF-21-3(6)38-	179	A. M. Cohron &	HP 10 X 42	33	7/14/1981	7/16/1981	Mixed	0.0	724.64
39	Iowa	Honey Creek	AXP1-8	BRF-21-3(6)38-	179	A. M. Cohron &	HP 10 X 42	33	7/17/1981	7/21/1981	Mixed	0.0	712.64
40	Linn	Washington	AXP1-9	I-380-6(77)280-	2777	Schmidt Constr	HP 10 X 42	37	8/4/1981	8/11/1981	Sand	0.0	684.37
41	Jackson	Monmouth	AXP1-11	BRF-64-2(25)--:	1078	Grimshaw Con:	HP 10 X 42	37	9/29/1981	10/8/1981	Sand	0.0	642.20

Record: 1 of 266 | No Filter | Search

Click here to print the Pile Load Test Record Form

Click here to close the Pile Load Test Record Form

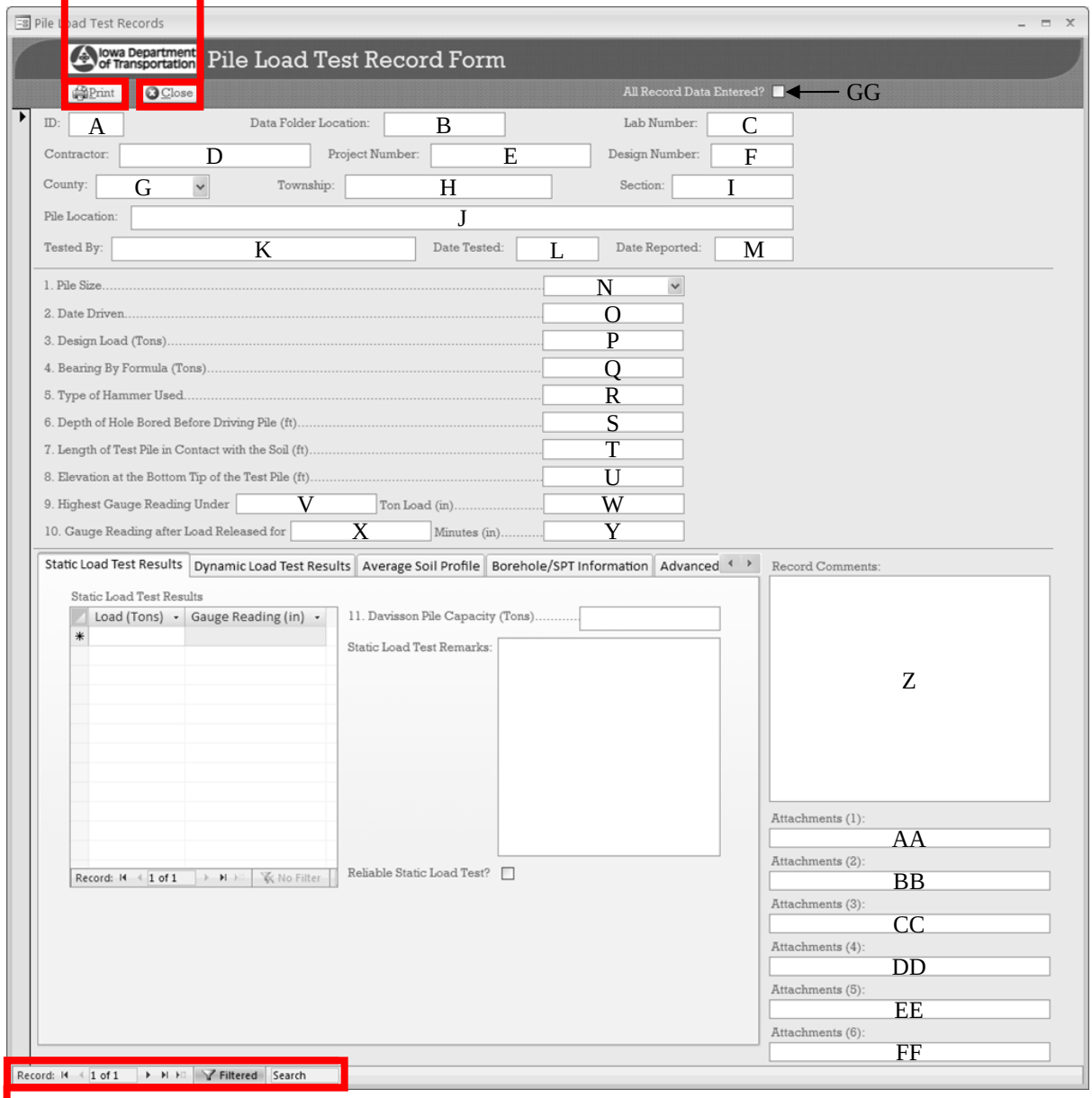

Figure 3.36: Pile Load Test Record Form (PLTRF)

Use these controls to navigate amongst the various records in PILOT-IA

3.4.2.2.1 General Pile Load Test Record Form Information

Described below are various fields included in the general Pile Load Test Record Form (PLTRF) with reference to labels included in Figure 3.36.

A. **ID:** A unique cataloging number automatically assigned by Microsoft Office Access™ to each record within PILOT-IA.
B. **Data Folder Location:** A database field that specifies the location of the pile load test records for each load test contained within the database. The directory housing these various pile load test records, the Pile Load Tests Records Directory, is organized by three volumes. Volume 1 consists of pile load test records for steel H-piles, Volume 2 consists of pile load test records for prestressed concrete, Monotube, and steel pipe piles, Volume 3 consists of pile load test records for timber piles, and Volume 4 consists of pile load test records for those piles tested as a part of the research defined in this thesis (i.e., Chapter 4). Therefore, the possible entries into this database field are as follows: Volume 1, Volume 2, Volume 3, or Volume 4.
C. **Lab Number:** The identification number used by the Iowa DOT to distinguish between the various test piles (e.g., AXP0-1, AXP1-9, etc.).
D. **Contractor:** The name of the contracting company responsible for the construction of the specified bridge project including driving of the test pile.
E. **Project Number:** The unique Iowa DOT cataloging number assigned to each construction project.
F. **Design Number:** This database field goes hand in hand with the previously described field E (i.e., Project Number). For every construction project in the State of Iowa, in addition to assigning a unique project number, each bridge project within the construction project is assigned a unique design number. The bridge design number corresponding to a specified pile load test is entered into this database field.
G. **County:** This database field utilizes a drop-down menu for simple selection of the Iowa County in which the specified bridge construction project is located.
H. **Township:** This field allows one to manually enter the name of the township corresponding to the location of the specified Iowa bridge construction project.

I. **Section:** This numerical database field allows one to manually enter the section number in which the specified Iowa bridge construction project is located.

J. **Pile Location:** This text database field allows one to manually enter a short description of the test pile location in relation to the features of the bridge under construction. For instance, a typical description will specify if the test pile was located near an abutment or a pier. Furthermore, either the pile number or a detailed narrative identifying the exact location of the pile within the abutment or pier is usually provided.

K. **Tested By:** This text database field allows one to manually enter the names of those people who were responsible for carrying out the pile load test on the specified pile.

L. **Date Tested:** In this database field, which has been formatted to accept dated entries of the form: Month/Day/Year (e.g., 3/8/1984), the date on which the pile static load test was conducted on the specified pile is specified.

M. **Date Reported:** In this database field, which has been formatted to accept dated entries of the form: Month/Day/Year (e.g., 3/8/1984), the date on which the pile load test results for the specified pile were reported to the Iowa DOT is specified.

N. **1. Pile Size:** This database field utilizes a drop-down menu for simple selection of the test pile type and size. The options available for selection in this database field are as follows: Steel H-Piles (10×42, 10×57, 12×53, 12×74, 14×73, 14×89, and Steel H – a generic option that may be utilized for instances where the exact Steel H pile size is unknown), Monotube Piles, Steel Pipe Piles (10”, 12”, 16”, and 18” outside diameter), and Timber Piles (18’, 20’, 25’, 30’, 34’, 35’, 40’, 45’, 50’, 55’, and 60’ length or Timber – a generic option that may be utilized for instances where the exact timber pile length is unknown).

O. **2. Date Driven:** In this database field, which has been formatted to accept dated entries of the form Month/Day/Year (e.g., 3/8/1984), the date on which the specified test pile was driven is included.

P. **3. Design Load (Tons):** This database field specifies the total sum of all design loads for which any given pile in the structure is anticipated to support based on the superstructure loading evaluation. In other words, the given pile must possess a bearing capacity equal to or greater than this value to ensure the safety of the structure.

Q. **4. Bearing by Formula (Tons):** This database field specifies the anticipated bearing capacity for a given pile as determined through the use of the Iowa DOT Modified ENR dynamic pile driving formula, which is supplied in Article 2501.13 of the Iowa Department of Transportation Standard Specifications, Series 2008 (Iowa DOT 2008) and was presented in Section 2.3.4 of this thesis.

R. **5. Type of Hammer Used:** This database field contains information about the type of hammer used for driving the test pile. Examples of possible entries into this database field include: Gravity, Kobe K-13, and Delmag D-12; the last two examples specify both a brand and series number.

S. **6. Depth of Hole Bored before Driving Pile (ft):** The depth, in feet, of the hole bored to initiate pile driving of the specified test pile. (A value of zero in this field indicates that no hole was bored prior to driving.)

T. **7. Length of Test Pile in Contact with the Soil (ft):** The length, in feet, of the test pile in direct contact with the soil.

U. **8. Elevation at the Bottom Tip of the Test Pile (ft):** The elevation, in feet, at which the toe of the driven test pile resides with reference to the mean sea level datum.

V & W. **9. Highest Gauge Reading Under ### Ton Load (in):** Based upon the SLT results for the specified pile (the location of the SLT results for each record in the database is shown in Figure 3.37), the maximum load experienced by the pile is recorded where the number signs (i.e., ###) appear in the above statement and the displacement gauge reading, in inches, corresponding to this maximum applied load is included in database field W.

X & Y. **10. Gauge Reading after Load Released for ### Minutes (in):** The final entry into each record's static load test table shows a load of zero tons and a corresponding non-zero gauge reading. This gauge reading represents the rebound of the specified pile

after the release of the maximum applied vertical load for a given period of time. The time between the release of the maximum applied load to the pile and the subsequent recording of the final gauge reading is added where the number signs (i.e., ###) appear in the above statement. The final gauge reading, in inches, is then specified in database field Y.

Z. **Record Comments:** Any pertinent additional information regarding the record as a whole is included in this text database field.

AA - FF. **Attachments (1) – (6):** These six hyperlink database fields were created so that important information related to each pile load test could be easily accessed from the PLTRF. The hyperlinked text descriptions found within these database fields maintain a direct path to the file of interest.

To add a new hyperlink to the PLTRF, follow the steps outlined below:

1) Open the desired PLTRF to which a new hyperlink will be added.
2) Position the cursor over the preferred location, Attachments (1) – (6), for the new hyperlink.
3) Right click with the mouse and select Hyperlink-Edit Hyperlink…
4) Locate the file to which the hyperlink will be tied and provide a concise but meaningful description of the file in the "Text to display:" option.

GG. **All Record Data Entered?:** This yes/no database field was created mostly for the one(s) responsible for the data entry procedures, so that an easy distinction could be made between those records still requiring data to be entered and those that had been termed complete. When all available information has been entered for a specific record, this field receives a check mark.

3.4.2.2.2 Static Load Test Results Tab of PLTRF

As illustrated in Figure 3.37, the first of nine tabs encountered on the PLTRF (i.e., Static Load Test Results) houses those results related to a pile static load test. Most importantly, this tab contains a table which displays the load versus displacement results obtained during static load testing of the pile. The remaining fields contained within this tab are elucidated below.

A. **11. Davisson Pile Capacity (Tons):** Utilizing the static load test results supplied for each pile, shown in Figure 3.37, the Davisson failure criterion was utilized to determine the ultimate pile capacity. The Davisson failure criterion states that the ultimate load of a pile subjected to a vertical load test is the load which the displacement of the pile exceeds the elastic compression of the pile by $0.15 + D/120$ inches, where D is the pile depth or diameter (Davisson 1972). The elastic compression of the pile is simply the length of the pile divided by its elastic modulus and cross-sectional area (i.e., the pile stiffness), then multiplied by the applied load. The Davisson pile capacity established for each pile SLT is provided in this numerical database field.

B. **Static Load Test Remarks:** Any additional comments or information relating to the pile SLT results are supplied in this text database field. Examples of information presented in this database field include the time duration step used for each load increment and pertinent test reliability information such as observed pile punching, pulling out of anchor piles, or no observed yielding of the test pile.

C. **Reliable Static Load Test?:** This yes/no database field receives a checkmark if the SLT data for the specified pile is considered reliable. A reliable test is one in which the test pile reached its displacement-based capacity (i.e., the Davisson pile capacity) with no anchor piles being pulled out prior to its achievement. If the SLT data for a specified test pile does not meet this criterion, then the test is considered unreliable and this database field is left unchecked.

3.4.2.2.3 Dynamic Load Test Results Tab of PLTRF

As illustrated in Figure 3.38, the second of nine tabs included on the PLTRF (i.e., Dynamic Load Test Results) houses those results obtained from a dynamic pile load test using PDA. The fifteen fields contained within this tab are described below.

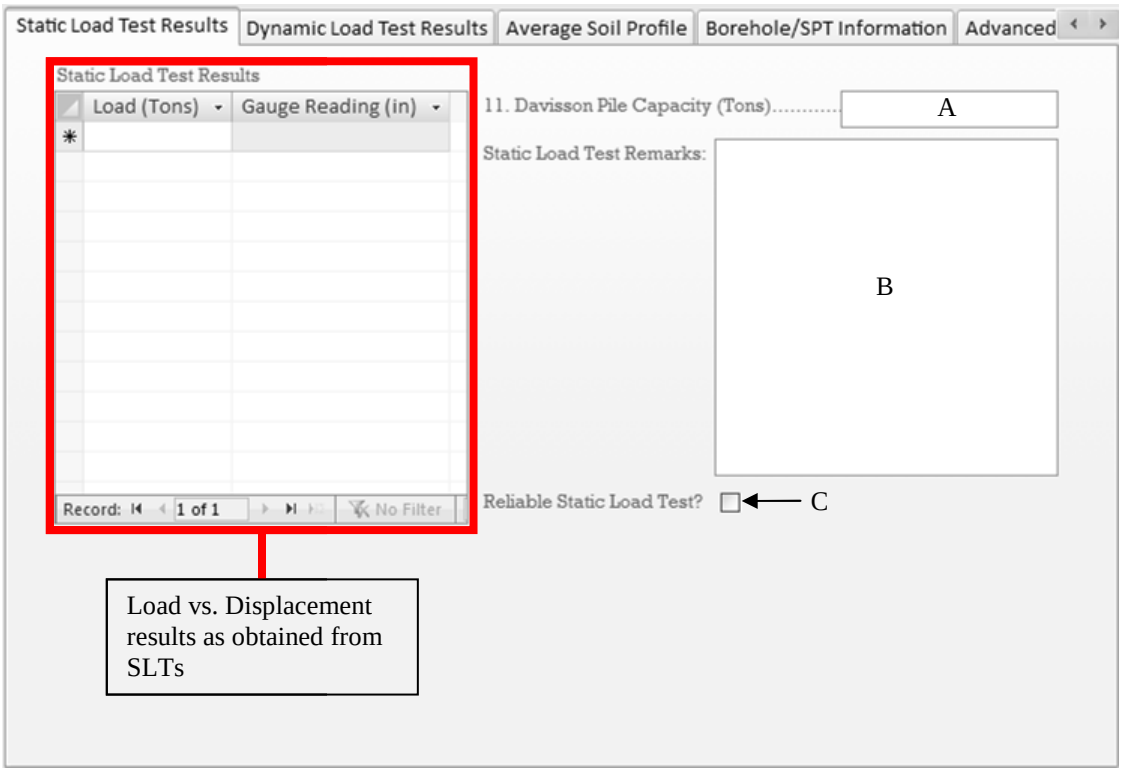

Figure 3.37: Static Load Test Results Tab of PLTRF

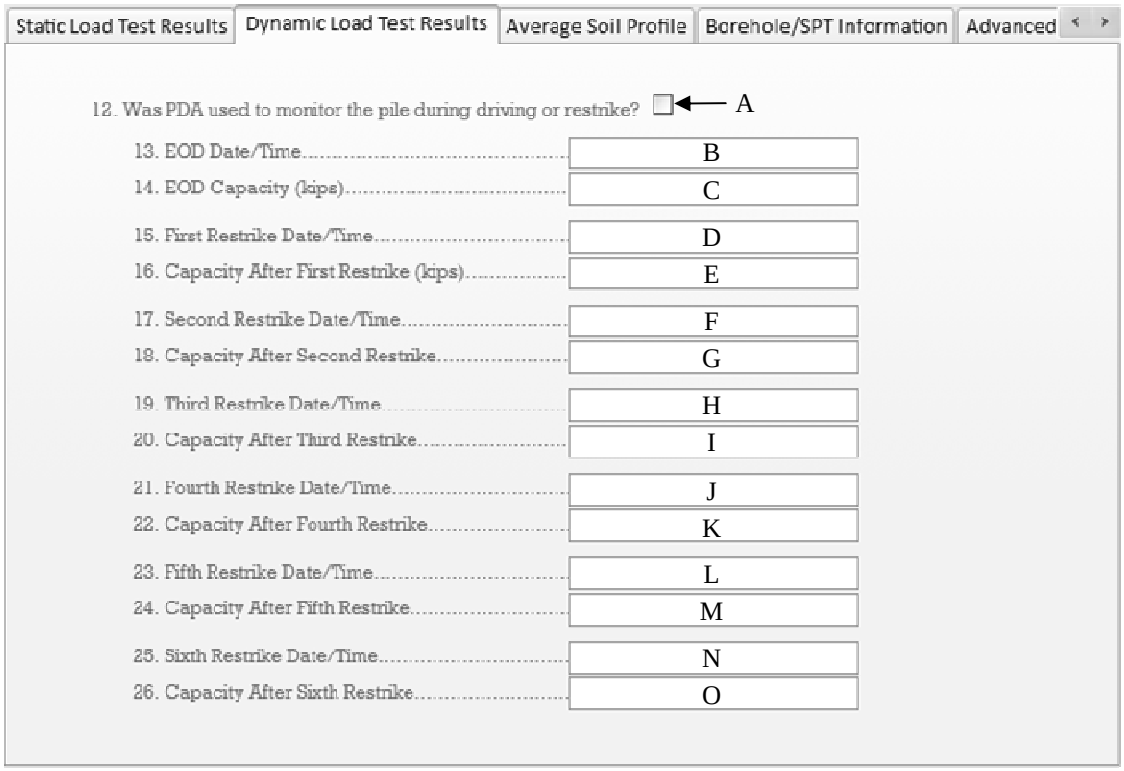

Figure 3.38: Dynamic Load Test Results Tab of PLTRF

A. **12. Was PDA used to monitor the pile during driving or restrike?:** This yes/no database field receives a checkmark when the Pile Driving Analyzer hardware product is used to monitor the installation of the test pile, which must be instrumented with accelerometers and strain transducers near the pile head, and assess its bearing capacity at either the EOD or BOR conditions; otherwise, this database field is left unchecked.

B. **13. EOD Date/Time:** In this database field, which has been formatted to accept dated entries of the form: Month/Day/Year Time-of-Day (e.g., 3/8/1984 10:12:55 AM), the date and time at which the EOD condition was achieved is input.

C. **14. EOD Capacity (kips):** The maximum static pile capacity estimate, in units of kips, provided by PDA at the EOD (i.e., RMX).

D. **15. First Restrike Date/Time:** In this database field, which has been formatted to accept dated entries of the form: Month/Day/Year Time-of-Day (e.g., 3/8/1984 10:12:55 AM), the date and time corresponding to the beginning of the first restrike are added.

E. **16. First Restrike Capacity (kips):** This field represents the maximum static pile capacity estimate, in units of kips, provided by PDA at the beginning of the first restrike (i.e., RMX).

F. **17. Second Restrike Date/Time:** In this database field, which has been formatted to accept dated entries of the form: Month/Day/Year Time-of-Day (e.g., 3/8/1984 10:12:55 AM), the date and time corresponding to the beginning of the second restrike are inserted.

G. **18. Second Restrike Capacity (kips):** This field represents the maximum static pile capacity estimate, in units of kips, provided by PDA at the beginning of the second restrike (i.e., RMX).

H. **19. Third Restrike Date/Time:** In this database field, which has been formatted to accept dated entries of the form: Month/Day/Year Time-of-Day (e.g., 3/8/1984 10:12:55 AM), the date and time corresponding to the beginning of the third restrike are input.

I. **20. Third Restrike Capacity (kips):** This field represents the maximum static pile capacity estimate, in units of kips, provided by PDA at the beginning of the third restrike (i.e., RMX).
J. **21. Fourth Restrike Date/Time:** In this database field, which has been formatted to accept dated entries of the form: Month/Day/Year Time-of-Day (e.g., 3/8/1984 10:12:55 AM), the date and time corresponding to the fourth restrike are added.
K. **22. Fourth Restrike Capacity (kips):** This field represents the maximum static pile capacity estimate, in units of kips, provided by PDA at the beginning of the fourth restrike (i.e., RMX).
L. **23. Fifth Restrike Date/Time:** In this database field, which has been formatted to accept dated entries of the form: Month/Day/Year Time-of-Day (e.g., 3/8/1984 10:12:55 AM), the date and time corresponding to the fifth restrike are inserted.
M. **24. Fifth Restrike Capacity (kips):** This field represents the maximum static pile capacity estimate, in units of kips, provided by PDA at the beginning of the fifth restrike (i.e., RMX).
N. **25. Sixth Restrike Date/Time:** In this database field, which has been formatted to accept dated entries of the form: Month/Day/Year Time-of-Day (e.g., 3/8/1984 10:12:55 AM), the date and time corresponding to the sixth restrike are input.
O. **26. Sixth Restrike Capacity (kips):** This field represents the maximum static pile capacity estimate, in units of kips, provided by PDA at the beginning of the sixth restrike (i.e., RMX).

3.4.2.2.4 Average Soil Profile Tab of PLTRF

As illustrated in Figure 3.39, the third of nine tabs included on the PLTRF (i.e., Average Soil Profile) houses information concerning various soil parameters characteristic of the average soil profile found at the location of the test pile. The various soil parameters included in the table provided in this tab include thickness, an average SPT blow count (NAVG), and a unit skin friction value specified by the design chart found in the *Iowa LRFD Bridge Design Manual* (Iowa DOT 2010) for each soil layer, as well as a total soil layer skin friction value resulting from the multiplication of the soil layer thickness by the unit skin friction value.

A. **27. Total Sum of Soil Layer Thicknesses (ft):** This database field refers to the average soil profile table illustrated in Figure 3.39. Based upon the average soil layer data found in this table, the sum of the thicknesses of the various soil strata identified in the table is reported in this field.

B. **28. Calculated Total Skin Friction Using Design Charts (Tons):** This field refers to the average soil profile table illustrated in Figure 3.39. Based upon the average soil layer data found in this table, the sum of the total skin friction values listed for each of the various soil strata identified in the table is reported in this database field.

C. **29. Calculated End Bearing Using Design Charts (Tons):** The value input into this field is determined through the use of the average soil profile table illustrated in Figure 3.39 and the design chart found in the *Iowa LRFD Bridge Design Manual* (Iowa DOT 2010). Based upon the average blow count (i.e., NAVG) value obtained for the soil layer in which the test pile toe resides and the aforementioned design chart, a total end bearing value is established and recorded into this database field.

D. **30. Total Pile Capacity Using Design Charts (Tons):** The value input into this database field is the result of the addition of the value found in the database field marked with a number 28 (i.e., Calculated Total Skin Friction Using Design Charts) and the value found in the database field marked with a number 29 (i.e., Calculated End Bearing Using Design Charts).

E. **31. Factor of Safety:** The value entered into this database field is the result of dividing the value found in the database field marked with a number 11 (i.e., Davisson Pile Capacity) by the value found in the database field marked with a number 3 (i.e., Design Load).

F. **Test Site Soil Classification:** This database field utilizes a drop-down menu for simple selection of the predominant soil medium (i.e., sand, clay, or, mixed) encountered along the shaft of the test pile. When at least two soil types are present along the shaft of the test pile and none account for 70 percent or more of the soil profile encountered along the shaft of the test pile, then a mixed soil classification is used to describe the predominant soil medium.

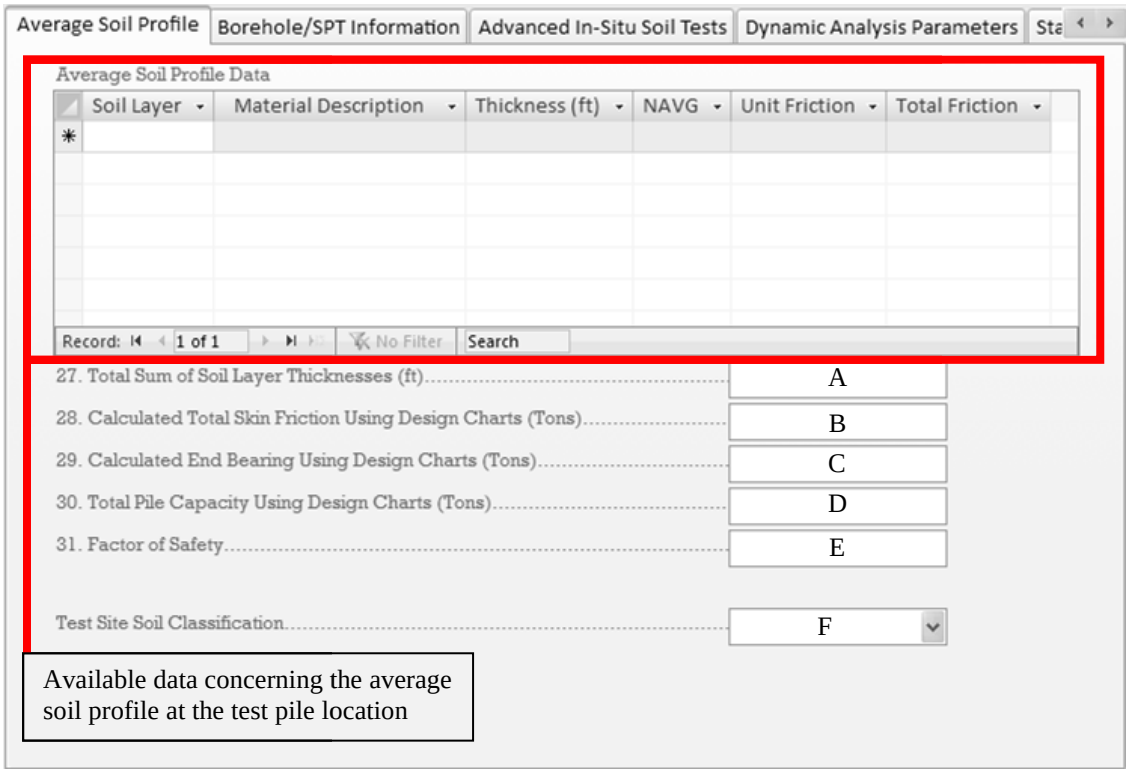

Figure 3.39: Average Soil Profile Tab of PLTRF

3.4.2.2.5 Borehole/SPT Information Tab of PLTRF

As illustrated in Figure 3.40, the fourth of nine tabs included on the PLTRF (i.e., Borehole/SPT Information) houses information concerning the availability of borehole and SPT data at the location of the test pile. Most importantly, this tab possesses a table that displays the available borehole and SPT data at the test pile location. The remaining fields contained within this tab are described below.

A. **32. Total Number of Boreholes:** The total number of boreholes drilled for the corresponding construction project. This information is taken from the relevant project Situation Plan Sheet.
B. **33. Total Number of Borehole with SPT Data:** The total number of boreholes possessing soil penetration data or SPT N-values. This information is taken from the relevant project Sounding Data Plan Sheet.
C. **34. Borehole(s) near Test Pile Location:** This yes/no database field receives a checkmark if a borehole is located within 100 feet of the specified test pile location.

If no borehole is located within 100 feet of the test pile location, the field is left without a checkmark.

D. **35. Borehole Number(s) near Test Pile Location:** When the Borehole(s) at Test Pile Location database field is checked, the identification number associated with each of the boreholes located within 100 feet of the test pile location is reported in this text database field. Otherwise, if no boreholes are located within 100 feet the test pile location, the word "None" is entered into this database field. When a borehole or boreholes are located within 100 feet of the location of the test pile, the resulting soil profiles are displayed in the table identified in Figure 3.40.

E. **36. SPT Data Available near Test Pile Location:** When any of the boreholes listed in the Borehole(s) at Test Pile Location database field possess SPT data, then the identification number of such boreholes is repeated in this database field, and the resulting data, soil profile and SPT values are entered into the table identified in Figure 3.40. If none of the boreholes listed in the Borehole(s) at Test Pile Location database field have SPT data, then the word "None" appears in this database field. Although, if the soil profile at the test pile location matches that of any of the boreholes with SPT data, even though these boreholes are not located at or within 100 feet of the test pile location, the resulting information for such boreholes is also provided in the table identified in Figure 3.40.

F. **Usable-Static Test?:** This yes/no database field receives a checkmark if a checkmark already exists in the Reliable Load Test? database field and if there is acceptable SPT data available at or within 100 feet of the test pile location.

3.4.2.2.6 Advanced In-Situ Soil Tests Tab of PLTRF

As illustrated in Figure 3.41, the fifth of nine tabs included on the PLTRF (i.e., Advanced In-Situ Soil Tests) houses those results obtained from advanced in-situ soil tests such as the CPT and the BST, as well as horizontal stress and porewater pressure data collected from push-in pressure cells. The twelve fields contained within this tab are described below.

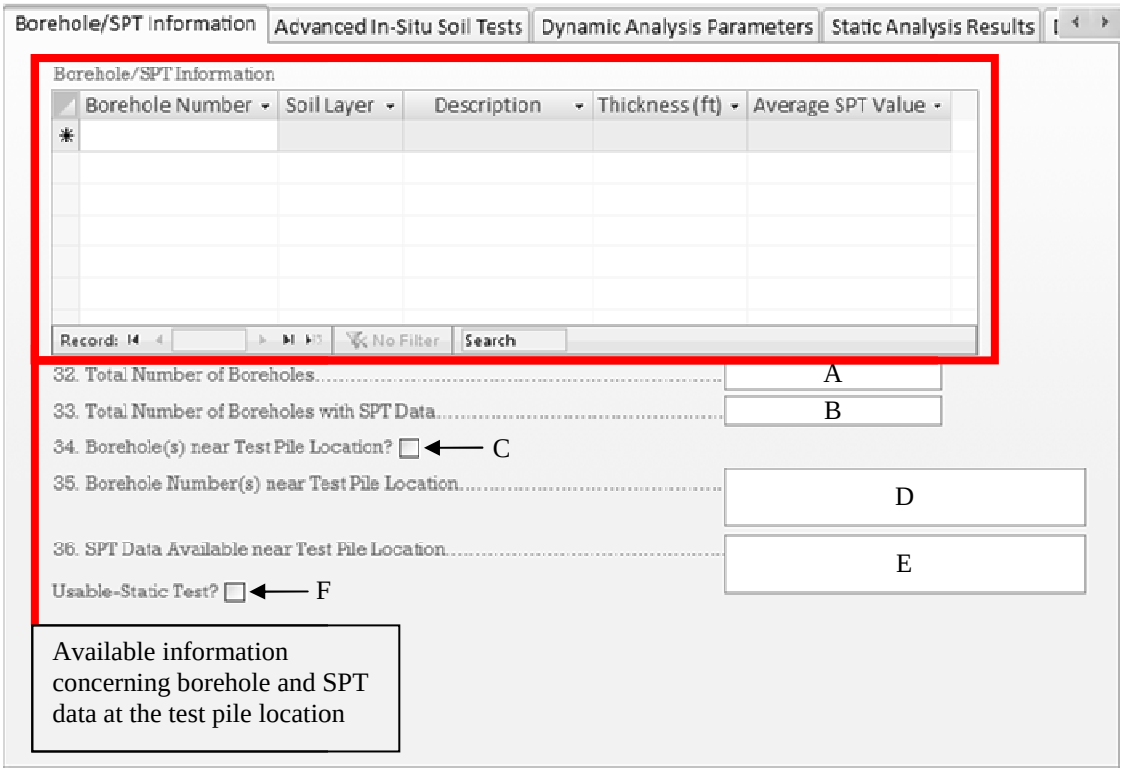

Figure 3.40: Borehole/SPT Information Tab of PLTRF

A. **37. Were Push-In Pressure Cells used to monitor lateral earth and porewater pressure?:** This yes/no database field receives a checkmark if one or more push-in pressure cells were installed near the location of the test pile for acquisition of horizontal stress and porewater pressure data; otherwise, this database field is left unchecked.

B. **38. Number of Pressure Cells Used:** When the database field marked with a number 37 (i.e., Were Push-In Pressure Cells used to monitor lateral earth and porewater pressure?) is checked, the total number of push-in pressure cells installed near the location of the test pile is reported in this text database field.

C. **39. Depth of Pressure Cells:** When the database field marked with a number 37 (i.e., Were Push-In Pressure Cells used to monitor lateral earth and porewater pressure?) is checked, the depths to which each of the push-in pressure cells identified in the database field marked with a number 38 (i.e., Number of Pressure Cells Used) were installed are reported in this text database field.

D. **40. Complete Pressure Cell Data:** This hyperlink database field allows for the establishment of a direct path to the file(s) holding all data acquired from the installed push-in pressure cells. The reader is referred to Section 3.4.2.2.1 for instructions on how to add a new hyperlink to the PLTRF.

E. **41. Was a Cone Penetration Test (CPT) Performed?:** This yes/no database field receives a checkmark if one or more CPTs were performed near the location of the test pile; otherwise, this database field is left unchecked.

F. **42. Number of CPT Soundings:** When the database field marked with a number 41 (i.e., Was a Cone Penetration Test (CPT) Performed?) is checked, the total number of soundings performed near the location of the test pile is reported in this text database field.

G. **43. Number of Pore Pressure Dissipation Tests:** When the database field marked with a number 41 (i.e., Was a Cone Penetration Test (CPT) Performed?) is checked, the number of pore pressure dissipation tests conducted in conjunction with each of the CPT soundings identified in the database field marked with a number 42 (i.e., Number of CPT Soundings) is reported in this text database field.

H. **44. Complete CPT Data:** This hyperlink database field allows for the establishment of a direct path to the file(s) holding all data acquired from the various CPTs performed near the location of the test pile. The reader is referred to Section 3.4.2.2.1 for instructions on how to add a new hyperlink to the PLTRF.

I. **45. Was a Borehole Shear Test (BST) Performed?:** This yes/no database field receives a checkmark if one or more BSTs were performed near the location of the test pile; otherwise, this database field is left unchecked.

J. **46. Number of BSTs Performed:** When the database field marked with a number 45 (i.e., Was a Borehole Shear Test (BST) Performed?) is checked, the total number of BSTs performed near the location of the test pile is reported in this text database field.

K. **47. Depths of BSTs:** When the database field marked with a number 45 (i.e., Was a Borehole Shear Test (BST) Performed?) is checked, the depths at which each of the BSTs identified in the database field marked with a number 46 (i.e., Number of BSTs Performed) were performed are reported in this text database field.

L. **48. Complete BST Data:** This hyperlink database field allows for the establishment of a direct path to the file(s) holding all data acquired from the various BSTs performed near the location of the test pile. The reader is referred to Section 3.4.2.2.1 for instructions on how to add a new hyperlink to the PLTRF.

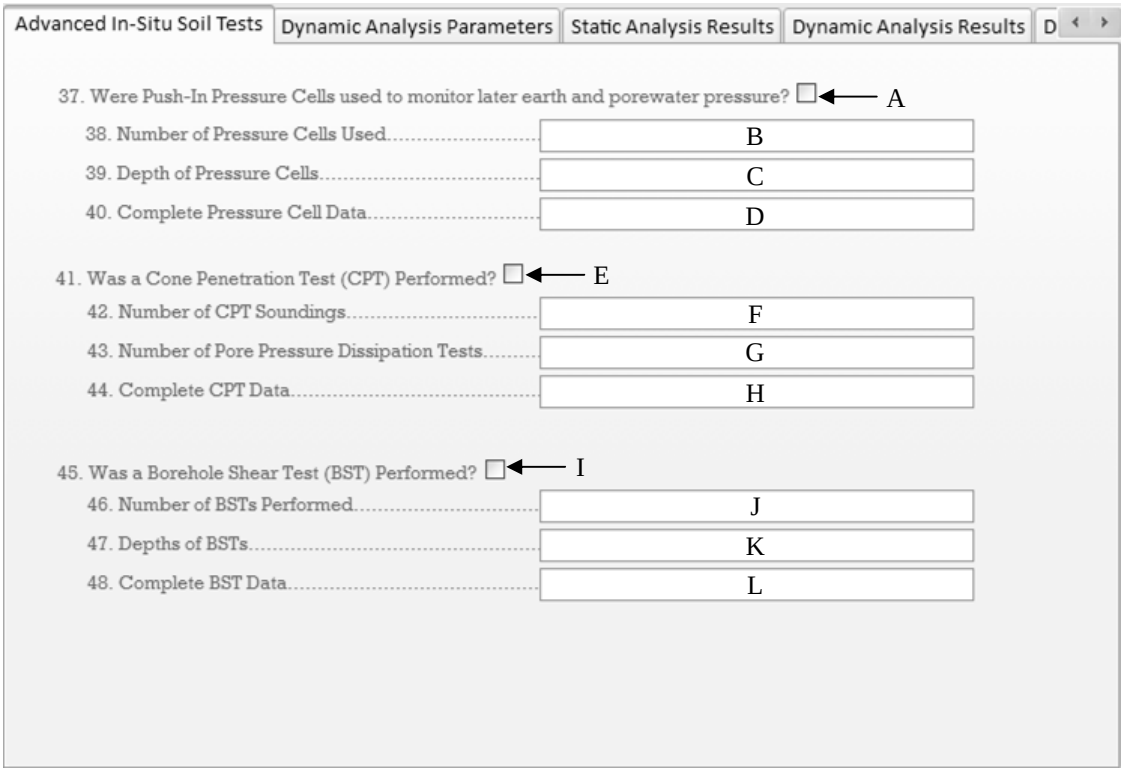

Figure 3.41: Advanced In-Situ Soil Tests Tab of PLTRF

3.4.2.2.7 Dynamic Analysis Parameters Tab of PLTRF

As illustrated in Figure 3.42, the sixth of nine tabs included on the PLTRF (i.e., Dynamic Analysis Parameters) houses information necessary for the prediction of pile capacity by means of dynamic methods (e.g., WEAP, PDA, CAPWAP, and dynamic pile driving formulas). The eleven fields contained within this tab are described below.

A. **49. Water Table Location:** The elevation at which the groundwater table is encountered at the site of the test pile is included in this database field. Such information is taken from the relevant Sounding Data Plan Sheet.

B. **50. Driven Pile Length (ft):** The total length of pile, in units of feet, placed in the leads of the pile driving rig is inserted into this database field.

C. **51. Pile Cross-Sectional Area (square inches):** The total cross-sectional area, in units of square inches, of the pile driven for load testing purposes is inserted into this database field.

D. **52. Pile Weight (lb):** The total weight, in units of pounds, of the pile driven for load testing purposes is inserted into this database field. This pile weight should be in agreement with the length of pile specified in the database field marked with the number 50 (i.e., Driven Pile Length).

E. **53. Hammer (Ram) Weight (lb):** This numerical database field presents the total dynamic weight, in units of pounds, of the hammer used for driving the test pile. The dynamic weight of the hammer is determined by taking the total static weight of the hammer less such deductions resulting from air resistance, lead friction, etc.

F. **54. Cap Weight (lb):** The total weight of the cap, in units of pounds, used while driving the test pile is inserted into this database field.

G. **55. Anvil Weight (lb):** The total weight of the anvil, in units of pounds, used while driving the test pile is inserted into this database field.

H. **56. Hammer Stroke (ft):** The average height above the pile head, in units of feet, from which the hammer is dropped during the final five to ten blows of driving is recorded in this database field.

I. **57. Developed Hammer Energy (ft-tons):** The total developed energy, in units of foot-pounds, imparted by the hammer to the test pile is recorded in this database field. Simply put, the total developed energy is determined by multiplying the hammer (ram) weight with the hammer stroke.

J. **58. Average Number of Blows per Foot of Pile Penetration (blows/ft):** The average number of blows needed to advance the test pile tip one foot near the end of driving is recorded in this database field. This value is determined from the average penetration of the test pile over the last five to ten blows (i.e., five blows for gravity hammers and 10 blows for steam or diesel hammers) as recorded on the “Log of Piling Driven” record.

K. **Usable-Dynamic Test?:** This yes/no database field receives a checkmark if a checkmark already exists in the Usable-Static Test? database field and if complete driving records and information concerning characteristics of the pile driving equipment are available for the test pile.

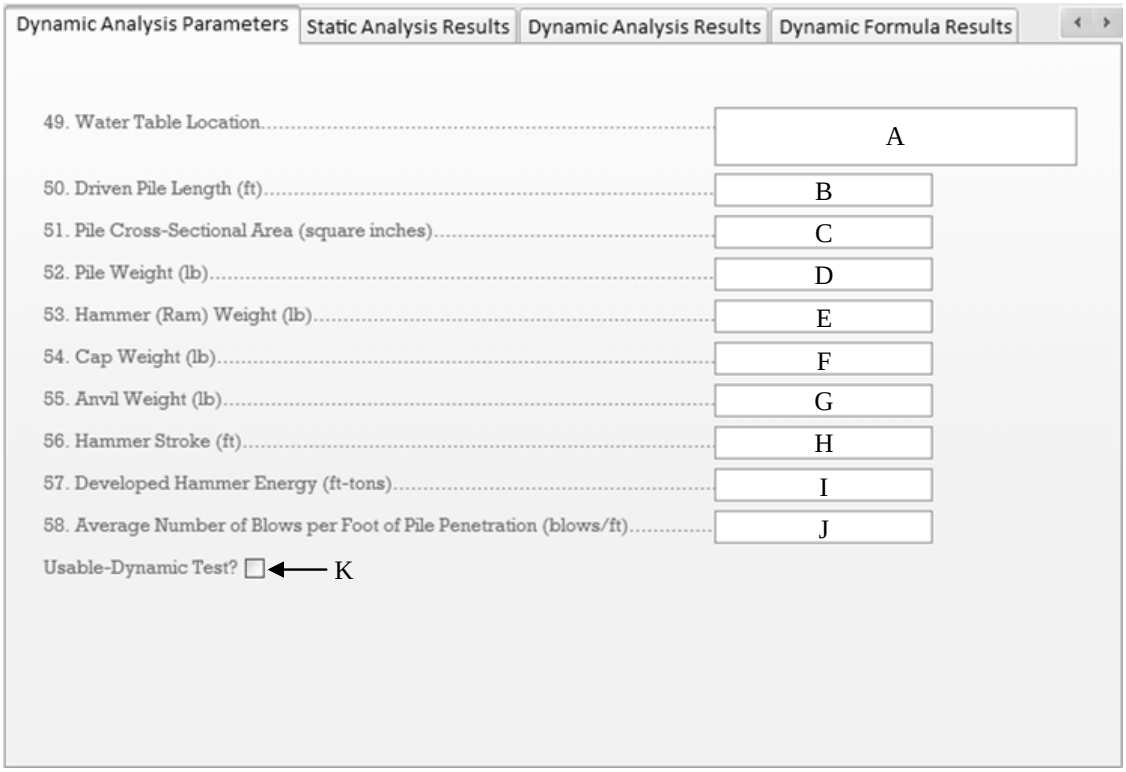

Figure 3.42: Dynamic Analysis Parameters Tab of PLTRF

3.4.2.2.8 Static Analysis Results Tab of PLTRF

As illustrated in Figure 3.43, the seventh of nine tabs included on the PLTRF (i.e., Static Analysis Results) displays the results obtained from the application of five static analysis methods upon the given test pile. The five static analysis methods displayed on this tab were chosen by AbdelSalam (2010) in response to an in-depth literature review of the most common and well-performing methods. The five fields contained within this tab are described below.

A. **59. Pile Capacity by Iowa Blue Book Method (Tons):** The pile capacity, in tons, predicted by the Iowa Blue Book static analysis method (Dirks and Kam 1989; AbdelSalam et al. 2010) is placed in this field.

B. **60. Pile Capacity by SPT Method (Tons):** The pile capacity, in tons, predicted by the SPT-Meyerhof static analysis method (Meyerhof 1976) is placed in this field.

C. **61. Pile Capacity by Alpha-API Method (Tons):** The pile capacity, in tons, predicted by the α-API (American Petroleum Institute) static analysis method (API 1984) is placed in this field.

D. **62. Pile Capacity by Beta Method (Tons):** The pile capacity, in tons, predicted by the β static analysis method (Burland 1973) is placed in this field.

E. **63. Pile Capacity by Nordlund Method (Tons):** The pile capacity, in tons, predicted by the Nordlund static analysis method (Nordlund 1963) is placed in this field.

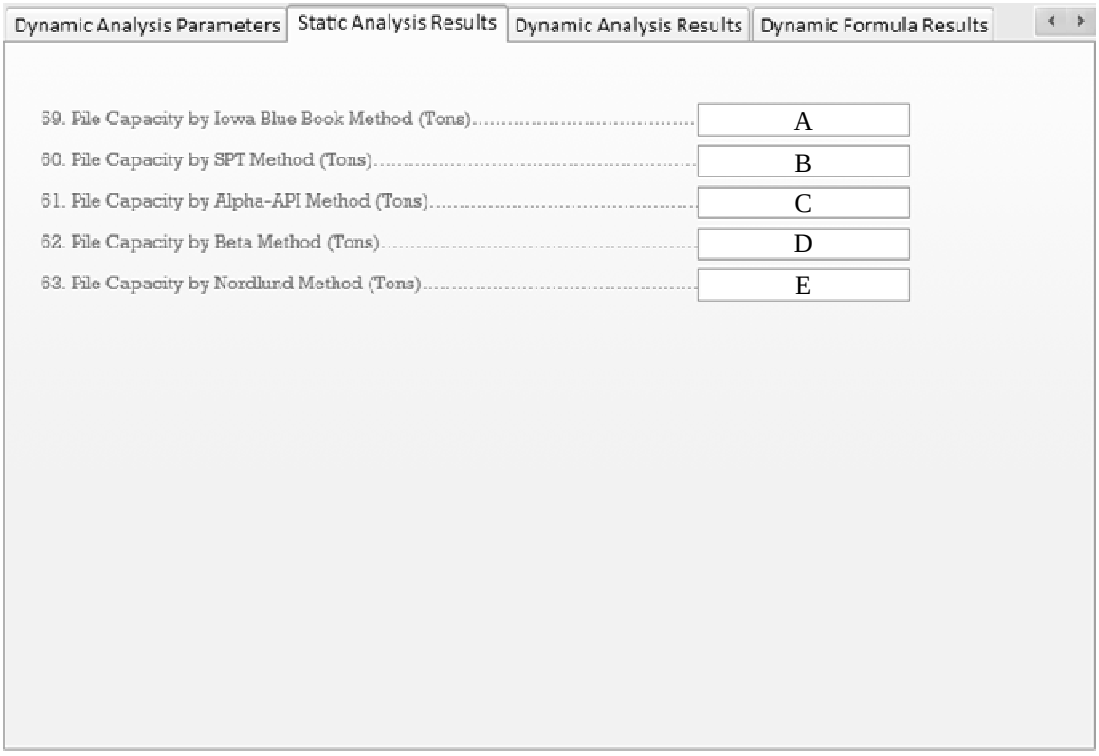

Figure 3.43: Static Analysis Results Tab of PLTRF

3.4.2.2.9 Dynamic Analysis Results Tab of PLTRF

As illustrated in Figure 3.44, the eighth of nine tabs included on the PLTRF (i.e., Dynamic Analysis Results) displays the results obtained from the application of three dynamic analysis methods upon the given test pile. The three dynamic analysis methods displayed on this tab were chosen by Ng (2011) in response to an in-depth literature review of the most common and well-performing methods. The fields contained within this tab are described below.

A. **64. Pile Capacity by WEAP (Tons):** The pile capacity, in tons, as predicted by the Wave Equation Analysis Program (Pile Dynamics Inc. 2005) is placed in this field.
B. **65. Shaft Quake used in WEAP Analysis:** The elastic compression limit or quake, in units of inches, for soil located along the shaft of the test pile that was used to determine the WEAP pile capacity is placed in this field.
C. **66. Toe Quake used in WEAP Analysis:** The elastic compression limit or quake, in units of inches, for soil located at the toe of the test pile that was used to determine the WEAP pile capacity is placed in this field.
D. **67. Shaft Damping Factor used in WEAP Analysis:** The damping factor for soil located along the shaft of the test pile that was used to determine the WEAP pile capacity is placed in this field.
E. **68. Toe Damping Factor used in WEAP Analysis:** The damping factor for soil located at the toe of the test pile that was used to determine the WEAP pile capacity is placed in this field.
F. **69. Pile Capacity from PDA (Tons):** The pile capacity, in tons, as predicted by PDA (Pile Dynamics Inc. 1992) is placed in this field.
G. **70. Case Damping Factor used by PDA:** The Case damping factor utilized by PDA to predict the ultimate capacity of the test pile is reported in this field.
H. **71. Pile Capacity from CAPWAP (Tons):** The pile capacity, in tons, as predicted by the CAse Pile Wave Analysis Program (Pile Dynamics Inc. 2000) is placed in this field.

I. **72. Smith Shaft Damping Factor Calculated by CAPWAP:** The damping factor for soil located along the shaft of the test pile that was calculated by CAPWAP in predicting the pile capacity is placed in this field.
J. **73. Smith Toe Damping Factor Calculated by CAPWAP:** The damping factor for soil located at the toe of the test pile that was calculated by CAPWAP in predicting the pile capacity is placed in this field.
K. **74. Shaft Quake Calculated by CAPWAP:** The elastic compression limit or quake, in units of inches, for soil located along the shaft of the test pile that was calculated by CAPWAP in predicting the pile capacity is placed in this field.
L. **75. Toe Quake Calculated by CAPWAP:** The elastic compression limit or quake, in units of inches, for soil located at the toe of the test pile that was calculated by CAPWAP in predicting the pile capacity is placed in this field.
M. **76. Case Shaft Damping Factor Calculated by CAPWAP:** The Case damping factor for soil located along the shaft of the test pile that was calculated by CAPWAP in predicting the pile capacity is reported in this field.
N. **77. Case Toe Damping Factor Calculated by CAPWAP:** The Case damping factor for soil located at the toe of the test pile that was calculated by CAPWAP in predicting the pile capacity is reported in this field.

3.4.2.2.10 Dynamic Formula Results Tab of PLTRF

As illustrated in Figure 3.45, the final tab included on the PLTRF (i.e., Dynamic Formula Results) displays the results obtained from the application of seven dynamic pile driving formulas upon the given test pile. The seven dynamic pile driving formulas displayed on this tab were chosen as a consequence of the results obtained from the in-depth literature review of the most common and well-performing formulas presented in Chapter 2 of this thesis. The fields contained within this tab are described below.

A. **78. Pile Capacity by ENR Formula (Tons):** The pile capacity, in tons, as predicted by the Engineering News Record formula (Wellington 1893) is reported in this field.

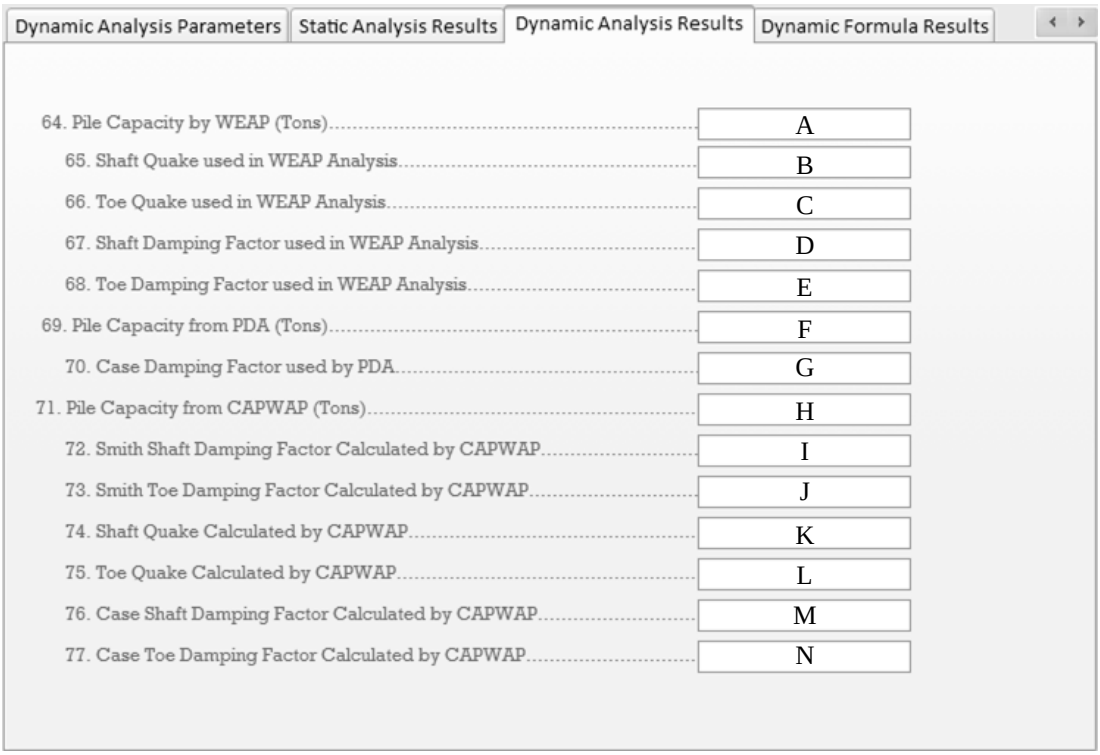

Figure 3.44: Dynamic Analysis Results Tab of PLTRF

B. **79. Pile Capacity by Iowa DOT Modified ENR Formula (Tons):** The pile capacity, in tons, as predicted by the Iowa DOT Modified Engineering News Record formula (Iowa DOT 2008) is reported in this field.

C. **80. Pile Capacity by Gates Formula (Tons):** The pile capacity, in tons, as predicted by the Gates formula (Gates 1957) is reported in this field.

D. **81. Pile Capacity by FHWA Modified Gates Formula (Tons):** The pile capacity, in tons, as predicted by the FHWA Modified Gates formula (AASHTO 2007) is reported in this field.

E. **82. Pile Capacity by Janbu Formula (Tons):** The pile capacity, in tons, as predicted by the Janbu formula (Bowles 1996) is reported in this field.

F. **83. Pile Capacity by Pacific Coast Uniform Building Code Formula (Tons):** The pile capacity, in tons, as predicted by the Pacific Coast Uniform Building Code formula (Bowles 1996) is reported in this field.

G. **4. Pile Capacity by Washington Department of Transportation Formula (Tons):** The pile capacity, in tons, as predicted by the Washington State Department of Transportation formula (Allen 2005) is reported in this field.

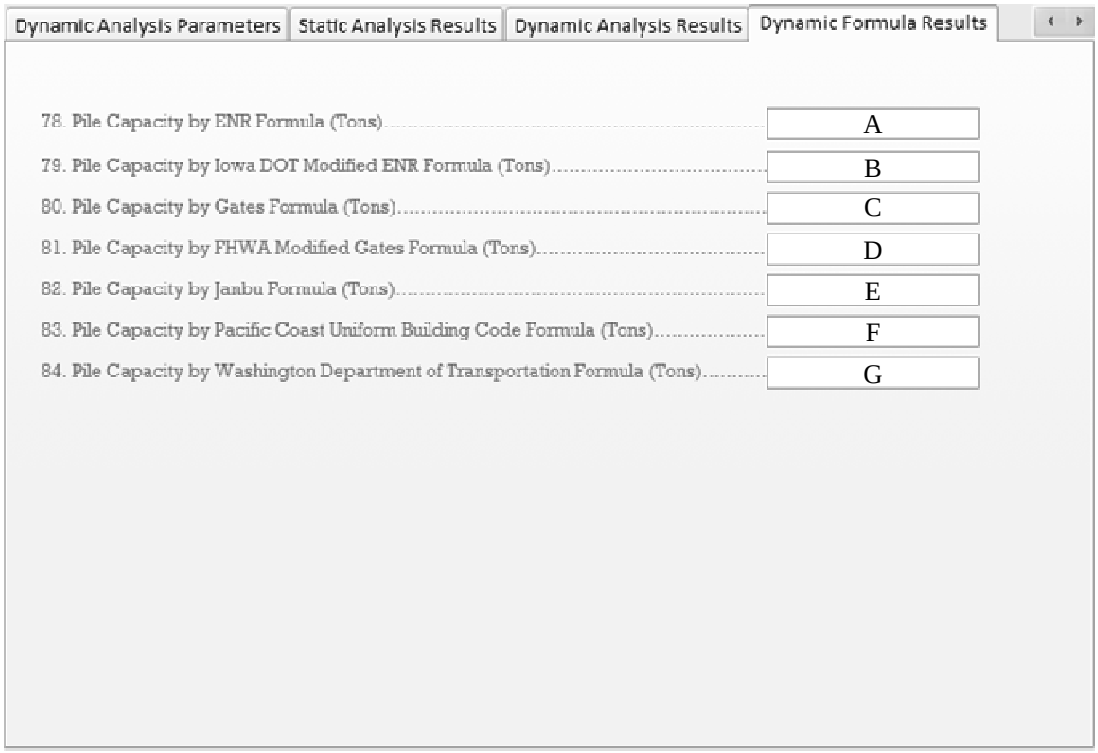

Figure 3.45: Dynamic Formula Results Tab of PLTRF

3.4.2.3 Disclaimer Notice

PILOT-IA was established as part of a research project (i.e., *TR-573: Development of LRFD Design Procedures for Bridge Piles in Iowa*) funded by the Iowa Highway Research Board (IHRB). Neither the IHRB nor the author of this thesis makes any warranty, express or implied, or assumes any legal liability or responsibility for the accuracy, completeness, or usefulness of any information contained in PILOT-IA. If a problem arises during the usage of PILOT-IA or more knowledge is required, contact those currently maintaining the database at the Iowa DOT.

CHAPTER 4: SUMMARY OF FIELD TESTING OF STEEL H-PILES

4.1 INTRODUCTION

For verification of the regionally calibrated LRFD resistance factors recommended in this thesis for the construction control of driven steel H-pile foundations via dynamic pile driving formulas, one HP 10×57 and eight HP 10×42 steel piles were driven and load tested in different counties spanning the five predominant soil regions encountered within the State of Iowa. Table 4.1 provides a summary of the location and subsurface characteristics for each of the nine tested steel H-piles. In addition to simply driving and statically load testing the piles to failure, most of the test piles were instrumented with strain gauges and dynamically monitored during driving and restrikes using the PDA device. Moreover, the subsurface conditions at the location of each of the test piles were characterized using various laboratory tests (e.g., moisture content, grain-size distribution, Atterberg limits, consolidation, and Triaxial Consolidated-Undrained compression tests) and in-situ tests (e.g., SPT, CPT, and BST). In some cases, ground instrumentation (i.e., push-in pressure cells) was used to capture horizontal stress and porewater pressure data near the test pile during driving and static load testing.

Table 4.1: Location and Subsurface Characteristics for Each of the Tested Steel H-Piles

Project ID	Pile Type	Iowa County	Soil Region	Test Site Soil Classification
ISU1	HP 10×57	Mahaska	Loess on top of Glacial	Mixed
ISU2	HP 10×42	Mills	Loess	Clay
ISU3	HP 10×42	Polk	Wisconsin Glacial	Clay
ISU4	HP 10×42	Jasper	Loess on top of Glacial	Clay
ISU5	HP 10×42	Clarke*	Loess on top of Glacial	Clay
ISU6	HP 10×42	Buchanan*	Loamy Glacial	Clay
ISU7	HP 10×42	Buchanan*	Loamy Glacial	Mixed
ISU8	HP 10×42	Poweshiek*	Loess on top of Glacial	Mixed
ISU9	HP 10×42	Des Moines	Alluvium	Sand

*Push-in pressure cells were installed at these sites near the test pile to capture horizontal stress and porewater pressure data during driving and static load testing

Since the majority of the aforementioned data can be considered superfluous for the performance of comparative analyses and LRFD resistance factor calibration efforts for dynamic pile driving formulas, a detailed presentation of such information has not been

provided in this thesis. In other words, given the scope of this thesis, only those details associated with the pile driving and axial load testing processes for each of the nine tested steel H-piles will be elaborated on in the following sections. However, the reader is referred to Ng et al. (2011) for a complete description of the procedures used as well as the data gathered from all tests performed at each of the nine test sites.

4.2 PILE DRIVING

4.2.1 Driving System

Summary characteristics of the pile driving hammers used to drive each of the nine test piles are provided in Table 4.2. Moreover, even though a total of four different hammer models (i.e., Delmag D16-32, Delmag D19-32, Delmag D19-42, and American Piledriving Equipment (APE) D19-42) were used for driving the nine test piles, all are open-ended, single-acting diesel hammers, where the term "open-ended" signifies that the hammer is open at the top, allowing the ram to become exposed during driving. Such a hammer type operates by manually raising the ram with a cable and then releasing it. As the ram free-falls within the cylinder, fuel is injected into the combustion chamber beneath the ram and the fuel/air mixture becomes pressurized. Once the ram strikes the anvil at the bottom of the cylinder, the fuel/air mixture ignites, pushing the ram back to the top of the stroke. This process, illustrated in Figure 4.1, will continue as long as fuel is injected into the combustion chamber and the stroke is sufficient to ignite the fuel.

Table 4.2: Characteristics of Pile Driving Hammers

Project ID	Hammer Type	Ram Weight (kips)	Cap Weight (kips)	Anvil Weight (kips)	Maximum Stroke (ft)	Maximum Rated Energy (kip-ft)
ISU1	Delmag D19-42	4.000	2.000	0.753	10.8	43.23
ISU2	Delmag D19-42	4.015	1.920	0.753	10.8	43.23
ISU3	Delmag D19-32	4.000	2.000	0.753	10.6	42.44
ISU4	Delmag D19-42	4.015	2.000	0.750	10.8	43.23
ISU5	Delmag D16-32	3.520	2.050	0.810	11.4	40.20
ISU6	Delmag D19-42	4.190	2.000	0.750	10.2	42.80
ISU7	Delmag D19-42	4.190	2.000	0.750	10.2	42.80
ISU8	Delmag D19-42	4.015	2.000	0.750	10.8	43.23
ISU9	APE D19-42	4.189	1.345	0.749	11.3	47.34

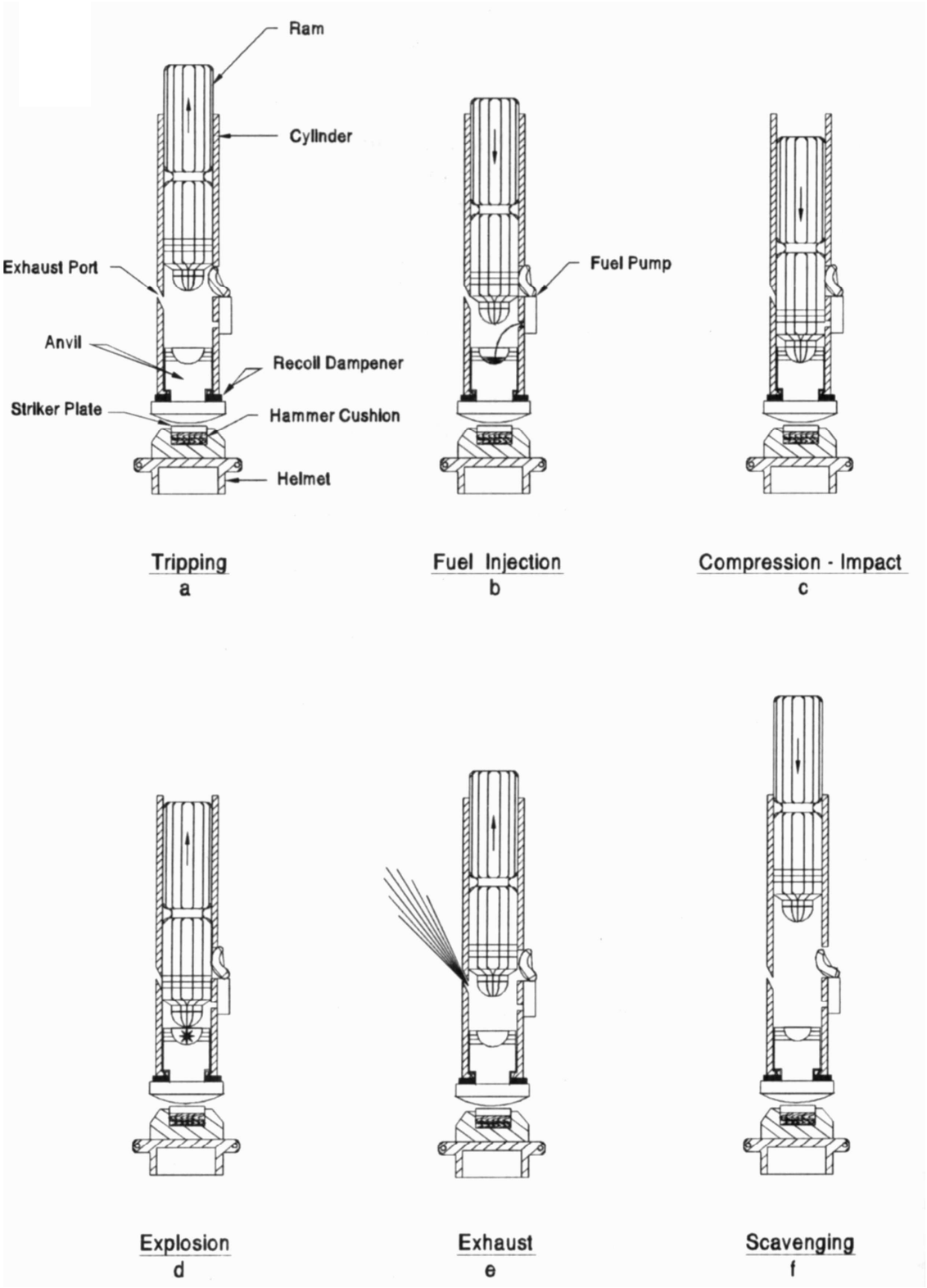

Figure 4.1: Single-Acting Diesel Hammer Operation (Pile Dynamics Inc. 2005)

4.2.2 Driving Process

Except for the testing conducted as a part of ISU1, two HP 10×42 piles were used at each test site to anchor the loading frame described in Section 4.3.1. These anchor piles were driven ahead of the test pile, but with all pile driving occurring on the same day. Upon achieving the EOD condition for all HP 10×42 test piles, restrikes were conducted according to the schedule outlined in Table 4.3 to examine the change in pile capacity as a function of time (i.e., soil set-up). The PDA device, which uses two strain gauges and two accelerometers to calculate the force and velocity imparted to the pile by the hammer, was used to monitor the driving and restriking of these HP 10×42 test piles. The PDA strain gauges and accelerometers were installed on the steel test piles by bolting them through drilled holes in the web approximately 30 inches from the pile head. The two PDA strain gauges were positioned opposite to one another on either side of the web, and the accelerometers were placed to the right of each of the strain gauges, as shown in Figure 4.2. Furthermore, resistance strain gauges were installed on both sides of the web along the pile centerline at different depths. Protected by a L2×2×3/16 welded to both sides of the web, these resistance strain gauges were primarily utilized during static load testing to characterize the load transfer mechanism of the test pile.

Table 4.3: Restrike Schedule from the EOD Condition

Project ID	Days After EOD Condition							
	1st Restrike	2nd Restrike	3rd Restrike	4th Restrike	5th Restrike	6th Restrike	7th Restrike	8th Restrike
ISU1	-	-	-	-	-	-	-	-
ISU2	0.1700	0.920	2.97	-	-	-	-	-
ISU3	0.00280	0.00730	0.01700	1.110	1.950	-	-	-
ISU4	0.00410	0.01600	0.0410	0.740	1.740	4.75	-	-
ISU5	0.00538	0.01300	0.0480	0.920	2.90	7.92	-	-
ISU6	0.001600	0.00440	0.01200	0.0700	0.830	2.82	6.79	9.81
ISU7	0.001860	0.00600	0.01500	0.800	2.77	6.76	9.76	-
ISU8	0.00707	0.01100	0.0390	0.970	3.97	4.95	-	-
ISU9	0.00384	0.01074	0.0375	0.690	2.87	9.77	-	-

As for ISU1, four HP 12×53 piles were used at the test site to anchor the load test frame. These anchor piles were driven one day before driving the HP 10×57 test pile. The PDA device was used to monitor the driving of the test pile and, unlike the other test piles, no

restrikes were performed upon achieving the EOD condition. Furthermore, resistance strain gauges were not installed along the HP 10×57 embedded pile length for characterization of the pile load transfer mechanism.

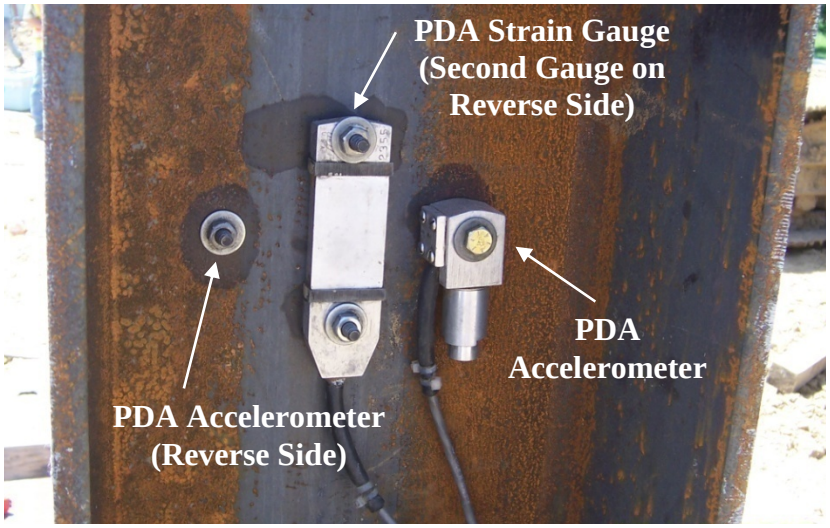

Figure 4.2: PDA Strain Gauge and Accelerometer Attached to the Web of a HP 10×42 Test Pile

In all cases, the steel H-shaped piles were lifted into position by cutting a hole in the web or flange and passing a lifting chain through it. The lifting chain was attached to the lower end of the hammer, as shown in Figure 4.3, such that as the hammer was raised, the pile was lifted into a vertical position beneath it. The hammer leads were then positioned in the desired location and adjusted until they were perfectly vertical. When the leads and pile were vertical, a worker climbed the ladder on the side of the leads, as seen in Figure 4.3, to guide the hammer helmet onto the top of the pile as the hammer and helmet were lowered. When the leads, hammer, and pile were in the correct position, the ram of the pile driving hammer was lifted manually by the crane and dropped. In some instances, the resistance provided by the soil to pile penetration was minimal for approximately the first five to ten feet of penetration and the ram needed to be raised manually several times before the hammer was able to develop enough combustion pressure to continue operating.

Figure 4.3: ISU4 Test Pile Lifted into Position via Pile Driving Hammer (Left) and Hammer Helmet Guided into Place via Construction Worker (Right)

4.2.3 Results

In addition to the pile driving hammer characteristics listed in Table 4.2, dynamic pile driving formulas require the measured pile penetration distance under one hammer blow, i.e., the pile set, as well as the observed hammer stroke at that particular blow for field estimation of a pile's ultimate bearing capacity. Table 4.4 provides a summary of these quantities as measured by PDA for both the EOD and BOR conditions. In addition, Table 4.5 presents a summary of the embedded pile lengths witnessed at the EOD and BOR conditions versus the total driven pile length.

It is important to point out that several of the piles experienced minimal local buckling or bending of the flanges near the pile top as a result of the pile driving process, which has been illustrated in Figure 4.4. When such flange local buckling was experienced, the damaged area was cut off to ensure uniform pile section at the top end for load testing purposes or to allow for correct assembly of the static load testing frame.

Table 4.4: Measured Pile Set and Hammer Stroke at EOD and BOR Conditions

Project ID	Pile Set (in)/Hammer Stroke (ft)								
	EOD	Restrike Number							
		1	2	3	4	5	6	7	8
ISU1	0.97/ 6.42	-	-	-	-	-	-	-	-
ISU2	0.95/ 5.80	0.73/ 6.48	0.52/ 7.29	0.46/ 7.15	-	-	-	-	-
ISU3	1.03/ 5.69	1.06/ 5.86	0.99/ 5.92	0.76/ 6.07	0.74/ 6.79	0.45/ 7.06	-	-	-
ISU4	0.62/ 6.24	0.64/ 6.51	1.05/ 6.63	0.73/ 7.00	0.61/ 8.97	0.26/ 7.48	0.33/ 7.39	-	-
ISU5	0.28/ 6.97	0.34/ 7.07	0.23/ 6.96	0.26/ 7.43	0.14/ 8.20	0.16/ 8.82	0.15/ 8.69	-	-
ISU6	0.54/ 6.25	0.54/ 6.85	0.59/ 6.86	0.45/ 6.55	0.50/ 8.26	0.31/ 8.20	0.07/ 8.47	0.15/ 8.75	0.21/ 8.26
ISU7	7.08/ 10.2†	4.30/ 10.2†	3.34/ 10.2†	4.27/ 10.2†	1.13/ 4.35	1.46/ 5.70	1.11/ 6.43	0.97/ 5.92	-
ISU8	0.62/ 6.74	0.32/ 6.82	0.44/ 7.15	0.23/ 7.11	0.46/ 7.39	0.65/ 7.46	0.38/ 7.43	-	-
ISU9	0.75/ 8.00†	0.94/ 7.39	0.86/ 7.71	0.79/ 7.81	0.72/ 8.14	0.82/ 7.66	0.68/ 7.57	-	-

† Approximate hammer stroke based on field observations due to the inability of the PDA device to capture such measurements.

Table 4.5: Embedded Pile Lengths at the EOD and BOR Conditions

Project ID	Driven Pile Length (ft)	Embedded Pile Length (ft)								
		EOD	Restrike Number							
			1	2	3	4	5	6	7	8
ISU1	36	32.5	-	-	-	-	-	-	-	-
ISU2	60	54.0	55.0	55.3	55.8	-	-	-	-	-
ISU3	60	48.0	48.5	49.0	49.5	50.2	51.0	-	-	-
ISU4	60	55.0	55.3	55.7	56.0	56.3	56.6	56.8	-	-
ISU5	60	55.0	55.3	55.7	56.0	56.3	56.5	56.7	-	-
ISU6	60	55.3	55.6	55.9	56.2	56.4	56.6	56.9	57.2	57.3
ISU7	35/40†	19.8	20.5	21.5	22.5	24.0	25.5	26.0	26.6	-
ISU8	60	55.0	55.5	56.2	56.5	56.8	57.1	57.3	-	-
ISU9	53	47.0	47.4	47.7	48.0	48.3	48.6	49.3	-	-

† A 10 foot deep hole was pre-bored before driving, and a five foot long extension was spliced to the test pile after the third restrike; in all other cases, no hole was pre-bored before driving of the test pile.

Figure 4.4: Local Buckling Damage of Test Pile Flanges for ISU5 (Left) and ISU8 (Right) due to Pile Driving

4.3 PILE AXIAL STATIC LOAD TEST

4.3.1 Loading Frame and Test Setup

Apart from the testing conducted as a part of ISU6 and ISU7, one steel H-shaped pile was load tested vertically at each test site using the configuration of test and anchor piles depicted in Figure 4.5. As indicated in this layout, a center-to-center spacing of 9*D*, where *D* refers to the section depth of the test piles, was maintained between the vertically tested pile and the adjacent anchor piles to ensure that a soil shear failure instigated by the stress intensity from overlapping stressed zones was minimized (Bowles 1996).

The two piles tested as a part of ISU6 and ISU7 were load tested vertically at the same test site, and the same loading frame was used to load both piles. The configuration of test and anchor piles used for this site is provided in Figure 4.6. As indicated in this layout, a center-to-center spacing of 5*D* was maintained between the two vertically tested piles, while a center-to-center spacing of 6*D* was maintained between each test pile and the adjacent anchor piles.

Plan, side and elevation views of the two employed loading frames are provided in Figure 4.7 and Figure 4.8. To assemble such loading frames, shorter pile segments, labeled as "Welded HP 10×42" pieces in the aforementioned loading frame figures, were welded onto either side of both anchor piles after they had been driven, as shown in Figure 4.9. The

welded HP 10×42 pieces were positioned so that the top of each piece was at the same elevation, providing level supports for the main reaction beam. Subsequently, the main reaction beam was lifted and placed on the protruding flanges of the welded HP 10×42 pieces, with the clamping beams and height adjusters being placed on top of the main reaction beam afterward. The three inch diameter rods were then lowered through the holes in the height adjusters and clamping beams and through the space bounded by the protruding flanges and web of the welded HP 10×42 pieces. Finally, sleeved nuts were tightened against a steel plate located directly underneath each welded HP 10×42 piece. A picture of the fully assembled loading frame is shown in Figure 4.10.

During testing, a hydraulic jack was used to apply the vertical load on the test pile, causing an equal load vertically upward on the main reaction beam. The main reaction beam reacted upward against the clamping beams extending across the top of each of its ends. The upward force on the clamping beams was transferred to the three inch diameter rods on either side of the main reaction beam. The rods reacted against the plates on the bottoms of each welded HP 10×42 piece, and the welds transferred the vertical load from the welded HP 10×42 pieces to the anchor piles, subjecting them to axial tension. Therefore, the load capacity of either test frame was controlled by the friction capacity of the anchor piles, which in turn was dependent upon the subsurface conditions encountered at each test site. If the friction capacity of the anchor piles was not exceeded first, the load test frame could be used to apply a maximum load of 670 kips to the ISU6 and ISU7 test piles, or a maximum load of 870 kips to the remainder of the tested piles. These maximum load values were controlled by the tension capacity of the three inch diameter rods.

4.3.2 Testing Equipment

A 200 ton hydraulic jack was used to apply the vertical load on the test piles, as noted previously, and a 300 kip load cell was used to measure the applied load. Four 10 inch stroke displacement transducers were used to measure the vertical displacement of the top of each test pile. These transducers were mounted on 2×4 inch wooden reference beams, which were supported on either side of the test pile by short ladders secured to the reference beams as illustrated in Figure 4.11.

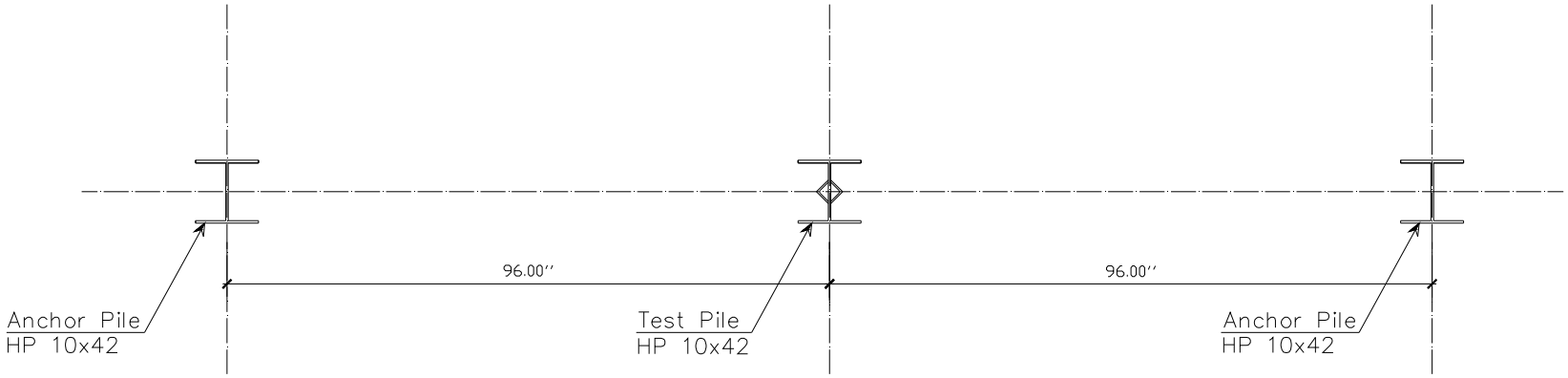

Figure 4.5: Typical Configuration of the Test and Anchor Piles used for Testing Piles in this Project

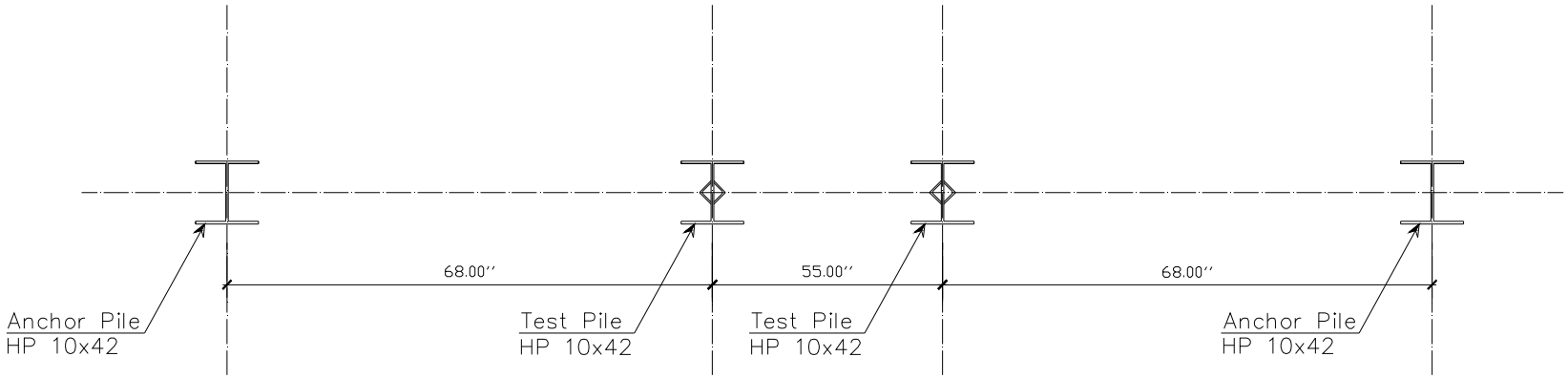

Figure 4.6: Configuration of the Test and Anchor Piles used for ISU6 and ISU7

Note: All dimensions are in inches.

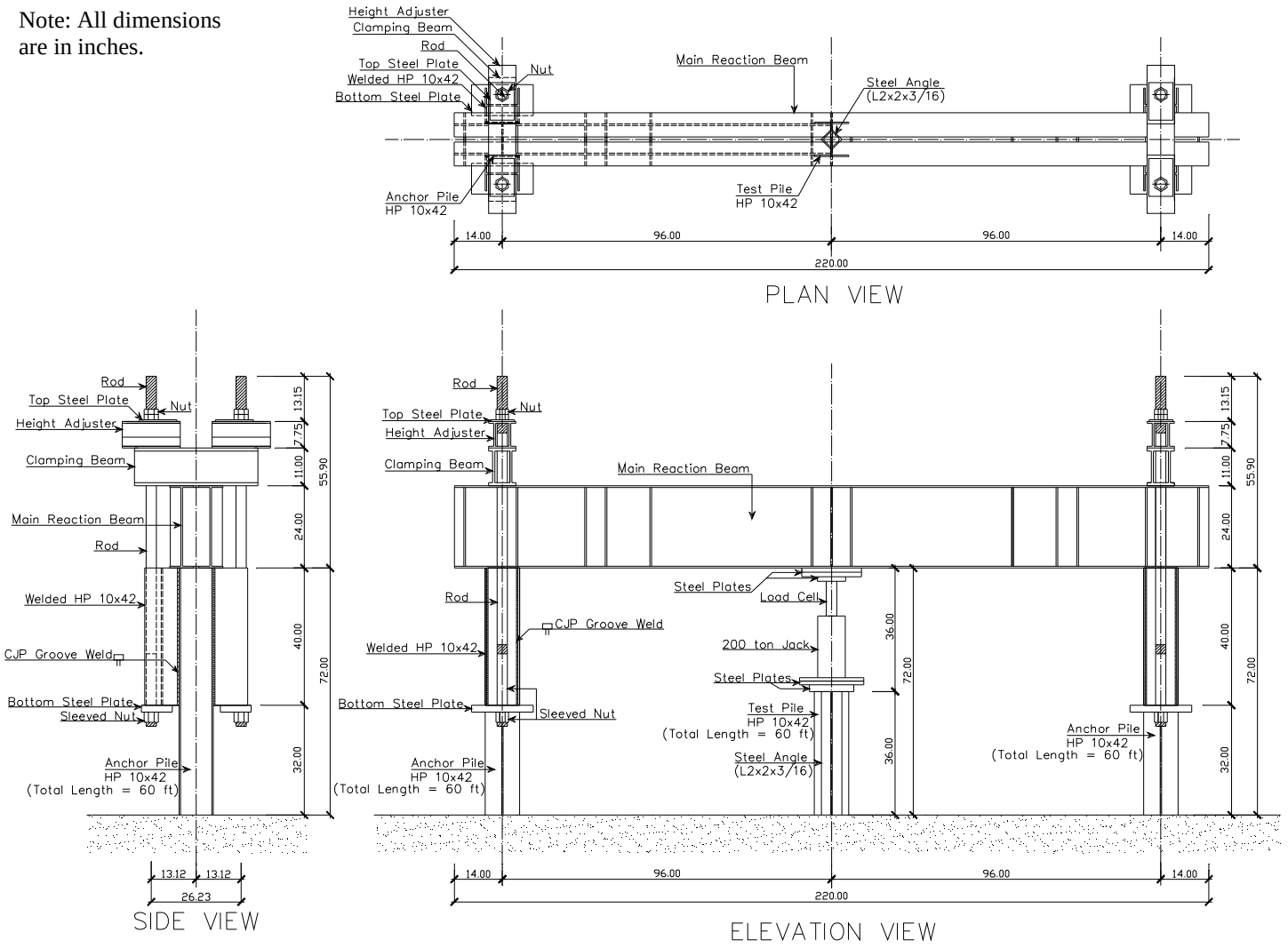

Figure 4.7: Typical Plan, Side and Elevation Views of the Vertical Load Test Setup used for Testing Piles in this Project

Note: All dimensions are in inches.

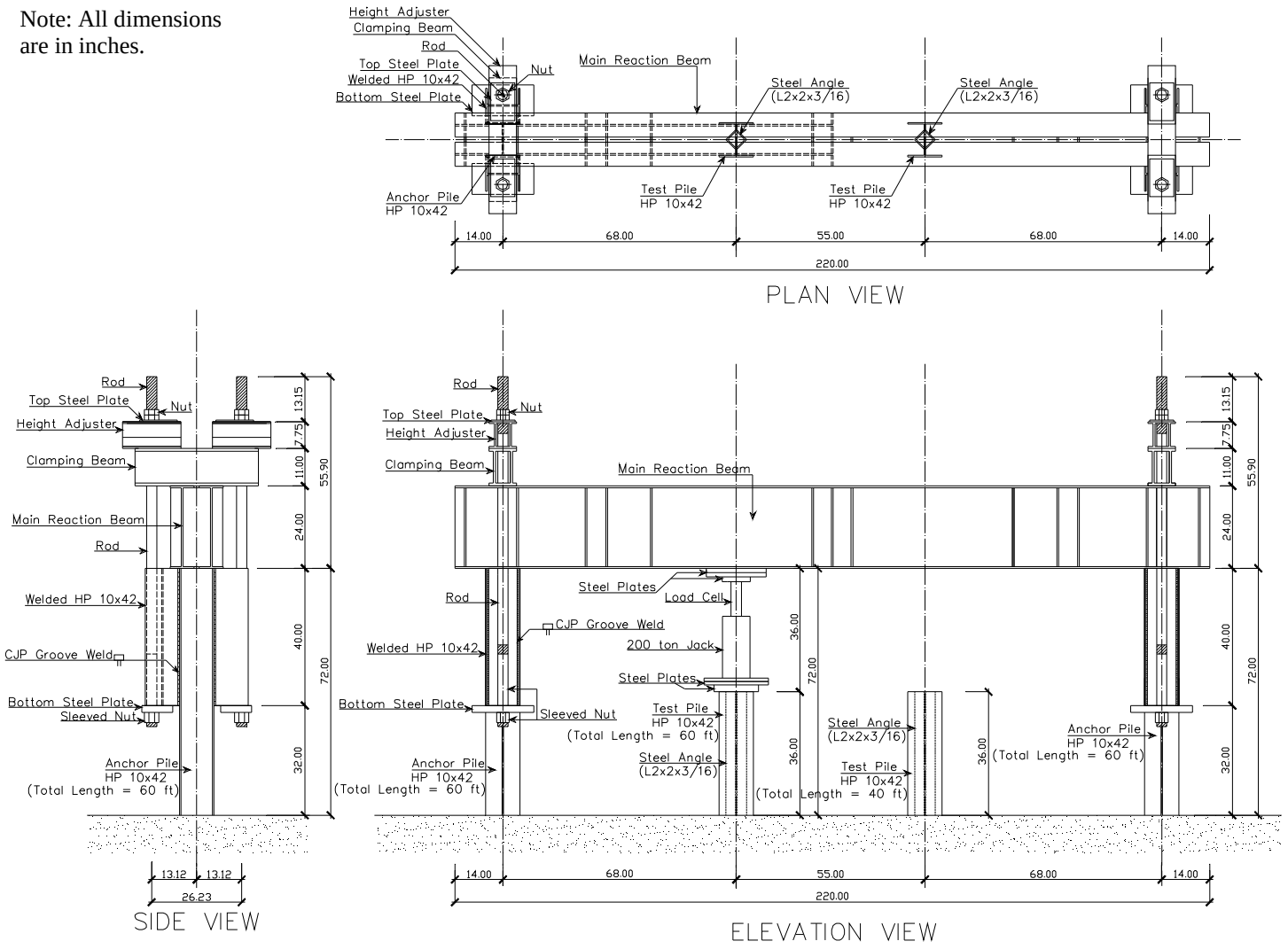

Figure 4.8: Plan, Side and Elevation Views of the Vertical Load Test Setup used for ISU6 and ISU7

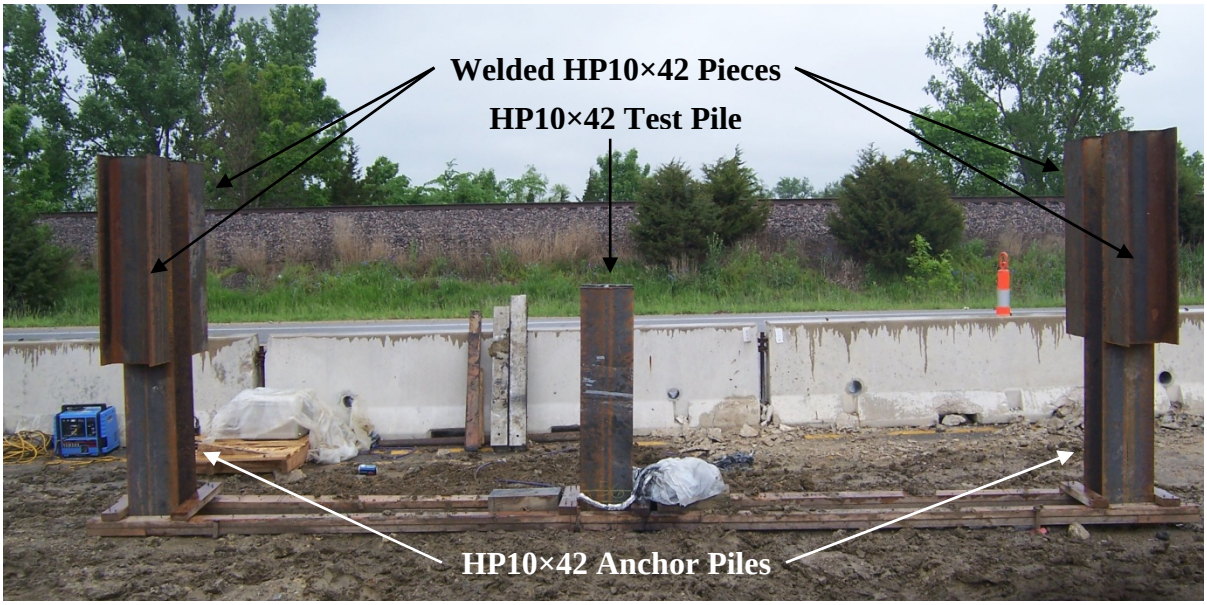

Figure 4.9: ISU5 Piles at Completion of the Driving and Restrikes, with the Welded HP 10×42 Pieces Secured to the Anchor Piles

Figure 4.10: Completed Vertical Load Test Setup used for ISU5

These short ladders were driven several inches into the soil at a distance of about four feet from the test pile to prevent any movement or instability issues, which in turn allowed for independent measurements of the absolute vertical movement of the pile. The transducers were connected to the top of the pile using eye hooks screwed into wooden blocks glued to the test piles, as illustrated in Figure 4.12.

The strain gauges, which were installed on both sides of the web along the pile centerline at different depths, were used to measure strains in the test pile at various depths below the ground surface. Ultimately, these strain measurements facilitated the characterization of the load transfer mechanism for a given test pile, as seen in Section 4.3.4. Data from these strain gauges as well as the load cell and deflection transducers was collected using a Megadac data acquisition system.

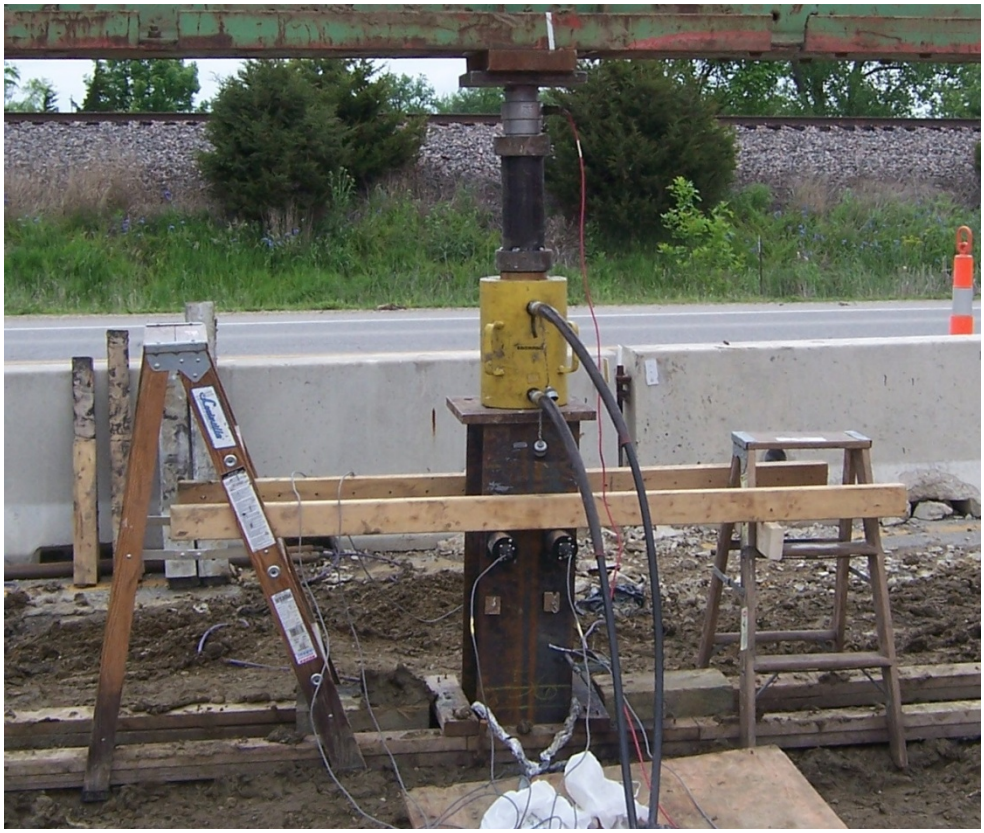

Figure 4.11: Wooden Reference Beams Supported by Short Ladders for ISU5

Figure 4.12: Displacement Transducers and Eye Hooks Mounted to the ISU4 Test Pile

4.3.3 Test Procedure

Vertical load testing of all test piles followed the "Quick Test" procedure outlined in American Society for Testing and Materials (ASTM) D 1143/D 1143 M – 07. Accordingly, each test pile was subjected to five percent load increments of the anticipated failure load given by PDA. The load was kept relatively constant during each load step until deflection readings had stabilized, which typically took between five and ten minutes for any given step. Deflection, strain, and load measurements were recorded electronically at every second for the duration of each sustained load increment. This process was followed until failure occurred, which was defined by the Davisson's displacement-based criterion. After experiencing failure, the test piles were unloaded in ten percent increments of the measured failure load, and the data was again recorded at the same frequencies used during the loading

stage. The load step durations were also increased to about fifteen to twenty minutes for the failure and final zero loads, as recommended by ASTM, to monitor creep and rebound behavior, respectively.

Furthermore, the load-displacement behavior of each test pile was monitored throughout each vertical load test. The Davisson failure criterion was used to determine the ultimate capacity of the pile and terminate the load test. As explained in the preceding chapter, the Davisson failure criterion defines the ultimate load of a pile subjected to a vertical load test as the load at which the displacement of the pile exceeds the elastic compression of the pile by $0.15 + D/120$ inches, where D is the pile depth or diameter (Davisson 1972). The elastic compression is simply the length of the pile divided by its elastic modulus and cross-sectional area (i.e., the pile stiffness), then multiplied by the applied load.

4.3.4 Results

From the deflection, strain, and load data collected during each axial static load test, the load-displacement behavior and the load transfer mechanism for each test pile were established. As an example, the load-displacement relationship of the ISU5 HP 10×42 test pile is provided in Figure 4.13. As seen in this figure, the pile was loaded to a maximum of 263 kips and the Davisson failure criterion for the steel H-shaped test pile was reached at a load of 243 kips. During this 243 kip load step, the pile experienced a maximum displacement of 0.90 inches. Additionally, the test pile experienced a permanent set of 0.56 inches according to measurements taken 10 minutes after the pile was unloaded. This permanent soil deformation indicates that the soil supporting the ISU5 test pile experienced plastic behavior during the load test. Although a summary of the Davisson failure criterion for each of the nine steel H-shaped test piles is provided in Table 4.6, the reader is referred to Ng et al. (2011) for a complete presentation of the load-displacement relationships associated with all nine test piles.

As for characterization of the load transfer mechanism for each test pile, the strain gauges were used to determine the skin friction along the embedded length of the pile. The loads in the pile at the location of each pair of strain gauges were calculated by multiplying the average strain by the elastic modulus and cross-sectional area of the pile. As an example,

the load transfer mechanism obtained for the ISU5 HP 10×42 test pile is provided in Figure 4.14, where about 22 percent of the Davisson failure criterion was resisted by end-bearing. The reader is referred to Ng et al. (2011) for a complete presentation of the load transfer mechanisms associated with all nine test piles.

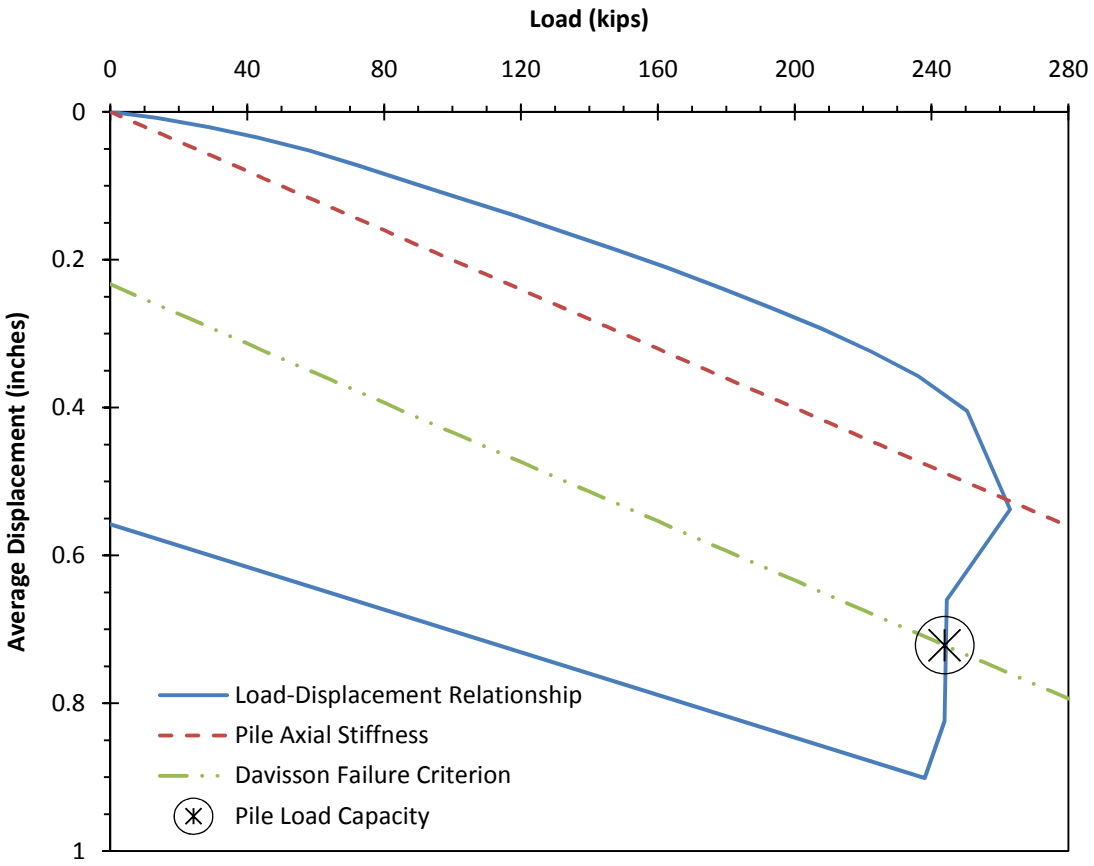

Figure 4.13: Load-Displacement Relationship and Davisson Failure Criterion for ISU5 Subjected to Axial Static Load

Table 4.6: Pile Capacities Established from the Davisson Failure Criterion

Project ID	Davisson Failure Criterion (kips)	Testing Time after EOD (days)
ISU1	198	100
ISU2	125	9
ISU3	150	36
ISU4	154	16
ISU5	243	9
ISU6	213	14
ISU7	53	13
ISU8	162	15
ISU9	182	25

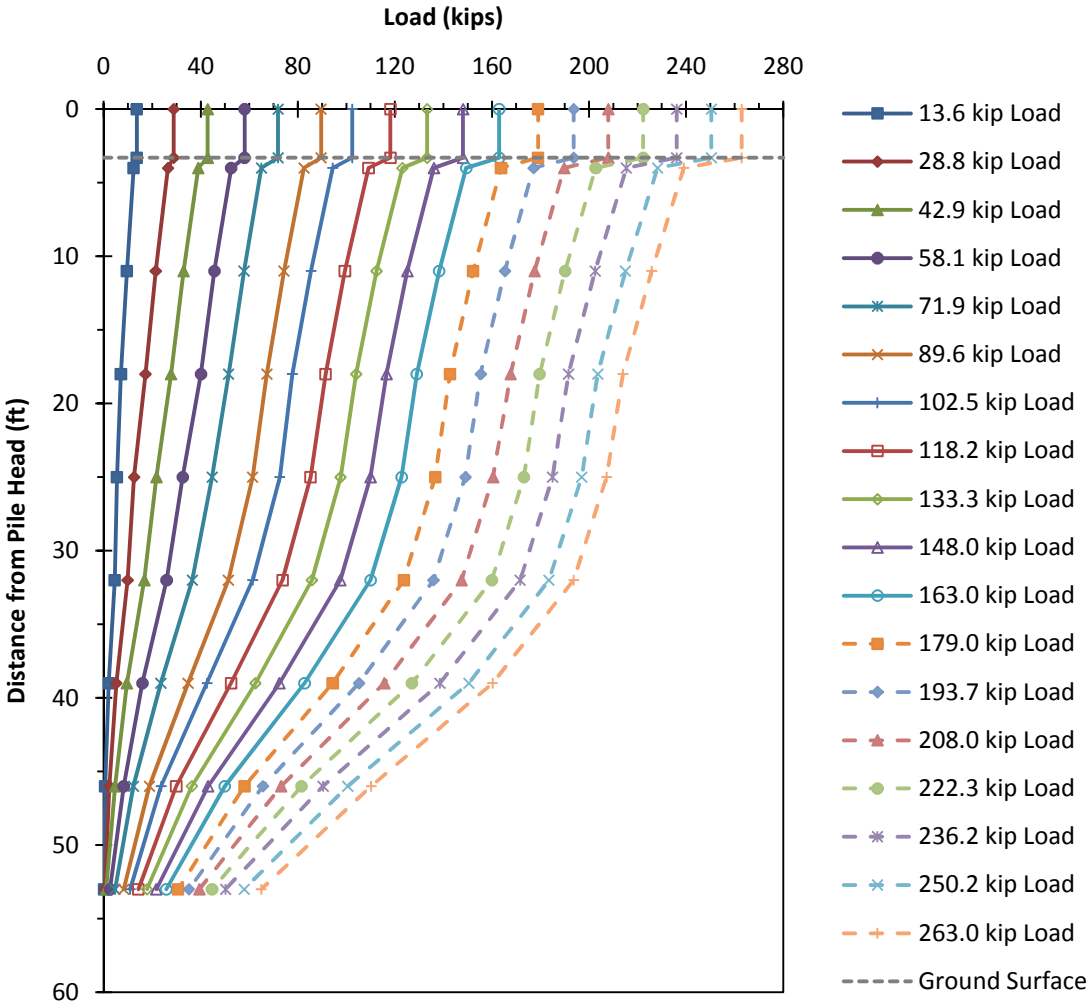

Figure 4.14: Load Transferred by Skin Friction to the Surrounding Soil for the ISU5 Test Pile, as Calculated from Measured Strain Gauge Data

CHAPTER 5: CALIBRATION OF LRFD RESISTANCE FACTORS

5.1 INTRODUCTION

As stated in Chapter 1, the LRFD approach, as it applies to deep foundation design, separates the uncertainties associated with the applied load and predicted pile foundation capacity and rationally quantifies them using probability-based methods aimed at achieving engineered designs with consistent levels of reliability. In the following sections, a description of the calibration process for estimating LRFD resistance factors for several dynamic pile driving formulas using reliability theory will be presented. Furthermore, the results obtained from calibration procedures carried out on the PILOT-IA usable-dynamic steel H-pile and timber pile data subsets will also be summarized prior to formulating the final recommendations.

5.2 FRAMEWORK OF CALIBRATION PROCESS

Based upon the results of numerous comparative studies, as summarized in Chapter 2, as well as the outcomes from a nationwide survey of state DOTs and a local survey of Iowa county engineers, which have been presented in Chapter 3, seven dynamic pile driving formulas were chosen for the LRFD resistance factor calibration process presented in this section; i.e., the Gates, FHWA Modified Gates, ENR, Iowa DOT Modified ENR, Janbu, PCUBC, and WSDOT formulas. This calibration process was carried out on the PILOT-IA usable-dynamic steel H-pile and timber pile data subsets in response to the feedback received from the Iowa DOT as well as the Iowa county engineers concerning the most commonly used types of driven pile foundations for bridge type structures.

5.2.1 Comparative Analyses

The first step in the LRFD resistance factor calibration process involves estimating the relationship between the measured ultimate pile capacity, as obtained through the application of Davisson's method (1972), and the predicted ultimate pile capacity, as estimated by a specified dynamic pile driving formula. To estimate this relationship, a pile load test dataset containing measured ultimate pile capacities from static load test results and sufficient information for the prediction of ultimate pile capacities using the dynamic pile driving formula of choice (i.e., complete pile driving records and information concerning the

characteristics of the pile driving equipment) is required. With this information, the resistance bias factor is determined for each pile load test record in the dataset, where the resistance bias factor is defined as follows:

$$\lambda_{Ri} = \frac{R_m}{R_n} \tag{5.1}$$

where: λ_{Ri} = resistance bias factor for the ith pile load test record in the dataset,

R_m = measured ultimate pile capacity for the ith pile load test record in the dataset, and

R_n = predicted ultimate pile capacity for the ith pile load test record in the dataset.

From the resulting set of resistance bias factors, the mean, standard deviation, and coefficient of variation parameters used to define the true population can be estimated by way of Eqs. (5.2), (5.3), and (5.4) (Withiam et al. 1997).

$$\bar{\lambda}_R = \frac{\sum \lambda_{Ri}}{N} \tag{5.2}$$

$$\sigma_{\lambda_R} = \sqrt{\frac{\sum\left(\lambda_{Ri} - \bar{\lambda}_R\right)^2}{N-1}} \tag{5.3}$$

$$COV_{\lambda_R} = \frac{\sigma_{\lambda_R}}{\bar{\lambda}_R} \tag{5.4}$$

where: $\bar{\lambda}_R$ = mean resistance bias factor,

N = sample size (i.e., number of elements in the analyzed dataset),

σ_{λ_R} = standard deviation of the resistance bias factor, and

COV_{λ_R} = coefficient of variation of the resistance bias factor.

Although these statistical parameters provide valuable information related to the distribution of the resistance bias factor for a particular dynamic pile driving formula, they yield no information regarding the overall shape of the distribution. Thus, the next task in the LRFD resistance factor calibration process involves determining the most probable probability distribution (i.e., either the normal or lognormal probability distribution) for the

set of resistance bias factors. To accomplish this task, the Anderson-Darling goodness-of-fit test is used. In general, for a set of observations λ_{R1}, λ_{R2}, ..., λ_{Rn} that are to be fit with a probability distribution, a goodness-of-fit test is a test of the following hypotheses (Fenton and Griffiths 2008):

H_o: the λ_{R1}, λ_{R2}, ..., λ_{Rn}'s are governed by the fitted distribution function.

H_a: the λ_{R1}, λ_{R2}, ..., λ_{Rn}'s are not governed by the fitted distribution function.

Typical of any hypothesis test, the null or default hypothesis, H_o, is only rejected if the data are sufficiently far from H_o. The Anderson-Darling test is essentially a numerical test of the empirical cumulative distribution function, determined from the set of observations, against the fitted cumulative distribution function. However, unlike other goodness-of-fit tests such as the Kolmogorov-Smirnov test, the Anderson Darling test is designed to better detect discrepancies in the tail regions of the probability distribution and is better able to discern differences between the hypothesized distribution and the actual distribution (Fenton and Griffiths 2008).

Once the most likely probability distribution, from which the sample set of resistance bias factors arose from, has been identified for a particular dynamic pile driving formula, a LRFD resistance factor can be calibrated using the selected statistical approach. As presented in Section 2.5, several statistical methods with varying degrees of sophistication have been used to calibrate LRFD resistance factors for driven pile foundation design and construction control methods. However, according to Kyung (2002), the most commonly used methods are the first-order, second-moment (FOSM) reliability approach and the first-order reliability method (FORM). Paikowsky et al. (2004) performed the LRFD resistance factor calibration using both the FOSM and FORM approaches and concluded that the resulting LRFD resistance factors differed by no more than about ten percent, with the FOSM approach providing the more conservative result. Given this information and the fact that the current *AASHTO LRFD Bridge Design Specifications* (2007) recommends resistance factors for the design and construction control of driven pile foundations that were calibrated using the FOSM approach, the FOSM reliability approach was chosen to conduct the LRFD

resistance factor calibrations presented in this thesis. The details surrounding this particular statistical approach are outlined in the following section.

5.2.2 FOSM Approach

As described by Fenton and Griffiths (2008), the FOSM approach uses a Taylor series expansion of the limit state function to be evaluated. This expansion is truncated after the linear, or first-order, terms and is used in conjunction with the first two moments of the input random variable(s) to determine the values for the first two moments of the dependent variable, i.e., the limit state function. Before any further explanation or derivation of the FOSM approach, as it applies to the calibration of geotechnical LRFD resistance factors, is given, a suitable limit state function must be defined.

As offered by Allen et al. (2005), a limit state is a condition, related to a design objective, in which a combination of one or more loads is just equal to the available resistance, so that the structure is at incipient failure defined by a prescribed failure criterion. In the context of the LRFD approach, this failure criterion can be represented by an equation having the following general form:

$$\sum \gamma_i Q_{ni} \leq \varphi R_n \tag{5.5}$$

where: γ_i = load factor applicable to a specific load component,

Q_{ni} = a specific nominal load component,

$\sum \gamma_i Q_{ni}$ = the total factored load for the load group applicable to the limit state being considered,

φ = the resistance factor, and

R_n = the predicted nominal resistance available.

Although Eq. (5.5) is a design equation, it can serve as the basis for the development of a limit state equation that can be used for calibration purposes. For instance, if only one load component, Q_n, is taken into consideration, Eq. (5.5) can be rewritten as:

$$\varphi R_n - \gamma_Q Q_n \geq 0 \tag{5.6}$$

where: R_n = the nominal resistance value,

Q_n = the nominal load value,

φ = a resistance factor, and

γ_Q = a load factor.

Consequently, the limit state equation that corresponds to Eq. (5.6) is as follows:

(5.7)

where: g = a random variable representing the safety margin,

R = a random variable representing resistance, and

Q = a random variable representing the load effect.

Within the LRFD framework, the magnitude of the load and resistance factors, and consequently the difference between R and Q, are determined such that the probability of failure, P_f, that Q is greater than R is acceptably small (Allen, Nowak, and Bathurst 2005). In other words, the goal of the LRFD approach is to separate the load and resistance probability distributions by a suitable margin so as to ensure an acceptably low probability of failure. This concept has been illustrated in the left-hand image of Figure 5.1 for the case of normally distributed load and resistance random variables. To quantify the probability of failure, a parameter known as the reliability index, β, is used, which is equal to the reciprocal of the coefficient of variation for the limit state function and is related to the probability of failure as shown in the right-hand image of Figure 5.1. It is here where the methodology of the FOSM approach is called upon to estimate the first two moments of the limit state function for quantification of the reliability index.

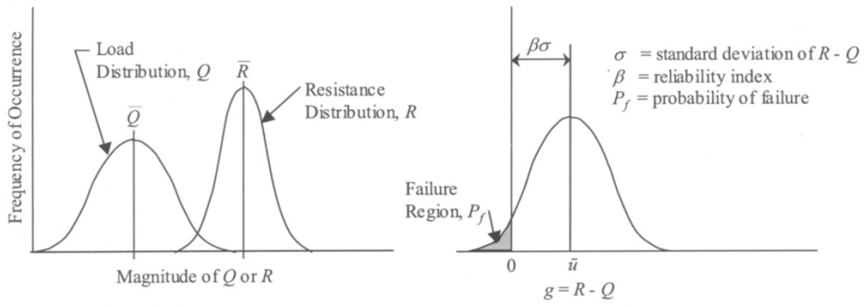

Figure 5.1: Probability of Failure (Left) and Reliability Index (Right) (Allen 2005)

For normally distributed random variables and the limit state function defined in Eq. (5.7), the FOSM approach quantifies the reliability index as:

$$\beta = \frac{\bar{R} - \bar{Q}}{\sqrt{\sigma_R^2 + \sigma_Q^2}} \tag{5.8}$$

where: $\bar{R}$ = the mean of the resistance random variable, *R*,

$\bar{Q}$ = the mean of the load random variable, *Q*,

σ_R = the standard deviation for the resistance random variable, *R*, and

σ_Q = the standard deviation for the load random variable, Q.

However, if the load and resistance random variables are lognormally distributed, the limit state function of Eq. (5.7) becomes:

$$g = \ln R - \ln Q = \ln \frac{R}{Q} \geq 0 \tag{5.9}$$

and the reliability index estimated by the FOSM approach takes on the form:

$$\beta = \frac{\ln\left[\frac{\bar{R}}{\bar{Q}}\sqrt{\frac{1 + COV_Q^2}{1 + COV_R^2}}\right]}{\sqrt{\ln\left[(1 + COV_R^2)(1 + COV_Q^2)\right]}} \tag{5.10}$$

where: COV_R = the coefficient of variation for the resistance random variable, *R*, and

COV_Q = the coefficient of variation for the load random variable, *Q*.

As alluded to previously, the statistics available for the performance of reliability analyses, i.e., mean, standard deviation, and distribution type, are generally expressed for load and resistance data points as a ratio of the measured to predicted values for a predefined prediction method (Allen, Nowak, and Bathurst 2005). However, the equations presented thus far in this section require that the load and resistance random variables, *Q* and *R*, as well as their associated statistical parameters be expressed as characteristic, or measured, values as opposed to a ratio of the measured to predicted values. Consequently, the biased data, or

the data corresponding to the ratio of measured to predicted values for load or resistance, must be scaled to obtain the associated characteristic statistics. Hence, as presented by Allen et al. (2005):

$$\bar{Q} = Q_n \cdot \bar{\lambda}_Q \tag{5.11}$$

$$\bar{R} = R_n \cdot \bar{\lambda}_R \tag{5.12}$$

$$\sigma_Q = COV_{\lambda_Q} \cdot \bar{Q} \tag{5.13}$$

$$\sigma_R = COV_{\lambda_R} \cdot \bar{R} \tag{5.14}$$

where: $\bar{Q}$ = the mean value of the measured load,

$\bar{R}$ = the mean value of the measured resistance,

Q_n = the nominal (or predicted) load value for the limit state considered,

R_n = the nominal (or predicted) resistance value for the limit state considered,

$\bar{\lambda}_Q$ = the mean value of the load bias factors,

$\bar{\lambda}_R$ = the mean value of the resistance bias factors,

σ_Q = the standard deviation of the measured load,

σ_R = the standard deviation of the measured resistance,

COV_{λ_Q} = the coefficient of variation of the load bias factors, and

COV_{λ_R} = the coefficient of variation of the resistance bias factors.

It is with this information that Eqs. (5.8) and (5.10) can be rewritten as that shown in Eqs. (5.15) and (5.16), respectively.

$$\beta = \frac{R_n \cdot \bar{\lambda}_R - Q_n \cdot \bar{\lambda}_Q}{\sqrt{\left(COV_{\lambda_Q} \cdot Q_n \cdot \bar{\lambda}_Q\right)^2 + \left(COV_{\lambda_R} \cdot R_n \cdot \bar{\lambda}_R\right)^2}} \tag{5.15}$$

$$\beta = \frac{\ln\left[\frac{R_n \cdot \bar{\lambda}_R}{Q_n \cdot \bar{\lambda}_Q}\sqrt{\frac{1 + COV_{\lambda_Q}^2}{1 + COV_{\lambda_R}^2}}\right]}{\sqrt{\ln\left[\left(1 + COV_{\lambda_R}^2\right)\left(1 + COV_{\lambda_Q}^2\right)\right]}} \tag{5.16}$$

Furthermore, by incorporating Eq. (5.6) into Eqs. (5.15) and (5.16), one ends up with the following two equations, by which a resistance factor can be estimated for a desired magnitude of β, depending on the assumed probability distribution for the load and resistance bias factors.

$$\beta = \frac{\left(\frac{\gamma_Q}{\varphi}\right) \cdot \bar{\lambda}_R - \bar{\lambda}_Q}{\sqrt{\left(COV_{\lambda_R} \cdot \frac{\gamma_Q}{\varphi} \cdot \bar{\lambda}_R\right)^2 + \left(COV_{\lambda_Q} \cdot \bar{\lambda}_Q\right)^2}} \tag{5.17}$$

$$\beta = \frac{\ln\left[\frac{\gamma_Q \cdot \bar{\lambda}_R}{\varphi \cdot \bar{\lambda}_Q}\sqrt{\frac{1 + COV_{\lambda_Q}^2}{1 + COV_{\lambda_R}^2}}\right]}{\sqrt{\ln\left[\left(1 + COV_{\lambda_R}^2\right)\left(1 + COV_{\lambda_Q}^2\right)\right]}} \tag{5.18}$$

Lastly, if it is desired that multiple load sources, e.g., dead and live load sources, be taken into account in the limit state equation provided in Eq. (5.7), then, with the use of the same principles employed for the derivation of Eqs. (5.17) and (5.18), these such equations become Eqs. (5.19) and (5.20), respectively.

$$\beta = \frac{\left(\frac{\bar{\lambda}_R}{\varphi}\right) \cdot \left(\frac{\gamma_{QD} \cdot Q_D}{Q_L} + \gamma_{QL}\right) - \left(\frac{\bar{\lambda}_{QD} \cdot Q_D}{Q_L} + \bar{\lambda}_{QL}\right)}{\sqrt{\left(COV_{\lambda_R} \cdot \frac{\gamma_{QD} \cdot \frac{Q_D}{Q_L} + \gamma_{QL}}{\varphi} \cdot \bar{\lambda}_R\right)^2 + \left(COV_{\lambda_{QD}} \cdot \frac{Q_D}{Q_L} \cdot \bar{\lambda}_{QD}\right)^2 + \left(COV_{\lambda_{QL}} \cdot \bar{\lambda}_{QL}\right)^2}} \tag{5.19}$$

$$\beta = \frac{\ln\left[\frac{\bar{\lambda}_R}{\varphi} \cdot \left(\frac{\frac{\gamma_{QD} \cdot Q_D}{Q_L} + \gamma_{QL}}{\frac{\bar{\lambda}_{QD} \cdot Q_D}{Q_L} + \bar{\lambda}_{QL}}\right)\sqrt{\frac{1 + COV_{\lambda_{QD}}^2 + COV_{\lambda_{QL}}^2}{1 + COV_{\lambda_R}^2}}\right]}{\sqrt{\ln\left[\left(1 + COV_{\lambda_R}^2\right)\left(1 + COV_{\lambda_{QD}}^2 + COV_{\lambda_{QL}}^2\right)\right]}} \tag{5.20}$$

where: γ_{QD}= dead load factor,

γ_{QL}= live load factor,

$\frac{Q_D}{Q_L}$ = dead-to-live-load ratio,

$\bar{\lambda}_{QD}$ = mean value of the dead load bias factors,

$\bar{\lambda}_{QL}$ = mean value of the live load bias factors,

$COV_{\lambda_{QD}}$ = the coefficient of variation of the dead load bias factors, and

$COV_{\lambda_{QL}}$ = the coefficient of variation of the live load bias factors.

For the LRFD resistance factor calibrations conducted in this thesis, both dead and live load sources were considered. Therefore, using the results of the comparative analyses performed according to Section 5.2.1, either Eq. (5.19) or (5.20) was utilized for the actual calculation of the LRFD resistance factors. Given that these comparative analyses only provide statistical information related to the distribution of the resistance bias factor, the following subsections have been provided to elaborate on the values assumed for the remaining unknown variables found in Eqs. (5.19) and (5.20).

5.2.3.1 Characteristics of the Dead and Live Load Bias Factors

In an effort to again maintain consistency with the current *AASHTO LRFD Bridge Design Specifications* (2007), the statistical characteristics for the dead and live load bias factors defined in this doument were used for the LRFD resitance factor calibrations conducted in this thesis. Assuming lognormal distributions, AASHTO's load factors and statistical characteristics for the dead and live load bias factors have been reproduced in Table 5.1.

Table 5.1: Load Factors and Statistical Characteristics for the Dead and Live Load Bias Factors (AASHTO 2007)

Load (Q)	Load Factor (γ_Q)	Load Bias ($\bar{\lambda}_Q$)	Coefficient of Variation (COV_{λ_Q})
Dead (D)	1.25	1.05	0.1
Live (L)	1.75	1.15	0.2

5.2.3.2 Target Reliability Index

The target reliability index, as defined in the current *AASHTO LRFD Bridge Design Specifications* (2007), is the measure of safety associated with a particular probability of failure, P_f. Moreover, the probability of failure, as defined previously, represents the

probability for the condition at which the resistance multiplied by the resistance factors will be less than the load multiplied by the load factors (Paikowsky et al. 2004). An approximate relationship between the probability of failure and the reliability index for lognormally distributed load and resistance bias factors was presented by Rosenbleuth and Esteva (1972) and has been reproduced in Eq. (5.21).

$$P_f = 460 \cdot e^{-4.3 \cdot \beta} \tag{5.21}$$

Baecher (2001) showed that this relationship is not very accurate for reliability index values of less than about 2.5, which is within the zone of interest for driven pile foundation design as shown by Barker et al. (1991). Namely, Barker et al. (1991) showed that a reliability index value in the range of 2.5 to 3 is appropriate for the design of driven pile foundations, and that this range could be reduced to a range of 2 to 2.5 given the redundancy in pile groups. Therefore, the following reliability indices and probabilities of failure were used for the LRFD resistance factor calibrations conducted in this thesis, which were developed and recommended by Paikowsky et al. (2004) for use with capacity evaluation methods for single pile foundations and adopted by the current edition of the *AASHTO LRFD Bridge Design Specifications* (2007):

- For redundant piles, defined as five or more piles per pile cap, the recommended probability of failure is 1%, corresponding to a target reliability index of 2.33.
- For non-redundant piles, defined as four or fewer piles per pile cap, the recommended probability of failure is 0.1%, corresponding to a target reliability index of 3.00.

5.2.3.3 Dead-to-Live Load Ratio

The dead-to-live load ratio for bridge type structures varies according to the span length of the bridge. For the design of most bridges, the live load effect is obtained by a standard procedure, while the dead load effect is determined based upon the size of the structure (Perez 1998). In other words, for most bridge structures, the live load effect will remain fairly constant, while the dead load effect will fluctuate. On account of the short span bridges typically constructed within the State of Iowa, the Iowa DOT employs a dead-to-live load ratio of 1.5. In the NCHRP 507 report, Paikowsky et al. (2004) used dead-to-live load

ratios of 2 and 2.5 in their NCHRP 507 report, while Allen (2005) used a relatively conservative dead-to-live load ratio of 3 in his Washington State DOT report. Since the studies conducted by Nowak (1999) and Paikowsky et al. (2004) both indicated that the effect of the dead-to-live load ratio on the calculated LRFD resistance factor is minimal, a dead-to-live load ratio of 2 was considered, in this thesis, to be a reasonable value for the LRFD resistance factor calibrations conducted in this thesis.

5.3 RESULTS OF CALIBRATION PROCESS

5.3.1 Steel H-Piles

5.3.1.1 Estimated Nominal Pile Capacities

Using the PILOT-IA usable-dynamic, steel H-pile data subset, the nominal pile capacity was estimated for each of the test piles using the seven dynamic pile driving formulas identified in Section 5.2. The corresponding measured and predicted nominal pile capacities for each of the test piles in the analyzed dataset have been summarized according to the predominant soil medium encountered along the embedded pile shaft, i.e., sand, clay, or mixed, in Table 5.2, Table 5.3, and Table 5.4, respectively.

5.3.1.2 Distribution of Resistance Bias Factors

As discussed earlier in Section 5.2.1, the first step in the LRFD resistance factor calibration process exploited in this thesis requires that the relationship between the measured and predicted nominal pile capacities be established for each of the seven dynamic pile driving formulas under investigation. Utilizing the Anderson-Darling goodness-of-fit test, this relationship was quantified through the determination of the most probable probability distribution (i.e., either the normal or lognormal probability distribution) from which the sample set of resistance bias factors arose from. With twenty-one different sample sets of resistance bias factors, corresponding to a particular dynamic pile driving formula used in combination with one of the three soil related subsets of the PILOT-IA usable-dynamic, steel H-pile dataset, the Minitab® (2009) statistical software package was employed to carry out the numerous goodness-of-fit tests.

Table 5.2: Measured and Calculated Nominal Axial Pile Capacities for the Sand Soil Subset of the PILOT-IA Usable-Dynamic, Steel H-Pile Dataset

ID #	County	Pile Type	Length[1] (ft)	Davisson (kips)	Dynamic Formula Predicted Nominal Pile Capacities (kips)							Days to SLT[2]
					Gates	FHWA Gates	ENR	IA DOT ENR	Janbu	PCUBC	WSDOT	
17	Fremont	HP 10 X 42	68	132	152	259	243	230	182	187	171	5
20	Muscatine	HP 10 X 42	65	120	136	203	387	153	146	126	140	5
24	Harrison	HP 10 X 42	89	184	188	346	312	218	209	184	216	9
25	Harrison	HP 10 X 42	60	224	164	264	549	209	193	164	210	4
34	Dubuque	HP 10 X 42	60	224	137	205	388	150	149	129	146	7
46	Iowa	HP 10 X 42	50	164	141	233	225	203	167	181	160	4
48	Black Hawk	HP 10 X 42	44	144	126	197	189	159	137	151	136	5
70	Mills	HP 10 X 42	80	128	156	246	480	160	159	135	200	5
74	Benton	HP 10 X 42	60	150	157	248	497	205	185	159	194	33
90	Black Hawk	HP 12 X 53	75	190	197	367	328	263	255	228	227	4
99	Wright	HP 10 X 42	59	104	107	154	156	137	106	123	115	7
151	Pottawattamie	HP 10 X 42	100	200	145	222	369	155	146	136	247	4
158	Dubuque	HP 14 X 89	110	582	315	601	2222	818	465	360	674	4

[1]Driven pile length
[2]Time between the EOD condition and the static load test in days

Table 5.3: Measured and Calculated Nominal Axial Pile Capacities for the Clay Soil Subset of the PILOT-IA Usable-Dynamic, Steel H-Pile Dataset

ID #	County	Pile Type	Length (ft)	Davisson (kips)	Dynamic Formula Predicted Nominal Pile Capacities (kips)							Days to SLT[10]
					Gates	FHWA Gates	ENR	IA DOT ENR	Janbu	PCUBC	WSDOT	
6	Decatur	HP 10 X 42	55	118	112	165	165	141	113	129	121	3
12	Linn	HP 10 X 42	30	204	163	263	570	243	241	211	194	5
42	Linn	HP 10 X 42	26	82	124	177	285	125	136	137	148	5
51	Johnson	HP 10 X 42	40	190	166	268	578	213	218	187	205	3
57	Hamilton	HP 10 X 42	66	168	137	225	211	168	150	154	150	4
67	Audubon	HP 10 X 42	35	140	144	221	395	155	171	160	185	4
102	Poweshiek	HP 10 X 42	45	130	120	184	152	143	128	140	107	3
109	Poweshiek	HP 12 X 53	55	176	140	212	424	158	168	145	142	4

Table 5.4: Measured and Calculated Nominal Axial Pile Capacities for the Mixed Soil Subset of the PILOT-IA Usable-Dynamic, Steel H-Pile Dataset

ID #	County	Pile Type	Length (ft)	Davisson (kips)	Dynamic Formula Predicted Nominal Pile Capacities (kips)							Days to SLT
					Gates	FHWA Gates	ENR	IA DOT ENR	Janbu	PCUBC	WSDOT	
7	Cherokee	HP 10 X 42	55	176	134	218	206	169	149	157	147	6
8	Linn	HP 10 X 42	60	170	162	261	536	222	195	168	209	8
10	Ida	HP 10 X 42	55	116	82	94	116	84	69	79	87	2
43	Linn	HP 10 X 42	46	142	146	226	403	186	176	165	196	5
44	Linn	HP 10 X 42	46	136	151	236	437	202	187	173	203	5
62	Kossuth	HP 10 X 42	47	100	116	157	249	107	113	109	124	5
63	Jasper	HP 10 X 42	65	66	131	211	182	155	140	144	128	2
64	Jasper	HP 10 X 42	75	122	138	226	192	161	146	145	135	1
66	Black Hawk	HP 10 X 42	45	180	156	247	488	189	192	169	197	5
73	Johnson	HP 10 X 42	60	232	156	247	482	166	173	149	201	6
76	Shelby	HP 10 X 42	50	526	174	286	601	252	226	196	246	8
77	Shelby	HP 10 X 42	50	354	183	308	738	291	243	199	235	12
106	Pottawattamie	HP 10 X 42	48	148	108	155	165	128	107	121	122	6

Provided in Figures 5.2 through 5.4, are the Minitab® probability distribution identification results for the Iowa DOT Modified ENR formula used in combination with the sand, clay, and mixed soil subsets of the PILOT-IA usable-dynamic, steel H-pile dataset, respectively. A complete summary of the Minitab® probability distribution identification results for all twenty-one sample sets of resistance bias factors has been supplied in Table 5.5.

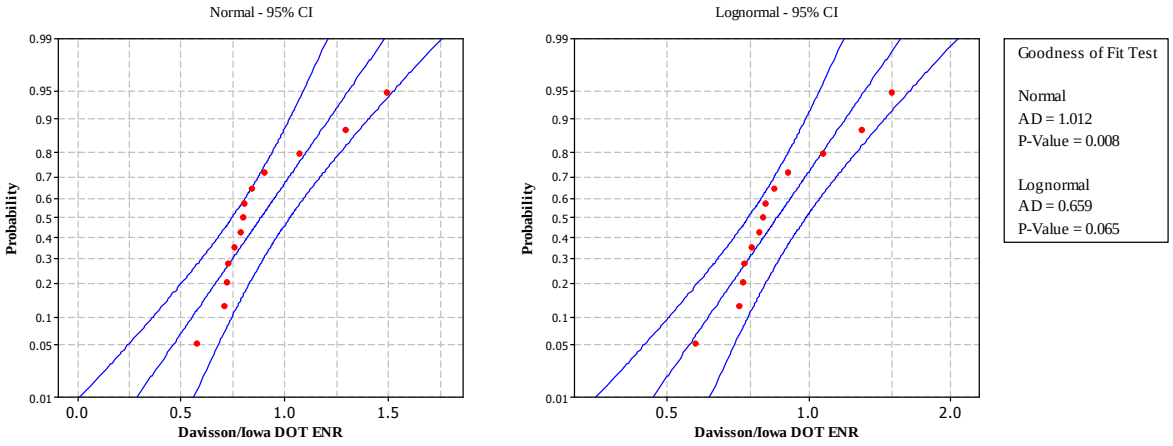

Figure 5.2: Anderson-Darling Goodness-of-Fit Test for the Iowa DOT Modified ENR Formula with the Sand Soil Subset of the PILOT-IA Usable-Dynamic, Steel H-Pile Dataset

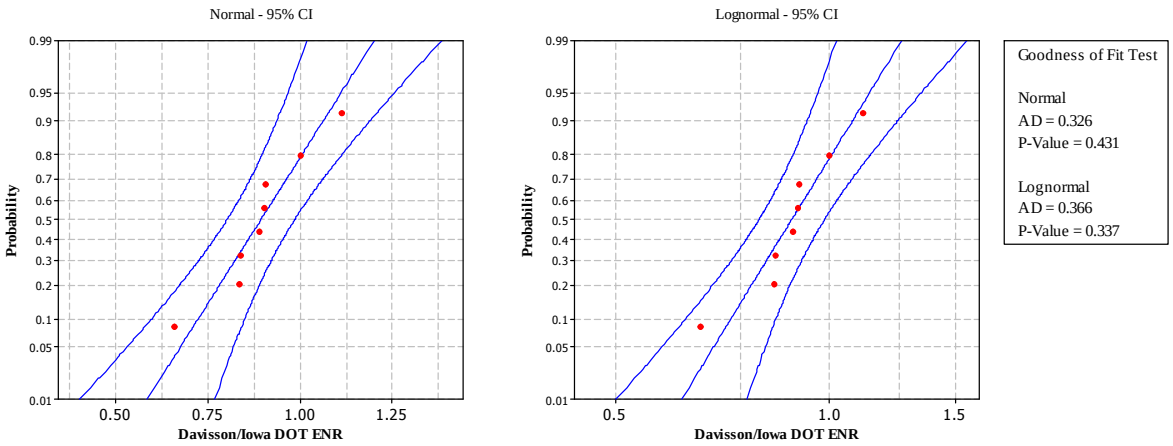

Figure 5.3: Anderson-Darling Goodness-of-Fit Test for the Iowa DOT Modified ENR Formula with the Clay Soil Subset of the PILOT-IA Usable-Dynamic, Steel H-Pile Dataset

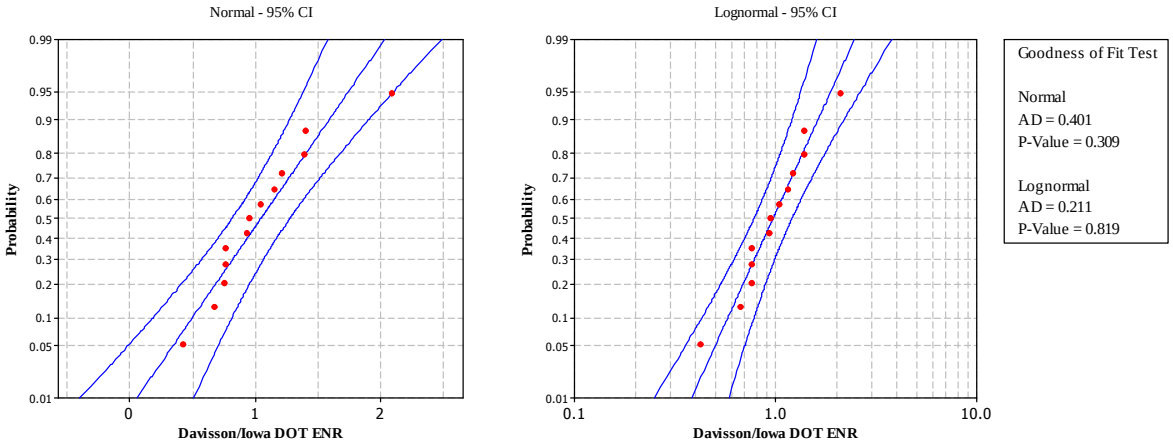

Figure 5.4: Anderson-Darling Goodness-of-Fit Test for the Iowa DOT Modified ENR Formula with the Mixed Soil Subset of the PILOT-IA Usable-Dynamic, Steel H-Pile Dataset

As indicated in Table 5.5, the assumption of a lognormal probability distribution for the various sample sets of resistance bias factors was accepted at the 5% significance level in all instances except for the cases in which the WSDOT formula was used in combination with the sand soil subset of the PILOT-IA usable-dynamic, steel H-pile dataset and the Gates and FHWA Modified Gates formulas were used in conjunction with the clay soil subset of the PILOT-IA usable-dynamic, steel H-pile dataset. However, the lognormal probability distribution was accepted for these three cases at the 1% significance level. Given this documented acceptance of the lognormal probability distribution for the various analyzed sample sets of resistance bias factors coupled with the assumed lognormal probability distributions for the dead and live load bias factors, Eq. (5.20) can be appropriately used for the calculation of LRFD resistance factors.

Before the calibrated LRFD resistance factors are presented, it is important to first discuss how each of the seven analyzed dynamic pile driving formulas compare in regards to prediction power and accuracy. Under the accepted assumption that the analyzed sample sets of resistance bias factors are lognormally distributed, the best-fit lognormal probability distributions were plotted for each method and can be observed in Figure 5.5, Figure 5.6, and Figure 5.7, which have been organized according to the three soil related subsets of the PILOT-IA usable-dynamic, steel H-pile dataset. It is important to point

Table 5.5: Summary of the Anderson-Darling Goodness-of-Fit Tests Carried Out on the Various Combinations of Dynamic Pile Driving Formulas and Soil Related Subsets of the PILOT-IA Usable-Dynamic, Steel H-Pile Dataset

Soil Type	N[1]	Dynamic Pile Driving Formula	Anderson-Darling Goodness-of-Fit Test							
			P^2_{Normal}	AD^3_{Normal}	$P^2_{Lognormal}$	$AD^3_{Lognormal}$	CV[4]	Best Distribution	Normal Assumption	Lognormal Assumption
Sand	13	Gates	0.045	0.720	0.145	0.526	0.702	Lognormal	Rejected	Accepted
	13	FHWA Gates	0.179	0.492	0.345	0.382	0.702	Lognormal	Accepted	Accepted
	13	ENR	0.191	0.482	0.057	0.681	0.702	Normal	Accepted	Accepted
	13	Iowa DOT ENR	0.008	1.012	0.065	0.659	0.702	Lognormal	Rejected	Accepted
	13	Janbu	0.222	0.456	0.483	0.323	0.702	Lognormal	Accepted	Accepted
	13	PCUBC	0.007	1.027	0.030	0.785	0.702	N/A	Rejected	Rejected
	13	WSDOT	0.016	0.889	0.122	0.554	0.702	Lognormal	Rejected	Accepted
Clay	8	Gates	0.141	0.503	0.039	0.705	0.666	Normal	Accepted	Rejected
	8	FHWA Gates	0.142	0.502	0.045	0.684	0.666	Normal	Accepted	Rejected
	8	ENR	0.035	0.721	0.080	0.594	0.666	Lognormal	Rejected	Accepted
	8	Iowa DOT ENR	0.431	0.326	0.337	0.366	0.666	Normal	Accepted	Accepted
	8	Janbu	0.353	0.359	0.195	0.453	0.666	Normal	Accepted	Accepted
	8	PCUBC	0.475	0.309	0.177	0.469	0.666	Normal	Accepted	Accepted
	8	WSDOT	0.674	0.240	0.280	0.396	0.666	Normal	Accepted	Accepted
Mixed	13	Gates	0.027	0.805	0.514	0.308	0.702	Lognormal	Rejected	Accepted
	13	FHWA Gates	0.122	0.554	0.731	0.237	0.702	Lognormal	Accepted	Accepted
	13	ENR	0.014	0.919	0.059	0.676	0.702	Lognormal	Rejected	Accepted
	13	Iowa DOT ENR	0.309	0.401	0.819	0.211	0.702	Lognormal	Accepted	Accepted
	13	Janbu	0.192	0.481	0.668	0.255	0.702	Lognormal	Accepted	Accepted
	13	PCUBC	0.091	0.604	0.753	0.231	0.702	Lognormal	Accepted	Accepted
	13	WSDOT	0.248	0.438	0.906	0.174	0.702	Lognormal	Accepted	Accepted

[1]N = Sample Size

[2]P = P-value; i.e., the probability that the sample being tested was drawn from a population with a specific distribution (i.e., normal or lognormal); if the P-value is less than 0.05, then the null hypothesis is likely to be false and differences between the samples are likely to exist

[3]AD = Anderson-Darling test statistic for the assumption of a normally or lognormally distributed set of resistance bias factors

[4]CV = Critical value at the 5% significance level for which the Anderson-Darling test statistic must not exceed, otherwise the assumed probability distribution is rejected

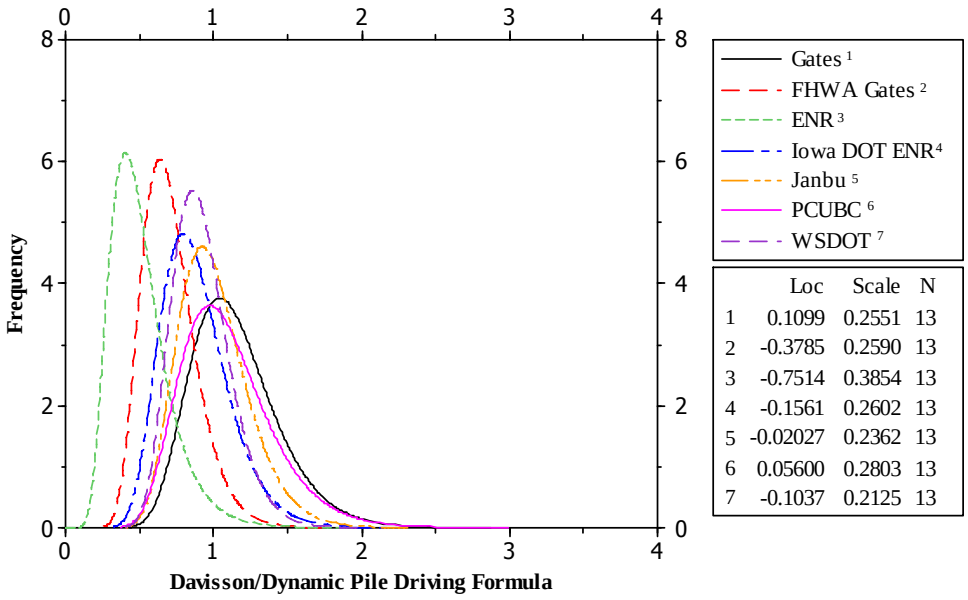

Figure 5.5: Summary of the Lognormally Distributed Resistance Bias Factors Using Seven Dynamic Pile Driving Formulas and the Sand Soil Subset of the PILOT-IA Usable-Dynamic, Steel H-Pile Dataset

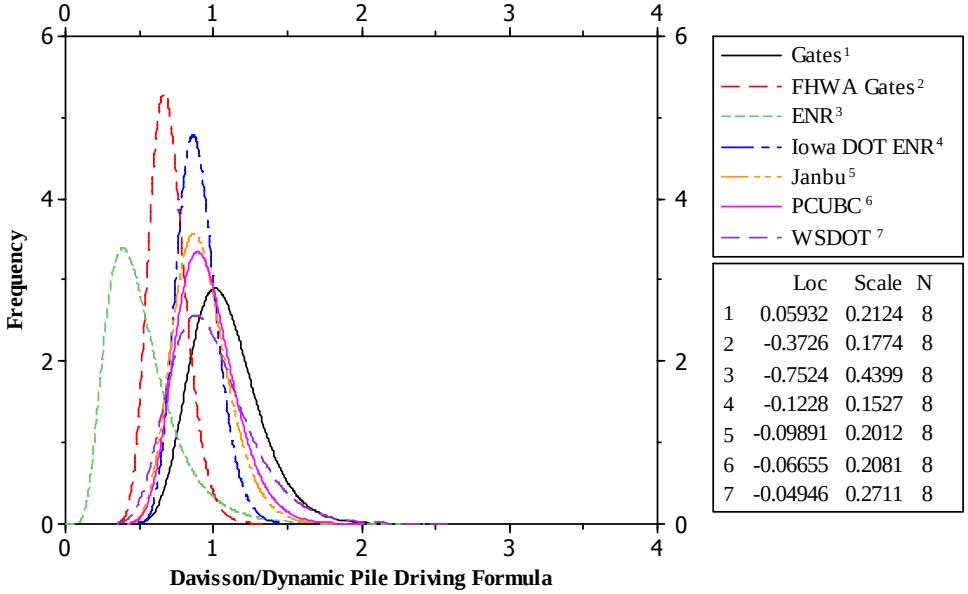

Figure 5.6: Summary of the Lognormally Distributed Resistance Bias Factors Using Seven Dynamic Pile Driving Formulas and the Clay Soil Subset of the PILOT-IA Usable-Dynamic, Steel H-Pile Dataset

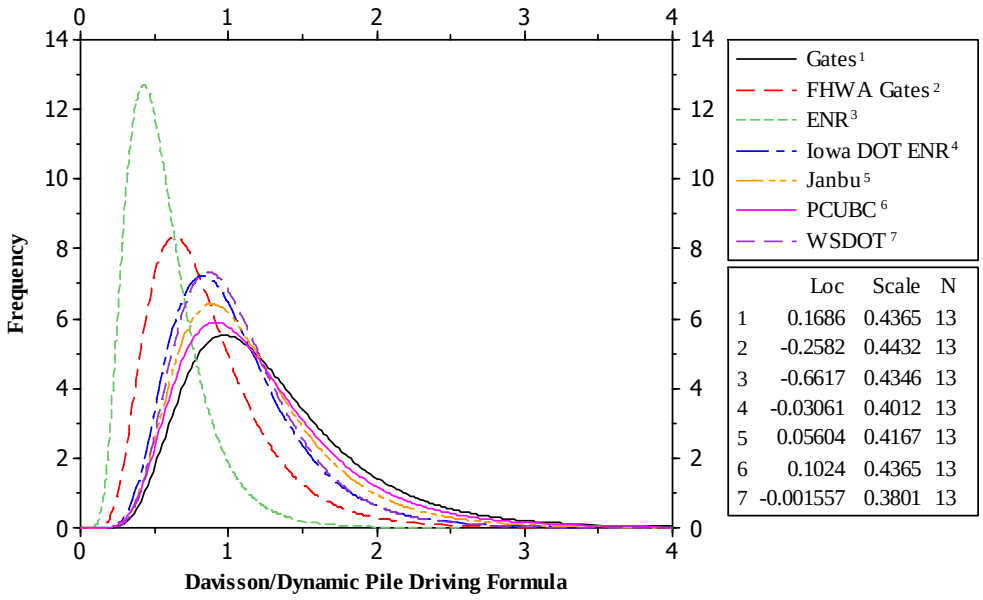

Figure 5.7: Summary of the Lognormally Distributed Resistance Bias Factors Using Seven Dynamic Pile Driving Formulas and the Mixed Soil Subset of the PILOT-IA Usable-Dynamic, Steel H-Pile Dataset

out that the legend in the lower right-hand corner of Figure 5.5, Figure 5.6, and Figure 5.7 presents the mean (Loc) and standard deviation (Scale) for the natural logarithm of the set of resistance bias factors identified in the upper right-hand legend of these figures.

By inspection of these figures it can be ascertained that the ENR and FHWA Modified Gates dynamic pile driving formulas produce small values for both the mean and standard deviation of the corresponding resistance bias factors regardless of the soil type under consideration. This implies that the ENR and FHWA Modified Gates formulas have a tendency to overpredict the measured pile capacity, but to a fairly consistent degree. Conversely, the Gates, Iowa DOT Modified ENR, Janbu, PCUBC, and WSDOT dynamic pile driving formulas produce values for the mean of the corresponding resistance bias factors that are very close to one, or zero when looking at the logarithmic mean, but with much larger standard deviation values. Consequently, these five formulas provide, on average, an accurate estimate of the measured pile capacity, but with a lesser degree of consistency.

5.3.1.3 Calibrated LRFD Resistance Factors

Using the statistical parameters determined in the previous section for the best-fit lognormal distribution to the various sample sets of resistance bias factors, the load factors and statistical parameters for the assumed lognormally distributed dead and live load bias factors presented in Section 5.2.3.1, a dead-to-live load ratio of two, and Eq. (5.20), LRFD resistance factors were calculated for each of the seven examined dynamic pile driving formulas on a soil type basis and at reliability indices of 2.33 and 3.00. Table 5.6 provides a summary of the preliminarily calibrated LRFD resistance factors for the construction control of driven steel H-pile foundations via selected dynamic pile driving formulas.

The results provided in this table show that the higher the resistance bias factor is for a particular dynamic pile driving formula, the higher the corresponding resistance factor will be. For instance, the ENR formula, when used with steel H-piles driven in a predominantly sand soil profile, produces a mean value for the resistance bias factor of 0.503 and a LRFD resistance factor of 0.25 for a reliability index of 2.33, whereas the Gates formula, when used with steel H-piles driven in a mixed soil profile, produces a mean value for the resistance bias factor of 1.297 and a LRFD resistance factor of 0.47 for a reliability index of 2.33. This observed phenomenon appears logical in terms of the definition for the resistance bias factor. As defined in Section 5.2.1, the resistance bias factor symbolizes the ratio between the measured and predicted ultimate pile capacities. Consequently, a large value for the resistance bias factor indicates an overly conservative pile capacity estimation method, which requires a higher resistance factor to achieve the target reliability index, or probability of failure.

Although the absolute value of the LRFD resistance factor is a good indicator of the degree of conservatism exhibited by a particular pile capacity estimation method, it does not provide a clear indication of the method's accuracy. However, the efficiency factor, which was first introduced in Section 2.5.1 as the ratio between the resistance factor and the mean value of the resistance bias factor for a particular pile capacity estimation method, provides an excellent criterion for the evaluation of a given method's accuracy. In essence, the efficiency factor, $\varphi/\bar{\lambda}_R$, indicates the percentage of the measured ultimate pile capacity that can be utilized in design to reach a predefined structural reliability. In other words, higher

values for the efficiency factor indicate a more reliable and overall superior pile capacity estimation method.

Table 5.6: Preliminary LRFD Resistance and Efficiency Factors Provided on a Soil Type Basis for the Construction Control of Driven Steel H-Pile Foundations via Dynamic Pile Driving Formulas

Soil Type	N	Dynamic Formula	$\bar{\lambda}_R$	σ_{λ_R}	COV_{λ_R}	β = 2.33		β = 3.00	
						φ	$\varphi/\bar{\lambda}_R$	φ	$\varphi/\bar{\lambda}_R$
	13	Gates	1.152	0.317	0.276	0.66	0.572	0.52	0.453
	13	FHWA Gates	0.707	0.191	0.270	0.41	0.578	0.32	0.459
	13	ENR	0.503	0.175	0.349	0.25	0.493	0.19	0.376
Sand	13	Iowa DOT ENR	0.885	0.257	0.291	0.49	0.556	0.39	0.437
	13	Janbu	1.006	0.248	0.247	0.61	0.605	0.49	0.486
	13	PCUBC	1.098	0.330	0.300	0.60	0.545	0.47	0.426
	13	WSDOT	0.922	0.220	0.239	0.57	0.615	0.46	0.495
	8	Gates	1.080	0.198	0.183	0.73	0.677	0.60	0.559
	8	FHWA Gates	0.698	0.110	0.158	0.49	0.704	0.41	0.587
	8	ENR	0.514	0.234	0.455	0.20	0.392	0.15	0.283
Clay	8	Iowa DOT ENR	0.893	0.132	0.148	0.64	0.714	0.53	0.598
	8	Janbu	0.921	0.169	0.184	0.62	0.676	0.51	0.558
	8	PCUBC	0.952	0.180	0.189	0.64	0.671	0.53	0.552
	8	WSDOT	0.980	0.234	0.239	0.60	0.614	0.49	0.495
	13	Gates	1.297	0.632	0.487	0.47	0.366	0.34	0.259
	13	FHWA Gates	0.846	0.392	0.463	0.33	0.385	0.23	0.277
	13	ENR	0.564	0.254	0.450	0.22	0.396	0.16	0.287
Mixed	13	Iowa DOT ENR	1.044	0.425	0.407	0.45	0.436	0.34	0.322
	13	Janbu	1.146	0.492	0.430	0.48	0.415	0.35	0.303
	13	PCUBC	1.211	0.564	0.466	0.46	0.383	0.33	0.275
	13	WSDOT	1.069	0.430	0.402	0.47	0.440	0.35	0.326

As presented in Table 5.6, for a reliability index of 2.33, it was found that the WSDOT formula was the most efficient method for the construction control of steel H-piles driven in a sand or mixed soil profile, while the Iowa DOT Modified ENR formula was

found to be the most efficient method when considering a clay soil profile. As was expected from the results of the comparative studies presented in Section 2.4, the ENR formula was shown to be one of the least efficient methods, regardless of the type of soil profile under consideration. Bearing in mind that the Iowa DOT Modified ENR formula is currently specified in the Iowa DOT's *Standard Specifications for Highway and Bridge Construction* manual as the preferred dynamic pile driving formula for the construction control of driven pile foundations, it is important to point out that this formula is only 9.59% and 0.91% less efficient than the WSDOT formula at a reliability index of 2.33, when consideration is given to a sand and mixed soil profile, respectively. Consequently, in an effort to avoid a comprehensive modification to the Iowa DOT's driven pile foundation design guide, the performance of the Iowa DOT Modified ENR formula is sufficient to allow for its recommended use with steel H-pile foundations driven in any soil type.

5.3.1.4 Sample Size Effects on Resistance Factors

Since the sizes of the sand, clay, and mixed soil subsets of the PILOT-IA usable-dynamic, steel H-pile dataset are all less than thirty, they are considered to be samples of "small" size by Miller and Miller (2004), as well as many other statistical references. Unfortunately, this implies that standard deviations or coefficients of variation of the resistance bias factors presented in Table 5.6 may not be representative of the true populations. Moreover, even for sample populations with similar statistical characteristics to the true populations, a random sampling may still generate significant variation in the computed LRFD resistance factors on account of the small sample size (McVay, Birgisson, and Lee 2004).

In order to check the sample sizes of the sand, clay, and mixed soil subsets of the PILOT-IA usable-dynamic, steel H-pile dataset on the variability of the LRFD resistance factors computed in the previous section, a Monte Carlo simulation was performed using MATLAB™ (2009). The Monte Carlo method, whose conceptual origins were first proposed by Pierre Simon Laplace in 1886, consists of finding a numerical value by realizing a random event many times and observing its outcome experimentally (Beckmann 1976). Focusing on the LRFD resistance factors calculated for the Iowa DOT Modified ENR formula, a random sample of resistance bias factors was selected from the assumed

distribution for the true population, which was formed using the statistical characteristics outlined in Table 5.6 for each of the sand, clay, and mixed soil type subsets. From this random sample, which was chosen to be of the same size as the sand (13), clay (8), and mixed (13) soil type subsets, the mean value and the coefficient of variation for the randomly selected resistance bias factors were determined. Then, using Eq. (5.20), the load factors and statistical parameters for the assumed lognormally distributed dead and live load bias factors presented in Section 5.2.3.1, a dead-to-live load ratio of two, and a reliability index of 2.33, a corresponding LRFD resistance factor was calculated. To replicate the random nature of the sample population, another random sample of resistance bias factors was selected from the assumed distribution for the true population. Upon computing the mean value as well as the coefficient of variation for this second set of randomly selected resistance bias factors, another LRFD resistance factor was calculated. Repeating this process a total of 1,000 times, a distribution of LRFD resistance factors was obtained for the Iowa DOT Modified ENR formula, as it is used for monitoring the driving of steel H-piles in sand, clay, and mixed soil profiles. Figure 5.8 and Figure 5.9 provide a summary of the results obtained from the formerly described Monte Carlo simulations.

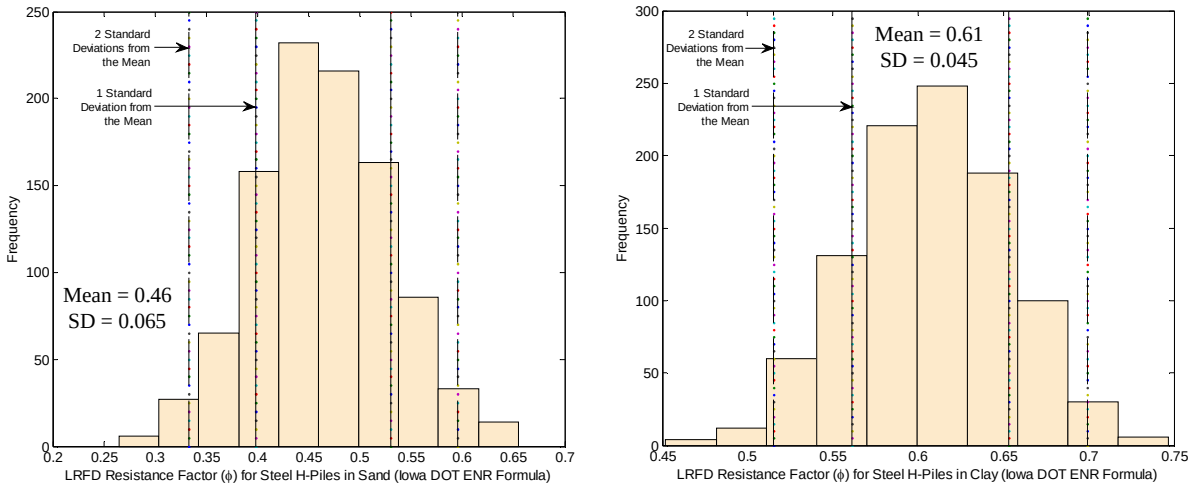

(a) Sand Soil Profile **(b) Clay Soil Profile**

Figure 5.8: Variations in LRFD Resistance Factors for the Iowa DOT Modified ENR Formula

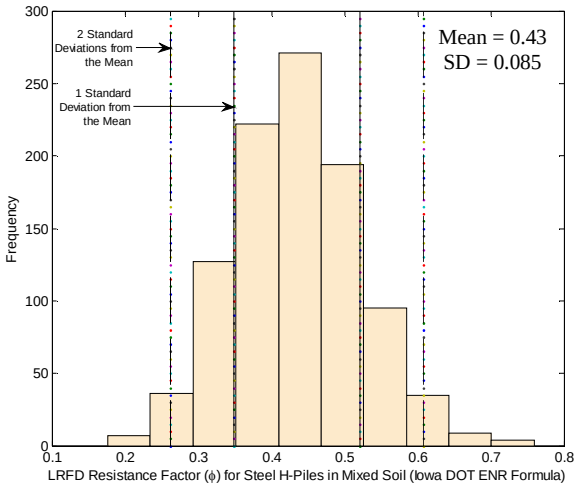

Figure 5.9: Variation in LRFD Resistance Factors for the Iowa DOT Modified ENR Formula used in Mixed Soil Profiles

The distributions provided in these figures indicate mean LRFD resistance factor values of 0.46, 0.61, and 0.43 for the sand, clay, and mixed soil type subsets, respectively. As was expected, these values compare quite favorably with the corresponding LRFD resistance factors provided in Table 5.6. Using one standard deviation above and below the mean resistance factors as a measure of variability, it was observed that such variability is directly related to the coefficient of variation assumed for the true distribution of resistance bias factors. In other words, if the true population statistics were to change from those assumed, a corresponding change in the variability of the computed LRFD resistance factors would be realized. However, since it must be assumed that the true population statistics have been correctly captured, the observed variability in the LRFD resistance factors can be used to determine whether or not the utilized sample size sufficiently captures the characteristics of the true population. As indicated in Figure 5.8 and Figure 5.9, the one standard deviation bounds on the mean resistance factors determined for the sand, clay, and mixed soil type subsets were found to be (0.40, 0.53), (0.56, 0.65), and (0.35, 0.52), respectively. Considering the fact that McVay, Birgisson, and Lee (2004) defined significant variability in computed LRFD resistance factors at the one standard deviation level to be about 0.15, it is appropriate to assume that the sample sizes available for the computation of LRFD resistance factors for the Iowa DOT Modified ENR formula, as it is used with sand, clay, and mixed

soil profiles, effectively capture the characteristics of the true population, given that the highest observed variability is only half of that value considered to be significant. Moreover, it is only at the two standard deviation level that the observed variability in LRFD resistance factors begins to encroach upon the significant value defined by McVay, Birgisson, and Lee (2004).

5.3.1.5 Verification with Full-Scale Pile Load Tests

As a means of verifying the performance of the LRFD resistance factors established in Section 5.3.1.3, the design, or factored, pile capacities estimated by the seven examined dynamic pile driving formulas were compared with the corresponding measured pile capacities for the nine steel H-piles tested as a part of the research outlined in this thesis. To begin with, the measured and predicted nominal pile capacities were established for these nine steel H-shaped test piles and the results have been summarized in Table 5.7. Using the appropriate preliminarily calculated LRFD resistance factors, as presented in Table 5.6, in conjunction with the nominal pile capacities predicted by the seven examined dynamic pile driving formulas, the predicted design pile capacities were determined and have been provided in Table 5.8. Figure 5.10 and Figure 5.11 present the same information contained in Table 5.7 and Table 5.8, respectively, but in a format that is much more conducive to the formation of comparisons.

Table 5.7: Measured and Predicted Nominal Pile Capacities for Nine Steel H-Piles

Project ID	Measured Capacity (kips)	Predicted Nominal Capacity (kips)						
		Gates	FHWA Gates	ENR	Iowa DOT ENR	Janbu	PCUBC	WSDOT
ISU1	198	128	184	288	131	137	141	186
ISU2	125	123	173	266	116	118	116	170
ISU3	150	117	161	242	104	108	107	160
ISU4	154	150	235	418	181	171	157	216
ISU5	243	191	326	775	306	244	201	272
ISU6	213	161	259	491	217	194	175	237
ISU7	53	24	0	71	36	34	38	46
ISU8	162	156	248	451	195	182	166	233
ISU9	182	162	260	473	233	203	194	269

Table 5.8: Measured and Predicted Design Pile Capacities for Nine Steel H-Piles

Project ID	Measured Capacity (kips)	Predicted Design Capacity (kips)						
		Gates	FHWA Gates	ENR	Iowa DOT ENR	Janbu	PCUBC	WSDOT
ISU1	198	60	61	63	59	66	65	87
ISU2	125	90	85	53	74	73	74	102
ISU3	150	86	79	48	67	67	68	96
ISU4	154	110	115	84	116	106	101	130
ISU5	243	140	160	155	196	151	128	163
ISU6	213	118	127	98	139	120	112	142
ISU7	53	11	0	16	16	16	18	22
ISU8	162	73	82	99	88	87	77	110
ISU9	182	107	107	118	114	124	116	153

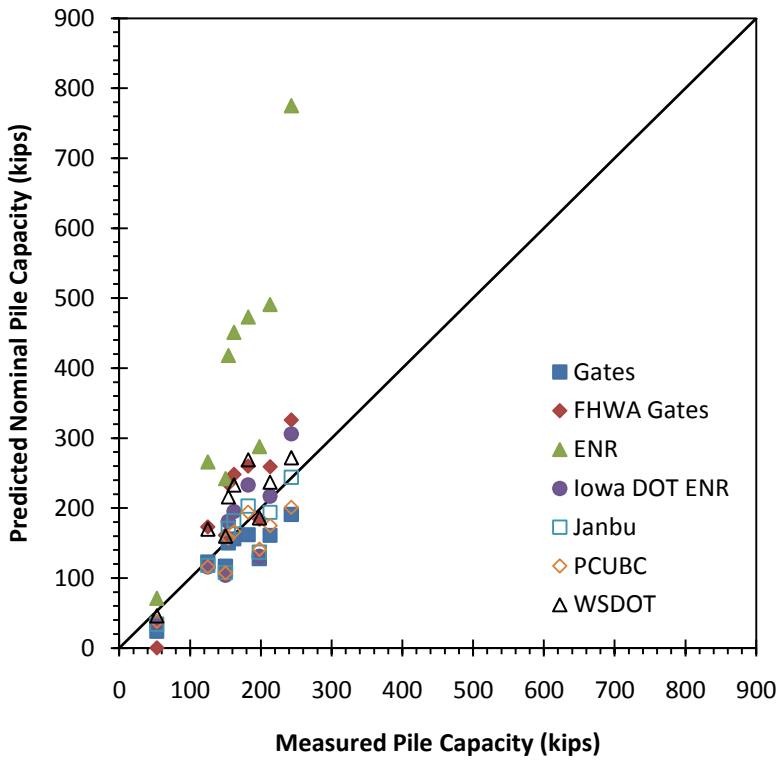

Figure 5.10: Nominal Pile Capacities Predicted by Dynamic Pile Driving Formulas versus Measured Pile Capacities obtained from Static Load Testing Nine Steel H-Piles

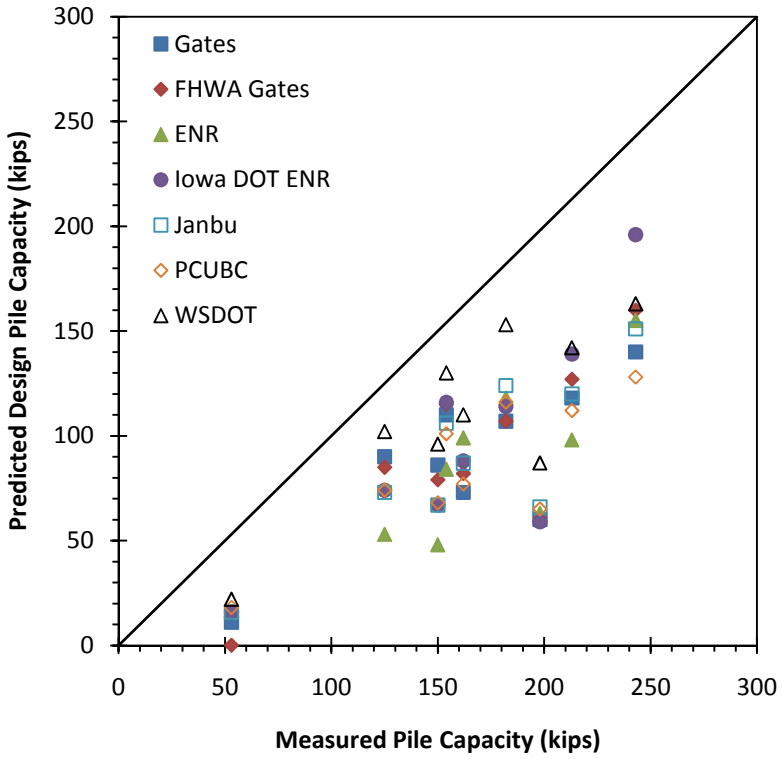

Figure 5.11: Design Pile Capacities Predicted by Dynamic Pile Driving Formulas versus Measured Pile Capacities obtained from Static Load Testing Nine Steel H-Piles

One important observation that should be drawn from Figure 5.10 and Figure 5.11 is that the preliminarily calculated LRFD resistance factors successfully establish safe design pile capacities for all soil types; i.e., the design pile capacities are always less than the measured pile capacities. Furthermore, Figure 5.11 provides a clear indication and verification of the efficiencies associated with each of the seven examined dynamic pile driving formula, which were first established in Section 5.3.1.3. More specifically, the elevated efficiencies of the WSDOT formula in sand and mixed soil profiles and the Iowa DOT Modified ENR formula in predominantly clay soil profiles are prominent in this graphical display. On another note, Figure 5.10 emphasizes the significant overprediction in pile capacity (i.e., poor performance) offered by the ENR formula.

Having verified the safety and efficiency of the preliminarily calculated LRFD resistance factors, the data obtained from the nine additional steel H-shaped test piles was combined with that from the PILOT-IA usable-dynamic, steel H-pile dataset to allow for further enhancement of the preliminarily calibrated resistance and efficiency factors.

Employing the same calibration procedures outlined previously, final LRFD resistance and efficiency factors were calculated for each of the seven dynamic pile driving formulas on a soil type basis. The results of this final calibration are provided in Table 5.9. Although the efficiency of the Iowa DOT Modified ENR formula decreased slightly from that reported in Table 5.6 for clay soils, this can be explained by the variations in the degree of soil set-up achieved at the time of testing.

Table 5.9: Final LRFD Resistance and Efficiency Factors Provided on a Soil Type Basis for the Construction Control of Driven Steel H-Pile Foundations using Different Dynamic Pile Driving Formulas

Soil Type	N	Dynamic Formula	$\bar{\lambda}_R$	σ_{λ_R}	COV_{λ_R}	β = 2.33		β = 3.00	
						φ	$\varphi/\bar{\lambda}_R$	φ	$\varphi/\bar{\lambda}_R$
	14	Gates	1.150	0.305	0.265	0.67	0.584	0.53	0.465
	14	FHWA Gates	0.706	0.184	0.260	0.42	0.590	0.33	0.471
	14	ENR	0.494	0.171	0.347	0.24	0.495	0.19	0.378
Sand	14	Iowa DOT ENR	0.877	0.248	0.283	0.49	0.564	0.39	0.445
	14	Janbu	0.998	0.240	0.241	0.61	0.612	0.49	0.492
	14	PCUBC	1.087	0.320	0.294	0.60	0.552	0.47	0.433
	14	WSDOT	0.904	0.221	0.245	0.55	0.608	0.44	0.488
	13	Gates	1.119	0.181	0.162	0.78	0.700	0.65	0.583
	13	FHWA Gates	0.728	0.111	0.153	0.52	0.709	0.43	0.592
	13	ENR	0.486	0.195	0.400	0.21	0.442	0.16	0.328
Clay	13	Iowa DOT ENR	0.945	0.191	0.202	0.62	0.656	0.51	0.537
	13	Janbu	0.986	0.188	0.191	0.66	0.668	0.54	0.550
	13	PCUBC	1.039	0.201	0.193	0.69	0.666	0.57	0.547
	13	WSDOT	0.924	0.202	0.219	0.59	0.637	0.48	0.518
	16	Gates	1.351	0.613	0.454	0.53	0.393	0.38	0.284
	15	FHWA Gates	0.848	0.372	0.438	0.35	0.407	0.25	0.296
	16	ENR	0.570	0.240	0.421	0.24	0.423	0.18	0.311
Mixed	16	Iowa DOT ENR	1.087	0.416	0.383	0.50	0.459	0.37	0.344
	16	Janbu	1.175	0.463	0.394	0.53	0.447	0.39	0.333
	16	PCUBC	1.219	0.513	0.421	0.52	0.423	0.38	0.311
	16	WSDOT	1.051	0.397	0.378	0.49	0.464	0.37	0.348

5.3.1.6 Comparison with Design Specifications

In the current edition of the *AASHTO LRFD Bridge Design Specifications*, resistance factors, developed for the EOD condition, are provided for the FHWA Modified Gates and ENR dynamic pile driving formulas. More specifically, resistance factors of 0.40 and 0.10 are recommended for use with the FHWA Modified Gates and ENR formulas, respectively. It is important to point out that these recommendations are provided without enhacement for particular pile types and/or soil profiles. In comparing these code recommended resitance factors with those recommended in the previous section, i.e., Table 5.10, the enhanced enconomy of the regionally calibrated factors is evidenced.

Table 5.10: Comparison of the Iowa (Steel H-Shaped) and AASHTO (2007) Recommended LRFD Resistance Factors for the FHWA Modified Gates, ENR, and Iowa DOT Modified ENR Formulas at a Reliability Index of 2.33

Soil Type	Dynamic Formula	Iowa Recommended Resistance Factor	AASHTO (2007) Recommended Resistance Factor	Economy Gain (%)
Sand	FHWA Gates	0.42	0.40	5
	ENR	0.24	0.10	140
	Iowa DOT ENR	0.49	-	5*
Clay	FHWA Gates	0.52	0.40	30
	ENR	0.21	0.10	110
	Iowa DOT ENR	0.62	-	30*
Mixed	FHWA Gates	0.35	0.40	-15
	ENR	0.24	0.10	140
	Iowa DOT ENR	0.50	-	-10*

*Gain in economy over AASHTO's (2007) recommended value for the FHWA Gates formula

In all instances outlined in Table 5.10, except for the combination of the FHWA Modified Gates formula with a mixed soil profile, the Iowa recommended resistance factors are greater in value than those recommended in the current edition of the *AASHTO LRFD Bridge Design Specifications*. This implies that, overall, the regionally calibrated resistance factors for the State of Iowa provide for the improved economy of bridge foundation elements, which was the goal set forth by AASHTO in allowing such regional calibration efforts. As for the combination of the FHWA Modified Gates formula with a mixed soil profile, the small reduction in economy indicated in Table 5.10 should not generate concerns since the resistance factors recommended by AASHTO (2007) were ultimately established as

a result of rounding prcoedures carried out to the nearest 0.05. Therefore, since the Iowa recommended resistance factor for this combination is within the 0.05 rounding tolerance of the AASHTO (2007) recommended value, the two should be considered equivalent, with no net loss in economy.

5.3.1.7 Enhancement of LRFD Resistance Factors for Static Analysis Methods

As indicated by AbdelSalam et al. (2010), the Iowa DOT currently uses an in-house static analysis method, known as the Iowa Blue Book method (Dirks and Kam 1989; Iowa DOT 2010), to predict the required length of piles to be driven in the field. Moreover, during actual pile driving, the Iowa DOT Modified ENR formula is used to determine when a pile has developed adequate axial capacity. Given that the results of the LRFD resistance factor calibration process presented in this thesis for dynamic pile driving formulas utilized in conjunction with steel H-piles, coupled with those similar results presented by AbdelSalam et al. (2010) for static analysis methods, indicate that the current design and construction control procedures for driven pile foundations in the State of Iowa are some of the most efficient, as expected, there exists no need for the recommendation of alternative methods. Provided this information, an attempt to further enhance the LRFD resistance factors recommended by AbdelSalam et al. (2010) for the Iowa Blue Book method can be made so that the recognized use of the Iowa DOT Modified ENR formula for pile driving termination is taken into account.

In an ideal situation, the design length of piling predicted by the Iowa Blue Book method would agree with that driven in the field, where the Iowa DOT Modified ENR formula is used to terminate driving. Due to uncertainties involved in the pile driving process, this ideal situation is never achieved. However, the probability that the length of piling driven will be greater or less than that predicted by the Iowa Blue Book method can be quantified by looking at the cumulative probability distribution for the ratio of the design, or factored, pile capacity predicted by the Iowa DOT ENR formula to that predicted by the Iowa Blue Book method.

Provided in Figures 5.12 through 5.14 are the Minitab® probability distribution identification results for the Iowa DOT Modified ENR to Iowa Blue Book design capacity ratio used in combination with the sand, clay, and mixed soil subsets of the amassed PILOT-

IA usable-dynamic, steel H-pile dataset, respectively. This amassed PILOT-IA usable-dynamic, steel H-pile dataset simply combines the original PILOT-IA usable-dynamic, steel H-pile dataset with the information acquired from the nine, full-scale field load tests conducted as a part of this research and summarized in Chapter 4. Furthermore, the design capacities established by the Iowa DOT Modified ENR formula were achieved through the application of the appropriate LRFD resistance factors recommended in Table 5.9 of this thesis, while for the Iowa Blue Book method, the appropriate LRFD resistance factors recommended by AbdelSalam et al. (2010) were used; namely, resistance factors of 0.47, 0.71, and 0.45 were used for piles embedded in sand, clay, and mixed soil profiles, respectively.

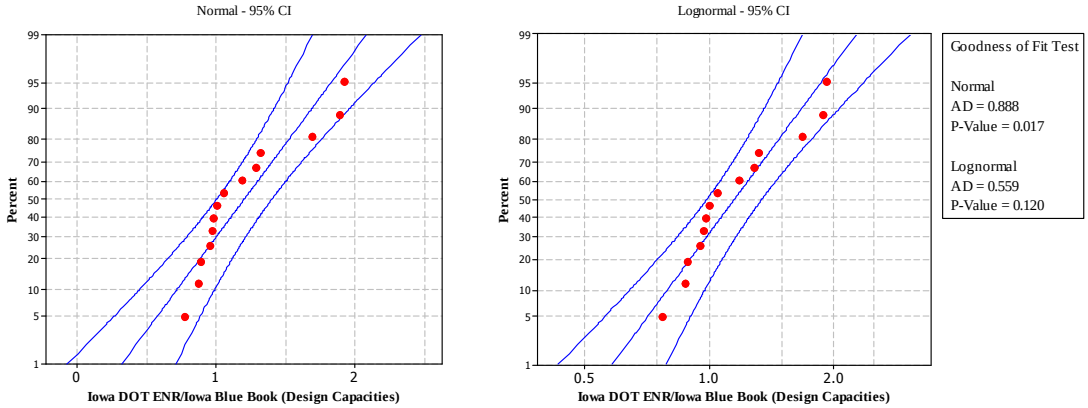

Figure 5.12: Anderson-Darling Goodness-of-Fit Test for the Iowa DOT Modified ENR to Iowa Blue Book Design Capacity Ratio used with the Clay Soil Subset of the Amassed PILOT-IA Usable-Dynamic, Steel H-Pile Dataset

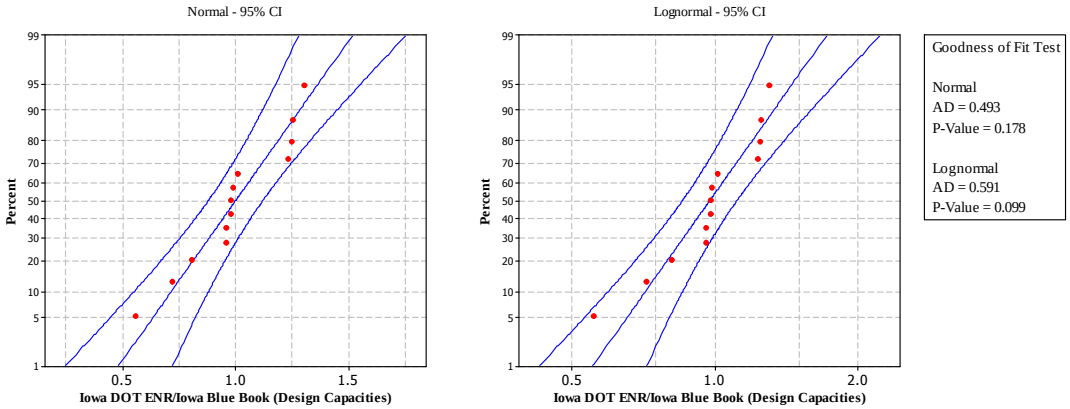

Figure 5.13: Anderson-Darling Goodness-of-Fit Test for the Iowa DOT Modified ENR to Iowa Blue Book Design Capacity Ratio used with the Clay Soil Subset of the Amassed PILOT-IA Usable-Dynamic, Steel H-Pile Dataset

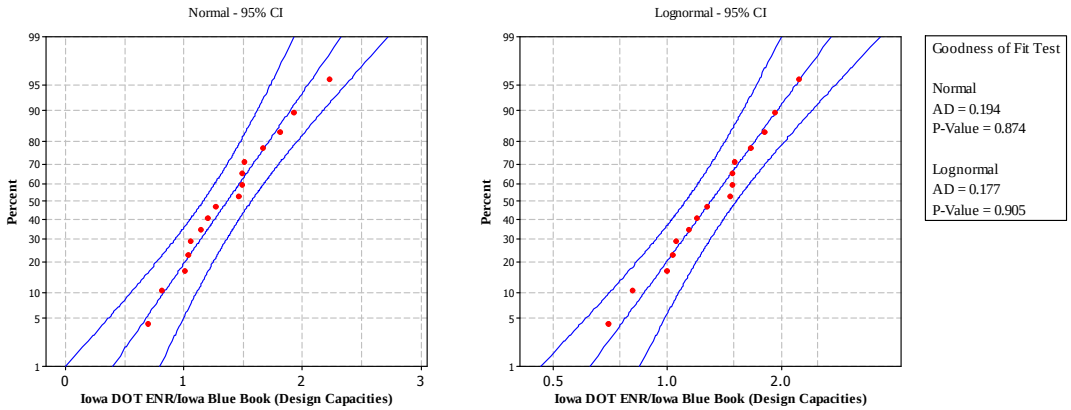

Figure 5.14: Anderson-Darling Goodness-of-Fit Test for the Iowa DOT Modified ENR to Iowa Blue Book Design Capacity Ratio used with the Mixed Soil Subset of the Amassed PILOT-IA Usable-Dynamic, Steel H-Pile Dataset

As evidenced from Figures 5.12 through 5.14, the assumption of a lognormal probability distribution for the three sample sets of Iowa DOT Modified ENR to Iowa Blue Book design capacity ratios was accepted at the 5% significance level in all cases. Therefore, for the development of enhanced LRFD resistance factors for the Iowa Blue Book method, the best-fit, lognormal, cumulative probability distributions depicted in the rightmost plots of Figures 5.12, 5.13, and 5.14 will be used. However, before such enhanced resistance factors are developed, an explanation of what these cumulative probability distributions actually indicate must be given. The y-axes of these plots designate the probability that the Iowa DOT Modified ENR to Iowa Blue Book design capacity ratio will be less than or equal to the specified design capacity ratio found on the x-axes. In other words, for piles driven in sand soil profiles, a value of unity for the design capacity ratio corresponds to a cumulative probability of about 31.6%, whereas for piles driven in clay and mixed soil profiles a value of unity for the design capacity ratio corresponds to cumulative probabilities of about 54.3% and 20.2%, respectively. This indicates that there is a 31.6% probability that the Iowa DOT Modified ENR to Iowa Blue Book design capacity ratio will be less than one for any given pile driven in a sand soil profile, while the probability that this design capacity ratio will be less than one for any given pile driven in a clay or mixed soil profile is 54.3% and 20.2%, respectively. So, for piles driven in a sand soil profile in particular, 31.6% of the time it can be expected that the length of piling driven in the field will be greater than that predicted by

the Iowa Blue Book method. Conversely, 68.4% of the time, the length of piling driven will be less than that predicted by the Iowa Blue Book method.

Hence, the design pile capacity established by either the Iowa Blue Book method or the Iowa DOT Modified ENR formula can be corrected to improve upon this probability. For instance, it may be desired that a majority of the time the length of piling driven in the field be less than that predicted by the Iowa Blue Book method in the design stages of the project. Driving piles longer than predicted may require splicing or even the acquisition of additional piling from off-site. On the other hand, it may also be desirable to correct one of the formulas so that half of the time the length of piling driven is shorter than that predicted and half of the time it is longer than predicted. Based on the available data, this would represent a best guess for making the actual and predicted pile lengths correlate. Thus, at a cumulative probability of 50%, the Iowa DOT Modified ENR to Iowa Blue Book design capacity ratio takes on values of 1.15, 0.97, and 1.33 when considering sand, clay, and mixed soil profiles, respectively. In other words, if it were desired that there be a 50% probability associated with the event that the driven pile lengths are longer than those predicted by the Iowa Blue Book method, then it would be necessary to multiply the design pile capacity established by the Iowa Blue Book method by a factor of 1.15, 0.97, or 1.33 depending on whether the embedded length of the pile was characterized by a sand, clay, or mixed soil profile. By incorporating these correction factors into the original LRFD resistance factors established for the Iowa Blue Book method, one arrives at the following enhanced LRFD resistance factors: 0.54, 0.69, and 0.60, which are to be used in conjunction with piles embedded in sand, clay, and mixed soil profiles, respectively.

As demonstrated in Figure 5.15 and Figure 5.16, the enhanced LRFD resistance factors for the Iowa Blue Book method, which account for the use of the Iowa DOT Modified ENR formula for pile design verification, successfully shift the lognormal probability distributions for the Iowa DOT Modified ENR to Iowa Blue Book design capacity ratios achieved in sand, clay and mixed soil profiles so that their expected value is approximately equal to one. Although the reliability assured by these enhanced LRFD resistance factors is no longer equal to 2.33, it is important to reiterate that these factors are to only be used in situations where it is known that the Iowa DOT Modified ENR formula

will be used in the field as a construction control measure. In other words, since embedded pile lengths will ultimately be determined via the Iowa DOT Modified ENR formula, regardless of what was established by the Iowa Blue Book method in the design stages of the project, a reliability of 2.33 is ensured by means of the LRFD resistance factors calibrated for the Iowa DOT Modified ENR formula. Once more, it is the sole function of these enhanced resistance factors to simply minimize the discrepancy between the design and production pile lengths.

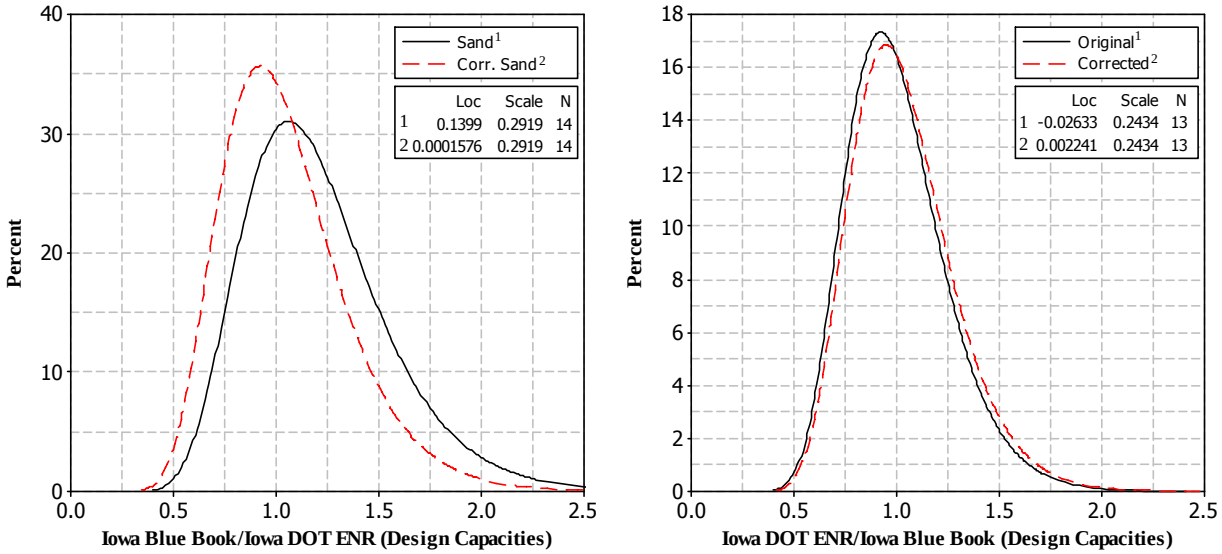

(a) Sand Soil Profiles **(b) Clay Soil Profiles**

Figure 5.15: Original and Corrected Lognormal Probability Distributions for the Iowa DOT Modified ENR/Iowa Blue Book Design Capacity Ratio

5.3.2 Timber Piles

5.3.2.1 Estimated Pile Capacities

Using the PILOT-IA usable-dynamic, timber pile dataset, the nominal pile capacity was estimated for each of the test piles using the seven dynamic pile driving formulas identified in Section 5.2. The corresponding measured and predicted nominal pile capacities for each of the test piles in the analyzed dataset have been summarized according to the predominant soil medium encountered along the embedded pile shaft, i.e., sand, clay, or mixed, in Table 5.11, Table 5.12, and Table 5.13, respectively.

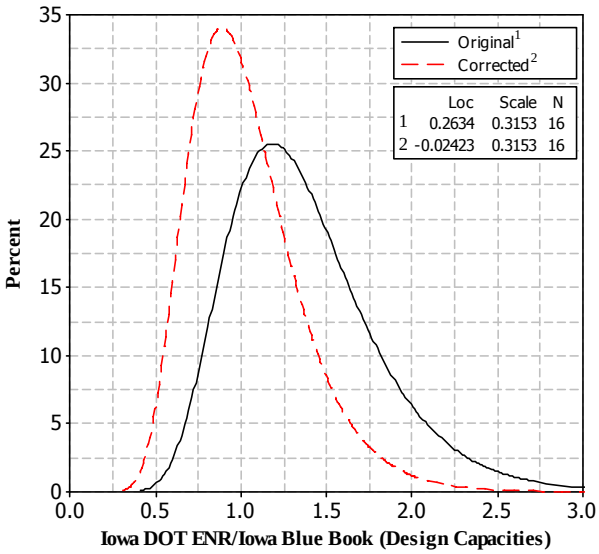

Figure 5.16: Original and Corrected Lognormal Probability Distributions for the Iowa DOT Modified ENR/Iowa Blue Book Design Capacity Ratio in Mixed Soil Profiles

5.3.2.2 Distribution of Resistance Bias Factors

As done in Section 5.3.1.2, the Anderson-Darling goodness-of-fit test was used to quantify the relationship between the measured and predicted nominal pile capacities established for the PILOT-IA usable-dynamic, timber pile dataset. Ignoring the soil type subdivisions of this dataset on account of the small available sample sizes, seven different sample sets of resistance bias factors, each corresponding to a particular dynamic pile driving formula, were analyzed using the Minitab® statistical software package to determine the most probable probability distribution from which these sets of resistance bias factors arose from.

Provided in Figure 5.17 is the Minitab® probability distribution identification results for the Iowa DOT Modified ENR formula used in combination with the PILOT-IA usable-dynamic, timber pile dataset. A complete summary of the Minitab® probability distribution identification results for all seven sample sets of resistance bias factors has been supplied in Table 5.14.

Table 5.11: Measured and Calculated Nominal Axial Pile Capacities for the Sand Soil Subset of the PILOT-IA Usable-Dynamic, Timber Pile Dataset

ID #	County	Pile Type	Length (ft)	Davisson (kips)	Dynamic Formula Predicted Nominal Pile Capacities (kips)							Days to SLT
					Gates	FHWA Gates	ENR	IA DOT ENR	Janbu	PCUBC	WSDOT	
180	Black Hawk	Ø 10" Timber	20	88	134	197	335	195	155	153	129	2
181	Black Hawk	Ø 10" Timber	25	200	188	318	792	448	243	203	189	12

Table 5.12: Measured and Calculated Nominal Axial Pile Capacities for the Clay Soil Subset of the PILOT-IA Usable-Dynamic, Timber Pile Dataset

ID #	County	Pile Type	Length (ft)	Davisson (kips)	Dynamic Formula Predicted Nominal Pile Capacities (kips)							Days to SLT
					Gates	FHWA Gates	ENR	IA DOT ENR	Janbu	PCUBC	WSDOT	
174	Linn	Ø 10" Timber	25	76	86	104	132	126	83	105	99	4
206	Lucas	Ø 10" Timber	40	88	80	78	112	52	52	54	60	2
229	Polk	Ø 10" Timber	25	138	127	182	313	171	138	130	109	2
235	Mitchell	Ø 10" Timber	20	152	99	119	175	94	86	89	78	5

Table 5.13: Measured and Calculated Nominal Axial Pile Capacities for the Mixed Soil Subset of the PILOT-IA Usable-Dynamic, Timber Pile Dataset

ID #	County	Pile Type	Length (ft)	Davisson (kips)	Dynamic Formula Predicted Nominal Pile Capacities (kips)							Days to SLT
					Gates	FHWA Gates	ENR	IA DOT ENR	Janbu	PCUBC	WSDOT	
175	Linn	Ø 10" Timber	30	94	54	28	90	79	52	67	62	6
201	Calhoun	Ø 10" Timber	20	72	68	62	103	89	61	77	76	5
209	Woodbury	Ø 10" Timber	20	110	101	140	147	120	95	107	109	7

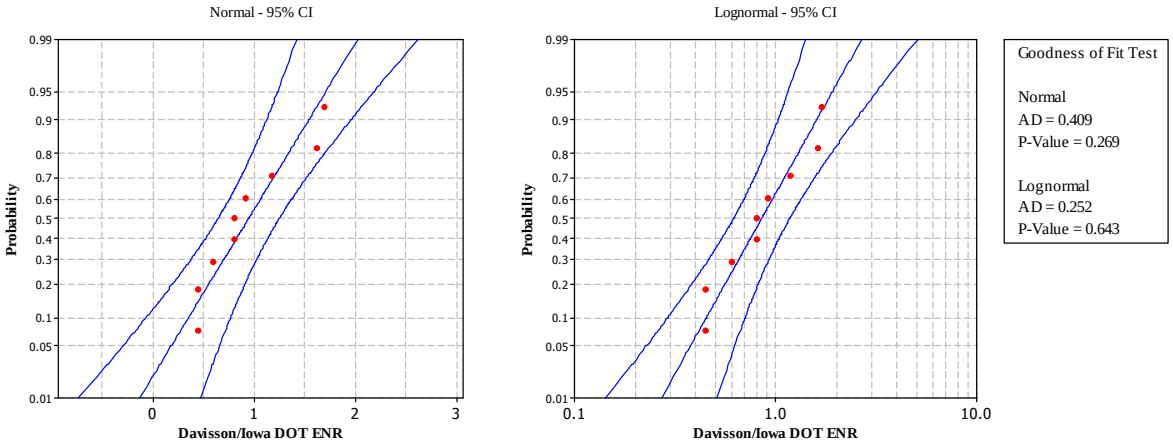

Figure 5.17: Anderson-Darling Goodness-of-Fit Test for the Iowa DOT Modified ENR Formula with the PILOT-IA Usable-Dynamic, Timber Pile Dataset

As indicated in Table 5.14, the assumption of a lognormal probability distribution for the various sample sets of resistance bias factors was accepted at the 5% significance level in all instances. Given this documented acceptance of the lognormal probability distribution for the various analyzed sample sets of resistance bias factors coupled with the assumed lognormal probability distributions for the dead and live load bias factors, Eq. (5.20) can be appropriately used for the calculation of LRFD resistance factors.

Before the calibrated LRFD resistance factors are presented, it is important to first discuss how each of the seven analyzed dynamic pile driving formulas compare in regards to prediction power and accuracy. Under the accepted assumption that the analyzed sample sets of resistance bias factors are lognormally distributed, the best-fit lognormal probability distributions were plotted for each method and can be observed in Figure 5.18.

By inspection of this figure it can be ascertained that the ENR dynamic pile driving formula produces a small value for both the mean and standard deviation of the resistance bias factor. This implies that the ENR formula has a tendency to overpredict the measured pile capacity, but to a fairly consistent degree. Conversely, the Gates, FHWA Modified Gates, Iowa DOT Modified ENR, Janbu, PCUBC, and WSDOT dynamic pile driving formulas produce a value for the mean of the corresponding resistance bias factors that is very close to one, but with larger standard deviation values. Consequently, these six formulas provide, on average, an accurate estimate of the measured pile capacity, but with a lesser degree of consistency.

Table 5.14: Summary of the Anderson-Darling Goodness-of-Fit Tests Carried Out on the Various Dynamic Pile Driving Formulas Used in Combination with the PILOT-IA Usable-Dynamic, Timber Pile Dataset

Soil Type	N	Dynamic Pile Driving Formula	Anderson-Darling Goodness-of-Fit Test							
			P_{Normal}	AD_{Normal}	$P_{Lognormal}$	$AD_{Lognormal}$	CV	Best Distribution	Normal Assumption	Lognormal Assumption
All	9	Gates	0.064	0.640	0.127	0.527	0.677	Lognormal	Accepted	Accepted
	9	FHWA Gates	< 0.005	1.207	0.233	0.432	0.677	Lognormal	Rejected	Accepted
	9	ENR	0.742	0.226	0.194	0.462	0.677	Normal	Accepted	Accepted
	9	Iowa DOT ENR	0.269	0.409	0.643	0.252	0.677	Lognormal	Accepted	Accepted
	9	Janbu	0.333	0.374	0.563	0.276	0.677	Lognormal	Accepted	Accepted
	9	PCUBC	0.426	0.333	0.657	0.248	0.677	Lognormal	Accepted	Accepted
	9	WSDOT	0.700	0.237	0.929	0.156	0.677	Lognormal	Accepted	Accepted

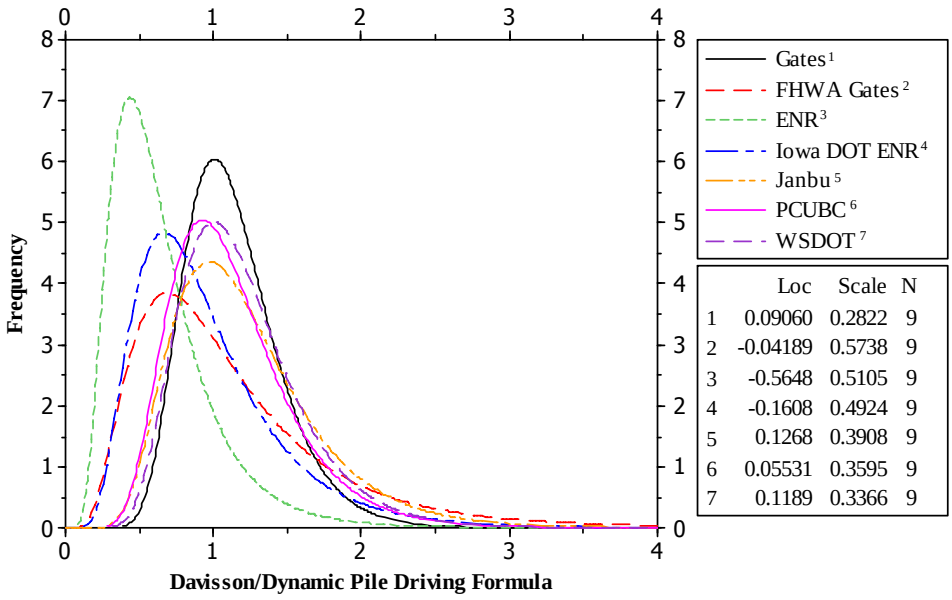

Figure 5.18: Summary of the Lognormally Distributed Resistance Bias Factors Using Seven Dynamic Pile Driving Formulas and the Clay Soil Subset of the PILOT-IA Usable-Dynamic, Steel H-Pile Dataset

5.3.2.3 Calibrated LRFD Resistance Factors

Using the statistical parameters determined in the previous section for the best-fit lognormal distribution to the various sample sets of resistance bias factors, the load factors and statistical parameters for the assumed lognormally distributed dead and live load bias factors presented in Section 5.2.3.1, a dead-to-live load ratio of two, and Eq. (5.20), LRFD resistance factors were calculated for each of the seven examined dynamic pile driving formulas at reliability indices of 2.33 and 3.00. Table 5.15 provides a summary of the calibrated LRFD resistance factors for the construction control of driven timber pile foundations via selected dynamic pile driving formulas.

As presented in Table 5.15, for a reliability index of 2.33, it was found that the Gates formula was the most efficient method for the construction control of timber piles driven into any type of soil profile. As was expected from the results of the comparative studies presented in Section 2.4, the ENR formula was shown to be one of the least efficient methods. Bearing in mind that the Iowa DOT Modified ENR formula is currently specified in the Iowa DOT's *Standard Specifications for Highway and Bridge Construction* manual as

the preferred dynamic pile driving formula for the construction control of driven pile foundations, it is important to point out that this formula is significantly less efficient, i.e., 35.2% less efficient, than the WSDOT formula at a reliability index of 2.33. Although timber piles are the second most frequently used pile type within the State of Iowa, this statistic should not skew the fact that, relative to steel H-piles, very few timber piles are actually driven for bridge foundations in any given year. Thus, seeing as the Iowa DOT Modified ENR formula was recommended for use with steel H-piles, it would seem acceptable to also recommend its use with timber piles in light of the aforementioned reality as well as for the maintenance of simplicity. Additionally, seeing as only a small sample size was available for the resistance factor calibrations presents in Table 5.15, the true population statistics for the various resistance bias factors may not have been adequately captured by the analyzed sample sets; thus, generating misleading results. The following section, however, will seek to address this specific issue.

Table 5.15: Final LRFD Resistance and Efficiency Factors for the Construction Control of Driven Timber Pile Foundations via Dynamic Pile Driving Formulas

Soil Type	N	Dynamic Formula	$\bar{\lambda}_R$	σ_{λ_R}	COV_{λ_R}	β = 2.33		β = 3.00	
						φ	$\varphi/\bar{\lambda}_R$	φ	$\varphi/\bar{\lambda}_R$
All	9	Gates	1.134	0.323	0.285	0.64	0.562	0.50	0.443
	9	FHWA Gates	1.140	0.870	0.763	0.23	0.203	0.14	0.126
	9	ENR	0.630	0.270	0.429	0.26	0.415	0.19	0.304
	9	Iowa DOT ENR	0.947	0.463	0.489	0.35	0.364	0.24	0.258
	9	Janbu	1.211	0.447	0.369	0.57	0.472	0.43	0.356
	9	PCUBC	1.118	0.389	0.348	0.55	0.494	0.42	0.377
	9	WSDOT	1.184	0.402	0.339	0.60	0.503	0.46	0.385

5.3.2.4 Sample Size Effects on Resistance Factors

As done in Section 5.3.1.4 for steel H-piles, a Monte Carlo simulation was performed using MATLAB™ to check the sample size of the PILOT-IA usable-dynamic, timber pile dataset on the variability of the LRFD resistance factors computed in the previous section. Focusing on the LRFD resistance factors calculated for the Iowa DOT Modified ENR

formula, a random sample of resistance bias factors was selected from the assumed distribution for the true population, which was formed using the statistical characteristics outlined in Table 5.15. From this random sample, which was chosen to be of the same size as the PILOT-IA usable-dynamic, timber pile dataset (9), the mean value and the coefficient of variation for the randomly selected resistance bias factors were determined. Then, using Eq. (5.20), the load factors and statistical parameters for the assumed lognormally distributed dead and live load bias factors presented in Section 5.2.3.1, a dead-to-live load ratio of two, and a reliability index of 2.33, a corresponding LRFD resistance factor was calculated. To replicate the random nature of the sample population, another random sample of resistance bias factors was selected from the assumed distribution for the true population. Upon computing the mean value as well as the coefficient of variation for this second set of randomly selected resistance bias factors, another LRFD resistance factor was calculated. Repeating this process a total of 1,000 times, a distribution of LRFD resistance factors was obtained for the Iowa DOT Modified ENR formula, as it is used for monitoring the driving of timber pile foundations. Figure 5.19 provides a summary of the results obtained from the formerly described Monte Carlo simulations.

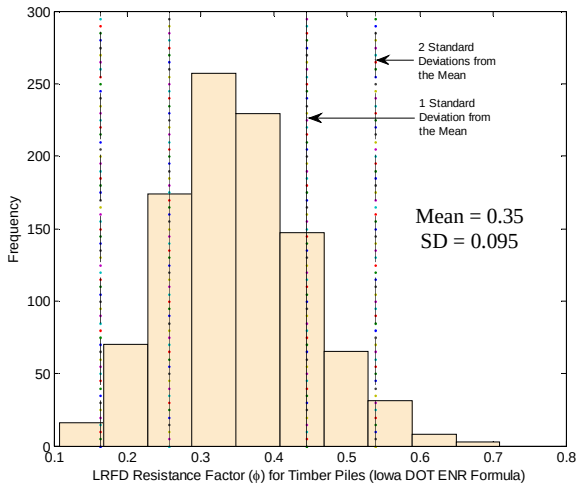

Figure 5.19: Variation in LRFD Resistance Factors for the Iowa DOT Modified ENR Formula used with Timber Pile Foundations

The distribution provided in this figure indicates a mean LRFD resistance factor value of 0.35. As was expected, this value compares quite favorably with the corresponding LRFD

resistance factor provided in Table 5.15. Using one standard deviation above and below the mean resistance factor as a measure of variability, it was observed that such variability is directly related to the coefficient of variation assumed for the true distribution of the resistance bias factor. In other words, if the true population statistics were to change from those assumed, a corresponding change in the variability of the computed LRFD resistance factors would be realized. However, since it must be assumed that the true population statistics have been correctly captured, the observed variability in the LRFD resistance factors can be used to determine whether or not the utilized sample size sufficiently captures the characteristics of the true population. As indicated in Figure 5.19, the one standard deviation bounds for the mean resistance factor were found to be (0.26, 0.46). Considering the fact that McVay, Birgisson, and Lee (2004) defined significant variability in computed LRFD resistance factors at the one standard deviation level to be about 0.15, it would be difficult to assume that the timber pile sample size available for the computation of LRFD resistance factors for the Iowa DOT Modified ENR formula effectively captures the characteristics of the true population, given that the observed variability is fairly close to this limit. As a consequence, the LRFD resistance and efficiency factors presented in Table 5.15 should be taken with caution until more information for driven and load tested timber pile foundations becomes available to further improve these results.

5.3.2.5 Comparison with Design Specifications

In the current edition of the *AASHTO LRFD Bridge Design Specifications*, resistance factors, developed for the EOD condition, are provided for the FHWA Modified Gates and ENR dynamic pile driving formulas. More specifically, resistance factors of 0.40 and 0.10 are recommended for use with the FHWA Modified Gates and ENR formulas, respectively. It is important to point out that these recommendations are provided without enhacement for particular pile types and/or soil profiles. In comparing these code recommended resitance factors with those recommended in Section 5.3.2.3, i.e., Table 5.15, an indication of the enhanced enconomy and dependability associated with regionally calibrated factors is evidenced. In other words, although it was advised in the previous section that the Iowa recommended resistance factors be taken with caution, what can be said about the comparisons made in Table 5.16 is that there exists a strong indication of the poor

dependability of the AASHTO (2007) recommended resistance factor for the FHWA Modified Gates formulawhen used with driven timber pile foundations. With only two of the 210 piles used for the calibration of the AASHTO (2007) recommended resistance factors being timber in type, it becomes quite clear that generalized resitance factors can lead to unsafe estimates of pile capacities when such generalizations are analyzed under much more stringent boundaries.

Table 5.16: Comparison of the Iowa (Timber) and AASHTO (2007) Recommended LRFD Resistance Factors for the FHWA Modified Gates, ENR, and Iowa DOT Modified ENR Formulas at a Reliability Index of 2.33

Soil Type	Dynamic Formula	Iowa Recommended Resistance Factor	AASHTO (2007) Recommended Resistance Factor	Economy Gain (%)
All	FHWA Gates	0.23	0.40	-43
	ENR	0.26	0.10	160
	Iowa DOT ENR	0.35	-	-10*

*Gain in economy over AASHTO's (2007) recommended value for the FHWA Gates formula

CHAPTER 6: A THEORETICAL DYNAMIC MODEL FOR PILE CAPACITY ESTIMATION

6.1 INTRODUCTION

Dynamic pile driving formulas have been criticized in many publications for their unsatisfactory prediction of pile capacity as summarized in Chapter 2. Most notably, in the FHWA's *Design and Construction of Driven Pile Foundations* workshop manual, Hannigan et al. (1998) writes:

> "Unfortunately, dynamic formulas have fundamental weaknesses in that they do not adequately model the dynamics of the hammer-pile impact, the influence of axial pile stiffness, or soil response. Dynamic formulas have also proven unreliable in determining pile capacity in many circumstances. Their continued use is not recommended on significant projects."

However, based on the efficiency factors determined in the previous chapter as well as those reported by AbdelSalam et al. (2010) for the Iowa Blue Book static analysis method, the Iowa DOT Modified ENR formula is just as efficient, if not more so, than the best performing static analysis method. On account of this observation, an investigation was undertaken with the objective of developing a means by which a more reliable, yet uncomplicated construction control method may be utilized for the design of driven pile foundations. This investigation was also intended to understand the discrepancies between the different dynamic formulas.

As developed in Chapter 2, for estimation of a driven pile's bearing capacity, typical dynamic pile driving formulas require knowledge of characteristics for the pile and the pile driving hammer as well as the observed permanent pile penetration under one hammer blow (i.e., pile set). Except for the pile set, values for all of these variables are available to an engineer in the design stages of a project. Consequently, for the successful use of a dynamic pile driving formula such as the Iowa DOT Modified ENR formula for the design of driven pile foundations, an accurate estimate or assumption of this pile set must be made. To accomplish this task, a one-dimensional pile-soil model, similar to that proposed by Smith (1962) and utilized by the Wave Equation Analysis Program (WEAP) a well as the CAse Pile Wave Analysis Program (CAPWAP), may be used. Furthermore, this process assumes that

additional parameters used to define the soil's dynamic characteristics can be quantified with sufficient accuracy in the design stages of a deep foundation project.

According to McVay and Kuo (1999), the best approach for determining these dynamic, or Smith, soil parameters is through the performance of CAPWAP analyses using PDA data. As a result, significant efforts were made towards the end of the twentieth century to compile numerical values of the CAPWAP estimated Smith soil parameters (McVay and Kuo 1999). However, the collected data exhibited a large degree of scatter and with no apparent trend as seen in the examples provided in Figure 6.1, making the establishment of empirical relations for the estimation of Smith's soil parameters practically impossible. Given that the purpose of a CAPWAP analysis is to determine the mobilized static capacity for a given pile through a trial and error signal (i.e., upward traveling force wave) matching technique, the actual Smith soil parameters of quake and damping used in a given analysis have a negligible effect on the end result (Svinkin 2004), which explains the large scatter and non-uniqueness of these parameters witnessed by McVay and Kuo (1999).

In an effort to improve the uniqueness of a CAPWAP analysis and, correspondingly, the estimated Smith soil parameters for a given set of conditions, a displacement-based signal matching procedure derived from the theory of structural dynamics is investigated in this chapter. Based upon the results obtained from this procedure on two steel H-piles driven in predominantly clay soil profiles, the ability to establish improved empirical relations for Smith's soil parameters is assessed, ultimately enabling for an improved approach concerning the use of a one-dimensional pile-soil model for the estimation of pile set.

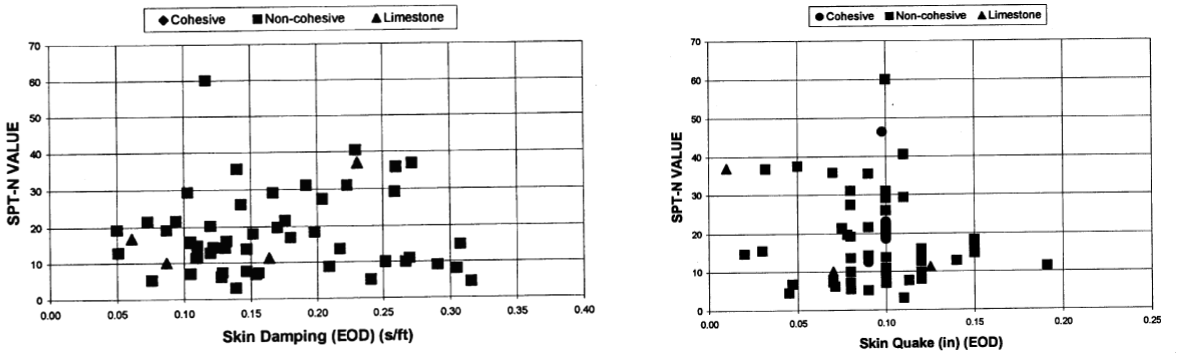

Figure 6.1: SPT-N Values versus Shaft Soil Damping Factors (Left) and Shaft Soil Quake Values (Right) from McVay and Kuo (1999)

6.2 BACKGROUND

6.2.1 One-Dimensional Pile-Soil Model

As expressed in the preceding section, the simplest way to predict the permanent displacement of a pile under the influence of a single hammer blow is through the use of a one-dimensional pile-soil model, like that proposed by Smith (1962). Illustrated in Figure 6.2, such a model assumes that the pile can be discretized into a finite number of lumped masses connected together by linear elastic spring and dashpot elements. These linear elastic spring elements defining the pile stiffness are characterized by the following spring constant:

$$k_{pi} = \frac{AE}{L_i} \tag{6.1}$$

where: k_{pi} = spring constant for the ith pile segment,
A = cross-sectional area of the pile,
E = modulus of elasticity of the pile material, and
L_i = length of the ith pile segment.

Unlike pile stiffness, pile damping does not significantly influence the dynamic response of the pile-soil system during driving because this structural related damping is assumed to produce relatively small energy losses when compared to the damping provided by the surrounding soil (Pile Dynamics, Inc. 2005). However, to model the pile as realistic as possible, a linear dashpot element characterized by the following viscous damping coefficient is typically used:

$$c_{pi} = 2\xi\sqrt{k_{pi}m_{pi}} \tag{6.2}$$

where: c_{pi} = viscous damping coefficient for the ith pile segment,
ξ = pile damping ratio; assumed to be about 1% for steel, 2% for concrete, and 3% for timber pile materials (Pile Dynamics, Inc. 2000), and
m_{pi} = mass of the ith pile segment.

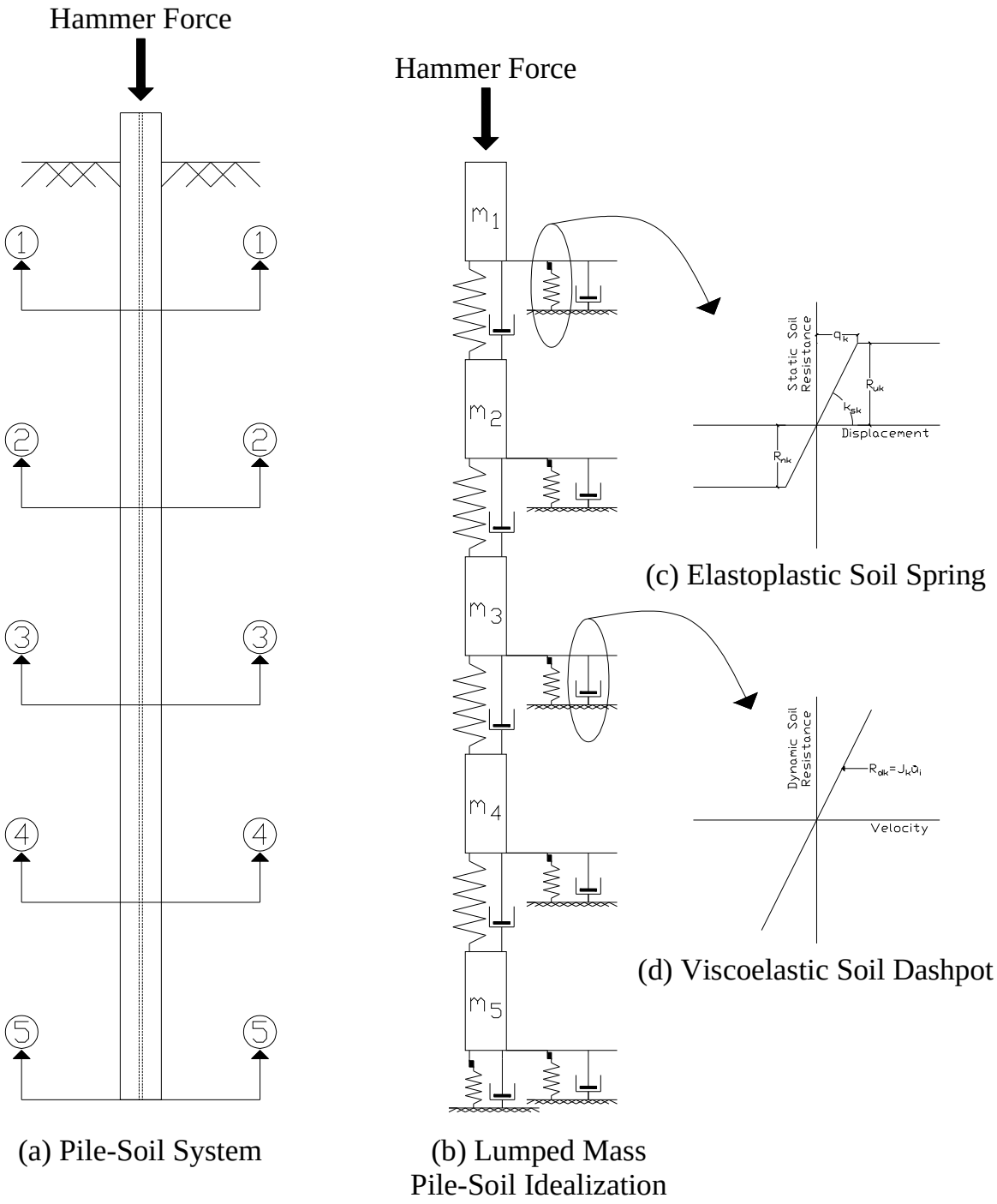

Figure 6.2: One-Dimensional Pile-Soil Idealization for Dynamic Analyses

Moreover, the pile-soil model depicted in Figure 6.2 assumes that the soil located along the pile shaft as well as that at the pile toe can be idealized by elastoplastic spring and

linear dashpot elements connected to the lumped mass points defining the pile. These elastoplastic spring elements defining the static soil resistance are pile displacement dependent and defined by the quantities q_k, R_{uk}, and R_{nk}, where q_k is the soil quake or maximum elastic soil deformation in the direction of installation for the kth soil segment, R_{uk} is the ultimate static soil resistance in the direction of installation for the kth soil segment, and R_{nk} is the ultimate static soil resistance in the direction opposite the installation direction for the kth soil segment. This cyclic behavior leads to a form of damping conveniently referred to as hysteretic damping. Such damping is assumed to be independent of the rate of loading and is solely defined by the relative displacement resulting from the pile-soil interaction mechanism. It is important to point out that R_{nk} will always be zero for the spring modeling the soil located at the pile toe to reflect the inability of end-bearing soil to provide tensile resistance. Additionally, Smith (1962) recommends a quake value equal to 0.10 inches for soils of any type located along the shaft of the pile as well as at the pile toe.

The dynamic soil resistance is handled by the linear dashpot elements, which are pile velocity dependent and defined by the following equivalent viscous damping coefficient:

$$c_{sk} = J_{sk} R_{uk} \tag{6.3}$$

where: c_{sk} = equivalent viscous damping coefficient for the kth soil segment, and

J_{sk} = Smith damping factor for the kth soil segment.

This equivalent viscous damping coefficient attempts to account for the viscous as well as the radiation, or inertial, damping of the soil. In essence, these viscoelastic dashpot elements attempt to model the increase in resistance provided under a rapidly applied displacement as compared to a slowly applied displacement. It is important to point out that as a pile is driven downward, the soil under the pile toe is displaced or caused to flow aside very rapidly. However, the soil alongside the pile is not correspondingly displaced. This implies that the value of J_{sk} for soil located along the pile shaft should be smaller than the value of J_{sk} for soil located beneath the pile toe. Hence, Smith (1962) recommends damping factors of 0.05 s/ft and 0.15 s/ft for soil located along the pile shaft and beneath the pile toe, respectively.

6.2.2 CAPWAP Signal Matching Technique

With measurements of pile top acceleration and force available at any given hammer blow from PDA, both input to and response of the pile top for a one-dimensional pile-soil model, like that presented in the previous section, are known. However, the soil portion of the pile-soil system, which dictates the measured response, is unknown. In order to calculate the static as well as the dynamic properties of the soil, a back-analysis must be performed, in which the unknown soil model parameters are quantified. This back-analysis, or signal matching analysis, requires an iterative procedure to converge at the solution. In other words, an assumption is first made of the unknown soil parameters and successively improved by performing an analysis using a one-dimensional pile-soil model with the measured force history as a pile top boundary condition. It is important to point out that in the CAPWAP signal matching procedure, one quake value and one Smith damping factor are used to characterize the soil located along the entire pile shaft regardless of the variation in the soil profile, but separate quake and Smith damping factor values are used for soil located beneath the pile toe. If there is disagreement between the measured upward traveling force wave and its calculated counterpart, then the procedure is repeated with the improved soil parameters. The upward traveling force wave, which is obtained from both force and velocity measurements, is defined as follows (Pile Dynamics, Inc. 2000):

$$F_{WU} = \frac{F(t) + Z\dot{u}(t)}{2} \tag{6.4}$$

where: F_{WU} = upward traveling force wave,

$F(t)$ = measured pile top force at time t,

$Z = \frac{EA}{c}$ = pile impedance,

$c = \sqrt{\frac{E}{\rho}}$ = wave speed,

ρ = mass density of the pile material, and

$\dot{u}(t)$ = measured pile top velocity, obtained from integration of the measured acceleration time history, at time t.

Obviously, the more realistic the soil model is, the more accurate the model will be in matching the measured quantities. On the other hand, a very sophisticated model may have too many unknowns and may not be uniquely defined by the matching process (Rausche, Robinson, and Liang 2000). For that reason, Smith's (1962) soil model, as presented in the preceding section, has been employed for CAPWAP's signal matching technique.

As pointed out by Rausche, Robinson, and Liang (2000), an important part of the CAPWAP signal matching procedure is the evaluation of the match quality, i.e., quantifying the difference between the measured and computed pile top quantities. In CAPWAP, the match quality is the normalized, weighted sum of the absolute values of the differences between computed and measured values of all analyzed time steps. Normalization is achieved with respect to both the maximum pile top force and the number of data points used. The match over a 3 millisecond time period, following the first return of the stress wave from the pile toe, is given a double weight because of its importance in determining the total pile capacity. Consequently, a satisfactory match quality may, in fact, correspond to a match that has failed to correctly or uniquely quantify the remaining soil model parameters, i.e., the quake values and Smith damping factors for soil located both along the pile shaft and beneath the pile toe, besides the fact that it cannot be realistically expected that the quake values and Smith damping factors will remain constant with increasing depth below the ground surface (Tomlinson 1971).

6.3 DISPLACEMENT-BASED SIGNAL MATCHING TECHNIQUE

Rausche, Robinson, and Liang (2000) suggested that it is reasonable to require that the CAPWAP signal matching process also produces a match of the measured and calculated pile top set, assuming that the PDA measured acceleration records can be satisfactorily doubly integrated to obtain the measured displacement histories. However, as will be shown in the following section, an acceptable wave-up (i.e., Eq. (6.4)) match does not always correlate to a match of the measured and computed pile top displacement histories due to inaccurately defined soil hysteretic and equivalent viscous damping parameters. To improve upon this reality and the fact that the current CAPWAP signal matching process places little emphasis on the soil quake values and Smith damping factors, a displacement-based signal matching technique is proposed.

When performing a CAPWAP signal matching analysis, the rationale behind changing such soil related parameters as the quake values and Smith damping factors is not at all intuitive given that the matching is done against a measured and computed upward traveling pile force wave. A more instinctive approach would be to look at matching the measured and computed pile top displacement histories given that soil quake values and Smith damping factors are more closely related to the displacement of the pile and not the force within the pile. For instance, an increase in the soil quake values decreases the elastic stiffness of the soil and causes the pile to undergo a more rapid penetration, i.e., increasing the rate of penetration. Additionally, by attempting to match the measured and computed pile top displacement time histories in entirety, as opposed to placing significant emphasis on a small portion of the response as is done in the CAPWAP signal matching process, an accurate quantification of the soil behavior under displacements imposed opposite to the loading direction can be obtained.

Derived using the theoretical concepts most commonly associated with the dynamic behavior of structural elements subjected to an impulsive loading, the proposed displacement-based signal matching technique begins by first assuming that the distribution of the static soil resistance at the EOD follows that provided by Schmertmann's (1978) correlated CPT sleeve friction and tip resistance data. This assumption eliminates a significant number of unknowns from the analysis and is an efficient estimation method for the ultimate static soil resistance as confirmed by comparisons conducted by Yoon et al. (2008).

The next step in the proposed signal matching process requires a breakdown of the typical pile top force history that is obtained from PDA measurements and input into a one-dimensional pile-soil model as a pile top boundary condition. As illustrated in Figure 6.3, a pile top force history is typically characterized by two successive impulsive loadings. The first impulsive loading results from the pile driving hammer impacting the pile head, while the successive impulsive loading results from the pile head rebounding and striking the pile driving hammer. If an emphasis is placed on the first impulsive loading, soil quake values can be quantified within this time duration to produce a match of the measured and computed pile top displacement time histories since damping mechanisms will not have had a chance to

respond. However, by the time the second impulsive load is applied, damping mechanisms will have had a chance to respond and influence the pile top displacement time history. Thus, after a successful match of the measured and computed pile top displacement time histories within the time interval of the first impulsive load has been achieved, Smith damping factors as well as ultimate static soil resistances for pile displacements opposite the installation direction can be quantified for each soil segment to complete the match of the measured and computed pile top displacement time histories.

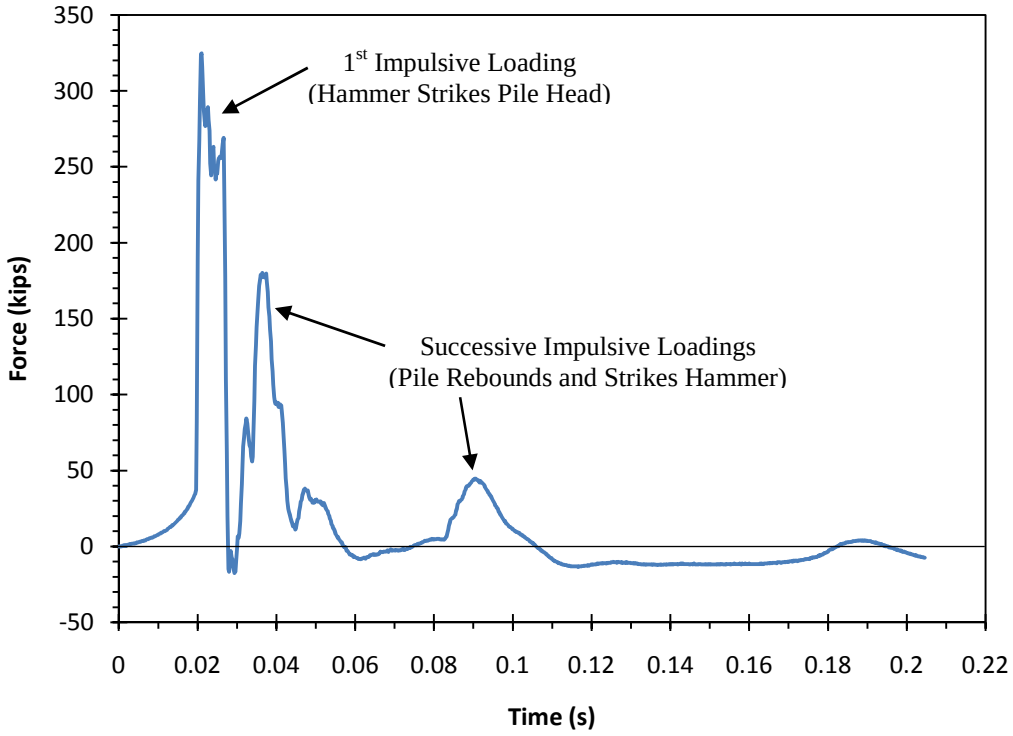

Figure 6.3: Pile Top Force History Obtained from ISU3 PDA Measurements at the EOD Condition (Blow Number 273)

To further elaborate on how soil parameters characteristic of specific soil segments in the pile-soil model are individually altered to provide the best possible match, a brief introduction to how wave propagation takes place in a pile element is first given. As a stress wave propagates along a pile, wave reflections are generated by changes in pile cross-sectional area, soil resistance forces along the shaft, and the pile toe resistance. Thus, the exact influence of any of these three wave reflection mechanisms can be located on a pile top

time history response plot by simply considering the distance between the pile top and the location of the wave reflection mechanism as well as the speed at which waves travel within the pile material. In other words, a stress wave originating at the pile head will travel to a specific wave reflection mechanism in a time period given by the following expression:

$$t = \frac{L}{c} \tag{6.5}$$

where: L = distance from the pile head to the wave reflection mechanism of interest, and
c = pile wave speed as defined previously.

Therefore, the influence of the specified wave reflection mechanism on the response of the pile top will be apparent at a time interval twice that determined by Eq. (6.5). Using this theoretical concept, soil parameters characteristic of specific soil segments can be individually adjusted using the proposed displacement-based signal matching technique by calculating the corresponding wave reflection times and locating them on the pile top displacement time history plot, where it is typically assumed that the time at which the maximum pile top velocity is achieved corresponds to the origination of the induced stress wave.

6.4 VERIFICATION RESULTS AND DISCUSSION

6.4.1 ISU3 EOD Condition

To verify the proposed displacement-based signal matching technique, the one-dimensional pile-soil model of Figure 6.2 was created in SAP2000, a professional finite element analysis program (Computers & Structures, Inc. 2008), for the ISU3 test pile at the EOD condition. The pile was discretized into 31 mass points connected by linear elastic spring and dashpot elements defined by a spring constant and damping coefficient of 16170 kip/in and 0.0367 kip-s/in (1% pile material damping ratio), respectively. The soil located along the pile shaft, which was mainly cohesive in nature, was discretized into thirteen segments and modeled by multi-linear plastic spring elements, with a kinematic hysteresis rule, and linear dashpot elements connected to alternating lumped pile mass points beginning at the pile toe. Similarly, the soil located beneath the pile toe, which again was cohesive in

nature, was modeled using the same multi-linear plastic spring and linear dashpot elements connected to the lumped pile mass point corresponding to the pile toe.

Using Schmertmann's (1978) correlated CPT sleeve friction and tip resistance data to arrive at the ultimate, static soil resistance distribution under both directions of loading (Figure 6.4) for this specific pile embedment condition and Smith's (1962) recommended soil quake values and damping factors, the pile top force history of Figure 6.3 was imposed as a boundary condition and the displacement-based signal matching technique outlined in the previous section was carried out using a non-linear, direct integration analysis with a time step of 0.0001 seconds to generate the computed pile top displacement time histories. A summary of the soil parameters associated with the best match of the pile top displacement time history depicted in Figure 6.5 has been provided in Table 6.1.

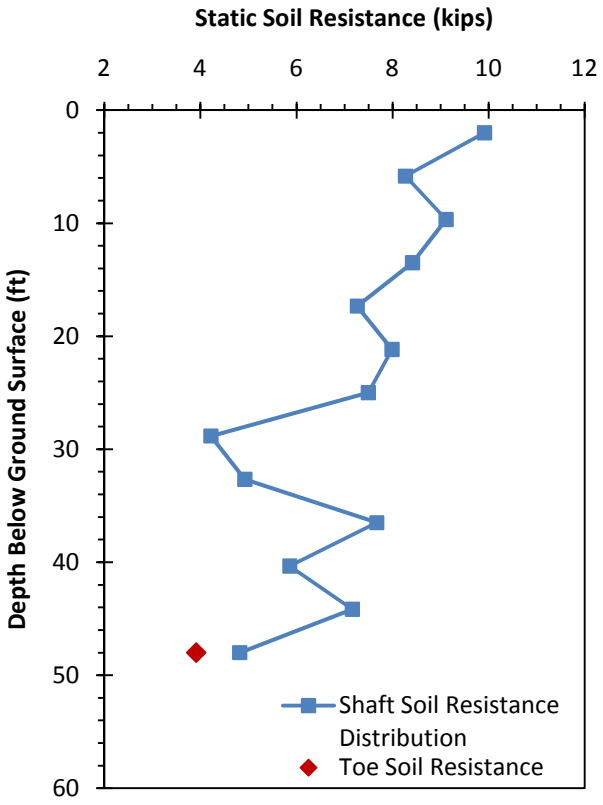

Figure 6.4: CPT Correlated Ultimate, Static Soil Resistance Distribution for ISU3 at EOD Condition

Table 6.1: Soil Model Parameters for the Best Match of Computed to Measured Pile Top Displacement Histories for ISU3 at EOD Condition

Shaft Soil Segment	Depth Below Ground Surface (ft)	R_{uk} (kips)	R_{nk} (% of R_{uk})	q_k (in)	J_{sk} (s/ft)
1	2.0	9.92	10	0.25	0.0309
2	5.8	8.27	10	0.25	0.0383
3	9.7	9.11	10	0.25	0.0481
4	13.5	8.41	10	0.20	0.0720
5	17.3	7.27	15	0.20	0.0841
6	21.2	7.99	15	0.20	0.0840
7	25.0	7.50	15	0.20	0.0961
8	28.8	4.22	10	0.15	0.1079
9	32.7	4.92	15	0.10	0.1080
10	36.5	7.67	15	0.05	0.1439
11	40.3	5.86	15	0.05	0.1440
12	44.2	7.16	15	0.05	0.1585
13	48.0	4.82	15	0.05	0.1582
Toe	48.0	3.91	0	0.30	0.2699

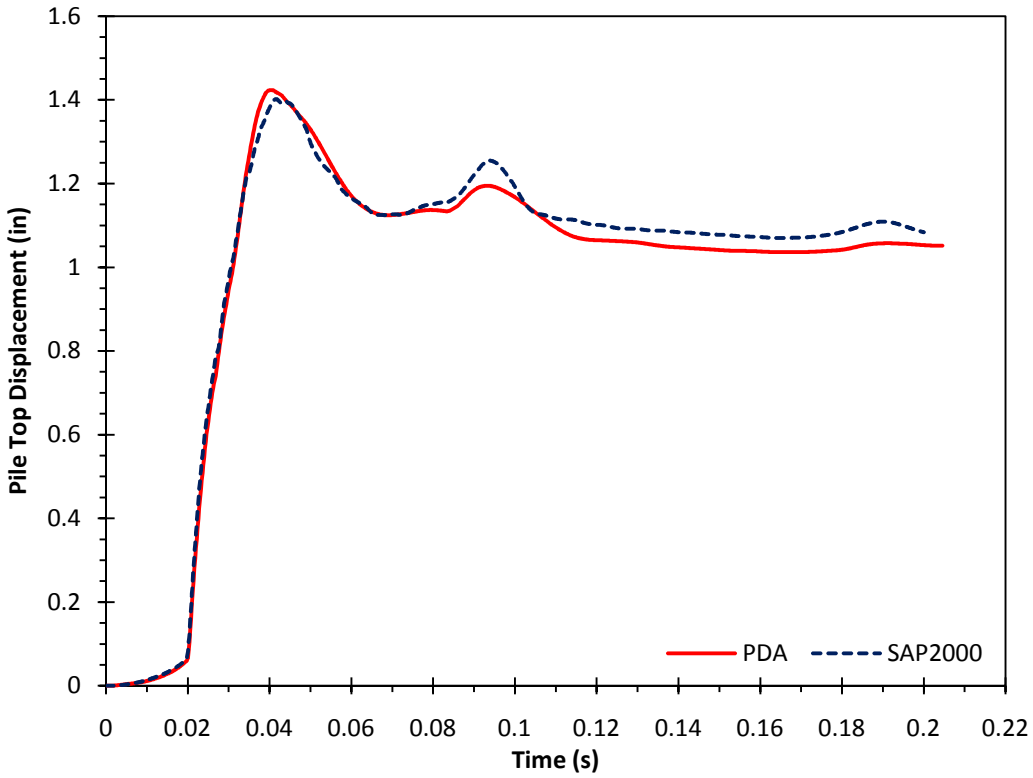

Figure 6.5: Best Match of Computed to Measured Pile Top Displacement Histories for ISU3 at EOD Condition

As further validation of the displacement-based signal matching technique, the upward traveling force wave time history computed at the pile head using the best match soil parameters found in Table 6.1, was compared against that measured by PDA and that computed by a CAPWAP analysis with a match quality of 3.72, where q_k is 0.27 inches and 0.06 inches for soil located along the pile shaft and beneath the pile toe, respectively, J_{sk} is 0.122 s/ft and 0.158 s/ft for soil located along the pile shaft and beneath the pile toe, respectively, R_{nk} is 10 percent of R_{uk} for soil located along the pile shaft, and the distribution of R_{uk} is as depicted in Figure 6.6. The results of this comparison, as presented in Figure 6.7, clearly show that the proposed displacement-based signal matching technique also provides for an acceptable match of the upward traveling force wave induced at the pile top. In fact, one could argue that the match achieved through the displacement-based signal matching procedure is better than that attained from the CAPWAP analysis.

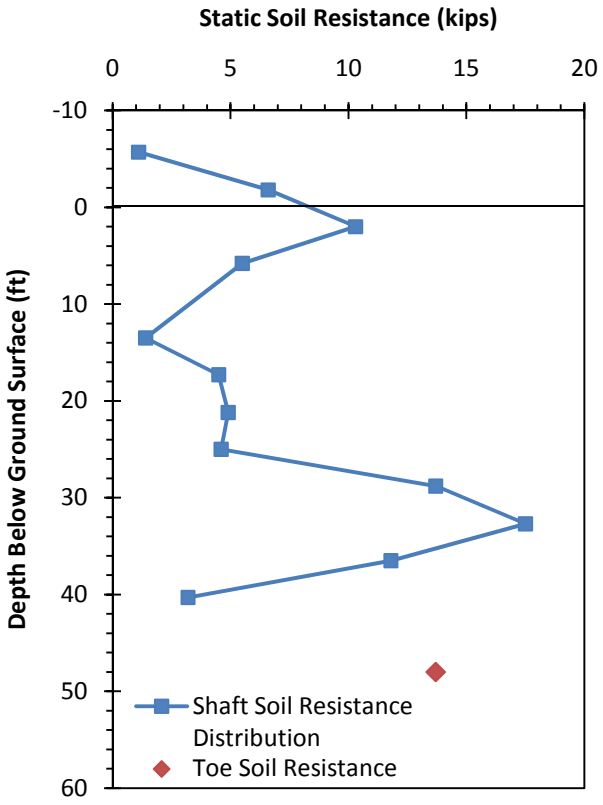

Figure 6.6: Ultimate, Static Soil Resistance Distribution Obtained from CAPWAP Signal Matching Analyses for ISU3 at EOD Condition

In comparing the shaft soil quake values and Smith damping factors computed by the displacement-based signal matching procedure in SAP2000 with those computed by the CAPWAP signal matching procedure, significant differences are observed, as seen in Figure 6.8. As pointed out previously, the CAPWAP analysis assumes a constant shaft soil quake value and Smith damping factor with increasing depth below the ground surface. As a result of the displacement-based signal matching procedure, a more realistic variation of the shaft soil quake values and Smith damping factors with increasing depth below the ground surface is achieved. In other words, it should be expected that as one moves deeper into a given soil profile the shaft soil quake values will decrease on account of the increasing overburden pressure. Likewise, the Smith damping factors for the shaft soil model can reasonably be expected to increase with increasing depth below the ground surface on account of the increase in soil stiffness provided by the decreasing shaft soil quake values.

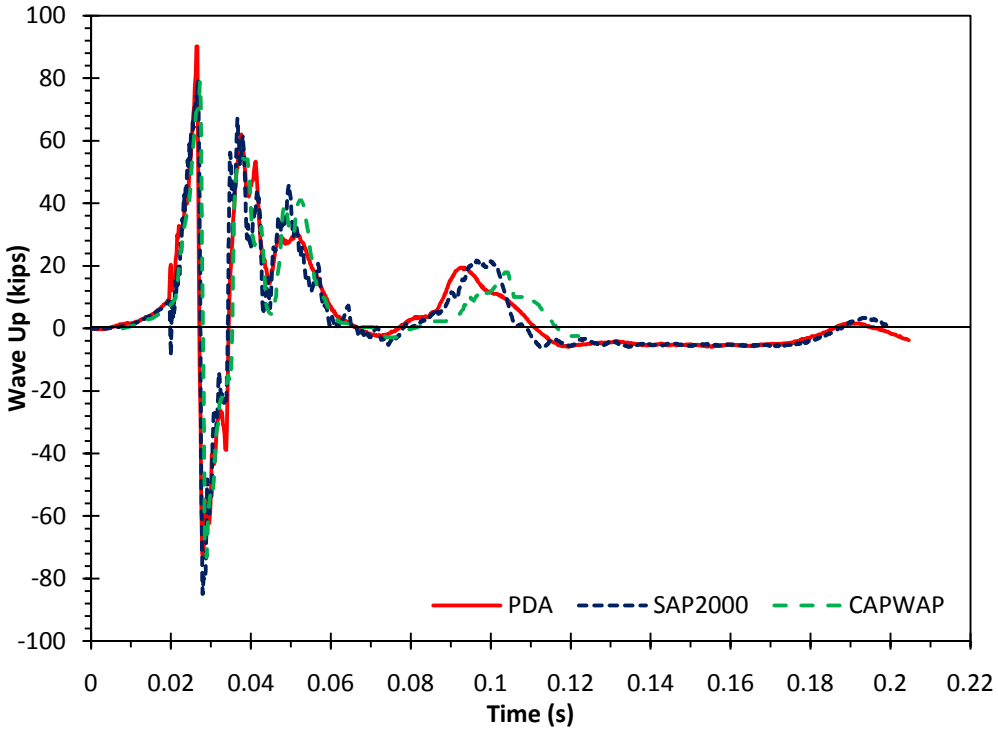

Figure 6.7: ISU3 EOD Wave-Up Comparison

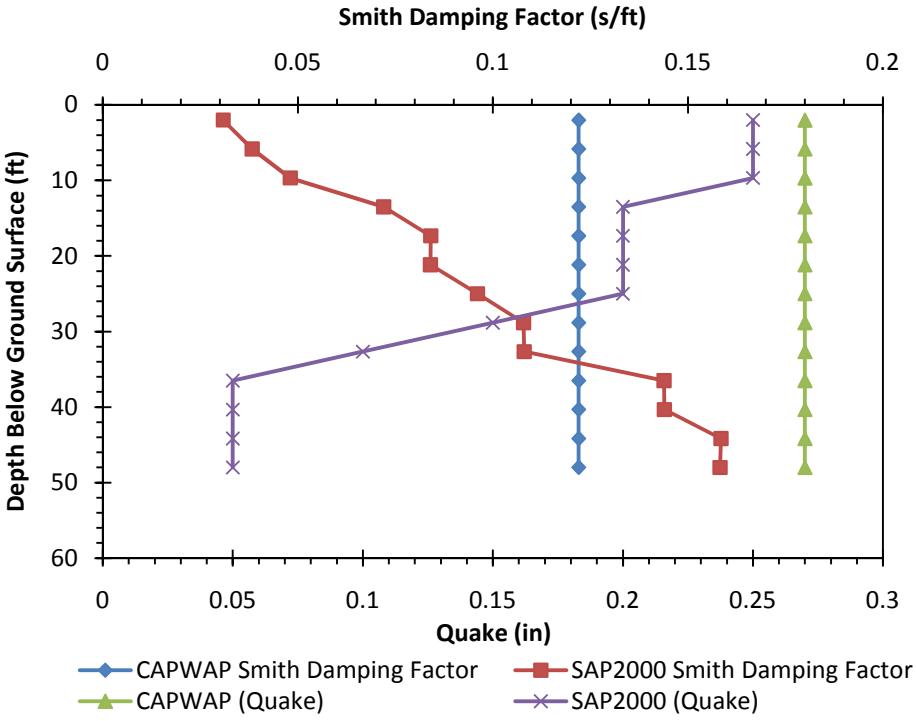

Figure 6.8: Shaft Soil Quake Values and Smith Damping Factors Comparison for ISU3 EOD Signal Matching Analyses Conducted by CAPWAP and SAP2000

Nonetheless, it is interesting to point out that although the Smith damping factor obtained from the CAPWAP analysis for the shaft soil model is somewhat comparable to the average value obtained from the displacement-based signal matching process, the CAPWAP obtained shaft soil quake value is exceedingly different from the average value obtained via the displacement-based signal matching process. One would expect that for such similar wave-up matches as those presented in Figure 6.7, the aforementioned comparisons would hold true. Given that this is not the case, the inefficiency of the CAPWAP signal matching technique in accurately and/or uniquely quantifying the soil quake values and Smith damping factors is again demonstrated.

6.4.2 ISU3 Partial Embedment Condition

To ensure the reproducibility of the proposed displacement-based signal matching technique, an earlier stage of embedment for the ISU3 test pile was first analyzed. Using the same pile model defined previously for the EOD condition and a soil model characterized by the parameters listed in Table 6.1 for a corresponding total pile embedded length of 25 feet,

the pile top force history of Figure 6.9 was imposed as a boundary condition and the proposed displacement-based signal matching technique was enacted upon the newly defined one-dimensional pile-soil model in SAP2000, using a non-linear, direct integration analysis with a time step of 0.0001 seconds to generate the computed pile top displacement time histories. A summary of the soil parameters associated with the best match of the pile top displacement time history depicted in Figure 6.10 has been provided in Table 6.2. Additionally, Figure 6.11 has been provided to show the comparison between the upward traveling force wave time history computed at the pile head using the best match soil parameters found in Table 6.2 with that measured by the PDA hardware product.

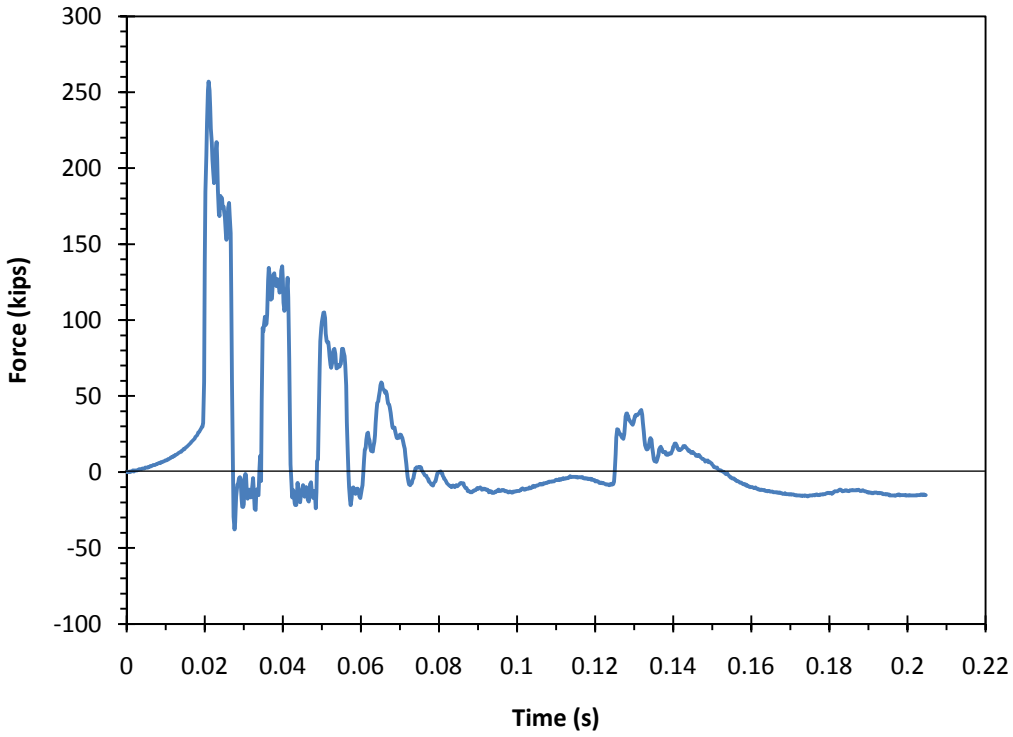

Figure 6.9: Pile Top Force History Obtained from ISU3 PDA Measurements at a 25 ft Embedment Condition (Blow Number 78)

Table 6.2: Soil Model Parameters for the Best Match of Computed to Measured Pile Top Displacement Histories for ISU3 at a 25 ft Embedment Condition

Shaft Soil Segment	Depth Below Ground Surface (ft)	R_{uk} (kips)	R_{nk} (% of R_{uk})	q_k (in)	J_{sk} (s/ft)
1	2.0	10.43	10	0.25	0.0162
2	5.8	8.59	12.5	0.25	0.0162
3	9.7	9.51	20	0.15	0.0163
4	13.5	8.82	35	0.15	0.0162
5	17.3	7.88	35	0.05	0.0161
6	21.2	8.78	35	0.05	0.0161
7	25.0	6.00	30	0.05	0.0116
Toe	25.0	2.00	0	0.10	0.0434

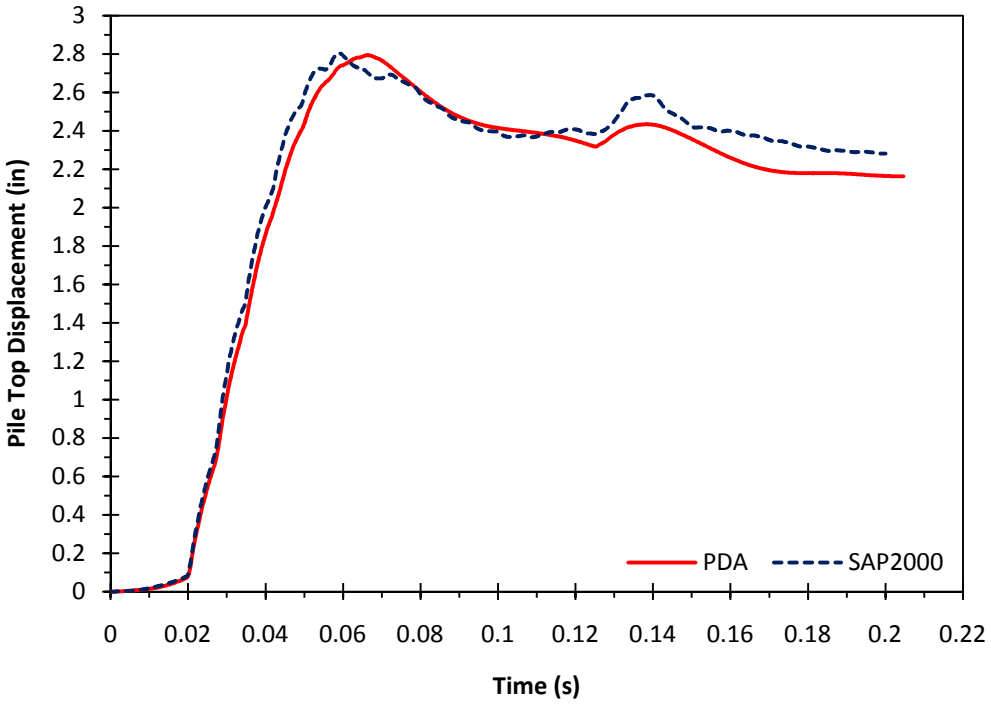

Figure 6.10: Best Match of Computed to Measured Pile Top Displacement Histories for ISU3 at a 25 ft Embedment Condition

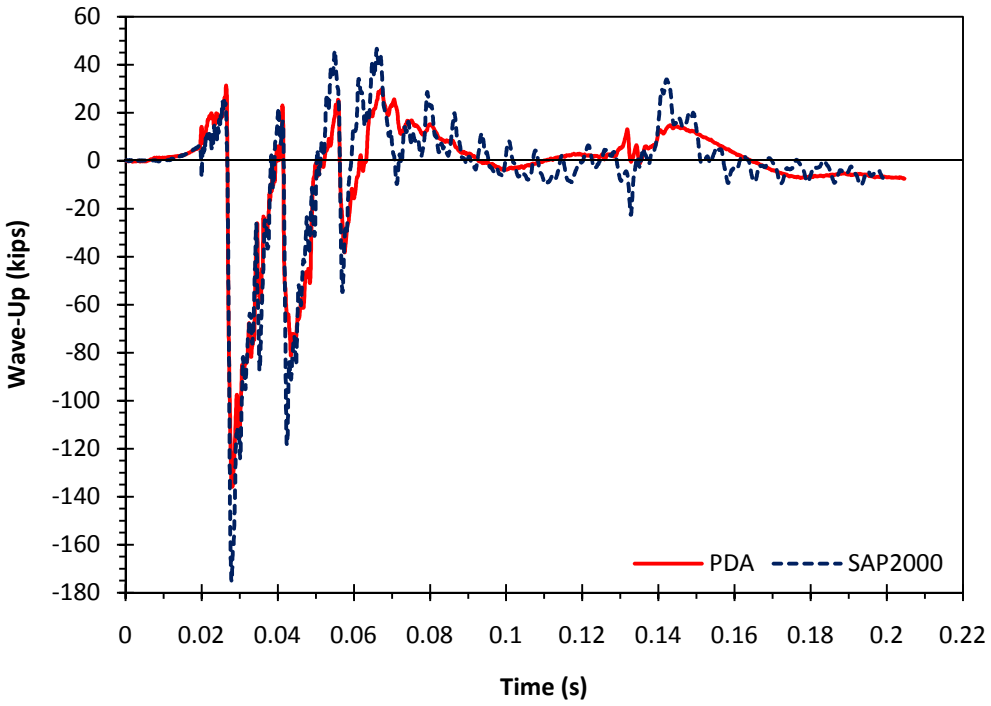

Figure 6.11: Measured and Calculated Wave-Up Comparison for ISU3 at 25 ft Embedment Condition

As evidenced by the results presented in Table 6.2, Figure 6.10, and Figure 6.11, the same conclusions drawn for the EOD analysis generally hold for this 25 foot embedment stage analysis. However, a few additional comments must be made regarding comparisons between the results obtained for the two separate stages of embedment. First, the Smith damping factors obtained for the 25 foot embedment condition are of smaller magnitude than those determined for the EOD condition. In other words, since the pile undergoes much larger displacements for the earlier stage of embedment, more energy is dissipated through hysteretic damping, thus dissipating a relatively low percentage of the input energy through equivalent viscous damping. That is to say, the magnitude of the Smith damping factor is dependent upon the stage of embedment.

Furthermore, if one looks closely at the parameters defining the soil hysteretic behavior in Table 6.1 and Table 6.2, a degradation of the shaft resistance and quake values corresponding to pile penetration depth is observed. To more easily view this degradation, the soil hysteretic behaviors at the 25 foot and 48 foot embedment conditions for shaft soil springs one and six have been provided in Figure 6.12 and Figure 6.13, respectively. As

illustrated in these figures, the observed degradation is more severe for shaft soil spring six than for shaft soil spring one because the soil corresponding to soil spring six for the 25 foot pile embedment condition is in a nearly virgin state of disturbance. Although insufficient data is available to accurately determine the relationship between the hysteretic behavior of the shaft soil resistance with pile embedment depth, what can be said is that when a soil segment (i.e., soil spring six) in a near virgin state is subjected to approximately 205 hammer blows, the ultimate, static resistance and quake values defining the soil hysteretic behavior degrade by approximately 9% and 300%, respectively. Similarly, when a soil segment (i.e., soil spring one), having already been subjected to nearly 71 hammer blows, is subjected to an additional 196 hammer blows, the ultimate, static resistance and quake values defining the soil hysteretic behavior degraded by only about 5% and 0%, respectively.

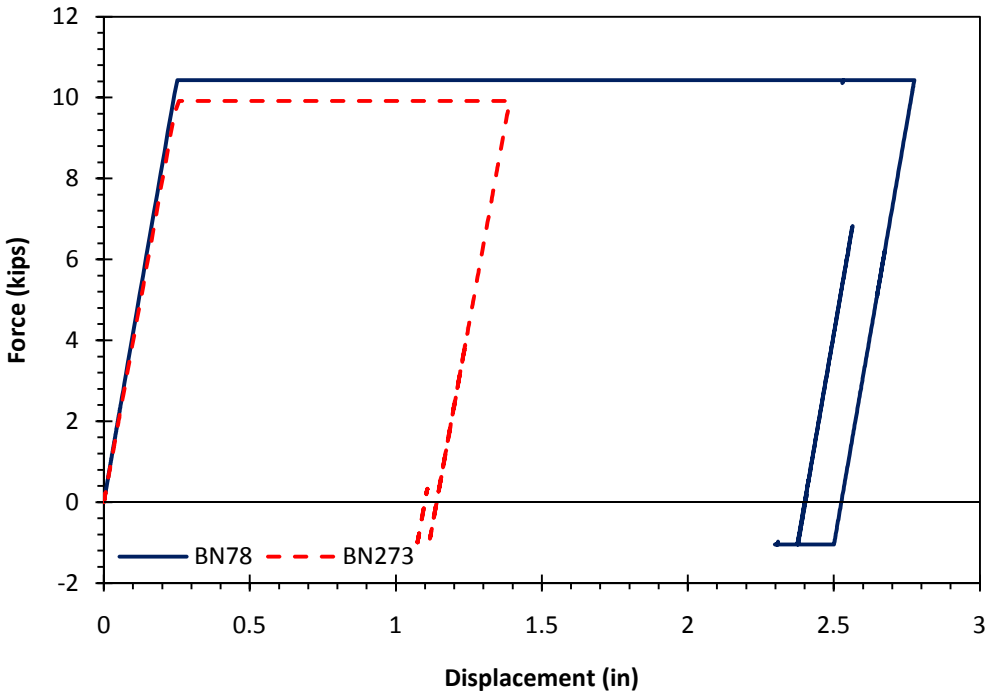

Figure 6.12: Theoretically Established Shaft Soil Spring #1 Hysteretic Responses for the 25 ft and 48 ft Embedment Conditions

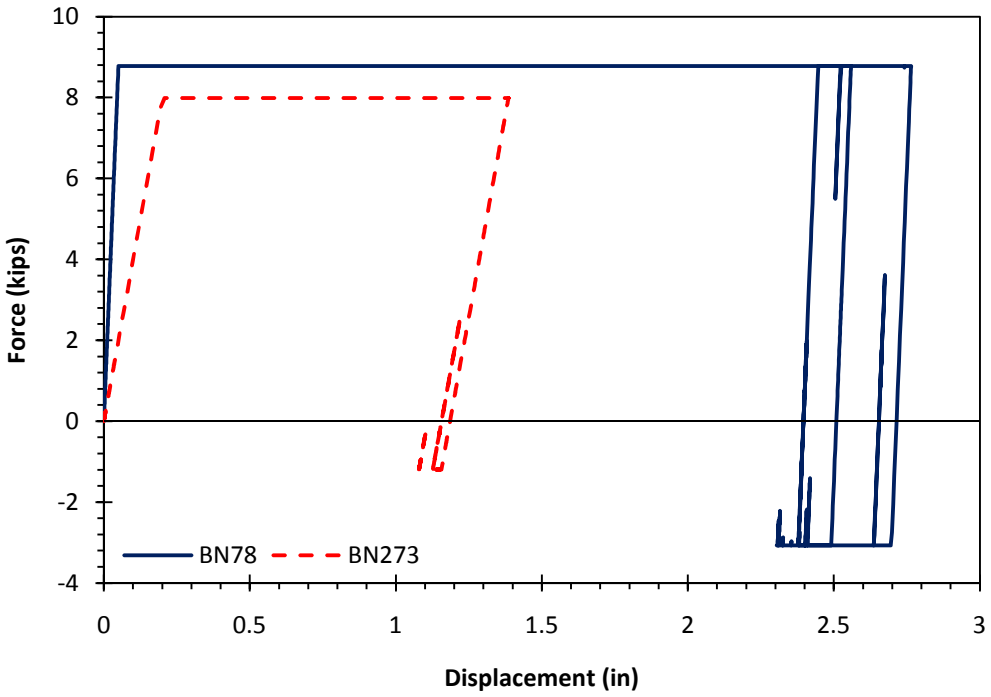

Figure 6.13: Theoretically Established Shaft Soil Spring #6 Hysteretic Responses for the 25 ft and 48 ft Embedment Conditions

6.4.3 ISU5 EOD Condition

To independently verify the proposed displacement-based signal matching technique, the EOD condition for the ISU5 test pile was analyzed. Using the same pile model defined previously for the ISU3 EOD condition, Schmertmann's (1978) correlated CPT sleeve friction and tip resistance data, which were used to obtain the ultimate, static soil resistance distribution under both directions of loading (Figure 6.14) for this specific pile embedment condition, and Smith's (1962) recommended soil quake values and damping factors, the pile top force history of Figure 6.15 was imposed as a boundary condition and the proposed displacement-based signal matching technique was enacted on the newly created one-dimensional pile-soil model in SAP2000, using a non-linear, direct integration analysis with a time step of 0.0001 seconds to generate the computed pile top displacement time histories. A summary of the soil parameters associated with the best match of the pile top displacement time history depicted in Figure 6.16 has been provided in Table 6.3.

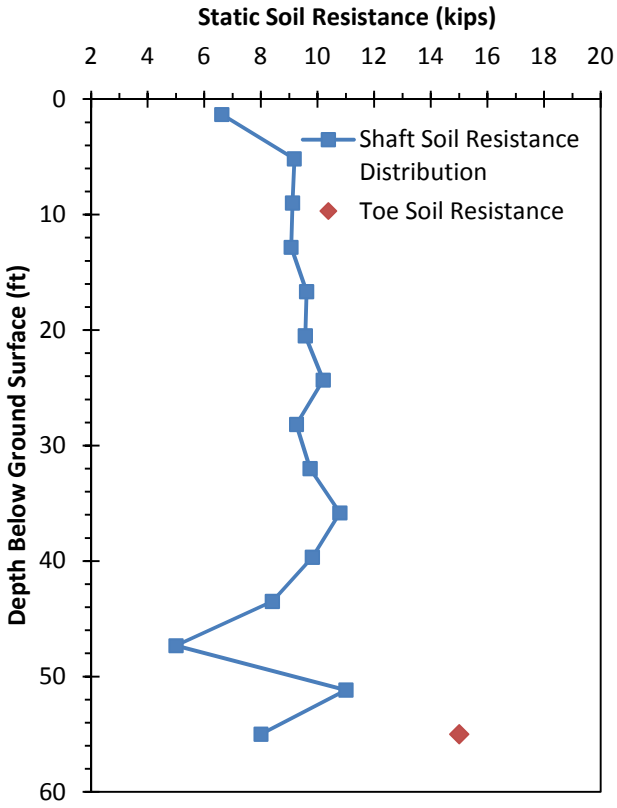

Figure 6.14: CPT Correlated Ultimate, Static Soil Resistance Distribution for ISU5 at EOD Condition

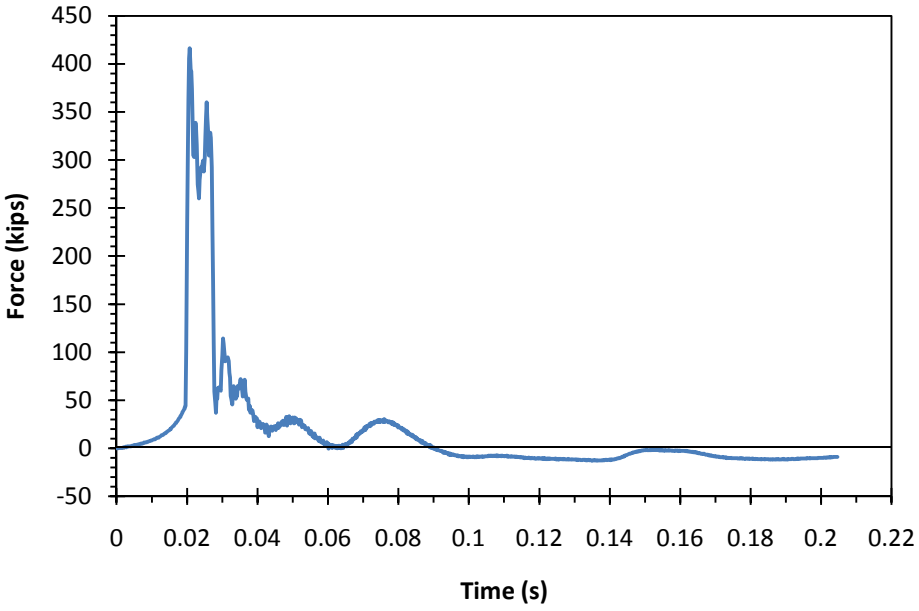

Figure 6.15: Pile Top Force History Obtained from ISU5 PDA Measurements at EOD Condition (Blow Number 602)

Table 6.3: Soil Model Parameters for the Best Match of Computed to Measured Pile Top Displacement Histories for ISU5 at EOD Condition

Shaft Soil Segment	Depth Below Ground Surface (ft)	R_{uk} (kips)	R_{nk} (% of R_{uk})	q_k (in)	J_{sk} (s/ft)
1	1.3	6.61	0	0.20	0.1905
2	5.2	9.18	5	0.20	0.1900
3	9.0	9.12	5	0.20	0.1903
4	12.8	9.07	5	0.20	0.l901
5	16.7	9.61	5	0.20	0.1904
6	20.5	9.57	5	0.20	0.1902
7	24.3	10.20	5	0.20	0.1900
8	28.2	9.26	5	0.15	0.1903
9	32.0	9.73	10	0.15	0.1902
10	35.8	10.78	10	0.15	0.1898
11	39.7	9.81	10	0.15	0.1902
12	43.5	8.40	10	0.15	0.1901
13	47.3	5.00	10	0.10	0.3041
14	51.2	11.00	10	0.10	0.1210
15	55.0	8.00	10	0.10	0.0831
Toe	55.0	15.00	0	0.30	0.3802

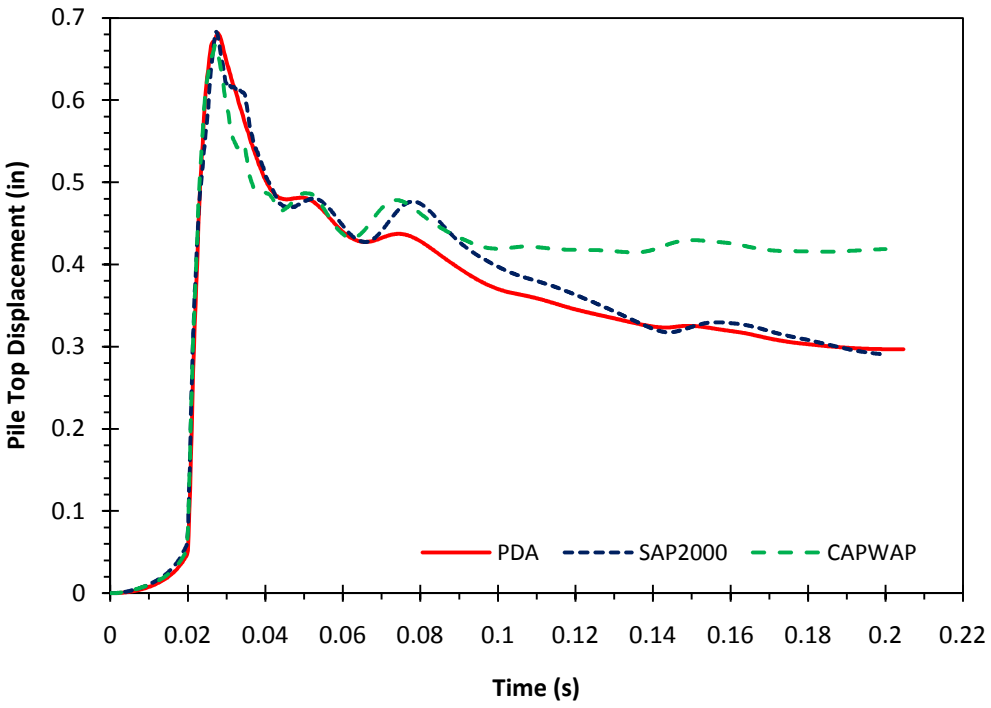

Figure 6.16: ISU5 EOD Condition Pile Top Displacement Comparison

As observed in Figure 6.16, the best fit pile top displacement time history obtained using the displacement-based signal matching technique has been compared against that measured by the PDA hardware product and that computed by a CAPWAP analysis with a suitable match quality (2.28), where q_k is 0.10 inches and 0.31 inches for soil located along the pile shaft and beneath the pile toe, respectively, J_{sk} is 0.166 s/ft and 0.162 s/ft for soil located along the pile shaft and beneath the pile toe, respectively, R_{nk} is 50 percent of R_{uk} for soil located along the pile shaft, and the distribution of R_{uk} is as depicted in Figure 6.17. The results of this comparison clearly show that although the CAPWAP analysis provided a suitable match of the upward traveling force wave time history computed at the pile head (Figure 6.18), a suitable match of the pile top displacement time history was not achieved. Once again, demonstrating the inefficiency of the CAPWAP signal matching technique to accurately and/or uniquely quantify the various one-dimensional soil model parameters.

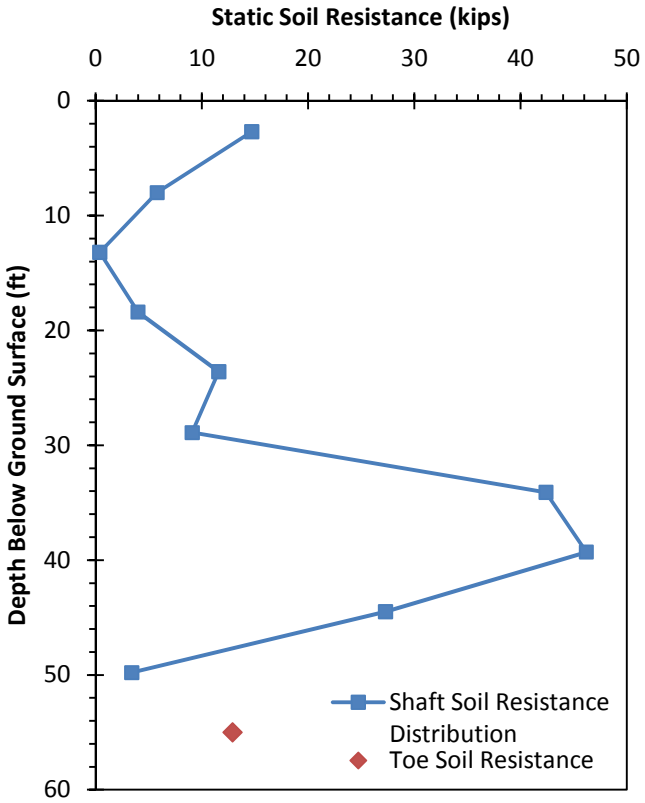

Figure 6.17: Ultimate, Static Soil Resistance Distribution Obtained from CAPWAP Signal Matching Analyses for ISU5 at EOD Condition

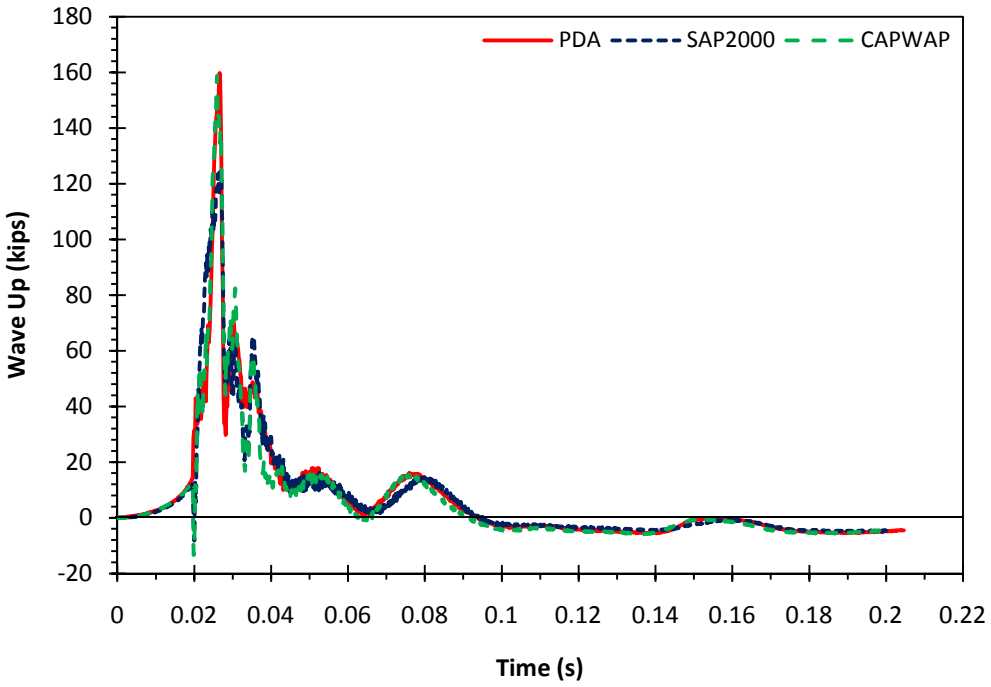

Figure 6.18: ISU5 EOD Condition Wave-Up Comparison

6.5 SUMMARY

The proposed displacement-based signal matching procedure, unlike the CAPWAP signal matching procedure, has been shown to not only produce a satisfactory match of the measured pile top displacement time history, but also produce a satisfactory match of the upward traveling force wave time history measured at the pile head. In fact, these satisfactory wave-up matches are often times better than those computed via a CAPWAP analysis for more accurate quantification of the one-dimensional soil model parameters. Consequently, the extended use of such a procedure on additional PDA datasets is recommended by the author to allow for the establishment of meaningful prediction correlations for soil quake values, Smith damping factors, the percentage of the ultimate, static soil resistance mobilized during pile rebound, and the degree-of-degradation experienced by static, soil shaft resistances and quake values as a function of pile penetration depth. Provided such prediction correlations can be established, it is safe to assume that a one-dimensional pile-soil model could be used to estimate the pile set and, with the application of a dynamic pile driving formula, establish the pile capacity more accurately in design, thereby improving the construction control procedures.

CHAPTER 7: SUMMARY, CONCLUSIONS, AND RECOMMENDATIONS

7.1 SUMMARY OF RESEARCH

The three main categories of pile bearing capacity estimation methods were introduced in Chapter 1, emphasizing how they fit into the current design and construction process used in the State of Iowa for driven pile foundations. Focusing the attention of this thesis on the use of dynamic pile driving formulas to predict driven pile foundation capacities, a comparison of the two main design approaches, i.e., WSD and LRFD, available for the evaluation of such predicted pile capacities was given in light of FHWA's mandate concerning the use of the LRFD approach for the design and construction of all new bridges initiated after October 1, 2007, and AASHTO's allowance for the development of regionally calibrated resistance factors.

A review of published literature in Chapter 2 has shown that the Hiley, Janbu, PCUBC, and Gates dynamic pile driving formulas are better on average than the remaining multitude of formulas in existence, with the ENR formula consistently displaying the worst performance. Three approaches for the performance of reliability analyses required for the development of LRFD resistance factors were discussed in Section 2.5, with an added presentation of the calibrated resistance factors generated by investigations that adopted these approaches.

Chapter 3 has presented the current state of practice with regards to the driven pile foundation design process via a discussion of the results obtained from a nationwide survey of state DOTs and a local survey of Iowa county engineers. Additionally, this chapter has provided a detailed description of the database for PIle LOad Tests in Iowa (PILOT-IA), which is an amalgamated, electronic source of information consisting of both static and dynamic data for pile driving and load tests conducted in the State of Iowa and is intended for use in the establishment of LRFD resistance factors for the design and construction control of driven pile foundations.

A brief summary of the adopted testing procedures and the corresponding results obtained for nine steel H-piles driven and load tested within the State of Iowa for LRFD resistance factor verification purposes has been presented in Chapter 4.

The methodology and framework utilized for the calibration of LRFD resistance factors for the construction control of driven pile foundations via seven dynamic pile driving formulas has been outlined in Chapter 5. In addition to presenting the pertinent calibration results for both steel H-shaped and timber pile types, enhanced LRFD resistance factors, which account for field capacity verification by means of the Iowa DOT Modified ENR formula, for the design of driven pile foundations via the Iowa Blue Book static analysis method have been presented.

Finally, the success of a newly proposed displacement-based signal matching technique over the more traditional CAPWAP signal matching procedure in providing accurate and unique estimates for various one-dimensional soil properties has been investigated in Chapter 6. The results of analyses carried out according to the rules of the proposed approach have shown that that soil quake values and Smith damping factors vary with increasing depth below the ground surface, besides the fact that static, soil shaft resistances and quake values have also been shown to degrade as a function of pile penetration depth.

7.2 CONCLUSIONS AND RECOMMENDATIONS

Conclusions drawn from the research investigation presented in this thesis are presented in the following subsections.

7.2.1 State- and County-Level Surveys

The results obtained from both a state- and county-level survey focused on characterizing current design and construction practices for bridge pile foundations showed that regional variation in pile foundation practice cannot be captured via a state-level investigation, thus inhibiting the performance of effective regional LRFD calibrations. For instance, the fairly common use of timber type piles by Iowa county engineers on low-volume and short-span bridges was not identified in the results of the state-level survey. Furthermore, the results of the county-level survey, which indicated that the degree-of-implementation of the LRFD approach at the county-level is about 84%, provided verification that the transition from the WSD approach to the LRFD approach for bridge foundation design, as indicated by the Iowa DOT's response in the state-level survey, is

almost complete. Additional conclusions drawn from the county-level survey, in particular, are provided below.

- 77% of the responding county engineers reported the use of pile design specifications that were based on the LRFD approach; however, none of the cited design specifications included the locally established *Iowa LRFD Bridge Design Manual*. Moreover, 100% of the responding engineering consulting firms reported the use of pile design specifications based on the LRFD approach, with the majority of respondents citing the use of the *Iowa LRFD Bridge Design Manual* as their primary driven pile design specification.
- During the construction of pile foundations, Iowa county engineers and consulting firms mainly rely on WEAP analyses and field observations to verify the pile capacity estimated by a static analysis method, which is consistent with the practice enacted at the state-level. However, in some instances, county engineers prefer to simply drive piles until refusal or bedrock has been reached. Such practices have the potential to yield uneconomical results given the average bedrock depths reported by various counties spanning the state.
- Although county engineers failed to report on the effect of soil setup or relaxation on pile capacity, about 70% of the responding engineering consulting firms indicated that such effects on pile capacity are neglected in design. However, one respondent indicated that soil setup affected pile capacity in a range from 5 to 10%, with another respondent indicating that soil setup can increase pile capacities from anywhere between 11 and 20%, depending on the soil type.
- The majority of Iowa county engineers and consulting firms responding to the survey indicated that quality control tests for driven pile foundations are never performed, including a unanimous agreement to the non-use of SLTs. Yet, about 22% and 19% of responding Iowa county engineers reported the use of such quality control tests on about 5% and less than 5% of installed piles, respectively.

7.2.2 PILOT-IA

An electronic, relational database management system for the amalgamation of information on pile load tests, both static and dynamic in nature, conducted within the State of Iowa was successfully formatted in Microsoft Office Access™ 2007 to allow for the efficient performance of filtering, sorting, and querying procedures on the amassed dataset. More specifically, this database was developed for use in the calibration of LRFD resistance factors for the design and construction of driven piles in Iowa after carefully verifying the interpreted test results from archived historical data dating back to 1966 on 264 piles statically load tested to failure. Conclusions drawn from the establishment of the PILOT-IA database are provided below.

- PILOT-IA uses a well-defined hierarchical classification scheme in addition to employing an appealing user-friendly interface. These features are unique to PILOT-IA and have not been seen for any other pile load test databases.
- Imposition of a strict acceptance criterion for each of the three hierarchical pile load test dependability classifications, i.e., reliable, usable-static, and usable-dynamic, ensures that the resulting data available in PILOT-IA for LRFD regional calibration is of superior quality and consistency.
- Of the 164 steel H-pile records contained within PILOT-IA, 82 are usable for investigations dealing with static analysis methods, while 34 are usable for investigations dealing with dynamic analysis methods, including dynamic pile driving formulas.
- Likewise, of the 75 PILOT-IA timber pile records, 24 were classified as usable for investigations dealing with static analysis methods, while 9 were considered usable for investigations dealing with dynamic analysis methods.

7.2.3 Full-Scale Pile Load Tests

Verification and enhancement of the LRFD resistance factors calibrated for steel H-shaped piles in this study was enabled through the performance of nine full-scale pile load tests distributed amongst the main geological soil formations found in the State of Iowa. Besides driving and statically load testing the piles to failure, a majority of the test piles were

instrumented with strain gauges and dynamically monitored during driving and restrikes using PDA. Additionally, the subsurface conditions at the location of each of the test piles were characterized using various laboratory tests (e.g., moisture content, grain-size distribution, Atterberg limits, consolidation, and Triaxial Consolidated-Undrained compression tests) and in-situ tests (e.g., SPT, CPT, and BST). In some cases, ground instrumentation (i.e., push-in pressure cells) was used to capture horizontal stress and porewater pressure data near the test pile during driving and static load testing. Conclusions drawn from the nine field tests are provided below.

- All piles were successfully driven, with only minimal local buckling or bending of the flanges near the pile top, using open-ended, single-acting diesel hammers, characterized by maximum rated hammer energies on the order of 40 kip-ft, to depths ranging from 30 to 60 feet.
- Dynamic measurements obtained from the PDA device during driving and restrikes captured the phenomenon of soil set-up, i.e., the increase in pile capacity as a function of time, for piles driven in a clay soil profile.
- Strain gauges, which were installed on both sides of the web along the pile centerline at different depths, successfully characterized the load transfer mechanism for each test pile, i.e., the percentages of load carried by skin friction and end-bearing. Moreover, all nine test piles carried the majority of the applied load by skin friction, with the end-bearing component not exceeding 30% at the displacement-based Davisson capacity.
- Based on the results of static load test, steel H-piles driven in clay soils to embedment depths of about 55 feet can effectively achieve ultimate static capacities in the range of about 125 to 240 kips, depending on the degree of soil setup experienced at the time of testing.

7.2.4 Regionally Calibrated LRFD Resistance Factors

For the design verification or construction control of Iowa driven pile foundations by means of a dynamic pile driving formula, the use of the Iowa DOT Modified ENR formula is recommended. When used in conjunction with steel H-shaped piles, LRFD resistance factors

of 0.49, 0.62, and 0.50 are recommended for use with sand, clay, and mixed soil profiles, respectively, assuming a 1% probability of failure. For timber piles, an LRFD resistance factor of 0.35 is recommended for use with all soil profile types, assuming, once again, a 1% probability of failure. Additionally, the regional LRFD resistance factor calibration procedures utilized in the development of these values were shown through various comparative studies to provide more reliable and economically efficient results than those provided in design codes and presented in similar studies. More specifically, the Iowa DOT Modified ENR formula showed improved economy over the AASHTO (2007) recommended values for the ENR and FHWA Modified Gates formulas of about 160% and 10%, respectively.

Based upon the results of Monte Carlo simulations, the previous soil specific resistance factors recommended for steel H-shaped piles were shown to exhibit acceptably small variation. However, the resistance factor recommended for use with timber piles in all soil profile types was shown to exhibit relatively high variation on account of the small sample size utilized in the calibration procedures. Thus, it is recommended that this LRFD resistance factor be taken with caution or altered to ensure a desired level of confidence; the 95% confidence interval for the timber pile type LRFD resistance factor was determined to be (0.17, 0.54).

To take advantage of the prescribed use of the Iowa DOT Modified ENR formula for the construction control of Iowa driven pile foundations, enhanced LRFD resistance factors are recommended for use with the Iowa Blue Book static analysis method with the goal of minimizing the difference between design and production pile lengths. More specifically, for driven steel H-shaped piles, enhanced LRFD resistance factors of 0.54, 0.69, and 0.60 are recommended for use with sand, clay, and mixed soil profiles, respectively. However, to ensure a 1% probability of failure, it is emphasized that the pile capacity predicted by the Iowa DOT Modified ENR formula should be considered final, regardless of what was estimated in the design stage by the Iowa Blue Book static analysis method.

7.2.5 Theoretical Dynamic Model

It was proposed that a one-dimensional pile-soil model can be used to predict the set of a driven pile provided the soil resistance distribution, soil quake values, Smith damping

factors, and the degree-of-degradation of such parameters with respect to pile penetration depth are known. A displacement-based signal matching technique is recommended for use with PDA measured data to arrive at prediction correlations for the aforementioned soil parameters. Although data from only two sites was analyzed by the author, the accuracy, uniqueness, and theoretical basis of the displacement-based signal matching approach over the more commonly employed CAPWAP approach was successfully demonstrated through matches of both the wave-up and pile top displacement time histories.

7.3 FUTURE RESEARCH

Additional full-scale dynamic and static pile load tests should be carried out on various pile types, especially timber, concrete, Monotube, and pipe piles, and in conjunction with varying soil profiles to allow for the expansion of the PILOT-IA usable datasets as well as a pile-type calibration of regional LRFD resistance factors.

To complete the transition from WSD to LRFD for deep foundations, data for load tests conducted on drilled shafts within the State of Iowa should be collected and an ensuing regional LRFD resistance factor calibration should be performed. However, it should be pointed out that work is currently underway to expand the structure of PILOT-IA to allow for the inclusion of drilled shaft load test data. Additionally, LRFD resistance factors should be regionally calibrated for both lateral strength and serviceability limit states for both driven piles foundations as well as drilled shafts.

Finally, to enable for the formation of prediction correlations for soil quake values, Smith damping factors, and the degree-of-degradation of these parameters with respect to pile penetration depth, numerous EOD PDA datasets should be collected and analyzed using the displacement-based signal matching technique proposed in this thesis. This in turn will allow for the future investigation of the efficiency and suitability of a pile design method utilizing a one-dimensional pile-soil model in combination with a dynamic pile driving formula to predict pile set and ultimate capacity, respectively, thus improving the construction control procedures for driven piles.

REFERENCES

AASHTO. 1994. *LRFD Highway Bridges Design Specifications, SI Units*. 1st ed. Washington, DC: AASHTO.

AASHTO. 1997. *Standard Specifications for Highway Bridges: 16th Edition (1996 with 1997 Interims)*. Washington, DC: AASHTO.

AASHTO. 2000. *LRFD Bridge Design Specifications: 2nd LRFD Edition - 2000 Interim Revisions*. Washington, DC: AASHTO.

AASHTO. 2006. *LRFD Bridge Design Specifications, Customary U.S. Units*. 3rd ed. Washington, DC: AASHTO.

AASHTO. 2007. *LRFD Bridge Design Specifications, Customary U.S. Units*. 4th ed. Washington, DC: AASHTO.

AbdelSalam, Sherif. 2010. Characterization of Axially Loaded Steel Piles and Development of the LRFD Resistance Factors, Department of Civil, Construction, and Environmental Engineering, Iowa State University, Ames, IA. PhD Dissertation.

AbdelSalam, Sherif S., Kam W. Ng, Matthew J. Roling, Sri Sritharan, and Muhannad T. Suleiman. 2010. Development of LRFD Procedures for Bridge Piles in Iowa - Volume III: LRFD Resistance Factor Calibration Efforts. Ames, IA: Iowa State University - Institute for Transportation.

AbdelSalam, Sherif, Sri Sritharan, and Muhannad T. Suleiman. 2010. Current Design and Construction Practices of Bridge Pile Foundations with Emphasis on Implementation of LRFD. *ASCE Journal of Bridge Engineering*.

Agerschou, Hans A. 1962. Analysis of the Engineering News Pile Formula. *ASCE Journal of Soil Mechanics and Foundation Division* 88 (No. SM 5):1-11.

Allen, T. M., A. S. Nowak, and R. J. Bathurst. 2005. *Calibration to Determine Load and Resistance Factors for Geotechnical and Structural Design, Transportation Research Circular*. Washington, DC: National Transportation Research Board.

Allen, Tony. 2005. Development of the WSDOT Pile Driving Formula and Its Calibration for Load and Resistance Factor Design (LRFD). Seattle, WA: Washington State Transportation Center.

Allen, Tony. 2007. Development of New Pile-Driving Formula. *Transportation Research Record: Journal of the Transportation Research Board* 2004:20-27.

Allen, Tony M. 2007. Development of New Pile-Driving Formula and Its Calibration for Load and Resistance Factor Design. *Transportation Research Record: Journal of the Transportation Research Board* 2004:20-27.

API. 1984. *API Recommended Practice for Planning, Designing and Constructing Fixed Offshore Platforms, API Recommended Practice 2A*. 15 ed: American Petroleum Institute.

Argo, Douglas E. 1987. Dynamic Formulas to Predict Driven Pile Capacity, Department of Civil and Environmental Engineering, Washington State University, Pullman, WA.

ASCE. 1941. Pile-Driving Formulas. *Proceedings ASCE* 67 (5):853-866.

ASCE. 1946. Pile Foundations and Pile Structures. *Manual of Engineering Practice* 27.

Ayyub, B., and I. Assakkaf. 1999. *LRFD Rules for Naval Surface Ship Structures: Reliability-Based Load and Resistance Factor Design Rules*: Naval Surface Warfare Center - Carderock Division - U.S. Navy.

Baecher, G. 2001. Contribution to a Progress Research Report as part of Project NCHRP 24-17, LRFD Deep Foundations Design, Unpublished Document.

Barker, R. M., J. M. Duncan, K. B. Rojiani, P. S. K. Ooi, C. K. Tan, and S. G. Kim. 1991. NCHRP Report 343: Manuals for the Design of Bridge Foundations. Washington, DC: Transportation Research Board - National Research Council.

Beardsley, Rufus Charles. 1907. *Design and Construction of Hydroelectric Plants: Including a Special Treatment of the Design of Dams*. New York, NY: McGraw Publishing Company.

Beckmann, Petr. 1976. *A History of PI*. New York, NY: St. Martin's Griffin.

Bowles, Joseph E. 1996. *Foundation Analysis and Design*. 5th ed. New York, NY: McGraw-Hill Science/Engineering/Math.

Burland, J. B. 1973. Shaft Friction of Piles in Clay. *Ground Engineering* 6 (3):3042.

Chellis, Robert D. 1949. The Relationship Between Pile Formulas and Load Tests. *American Society of Civil Engineers Transactions* 114:290-320.

Chellis, Robert D. 1961. *Pile Foundations*. 2nd ed. New York, NY: McGraw-Hill Book Company, Inc.

Chin, F. K. 1970. Estimation of the Ultimate Load of Piles Not Carried to Failure. Paper read at The 2nd Southeast Asian Conference on Soil Engineering, at Singapore.

Chin, F. K. 1971. Discussion on Pile Test: Arkansas River Project. *ASCE Journal of Soil Mechanics and Foundation Division* 97 (No. SM 6):930-932.

Computers and Structures, Inc. (CSI). 2008. *CSI Analysis Reference Manual For SAP2000®, ETABS®, and SAFE™*. Berkeley, CA: CSI.

Cummings, A. E. 1940. Dynamic Pile Driving Formulas. *Journal of the Boston Society of Civil Engineers* 27:6-27.

Davisson, M. T. 1972. High Capacity PIles. Paper read at The Soil Mechanics Lecture Series on Innovations in Foundation Construction, at Chicago, IL.

De Beer, E. 1967. Bearing Capacity and Settlement of Shallow Foundations on Sand. Paper read at The Symposium on Bearing Capacity and Settlement of Foundations, at Durham, NC.

DiMaggio, Jerry, Tom Saad, Tony Allen, Barry R. Christopher, Al DiMillio, George Goble, Paul Passe, Terry Shike, and Gary Person. 1999. Geotechnical Engineering Practices in Canada and Europe. Washington, D.C.: U.S. Department of Transportation - FHWA.

Dirks, Kermit L., and Patrick Kam. 1989. *Foudation Soils Information Chart: Pile Foundation*. Ames, IA: Iowa DOT - Highway Division - Soils Survey Section.

Faber, O., E. S. Andrews, A. Hiley, J. P. Porter, G. B. R. Pimm, R. D. Brown, Lee H. Donovan, H. D. Lee, M. Nachsen, A. S. E. Ackermann, J. S. Henzell, G. P. Manning, S. Packshaw, and G. Wilson. 1947. Discussion on A New Piling Formula. *Journal of the Institution of Civil Engineers* 28 (5):55-86.

Fenton, Gordon A., and D. V. Griffiths. 2008. *Risk Assessment in Geotechnical Engineering*. Hoboken, NJ: John Wiley and Sons, Inc.

Flaate, Kaare S. 1964. An Investigation of the Validity of Three Pile Driving Formulae in Cohesionless Material. *Norwegian Geotechnical Institute* (No. 56):11-22.

Folse, Michael D., Kenneth L. McManis, and Janet S. Elias. 1989. Study of Dynamic Methods of Predicting Pile Axial Load Capacity by Louisiana Department of Transportation and Development. *Transportation Research Record: Journal of the Transportation Research Board* 1219:13-20.

Fragaszy, Richard J., Douglas E. Argo, and Jerry D. Higgins. 1989. Comparison of Formula Predictions with Pile Load Tests. *Transportation Research Record: Journal of the Transportation Research Board* 1219:1-12.

Fragaszy, Richard J., Jerry D. Higgins, and Evert C. Lawton. 1985. Development of Guidelines for Construction Control of Pile Driving and Estimation of Pile Capacity. Olympia, WA: Washington State Transportation Center.

Fuller, Charles E., and William A. Johnston. 1915. *Applied Mechanics (Volume 1: Statics and Kinetics)*. 1st ed. New York, NY: John Wiley and Sons, Inc.

Gates, Marvin. 1957. Empirical Formula for Predicting Pile Bearing Capacity. *Civil Engineering*, 65-66.

Goble, George G. 2005. Reflections on LRFD for Geotechnical Applications. *ASCE Geotechnical Special Publication (GSP) No. 131: Contemporary Issues in Founation Engineering*, ASCE GeoFrontiers, Austin, TX, January 24-26.

Gulhati, Sahashi K., and Manoj Datta. 2005. *Geotechnical Engineering*. New Delhi, Haryana India: Tata McGraw-Hill Publishing Company Limited.

Gutierrez, M. A. 1978. Dynamic Methods for Predicting Pile Capacity. Masters Special Research Problem, School of Civil Engineering, Georgia Institute of Technology, Atlanta, GA.

Hannigan, P. J., G. G. Goble, G. Thendean, G. E. Likins, and F. Rausche. 1998. Design and Construction of Driven Foundations - Volume II. Washington, DC: Federal Highway Administration.

Hasofer, A. M., and N. C. Lind. 1974. An Exact and Invariant First-Order Reliability Theory. *Journal of Engineering Mechanics* 100 (EM1):111-121.

Housel, William S. 1966. Pile Load Capacity: Estimates and Test Results. *ASCE Journal of Soil Mechanics and Foundation Division* 92 (No. SM 4):1-30.

Iowa DOT. 2008. Standard Specifications with GS-01014 Revisions. *Iowa DOT Electronic Reference Library*, http://www.erl.dot.state.ia.us/Apr_2008/GS/frames.htm. Accessed April 2010.

Iowa DOT. 2009. Iowa County Bridge Standards. http://www.iowadot.gov/bridge/countybrgstd.htm. Accessed April 2010.

Iowa DOT. 2010. Iowa ASD/LFD Bridge Design Manual. http://www.iowadot.gov/bridge/manualasd.htm. Accessed April 2010.

Iowa DOT. 2010. Iowa LRFD Bridge Design Manual. http://www.iowadot.gov/bridge/manuallrfd.htm. Accessed April 2010.

Jacoby, Henry S., and Roland P. Davis. 1914. *Foundations of Bridges and Buildings*. 1st ed. New York, NY: McGraw-Hill Book Company, Inc.

Jumikis, Alfreds R. 1971. *Foundation Engineering*. New York, NY: Intext Educational Publishers

Kazmierowski, T., and M. Devata. 1978. Pile Load Capacity Evaluation: Highway 404 Structures. Ontario Ministry of Transportation and Communications.

Kerkhoff, G. O., L. T. Oehler, and W. S. Housel. 1965. A Performance Investigation of Pile Driving Hammers and Piles. Lansing, MI: Michigan State Highway Commission.

Kyung, K. J. 2002. Development of Resistance Factors for Axial Capacity of Driven Piles in North Carolina, Department of Civil, Construction, and Environmental Engineering, North Carolina State University, Raleigh, NC.

Long, James H., Joshua Hendrix, and Alma Baratta. 2009. Evaluation/Modification of IDOT Foundation Piling Design and Construction Policy. Urbana, IL: Illinois Center for Transportation.

Long, James H., Joshua Hendrix, and David Jaromin. 2009. Comparison of Five Different Methods for Determining Pile Bearing Capacities. Urbana, IL: University of Illinois Department of Civil Engineering.

Mansur, Charles I., and Alfred H. Hunter. 1970. Pile Tests - Arkansas River Project. *ASCE Journal of Soil Mechanics and Foundation Division* 96 (No. SM 5):1545-1582.

MATLAB. 2009. MATLAB® *The Language of Technical Computing*, Release 7.9.0 (R2009b) [Computer Software]. Natick, MA: The MathWorks, Inc.

McVay, Michael, Bjorn Birgisson, and Sangmin Lee. 2004. Influence of Sample Size, and Strength Variability on LRFD Resistance Factors. Paper read at Geo-Trans 2004, at Los Angeles, CA.

McVay, Michael C., Bjorn Birgisson, Limin Zhang, Ariel Perez, and Sastry Putcha. 2000. Load and Resistance Factor Design (LRFD) for Driven Piles Using Dynamic Methods - A Florida Perspective. *Geotechnical Testing Journal* 23 (1):55-66.

McVay, Michael, and Ching Kuo. 1999. Estimate Damping and Quake by Using Traditional Soil Testing. Gainesville, FL: University of Florida - Department of Civil Engineering.

Meyerhof, G. 1976. Bearing Capacity and Settlement of Pile Foundations. *ASCE Journal of the Geotechnical Engineering Division* 102 (3):195-228.

Miller, Irwin, and Marylees Miller. 2004. *John E. Freund's Mathematical Statistics with Applications*. 7th ed. Upper Saddle River, NJ: Pearson Prentice Hall.

Minitab. 2009. Minitab Statistical Software, Release 15.1.3 [Computer Software]. State College, PA.

Morris, Philip Scott Morris, and Richard D. Barksdale. 1982. A New Pile-Driving Formula. *The Military Engineer* (480):211-213.

Ng, Charles W. W., Noel Simons, and Menzies Bruce. 2004. *A Short Course in Soil-Structure Engineering of Deep Foundations, Excavations, and Tunnels*. London, UK: Thomas Telford Publishing.

Ng, Kam W. 2011. Behaviors Characterization and LRFD Developments of Bridge Foundations using Dynamic Analysis Methods, Department of Civil, Construction, and Environmental Engineering, Iowa State University, Ames, IA. PhD Dissertation.

Ng, Kam W., Matthew J. Roling, Sherif S. AbdelSalam, Sri Sritharan, and Muhannad T. Suleiman. 2010. Development of LRFD Design Procedures for Bridge Piles in Iowa - Volume II: Soil Investigation and Full-Scale Pile Tests. Ames, IA: Iowa State University - Institute for Transportation.

Nordlund, R. L. 1963. Bearing Capacity of Piles in Cohesionless Soils. *Journal of Soil Mechanics and Foundation Engineering* 89 (SM 3):1-36.

Nowak, A. S. 1999. NCHRP Report 368: Calibration of LRFD Bridge Design Code. Washington, DC: Transportation Research Board.

NRCS (Natural Resources Conservation Service). 2010. Iowa Soil Regions Map. http://www.ia.nrcs.usda.gov/soils.html

Olson, Roy E., and Kaare S. Flaate. 1967. Pile-Driving Formulas for Friction Piles in Sand. *ASCE Journal of Soil Mechanics and Foundation Division* 93 (No. SM 6):279-296.

Paikowsky, Samuel G., Bjorn Birgisson, Michael McVay, Thai Nguyen, Ching Kuo, Gregory Baecher, Bilal Ayyub, Kirk Stenersen, Kevin O'Malley, Les Chernauskas, and Michael O'Neill. 2004. NCHRP Report 507: Load and Resistance Factor Design (LRFD) for Deep Foundations. Washington, D.C.: Transportation Research Board.

Perez, Ariel. 1998. Load and Resistance Factor Design (LRFD) for Driven Piles based on Dynamic Methods with Assessment of Skin and Tip Resistance from PDA Signals, Department of Civil and Coastal Engineering, University of Florida, Gainesville, FL.

Pile Dynamics Inc. 1992. *Pile Driving Analyzer Manual*. Cleveland, OH.

Pile Dynamics Inc. 2000. *CAse Pile Wave Analysis Program - CAPWAP for Windows Manual*. Cleveland, OH.

Pile Dynamics Inc. 2005. *GRLWEAP Wave Equation Analysis of Pile Driving - Procedures and Models*. Cleveland, OH.

Poplin, J. K. 1971. Preliminary Evaluation of Test Pile Records for Highway Structures in Louisiana. *Engineering Research Bulletin* (No. 106).

Ramey, G. E., and A. P. Hudgins. 1975. Modification of Pile Capacity and Length Prediction Equations Based on Historical Alabama Pile Test Data. Montgomery, AL: State of Alabama Highway Department - Bureau of Research and Development.

Ramey, G. E., and A. P. Hudgins. 1977. Sensitivity and Accuracy of the Pile Wave Equation. *Ground Engineering*:45-47.

Rausche, F., B. Robinson, and L. Liang. 2000. Automatic Signal Matching with CAPWAP. Paper read at Sixth International Conference on the Application of Stress-Wave Theory to Piles, at Sao Paulo, Brazil.

Roling, Matthew J., Sri Sritharan, and Muhannad T. Suleiman. 2010. Development of LRFD Procedures for Bridge Piles in Iowa - Volume I: An Electronic Database for PIle LOad Tests in Iowa (PILOT-IA). Ames, IA: Iowa State University - Institute for Transportation.

Rosenblueth, E., and L. Esteva. 1972. *Reliability Basis for Some Mexican Codes*. Vol. ACI Publication SP-31. Detroit, MI: American Concrete Institute.

Schmertmann, J. H. 1978. Guidelines for Cone Penetration Test Performance and Design. Washington, DC: US Department of Transportation - Federal Highway Administration - Offices of Research and Development.

Smith, E. A. L. 1962. Pile-Driving Analysis by the Wave Equation. *American Society of Civil Engineers Transactions* 127:1145-1193.

Sörensen, T., and B. Hansen. 1957. Pile Driving Formulae - An Investigation Based on Dimensional Considerations and a Statistical Analysis. Paper read at Fourth International Conference on Soil Mechanics and Foundation Engineering, at London, UK.

Spangler, M. G., and H. F. Mumma. 1958. Pile Test Loads Compared with Bearing Capacity Calculated by Formulas. Paper read at Thirty-Seventh Annual Meeting of the Highway Research Board, at Washington, DC.

Svinkin, Mark. 2004. Some Uncertainties in High-Strain Dynamic Pile Testing. Paper read at Geo-Trans 2004, at Los Angeles, CA.

Thoft-Christensen, P., and M. J. Baker. 1982. *Structural Reliability Theory and Its Applications*. Berlin, Germany: Springer-Verlag.

Tomlinson, M. J. 1971. Some Effects of Pile Driving on Skin Friction. Paper read at Conference on Behaviour of Piles, at London, UK.

Van der Veen , C. 1953. The Bearing Capacity of a Pile. Paper read at The 3rd International Conference on Soil Mechanics and Foundation Engineering.

Wellington, A. M., ed. 1893. *Piles and Pile-Driving*. New York, NY: Engineering News Publishing Company.

Withiam, J. L., E. P. Voytko, R. M. Barker, J. M. Duncan, B. C. Kelly, S. C. Musser, and V. Elias. 1997. Load and Resistance Factor Design (LRFD) for Highway Bridge Substructures. Washington, DC: Federal Highway Administration.

Yoon, Sungmin, Murad Abu-Farsakh, Ching Tsai, and Zhongjie Zhang. 2008. LRFD Calibration of Axially-Loaded Concrete Piles Driven into Soft Soils. Paper read at 87th Annual Meting of the Transportation Research Board, at Washington, DC.

ACKNOWLEDGMENTS

The author would like to thank the Iowa Highway Research Board for sponsoring the research outlined in this thesis. The author would also like to thank Sandra Larson and Mark Dunn, from the Research and Technology Bureau of the Iowa DOT, for their coordination and support of the research, as well as the following members of the Technical Advisory Committee for their guidance and advice: Ahmad Abu-Hawash, Dean Bierwagen, Lyle Brehm, Ken Dunker, Kyle Frame, Steve Megivern, Curtis Monk, Michael Nop, Gary Novey, John Rasmussen, and Bob Stanley. The members of this committee represent Bridges and Structures, Soils, and Construction Divisions of the Iowa DOT, the FHWA Iowa Division, and Iowa county engineers. The author wishes to thank his major professor, Dr. Sri Sritharan, for his knowledge, guidance, and commitment to the success of the investigation detailed in this thesis. Furthermore, the advice and cooperation received from all other members of the Program of Study Committee, especially that provided by Dr. Muhannad Suleiman concerning the geotechnical aspects of this study, is much appreciated.

With regards to the field testing portion of this research, the author acknowledges Team Services, Inc. for their conduction of SPTs, Geotechnical Services, Inc. for their conduction of CPTs, Erica Velasco for her assistance with laboratory soil tests, and the following bridge construction contractors for their help with the pile driving and restriking procedures as well as the assembly of the static load testing frame: Cramer & Associates, Inc. (ISU1 and ISU3), Dixon Construction Company (ISU2), Peterson Contractors, Inc. (ISU4 and ISU8), Herberger Construction Company, Inc. (ISU5), Taylor Construction, Inc. (ISU6 and ISU7), and Iowa Bridge and Culvert, LLC (ISU9). In addition, special gratitude is due to Doug Wood for his assistance with the Megadac data acquisition system as well as Kam Weng Ng and Sherif AbdelSalam for their contribution to the field testing.

Finally, the author would like to especially thank his parents, sister, fiancé, and friends for their love, prayers, and support over these past two years. Giving thanks to God, the Lord and Savior, the author acknowledges the following words of the prophet Isaiah for their calming and strengthening influence throughout the entirety of my graduate studies: "...but those who hope in the Lord will renew their strength. They will soar on wings like eagles; they will run and not grow weary, they will walk and not be faint."